MONASH University

Molecular mechanism of GPCRs mediating metabolic responses – The role of adrenoceptors in glucose metabolism

Saori Mukaida

Master of Biotechnology

Copyright notice

Table of contents

Chapter 3 BRL37344 stimulates GLUT4 translocation and glucose uptake in skeletal muscle via β₂-adrenoceptors without causing classical receptor desensitisation 110

Abstract

Insulin-stimulated glucose uptake requires an intricate network of proteins including phosphoinositide 3-kinase, Akt and glucose transporter 4 (GLUT4), and is key to maintaining whole body glucose homeostasis. Dysfunction of insulin action causes diminished glucose uptake/utilization in insulin target tissues. Adrenoceptors (ARs), members of the G protein-coupled receptor superfamily, are also involved in glucose metabolism, and activation of α_{1A}-ARs, β_2-ARs and β_3-ARs increases glucose uptake in cardiomyocytes, skeletal muscle and brown adipocytes, respectively. However, there is a knowledge gap on the mechanisms involved in AR-mediated glucose uptake, and how they differ from that of insulin, which may be important in disease context (such as type 2 diabetes) where the insulin-signaling pathway is down-regulated.

We examined the differences in signalling profiles between two β_2-AR agonists, isoprenaline and BRL37344, in skeletal muscle. BRL37344 increased skeletal muscle glucose uptake *in vivo* and improved glucose tolerance *in vivo* in insulin-resistant mice, showing potential anti-diabetic effects. In skeletal muscle cells *in vitro*, BRL37344 increased GLUT4 translocation and glucose uptake with a similar potency and efficacy to that of isoprenaline. However, BRL37344 was a weak partial agonist for cAMP production and failed to desensitise the β_2-AR, as it was unable to promote β-arrestin1/2 binding to the β_2-AR. The role of GRK (which has a primary role in receptor desensitisation) was further investigated in a recombinant system using several mutant β_2-ARs partially or completely lacking putative GRK/PKA phosphorylation sites, since siRNA directed against GRK2 abolished β_2-AR mediated glucose uptake. Attenuation of GRK phosphorylation sites disrupted isoprenaline-stimulated receptor internalisation but did not affect GLUT4 translocation/glucose uptake. In contrast, BRL37344 stimulation did not induce internalisation and did not alter GLUT4 translocation/glucose uptake in the presence or absence of GRK phosphorylation sites. This suggested that GRK phosphorylation sites in β_2-AR C-terminal do not affect β_2-AR mediated glucose uptake, and that GRK may function in a novel manner to regulate this pathway.

Stimulation of cardiomyocyte α_{1A}-ARs prevents pathologic remodeling in heart failure, potentially due to increased glucose uptake and protein synthesis. In a recombinant system, we assessed the signalling pathways activated by two α_{1A}-AR agonists: A61603 and dabuzalgron. A61603 increased cAMP production, which is partially involved in glucose uptake. In contrast, dabuzalgron increased glucose uptake independently of cAMP. Both A61603 and dabuzalgron were full agonists for glucose

uptake and extracellular signal-regulated kinases1/2 phosphorylation (associated with cell survival), but dabuzalgron was a partial agonist for Ca^{2+} mobilization (contractility), S6 ribosomal protein phosphorylation (hypertrophy), and N-Myc Downstream Regulated 1 phosphorylation (downstream of mTORC2). This suggests that dabuzalgron may be a biased agonist with respect to cell survival and glucose uptake in contrast to contractility and hypertrophy. These findings establish a novel link between α_{1A}-ARs, cAMP and glucose uptake, and provide an improved framework for examining the utility of α_{1A}-AR agonists as cardioprotective agents. These studies collectively advance our basic understanding of how ARs can increase glucose uptake.

(473 words)

Declaration

This thesis contains no material which has been accepted for the award of any other degree or diploma at any university or equivalent institution and that, to the best of my knowledge and belief, this thesis contains no material previously published or written by another person, except where due reference is made in the text of the thesis.

Signature:

Print Name: Saori Mukaida

Date:

Thesis including published works declaration

I hereby declare that this thesis contains no material which has been accepted for the award of any other degree or diploma at any university or equivalent institution and that, to the best of my knowledge and belief, this thesis contains no material previously published or written by another person, except where due reference is made in the text of the thesis.

This thesis includes (1) submitted publication. The core theme of the thesis is "Molecular mechanism of GPCRs mediating metabolic responses – The role of adrenoceptors in glucose metabolism". The ideas, development and writing up of all the papers in the thesis were the principal responsibility of myself, the student, working within the Drug Discovery Biology Laboratory and the Cell Signalling Laboratory under the supervision of Dana S Hutchinson, Nick D Holliday, Masaaki Sato, Bronwyn A Evans, and Roger J Summers.

The inclusion of co-authors reflects the fact that the work came from active collaboration between researchers and acknowledges input into team-based research.

In the case of Chapter 3 and Appendices 1 my contribution to the work involved the following:

Thesis Chapter	Publication Title	Status *(published, in press, accepted or returned for revision, submitted)*	Nature and % of student contribution	Co-author name(s) Nature and % of Co-author's contribution*	Co-author(s), Monash student Y/N*
Chapter 3	BRL37344 stimulates GLUT4 translocation and glucose uptake in skeletal muscle via β_2-adrenoceptors without causing classical receptor desensitisation	Published	Performed 60% of the experiments (*in vitro* assays (Fig 3.1 A, Fig 3.3 A, B, D, E, Fig 3.4 A, B, E, Fig 3.5 A, B, C, D, E, F, G, H) except GLUT4 translocation assays, glucose uptake assays in L6 GLUT4myc cells and SkMC cells, glucose uptake assays using inhibitors, p-CREB phosphorylation assay and mTOR phosphorylation assay), analysed data, and contributed to the writing of the manuscript	1 Masaaki Sato, 10%, supervised the project and performed experiments 2 Anette I. Öberg, performd 3% of the experiments 3 Nodi Dehvari, performed 3% of the experiments 4 Jessica M. Olsen, performed 1% of the experiments 5 Martina Kocan, 1%, supervised the BRET experiments 6 Michelle L. Halls, 1%, supervised the FRET cAMP experiments 7 Jon Merlin, 1%, assisted in cell culture 8 Anna L. Sandström, performed 1% of the experiments	1, N 2, N 3, N 4, N 5, N 6, N 7, N 8, N

				9 Robert I. Csikasz, performed 1% of the experiments	9, N
			15	10 Bronwyn A. Evans, 3%, supervised the project	10, N
				11 Roger J. Summers, 5%, supervised the project and original concept	11, N
				12 Dana S. Hutchinson, 5%, supervised the project, original concept and wrote the manuscript	12, N
				13 Tore Bengtsson, 5%, supervised the project and original concept	13, N
Appendix 1	Adrenoceptors promote glucose uptake into adipocytes and muscle by an insulin-independent signalling pathway involving mechanistic target of rapamycin complex 2	Published	50%, contributed to writing of the review	1 Bronwyn A Evans, 10%, writing and editing of the review	1, N
				2 Tore Bengtsson, 10%, writing and editing of the review	2, N
				3 Dana S Hutchinson, 10%, writing and editing of the review	3, N
				4 Masaaki Sato, 20%, writing and editing of the review	4, N

I have renumbered sections of submitted paper in order to generate a consistent presentation within the thesis.

Student signature: **Date:**

The undersigned hereby certify that the above declaration correctly reflects the nature and extent of the student's and co-authors' contributions to this work. In instances where I am not the responsible author I have consulted with the responsible author to agree on the respective contributions of the authors.

Main Supervisor signature: **Date:**

Publications and Communications

Peer-reviewed articles

-Published

Mukaida, S., M. Sato, A. I. Oberg, N. Dehvari, J. M. Olsen, M. Kocan, M. L. Halls, J. Merlin, A. L. Sandstrom, R. I. Csikasz, B. A. Evans, R. J. Summers, D. S. Hutchinson, and T. Bengtsson. 2019. 'BRL37344 stimulates GLUT4 translocation and glucose uptake in skeletal muscle via beta2-adrenoceptors without causing classical receptor desensitization', Am J Physiol Regul Integr Comp Physiol 316:R666-R677.

Sato, M., B. A. Evans, A. L. Sandstrom, L. Y. Chia, **S. Mukaida**, B. S. Thai, A. Nguyen, L. Lim, C. Y. R. Tan, J. A. Baltos, P. J. White, L. T. May, D. S. Hutchinson, R. J. Summers and T. Bengtsson (2018). "α_{1A}-Adrenoceptors activate mTOR signalling and glucose uptake in cardiomyocytes." Biochem Pharmacol 148: 27-40.

Reviews

-Published
Yeong, L., B. A. Evans, **S. Mukaida**, T. Bengtsson, D. S. Hutchinson and M. Sato (2018). "Adrenoceptor regulation of mTOR in muscle and adipose tissue." BJ Pharmacol 1-16.

Mukaida, S., B. A. Evans, T. Bengtsson, D. S. Hutchinson and M. Sato (2017). "Adrenoceptors promote glucose uptake into adipocytes and muscle by an insulin-independent signalling pathway involving mechanistic target of rapamycin complex 2." Pharmacol Res 116: 87-92.

Conference abstracts

-**Saori Mukaida**, Masaaki Sato, Michelle Halls, Martina Kocan, Bronwyn Evans, Roger Summers, Tore Bengtsson, Dana Hutchinson. *BRL37344 stimulates glucose uptake into skeletal muscle by β_2-adrenoceptor mediated translocation of GLUT4 without causing receptor desensitisation.* Oral presentation. 2018. 18th World Congress of Basic and Clinical Pharmacology (Kyoto, Japan).

-**Saori Mukaida**, Masaaki Sato, Michelle Halls, Martina Kocan, Bronwyn Evans, Roger Summers, Tore Bengtsson, Dana Hutchinson. *BRL37344 stimulates glucose uptake into skeletal muscle by β_2-adrenoceptor mediated translocation of GLUT4 without causing receptor desensitisation.* Oral presentation. 2018. 10th Adrenoceptor Symposium (Shizuoka, Japan).

- **Saori Mukaida**, Bronwyn Evans, Roger Summers, Dana Hutchinson, Masaaki Sato. α_{1A}-adrenoreceptors stimulate glucose uptake and cell growth by activating mTOR. Oral presentation. 2017. British Pharmacological Society Meeting (London, UK).

- **Saori Mukaida**, Bronwyn Evans, Roger Summers, Dana Hutchinson, Masaaki Sato. α_{1A}-adrenoreceptors stimulate glucose uptake and cell growth by activating mTOR. Oral presentation. 2017. British Biochemical Society (Bath, UK).

- **<u>Saori Mukaida</u>**, Bronwyn Evans, Roger Summers, Dana Hutchinson, Masaaki Sato. α_{1A}-*adrenoreceptors stimulate glucose uptake and cell growth by activating mTOR*. Poster presentation. 2016. ASCEPT-MPGPCR Joint Scientific Meeting (Melbourne, Australia).

- **<u>Saori Mukaida</u>**, Bronwyn A Evans, Michelle L Halls, Martina Kocan, Masaaki Sato, Roger J Summers and Dana S Hutchinson. *Role of cAMP in BRL37344 and isoprenaline-mediated glucose uptake by β_2-adrenoceptors*. Poster presentation. 2015. Victorian Obesity Consortium (Melbourne, Australia).

- **<u>Saori Mukaida</u>**, Bronwyn A Evans, Michelle L Halls, Martina Kocan, Masaaki Sato, Roger J Summers and Dana S Hutchinson. *Role of cAMP in BRL37344 and isoprenaline-mediated glucose uptake by β_2-adrenoceptors. Poster presentation*. 2015. ASCEPT-MPGPCR Joint Scientific Meeting (Tasmania, Australia).

Acknowledgements

I would like to thank my supervisors, Dana, Bronwyn, Masa, Nick and Roger. Dana, thank you for accepting me having no background on biology but believing in my motivation and enthusiasm in this field of science. Dana, Bronwyn and Nick were also very patient and corrected my writing/slides over and over again. They gave me a great opportunity to learn academic writing. Bronwyn, your smile and advice always encouraged me to work more. Masa, thank you for showing me all your techniques in the lab and training me to become a researcher. You also listened to me whenever I was upset like a real brother. Thanks to Nick, for letting me work at relaxed and friendly environment. Roger, thank you for giving a warm welcome to be a member of your group. I was very honoured that I could work with you. Thank you to my rotation supervisors, Ann, Michelle and Martina for showing me new techniques including molecular biology, FRET and BRET. Thanks to Steven Charlton and David for using their facility and showing me TR-FRET, and also Jill for giving me a great advice for bindings. Thanks to my panels, Karen, Meri, Srgjan and Glenn for giving me suggestions and good ideas toward the goals of my study. Thanks to Jon, Linzi, Edilson and Ling for being great senpai! So, I appreciate all of you for directing me. I could not make this achievement without your continuous support.

Also, I cannot forget about my industry placement. Benjamin, Tore and Nodi helped me to survive in Stockholm and I had a great experience working at Atrogi thanks to them. Jessica, Calina, Anna, Robert and Anastasia were such lovely colleagues and I loved to have lunch and some teas between experiments.

During this 4 years, I had amazing friends who stood by my side through the good and tough times. I always hung out with Sheng and Mei Fern. They listened to me whenever I was overwhelmed and cooked gorgeous dishes. Kathy and Quynh cared so much about me even after they left Melbourne, and made it much easier for me to have a new life in Nottingham. Ee Von asked me to join lots of fun activities and I had countless lovely memories thanks to her. Alastair, thank you for letting me stay at your apartment and often offering me help before I asked. Thanks to Marleen and her family for treating me like a real family member. I loved travelling with my Brazilians friends, Liciane, Andrea, Juliana and Stefania, and having so many gatherings with them plus Vivi, Dani O, Dani G and Diana. Obrigado! Thanks to Maxine, Laura K, Mark, Carl, Pradeep, Chris DJ, Liz, Sai Fei, Yue, Lih En, Arisbel, Eunice, Emma, Anna, Adrian for being good friends. I love all of you!!

Abbreviations

2DG – 2-Deoxyglucose
AC – adenylyl cyclase
Alpha - amplified luminescent proximity homogeneous
AMPK – AMP-activated protein kinase
ANOVA – analysis of variance
AR – adrenoceptor
α-AR – α-Adrenoceptor
AS160 - Akt substrate of 160 kDa
att - site-specific attachment
ATP – adenosine triphosphate
b-cAMP – biotin cAMP
BCA - bicinchoninic acid
β-AR – β-Adrenoceptor
BF - bias factor
BRET – bioluminescence resonance energy transfer
BSA – bovine serum albumin
C - catalytic
Ca^{2+} – calcium
CAD - carbamoyl-phosphate synthetase
CaMKK – Calcium/Calmodulin-dependent protein kinase kinase
cAMP – cyclic adenosine monophosphate
CRISPR - clustered regularly interspaced short palindromic repeats
cDNA – complementary deoxyribonucleic acid
DNA – deoxyribonucleic acid
CHO – Chinese hamster ovary
DAG – diacylglycerol
DAPI – 4',6-Diamidino-2-Phenylindole dihydrochloride
ddH_2O - double distilled water
Deptor - DEP domain-containing mTOR interacting protein
DMEM – Dulbecco's modified Eagle's media
DMSO – dimethyl sulfoxide
DSS – dextran sulfate sodium
Dyn - dynamin
ECL – extracellular loop
EDTA - ethylenediaminetetraacetic acid
EPAC – exchange protein activated by cAMP
ER - endoplasmic reticulum
ETC – electron transport chain
FRET - fluorescence resonance energy transfer technology
ERK1/2 – extracellular signal regulated kinases 1 and 2
FCS - foetal calf serum
FBS – foetal bovine serum
FKBP12 - FK506-binding protein 12
FSK – forskolin
Gα – G alpha subunit
Gβγ – G beta-gamma complex

GLP-1 - glucagon-like peptide-1

GLUT – glucose transporter

GLUT4 - glucose transporter 4

GSVs - GLUT4 storage vesicles

G protein – guanine nucleotide-binding protein

GPCR – G protein-coupled receptor

GRK - G protein receptor kinase

GRK2 – G protein receptor kinase 2

GRK5 – G protein receptor kinase 5

H33342 - hoechst 33342

$[^3H]$-2DG – tritiated-2-Deoxyglucose

HEK – human embryonic kidney

HEPES – 4-(2-hydroxyethyl)-1-piperazineethanesulfonic acid

IBMX – 3-isobutyl-1-methylxanthine

ICL – intracellular loop

IP3 – inositol 1,4,5-trisphosphate

IR/IRS – insulin receptor/insulin receptor substrate

KO – knockout

LB - Luria-Bertani

LR – linear recombination

MEK – mitogen-activated protein kinase kinase

mLST8 - mammalian lethal with Sec13 protein

mRNA – messenger ribonucleic acid

mSIN1 - mammalian stress-activated protein kinase interacting protein

mTOR – mammalian target of rapamycin

mTORC1 – mammalian target of rapamycin complex 1

mTORC2 – mammalian target of rapamycin complex 2

NDRG1 - N-myc downstream regulated gene 1

NRVM - neonatal rat ventricular myocytes

PBS – phosphate-buffered Saline

PDK1 – phosphoinositide-dependent Kinase-1

PDZ - PSD95–Dlg–ZO1

PI3K – phosphatidylinositol-3 kinase

PIP2 – phosphatidylinositol 4,5-bisphosphate

PIP3 – phosphatidylinositol 3,4,5-triphosphate

PKA – protein kinase A

PKB – protein kinase B/AKT

PKC - protein kinase C

PLC – phospholipase C

Protor-1 - PRAS40 - proline rich Akt substrate 40 kDa

R - regulatory

RE - relative effectiveness

RFU - relative fluorescence units

RhoGEFs - RhoGTPase nucleotide exchange factors

Rluc – Renilla luciferase

RT – room temperature

S6K/S6RP – S6 kinase/S6 ribosomal protein

SDS – sodium dodecyl sulfate

S.e.mean – standard error of the mean
Ser/S - serine
SGLT - sodium-dependent glucose co-transporter
SOC - super optimal broth with catabolite repression
SR - sarcoplasmic reticulum
SREBP - sterol-regulatory-element-binding protein
SH2 – Src homology 2
SiRNA - small interfering RNA
SNX27 - sorting nexin 27
SNARE - soluble N-ethylmaleimide-sensitive factor attachment protein receptor
T2D – type 2 diabetes
TCA cycle - tricarboxylic acid cycle
TfR - transferrin receptor
TGN - Trans-Golgi network
Thr/T - threonine
TIRF - total internal reflection fluorescence
TM – transmembrane
TR - time-resolved measurement
UV - ultraviolet
WT – wild type

CHAPTER 1

General introduction

1.1 Glucose homeostasis

Glucose is a vital energy source, with the concentration in blood maintained within a range of 4.0 – 8.0 mmol/L (72–144 mg/dl) in the fasted state (Consoli et al., 1987; **Sprague & Arbelaez, 2011**)(**Bold** indicates a review paper). This occurs through the actions of several metabolic hormones including insulin, glucagon, and glucagon-like peptide 1 (GLP-1), acting at different organs and tissues including the gastrointestinal system, pancreas, brain, liver, adipose tissue, and skeletal muscle.

After a meal, nutrients from food are broken down in the gastrointestinal tract and appear in the blood in several forms, comprising sugars (including glucose), amino acids, fatty acids, and triacylglycerides. The β-cells of the pancreas sense the elevation in blood glucose levels, leading to the secretion of the anabolic hormone insulin. Insulin acts on several insulin-sensitive tissues in the body, to increase glucose uptake (Figure 1.1) (Satake et al., 2002; **Satoh, 2014**). Once glucose is taken up into tissues, it can be stored for later use either as glycogen (liver, skeletal muscle) or triacylglycerides (adipose tissue, liver). In the fasted state, when blood glucose concentrations are low, the α-cells of the pancreas secrete glucagon, the major counter-regulatory hormone to insulin, which acts exclusively on the liver to increase endogenous glucose output by promoting glycogenolysis and gluconeogenesis (**Bano, 2013**; Sprague & Arbelaez, 2011). As such, both insulin-dependent and insulin-independent processes are required to maintain normoglycaemia (**Roder et al., 2016**). Disruption of this finely balanced dynamic interaction of organs and hormones results in impaired glucose homeostasis, that can lead to the development of type 2 diabetes (T2D).

1.2 Type 2 diabetes

Diabetes is classed into two types: Type 1 that is strongly associated with genetic components, and is primarily the result of insufficient insulin production due to autoimmune destruction of pancreatic β-cells (**Bakay et al., 2013**), and Type 2 that is closely correlated with multiple factors such as sedentary lifestyle, physical inactivity, smoking, alcohol consumption, and obesity (**Wu et al., 2014**). The increased prevalence of T2D worldwide is a significant health concern. In 2012, the number of patients with T2D reached 371 million worldwide, and it is estimated that this figure will increase to 552 million by 2030. Furthermore, T2D has a huge impact on mortality, and accounts for 5% of all deaths in the world (**Lyssenko & Laakso, 2013**).
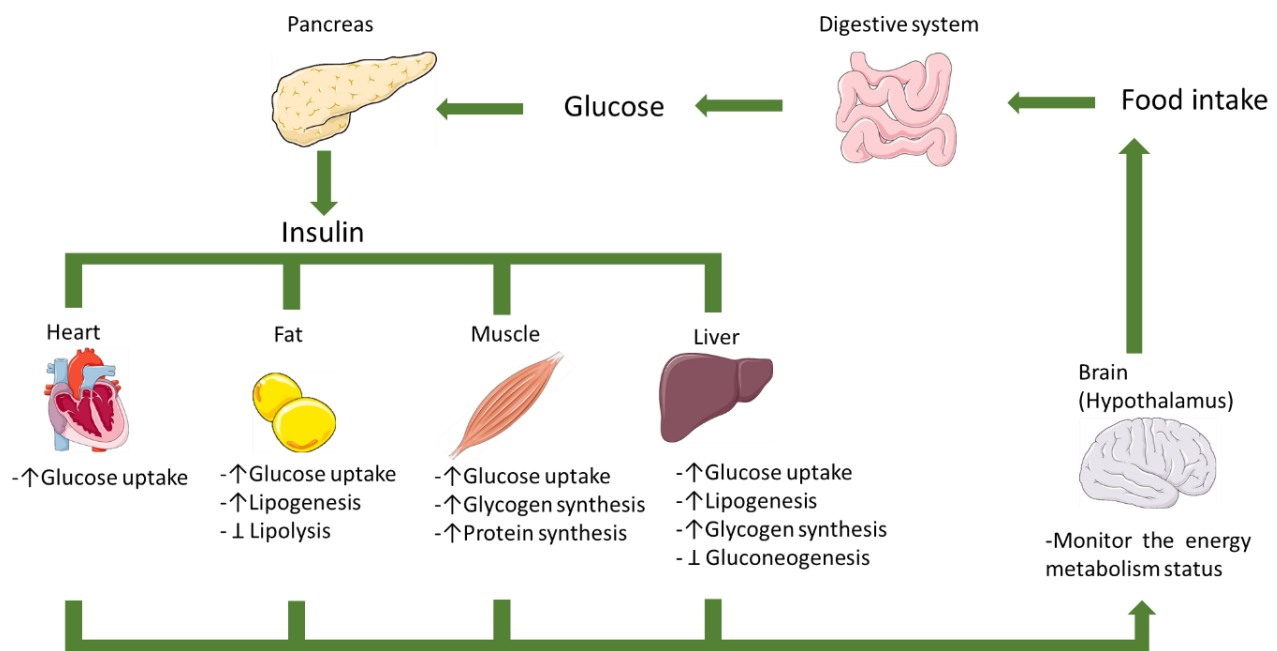
Figure 1.1: Regulation of glucose in the body

An elevated blood glucose level following a meal stimulates insulin secretion from the pancreas. Insulin in turn acts at many tissues and produces a variety of effects (**Dimitriadis et al., 2011**; **Lambadiari et al., 2015**; **Roh et al., 2016**). Images of tissues were obtained from www.servier.com.

The progression of T2D is summarised in Figure 1.2. Excessive and continual high blood glucose levels following a meal stimulates excess insulin production and release from the pancreas (hyperinsulinaemia). This leads to insulin insensitivity in peripheral tissues, including a reduction of insulin-stimulated glucose uptake in target tissues (**Abdul-Ghani, 2013**; **DeFronzo & Tripathy, 2009**). This is characteristic of the pre-diabetic state. In chronic hyperglycaemia, this leads to insulin deficiency, due to depletion of insulin stores from β-cells, leading to functional exhaustion, loss of β-cell mass, and finally β-cell death (**Chen et al., 2017**). Furthermore, diabetes increases the risk of developing long-term life threatening complications, such as cardiovascular disease, renal failure, retinopathy and neuropathy (**Kahn, 1994**; Turner et al., 1998).

The most common strategies for the treatment of T2D are lifestyle modifications aimed at reducing caloric/carbohydrate intake, and increasing energy expenditure through physical activity. However, compliance to diet modification is poor, and exercise is limiting for older people with limited mobility. Hence, there is a need for pharmacological management for diabetic patients. Currently available therapeutics for T2D work by (1) decreasing hepatic glucose production, (2) increasing insulin release/sensitivity, (3) decreasing glucagon release, (4) increasing incretin levels, and/or (5) increasing satiety (**Lee & Halter, 2017**). A brief overview of current medications in Australia is shown in Table 1.1 (**Chaudhury et al., 2017**; **Lee & Halter, 2017**; **Marin-Penalver et al., 2016**).

1.3 Glucose uptake into cells

Skeletal muscle is the major site of glucose utilization or uptake into the body, accounting for ~70% of glucose uptake in the fed state, and will be used as an example of how glucose transport occurs. Glucose uptake into skeletal muscle is comprised of 3 main processes: (1) glucose delivery, (2) glucose transport, and (3) glucose metabolism (Figure 1.3). Glucose delivery, which supplies glucose from the blood to the interstitium depends on several factors such as blood glucose levels and muscle blood flow (Wasserman et al., 2011). Glucose transport from the interstitium to the myocyte is determined by the content of glucose transporters (GLUTs) on the plasma membrane (see Section 1.4). Once glucose is taken up, it is phosphorylated to glucose 6-phosphate (G-6-P) via a non-reversible reaction (Wasserman et al., 2011), and can undergo several fates: it can enter the glycolysis pathway leading to its use in the tricarboxylic acid cycle (TCA cycle)/ electron transport chain (ETC) to result in the generation of ATP, or it can enter the glycogenesis pathway which results in synthesis of glycogen (**Richter & Hargreaves, 2013**).
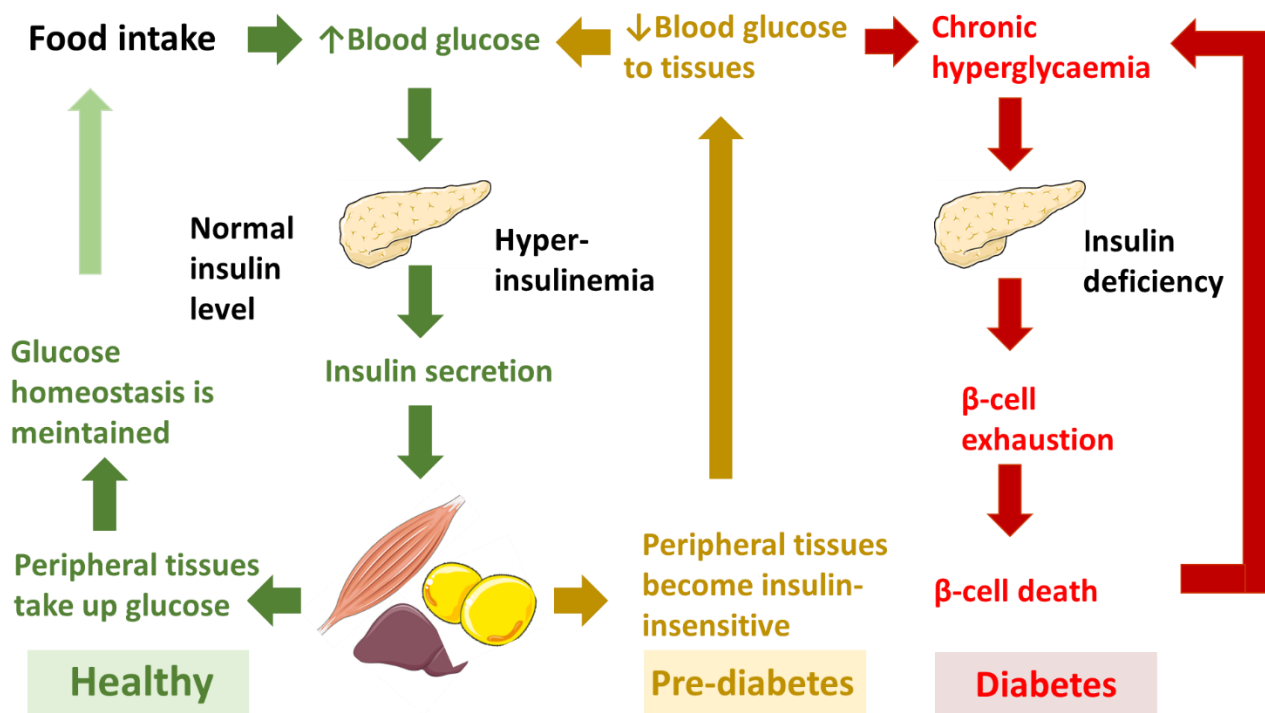
Figure 1.2: Progression of diabetes

The progression to prediabetes and diabetes is associated with insulin resistance in peripheral tissues, including decreased insulin-stimulated glucose uptake, which increases insulin demand on the pancreas. This pre-diabetic state is reversible if hyperglycaemia and insulin resistance is addressed through lifestyle or pharmacological interventions. However prolonged and chronic hyperglycaemia causes stress on pancreatic β-cells, resulting in the inability of the pancreas to produce enough insulin to meet demands, leading to eventual β-cell death. Images of tissues were obtained from www.servier.com.

Table 1.1: Current pharmacological treatments for type 2 diabetes in Australia (Chaudhury et al., 2017; Gunton et al., 2014; Lee & Halter, 2017; Marin-Penalver et al., 2016)

In general, metformin is the first-line therapy. If it is not tolerated, sulfonylureas are the second-line option. However, most patients progress to combination therapy with a number of agents, and a proportion require insulin at later stages of the disease (www.ndss.com.au; National Diabetes Services Scheme, viewed on 11th November 2018).

Class	Drug	Action	Adverse effects
Biguanide (Tablets)	Metformin	-↓glucose production in liver -↑insulin-stimulated glucose uptake in skeletal muscle	-Gastrointestinal effects -↓Vitamin B12 absorption
Thiazolidinediones (Tablets)	Rosiglitazone Pioglitazone	- PPARγ activator - ↑Insulin sensitivity	-Weight gain -Rosiglitazone; risk of cardiovascular diseases -Pioglitazone; risk of pancreatic cancers
α-Glucosidase Inhibitors (Tablets)	Acarbose Miglitol	-↓Intestinal carbohydrate Absorption	-Gastrointestinal effects
Sulfonylureas (Tablets)	Glipizide Glyburide Glimepiride Gliclazide	-Inhibit β-cell K_{ATP} channels -↑Insulin secretion	-Hypoglycaemia -Weight gain
Sodium glucose co-transporter 2 inhibitors (Tablets)	Canagliflozin Empagliflozin Dapagliflozin	-↓Glucose reabsorption in kidney -↑Urinary glucose excretion	-Urogenital tract infections
GLP-1 receptor agonists (Injection)	Exenatide Liraglutide Dulaglutide Albiglutide Lixisenatide	-↑Insulin secretion -↓Glucagon secretion -Slowing of gastric emptying -↑Satiety	-Gastrointestinal effects
Dipeptidyl peptidase-4 inhibitors (Tablets)	Sitagliptin Saxagliptin Vildagliptin Linagliptin Alogliptin	-↑Insulin secretion -↓Glucagon secretion	-Headache -Nasopharyngitis -Upper respiratory tract infection
Insulin (Injection)	Many different trade names: can be long and short acting or combined with other T2D medications	-Activation of insulin receptors and insulin-stimulated signalling (-↑Adipose and skeletal muscle glucose uptake) (-↓Liver glucose production)	-Risk of hypoglycaemia
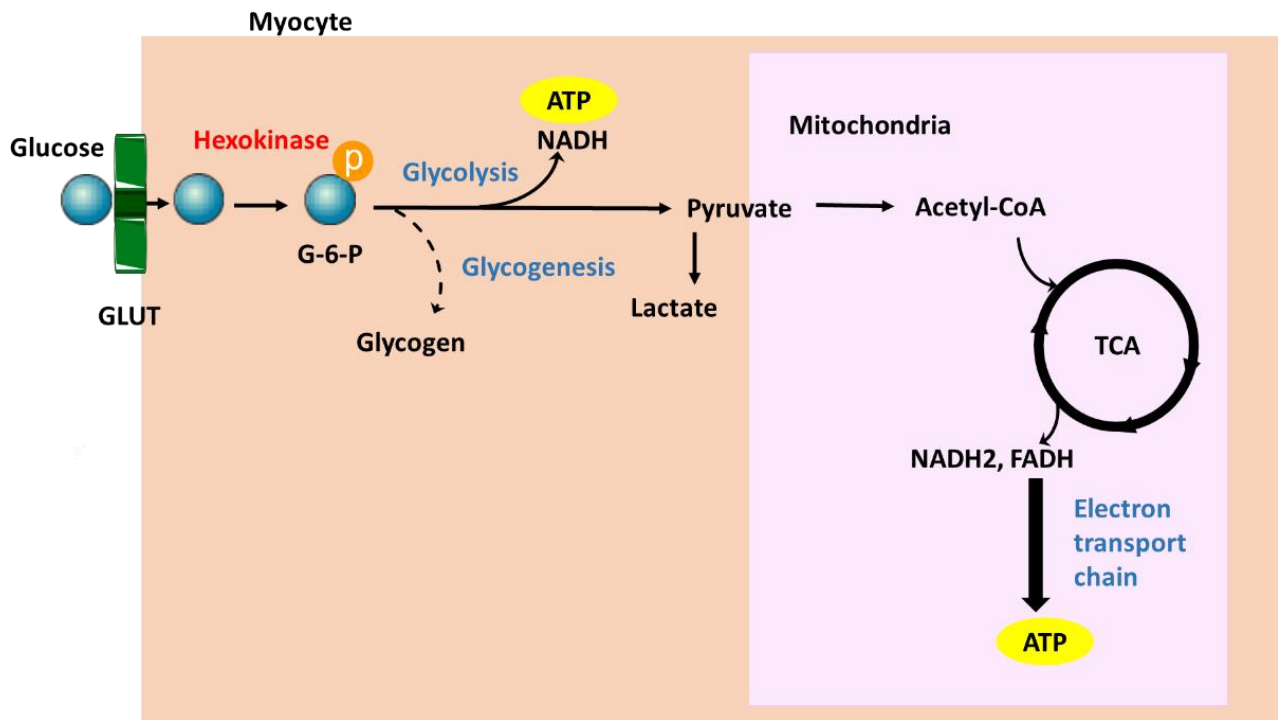
Figure 1.3: Glucose metabolism in the myocyte

In myocytes, glucose enters the cell via GLUTs, and is phosphorylated to G-6-P by hexokinase. It can then be used in two main pathways: for energy use in the glycolysis pathway/TCA cycle/electron transport chain or to be stored for later energy release by entering the glycogenesis pathway (**Doenst et al., 2013**; **Kolwicz & Tian, 2011**; **Nagoshi et al., 2011**). Figure was adapted from (**Richter & Hargreaves, 2013**).

Abbreviations; FADH - flavin adenine dinucleotide, G-6-P - glucose-6-phosphate, NADH - nicotinamide adenine dinucleotide, TCA - tricarboxylic acid cycle.

1.4 Glucose transporters

Glucose transporters (GLUTs) are key regulators of glucose homeostasis, and transport glucose (and other sugars depending on the GLUT isoform) into the cell. GLUTs are comprised of approximately 500 amino acid residues, and characterized by 12 membrane-spanning domains, a N-linked glycosylation site, and an intracellularly located amino and carboxyl terminus (**Mueckler & Thorens, 2013**).

To date, 14 GLUTs have been identified in mammals and they are divided into 3 classes as follows: Class I (GLUT1, GLUT2, GLUT3, GLUT4, and GLUT14), Class II (GLUT5, GLUT7, GLUT9, and GLUT11), and Class III (GLUT6, GLUT8, GLUT10, GLUT12, and GLUT13/ Proton myo-Inositol Transporter or H(+)-myo-inositol symporter, HMIT). These GLUTs are facilitative transporters (with the exception of HMIT), and transfer their substrates across cell membranes in a tissue specific manner (**Mueckler & Thorens, 2013**). They have different substrate specificity, regulatory and kinetic properties, which defines their specific roles in the regulation of glucose uptake as summarised in Table 1.2.

In human skeletal muscle, GLUT4, GLUT5 and GLUT12 mRNA/protein are highly expressed (Stuart et al., 2006), with much lower levels of GLUT1 mRNA/protein. Expression levels of these GLUT isoforms are different depending on the muscle fibre, with GLUT4 and GLUT12 predominantly expressed in type I fibres, whereas GLUT5 is predominately expressed in type II fibres (Stuart et al., 2006). In addition, GLUT4 and GLUT1 are the predominant GLUT isoforms expressed in cardiac muscle (Fischer et al., 1997). Their mRNA/protein expression level is highly regulated during development: GLUT1 is abundant in foetal myocardium but is down-regulated with ageing, whereas GLUT4 is up-regulated with ageing and becomes the primary GLUT isoform in adult cardiomyocytes (Depre et al., 1999). Other GLUT and sodium-dependent glucose co-transporter (SGLT) isoforms (GLUT3, GLUT8, GLUT10, GLUT11, GLUT12 and SGLT1 genes) are detected in the heart but are expressed at much lower levels (Szablewski, 2017).

Table 1.2: GLUT transporter family

Data compiled from (Aerni-Flessner et al., 2012; **Cheeseman, 2008**; Doege et al., 2000; Doege et al., 2001; **Douard & Ferraris, 2008**; McVie-Wylie et al., 2001; **Navale & Paranjape, 2016**; Rogers et al., 2002; **Simpson et al., 2008**; **Thorens, 1992**; **Thorens & Mueckler, 2010**; Uldry et al., 2001).

Class	GLUT isoform	Location	Substrates	Function
Class I	GLUT1	Many tissues including erythrocytes, blood-tissue barriers, muscle and fat	Glucose	Basal glucose uptake
	GLUT2	Liver, pancreatic β-cell, kidney proximal tubule and small intestine	Glucose, fructose, galactose, mannose, glucosamine	Low-affinity glucose/fructose transporter
	GLUT3	Brain	Glucose	High-affinity glucose transporter
	GLUT4	Muscle, heart and fat	Glucose	Insulin-responsive glucose transporter
	GLUT14	Testis	Unknown	Orphan transporter
Class II	GLUT5	Intestine, and low in kidney, skeletal muscle and fat	Fructose	Fructose transporter
	GLUT7	Small intestine, colon	Glucose, fructose	High-affinity glucose/fructose transporter
	GLUT9	Liver and kidney	Glucose, fructose urate	High capacity urate transporter
	GLUT11	Heart and muscle	Glucose, fructose	Glucose/fructose transporter
Class III	GLUT6	Brain, spleen and leukocytes	Glucose	Low affinity glucose transporter
	GLUT8	Testis	Glucose	High-affinity glucose transporter
	GLUT10	Liver and pancreas, and low in heart, skeletal muscle, placenta, kidney, lung, brain and liver	Glucose	High affinity glucose transporter
	GLUT12	Muscle, small intestine, prostate and heart	Glucose	Glucose transporter
	GLUT13 (HMIT)	Brain	Myo-inositol	H+/myo-inositol co-transporter

1.4.1 GLUT4

GLUT4, encoded by the Slc2a4 gene, was first identified by a monoclonal antibody screen in rat adipocytes, and was found to be translocated from the cytosol to the plasma membrane in response to insulin stimulation (James et al., 1988). It is the major GLUT isoform in adipose tissue, skeletal and cardiac muscle, (Charron et al., 1999; Guillet-Deniau et al., 1994; Mueckler & Thorens, 2013). When skeletal muscle is stimulated with insulin, it promotes a rapid increase in GLUT4 abundance at the plasma membrane from intracellular storage vesicles (Section 1.4.2). The important role of GLUT4 in glucose uptake has been demonstrated by numerous studies using transgenic and knockout mouse models, suggesting that disruption of GLUT4 regulation/function is associated with T2D (**Wallberg-Henriksson & Zierath, 2001**). Transgenic mice carrying muscle and fat specific overexpression (approximately 10-fold) of GLUT4 levels showed a marked reduction of plasma glucose and insulin levels under both fasted and fed conditions (Liu et al., 1993), and mice overexpressing GLUT4 in muscle showed enhanced basal- and insulin-stimulated whole-body glucose uptake (Buse et al., 1996; Ren et al., 1995). Moreover, a study in GLUT4 knockout mice demonstrated reduced basal- and insulin-stimulated glucose uptake and glycogen synthesis in isolated Extensor digitorum longus (EDL) muscles (Stenbit et al., 1996), and elevated serum glucose and insulin levels compared to control mice, (Stenbit et al., 1997). In addition, diabetic db/db mice carrying overexpression of muscle GLUT4 showed significantly increased GLUT4 translocation to the cell surface following insulin stimulation compared to control db/db mice (Gibbs et al., 1995).

1.4.2 GLUT4 trafficking

GLUT4 is a long lived protein which continuously moves between the plasma membrane and intracellular compartments (Martin et al., 2006; Satoh et al., 1993). In unstimulated adipocytes, for example, the half-life of GLUT4 is 50 h (Sargeant & Paquet, 1993). In muscle, the level of GLUT4 stays high at plasma membrane for 24 h following acute exercise, and it returns to basal levels 48 h after the last set of exercise (Reynolds et al., 2000). The majority of studies investigating GLUT4 trafficking were performed in three cellular systems: primary rat adipocytes, 3T3-L1 mouse adipocytes, and rat L6 skeletal muscle cells (**Foley et al., 2011**). Under basal conditions, the majority of GLUT4 (>90%) is stored in intracellular vesicles. Following insulin treatment, GLUT4 is rapidly transported to the plasma membrane, leading to an increase in glucose uptake (Yang & Holman, 1993). Upon removal of insulin, GLUT4 at the plasma membrane is internalised to intracellular compartments, and packed for storage (Livingstone et al., 1996). As such, it has been suggested that a single GLUT4 molecule

repeats this cycle (exocytosis and endocytosis) multiple times during the course of its lifetime, as described below.

GLUT4 exocytosis (also called GLUT4 translocation) is the combination of several distinct processes: vesicle mobilization, vesicle tethering, vesicle docking, and membrane fusion (Figure 1.4). High resolution imaging techniques such as confocal and immunofluorescence microscopy have captured the movement of GLUT4 vesicles along the cytoskeletal tracks to the cell surface (Fletcher et al., 2000; Patki et al., 2001; Semiz et al., 2003). Disruption of actin and/or microtubules leads to reduced GLUT4 translocation in response to insulin (Fletcher et al., 2000; Huang et al., 2005b; Omata et al., 2000; Patki et al., 2001; Wang et al., 1998). Vesicle tethering is regulated by a number of small GTPase Rab-family proteins and actin (Babbey et al., 2010; Lopez et al., 2009; **Zerial & McBride, 2001**). Vesicle docking and membrane fusion are associated with the actions of soluble N-ethylmaleimide-sensitive factor attachment protein receptor (SNARE) and SNARE associated proteins (Cheatham et al., 1996; D'Andrea-Merrins et al., 2007). Glucose uptake into tissues is initiated once GLUT4 appears and is integrated at the cell surface (Figure 1.4).

The internalisation of GLUT4 is mediated via clathrin-mediated endocytosis and/or cholesterol-dependent endocytosis (Figure 1.4). In muscle cells, clathrin-mediated endocytosis is the predominant mechanism for GLUT4 internalisation, whereas in adipocytes, GLUT4 is internalised by both clathrin-mediated and cholesterol dependent endocytosis (Ros-Baro et al., 2001; Shigematsu et al., 2003). When internalised through clathrin-mediated endocytosis, the adaptor protein AP2 binds to a N-terminal portion of GLUT4 and packs GLUT4 into endocytic vesicles (Al-Hasani et al., 2002; Blot & McGraw, 2006). Cholesterol dependent endocytosis, on the other hand, is due to caveolin, which forms large cave-like structures through oligomerization in lipid rafts (Ros-Baro et al., 2001). Membrane rafts, or lipid rafts, are lipid domains that are enriched in cholesterol and sphingolipids (**Munro, 2003**). For both pathways, the GTPase dynamin seems to be required for the vesicle scission from the plasma membrane (Kao et al., 1998; Mettlen et al., 2009). Once the vesicles are formed, they move to the interior of the cells (Guilherme et al., 2000).
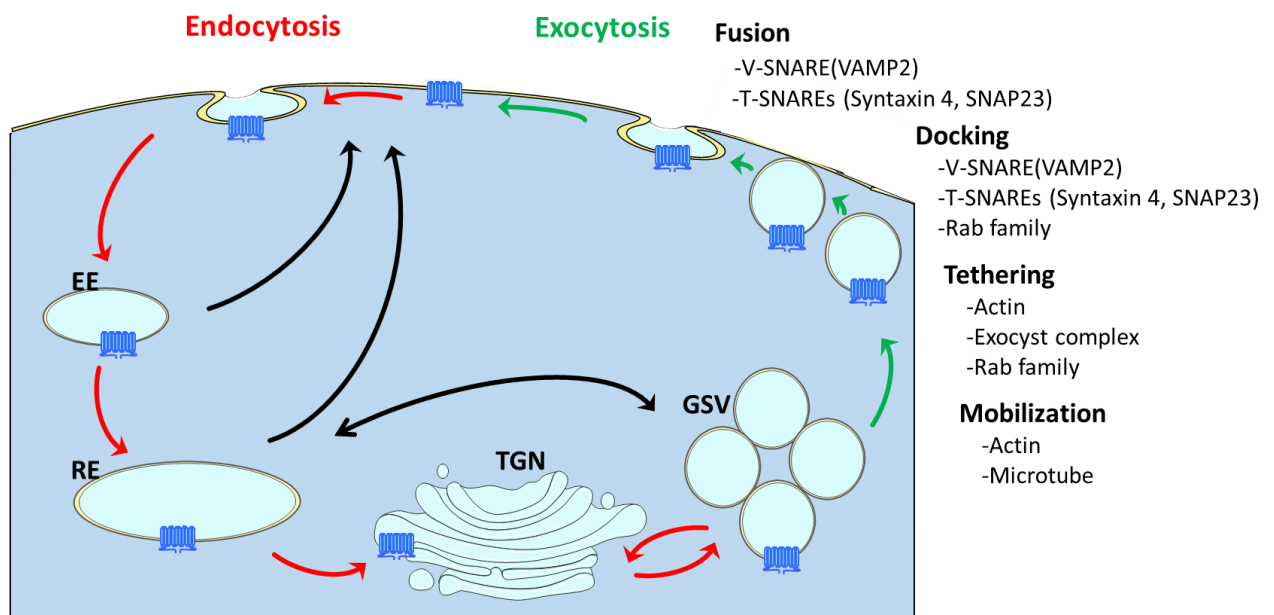
Figure 1.4: Exocytosis and endocytosis of GLUT4

Upon stimulation, GLUT4 localised in the GSV is translocated to the plasma membrane via vesicle tethering, docking and membrane fusion. In the absence of stimuli, GLUT4 is internalised to several different cytosolic compartments including (1) EE - early endosomes, (2) RE - recycling endosomes, (3) TGN - trans Golgi network and (4) GSV - GLUT4 storage vesicle (**Foley et al., 2011; Stockli et al., 2011**). TGN image was obtained from www.servier.com.

Abbreviations: SNARE - soluble N-ethylmaleimide-sensitive factor attachment protein receptor, V-SNARE – vesicle SNARE, T-SNARE – target localised SNARE, VAMP2 - vesicle-associated Membrane Protein-2, SNAP23 - synaptosomal-associated protein-23.

The use of total internal reflection fluorescence (TIRF) microscopy, electron microscopy and immunofluorescent assays showed that GLUT4 is localized to early endosomes, recycling endosomes, the Trans-Golgi network (TGN) and GLUT4 storage vesicles (GSVs) (**Foley et al., 2011**; Fujita et al., 2010; Ishiki et al., 2005; Smith et al., 1991). There are several different routes that GLUT4 can travel and return to the plasma membrane. Fast recycling back to the plasma membrane is carried out through early endosomes, whereas slow recycling happens when GLUT4 passes through early endosome en route to recycling endosomes marked by the transferrin receptor (TfR), after which GLUT4 is sorted back to the plasma membrane. GLUT4 can also be packed into GSVs, which are formed from recycling endosomes and/or TGN. GSVs represent lipid bilayer bound structures that have a capacity to pack about 25 GLUT4 molecules. When GLUT4 reaches the end of its lifespan, it is degraded by the ubiquitin-proteasome system or by lysosomes (Liu et al., 2007).

1.5 Signalling mechanisms involved in muscle glucose uptake

Muscle glucose uptake is mediated by at least two separate actions: (i) stimulation with insulin/insulin mimicking agents, and (ii) muscle contraction/exercise.

1.5.1 Insulin signal transduction leading to increased glucose uptake

The insulin receptor (IR) is a tyrosine kinase receptor, composed of two α-subunits and two β-subunits, and is distributed in a variety of tissues/cells including the brain, liver, skeletal muscle, adipose tissue, spleen and leukocytes (**Boucher et al., 2014**; Desbuquois et al., 1993).

Insulin signal transduction is initiated by insulin binding to the extracellular α-subunits of the receptor, which leads to a change in its conformation that brings the two α-subunits closer, resulting in rapid autophosphorylation of tyrosine residues on the β-subunits (Kasuga et al., 1982; Wilden et al., 1992). The activated receptor, in turn, stimulates multiple tyrosine phosphorylation of the insulin receptor substrate family (IRS 1 to 4) and proto-oncogene Cbl (Bjornholm & Zierath, 2005; Fantin et al., 2000; Huang et al., 2005a; Laustsen et al., 2002; Ribon & Saltiel, 1997). When these substrates are phosphorylated, they bind adapter molecules which contain Src homology 2 (SH2) domains (important for the interaction with the phosphorylated receptor) and activate many downstream effectors. The pathway linking IRS to the activation of phosphoinositide 3-kinase (PI3K) is common to skeletal muscle and other insulin target tissues. In adipocytes, a Cbl dependent pathway is also able to increase glucose uptake (Satoh, 2014), and will not be further discussed here.

PI3K is divided into three classes (I, II, III), and class I is subdivided into class IA and class IB based on their activation mechanisms. Class IA PI3Ks are heterodimeric lipid kinases composed of a p85 regulatory subunit and a p110 catalytic subunit, and studies using inhibitors and dominant negative constructs have shown that class IA PI3Ks have a central role in stimulating insulin-stimulated glucose transport, and glycogen synthesis (Hiles et al., 1992; Utermark et al., 2012). Pharmacological inhibition of PI3K by wortmannin dramatically blocks insulin-stimulated glucose uptake in both isolated rat skeletal muscle and adipocytes (Okada et al., 1994; Yeh et al., 1995), and another PI3K inhibitor (LY294002) inhibits both insulin-stimulated GLUT4 translocation and glucose uptake in L6 cells (Somwar et al., 2001). In addition, mice lacking class IA PI3Ks in skeletal muscle develop not only muscle insulin resistance, but also whole-body glucose intolerance (Luo et al., 2006).

Akt (also called protein kinase B) is a serine/threonine kinase, and phosphorylation at both Thr308 (phosphorylated by PDK1) and Ser473 (phosphorylated by mammalian target of rapamycin complex 2, mTORC2) is required for its full activation (Tsuchiya et al., 2014). In mammals, three homologous isoforms (Akt1/PKBα, Akt2/PKBβ, and Akt3/PKBγ) were identified (Bellacosa et al., 1993; Jones et al., 1991). Of all, Akt2 is the most abundant Akt isoform in insulin sensitive tissues (liver, skeletal muscle and adipose), and is most likely responsible for glucose metabolism. 3T3-L1 adipocytes transfected with Akt2 siRNA showed reduced insulin responsiveness (Jiang et al., 2003), and Akt2 knockout mice showed reduced glucose transport in muscle, and developed hyperglycaemia and diabetes (Cho et al., 2001; Garofalo et al., 2003). The PI3K and Akt dependent glucose uptake pathway is shown in Figure 1.5.

Patients with T2D have defects in the ability of insulin to activate intracellular components such as IRS-1 and Akt, rather than defects in the IR itself (Boucher et al., 2014; George et al., 2004; Hribal et al., 2008). Dysfunction of these proteins significantly reduces the activity of insulin-stimulated GLUT4 translocation/glucose uptake in muscle although it does not affect transcriptional and translational regulation of GLUT4 (Widen et al., 1992).
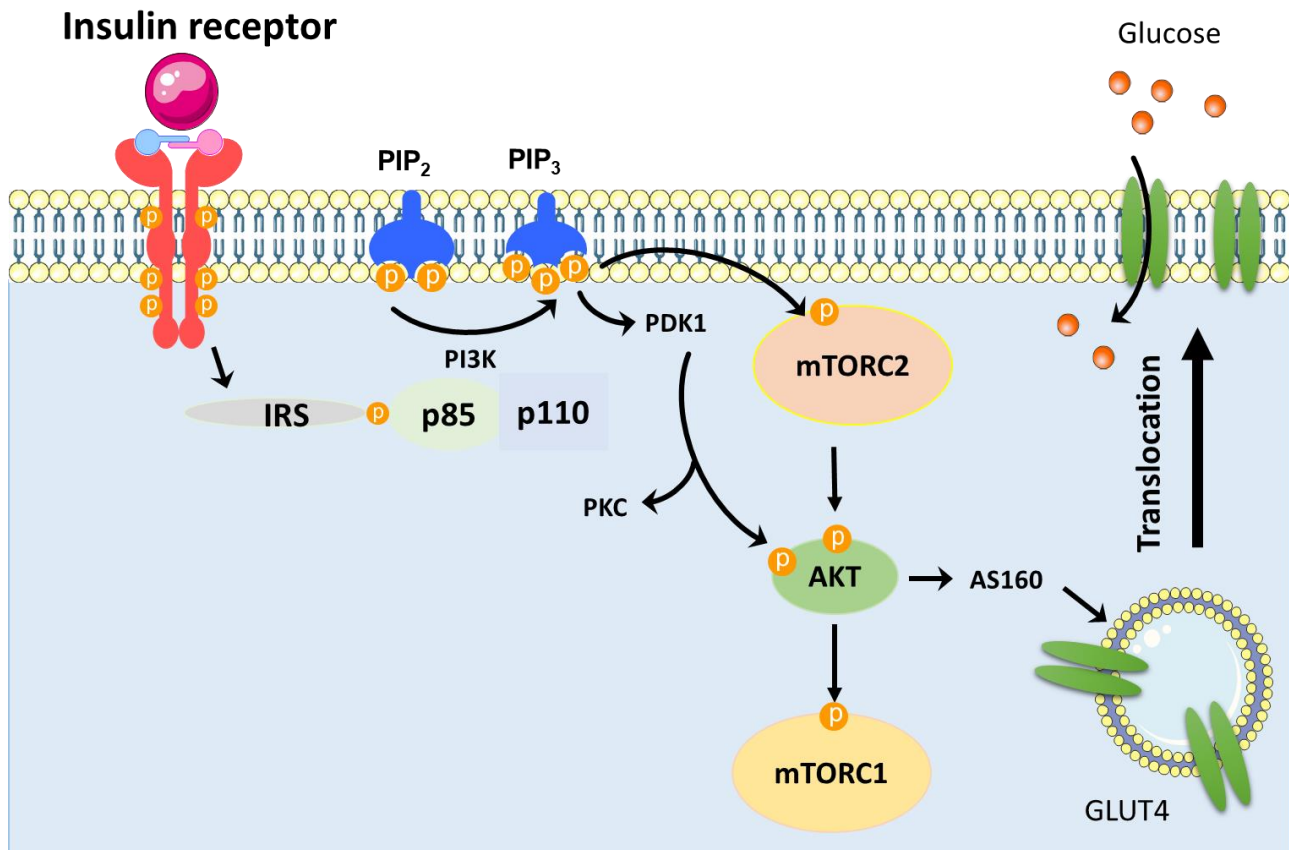
Figure 1.5: Insulin-stimulated glucose uptake pathway

Upon stimulation, insulin binds to the insulin receptor, which causes phosphorylation of IRS. Class IA PI3Ks are recruited to the plasma membrane, and their activation by IRS phosphorylates the membrane PIP2, and generates the lipid second messenger PIP3 (**Avogaro et al., 2010; Saltiel & Kahn, 2001**; **Sesti, 2006**; **Thorpe et al., 2015**). Increased PIP3 then recruits PDK1 to the plasma membrane, leading to the phosphorylation of Akt and subsequently activation of the atypical PKC isoforms PKCζ and PKCλ (**Avogaro et al., 2010; Bevan, 2001; Zierath & Wallberg-Henriksson, 2002**). PIP3 also promotes mTORC2 activity (Glidden et al., 2012; Liu et al., 2015). Activation of Akt by PDK1 and mTORC2 leads to phosphorylation of AS160, leading to GLUT4 translocation to plasma membrane, which in turn increases glucose uptake (Bjornholm & Zierath, 2005**; Ramalingam et al., 2013**). Images of insulin receptor, PIP$_2$, PIP$_3$, lipid membrane and glucose molecule, were obtained from www.servier.com.

Abbreviations: AS160 - Akt substrate of 160 kDa, IRS - insulin receptor substrates, mTORC2 - mammalian target of rapamycin complex 2, PDK1 - phosphoinositide-dependent Kinase-1, PI3K - phosphoinositide 3-kinase, PIP2 - phosphatidylinositol 4,5-bisphosphate, PIP3 - phosphatidylinositol 3,4,5-triphosphate, PKC – protein kinase C.

Mammalian target of rapamycin (mTOR) is another signalling molecule involved in insulin-stimulated glucose uptake. mTOR is a 289-kDa serine-threonine kinase in the family of PI3K related kinases. There are 2 different complexes, mTORC1 and mTORC2, which have different structures and functions (**Laplante & Sabatini, 2009**) (Figure 1.6).

mTORC1 is composed of 5 different subunits: mTOR, Raptor, the proline rich Akt substrate 40 kDa (PRAS40), the DEP domain-containing mTOR interacting protein (Deptor), and the mammalian lethal with Sec13 protein 8 (mLST8). It is sensitive to inhibition by rapamycin, as the mTOR kinase activity is inhibited by an FK506-binding protein 12 (FKBP12)-rapamycin complex (Choi et al., 1996; **Weichhart et al., 2015**). Activation of mTORC1 is elicited by a range of stimuli including growth factors/insulin, nutrients (amino acids), oxygen and a high ATP/AMP ratio (Arsham et al., 2003; Hahn-Windgassen et al., 2005; Suryawan & Davis, 2010). Several intracellular signalling molecules such as Akt and Erk are also likely to activate mTORC1 (Carriere et al., 2011; Dan et al., 2014). Following activation, mTORC1 stimulates several downstream effectors such as ribosomal protein S6 kinase (S6K)/ S6 ribosomal protein (S6RP), and promotes cell growth by promoting synthesis of proteins, lipids and nucleotides. Protein is synthesized by cap-dependent translation and ribosome biogenesis through the activation of S6K and the phosphorylation-mediated inhibition of the eukaryotic initiation factor 4E-binding protein 1 (4EBP1) (Fingar et al., 2002). Lipid synthesis is increased due to activation of both sterol-regulatory-element-binding protein (SREBP) and S6K (Porstmann et al., 2008; Wang et al., 2011), while nucleotide synthesis is up-regulated due to the phosphorylation of carbamoyl-phosphate synthetase (CAD) by S6K (Robitaille et al., 2013). In addition, some studies indicate that mTOR/S6K1 over-activation causes elevation of IRS-1 phosphorylation, which blunts PI3K/Akt signalling, leading to alterations in glucose metabolism (Khamzina et al., 2005; Um et al., 2004).

mTORC2 is also composed of mTOR, mLST8, and Deptor but differs from mTORC1 in that it contains rictor that associates with the mammalian stress-activated protein kinase interacting protein (mSIN1) and protein observed with Rictor-1 (Protor-1)(Pearce et al., 2007; Peterson et al., 2009). In contrast to mTORC1, mTORC2 is rapamycin insensitive. However, it has been reported that long-term treatment with rapamycin in some cell types prevents mTORC2 assembly (Ballou & Lin, 2008; Sarbassov et al., 2006).
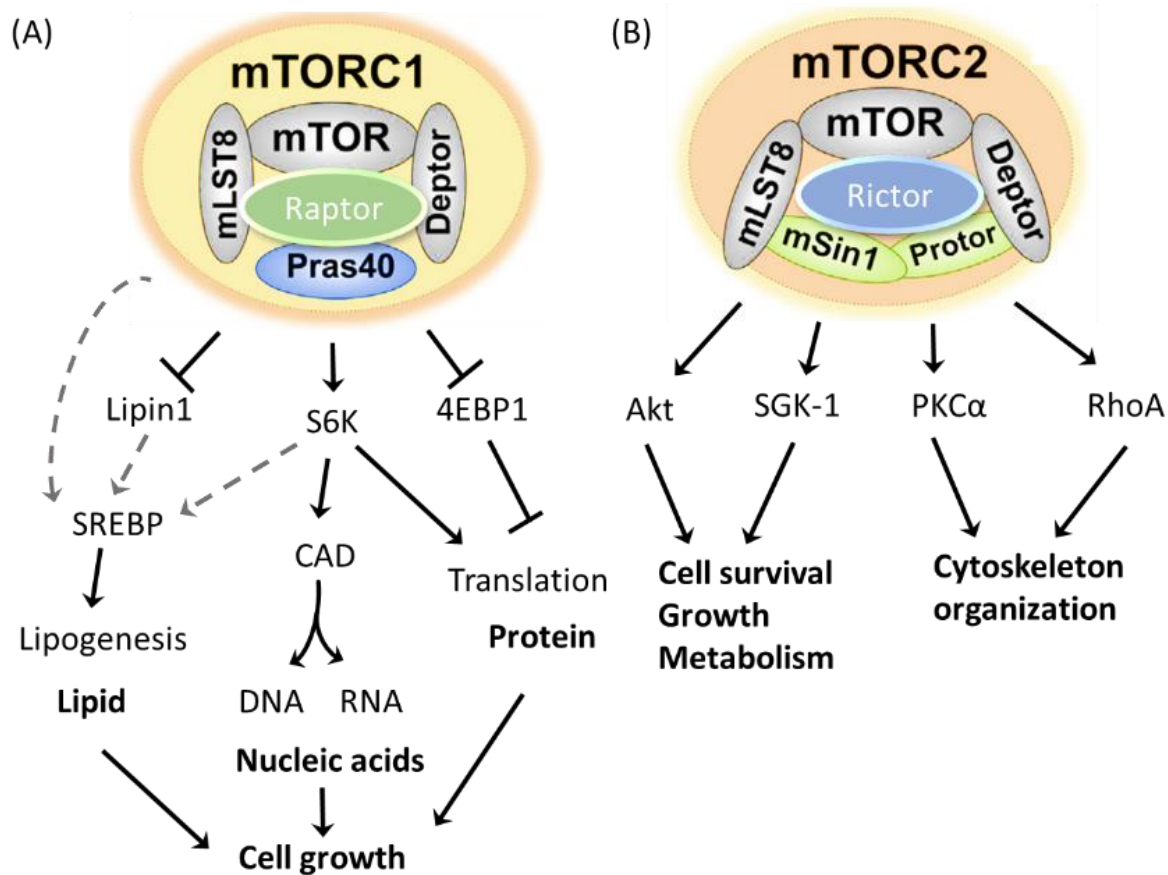
Figure 1.6: mTORC1 and mTORC2

(A) mTORC1 is composed of 5 different subunits including mTOR, Raptor, PRAS40, Deptor, and mLST8. It is involved in cellular growth by promoting lipid synthesis, nucleic acid synthesis and protein synthesis. (B) mTORC2 is composed of 6 different subunits including mTOR, Rictor, mLST8, and Deptor, mSin1 and Protor. It is involved in cell survival, metabolism and cytoskeletal reorganization. Figure was adapted from (Howell et al., 2013; **Huang & Fingar, 2014**).

Abbreviations: 4EBP1 - 4E-binding protein 1, CAD - carbamoyl-phosphate synthetase, RhoA - Ras homolog gene family member A, S6K - S6 kinase, SGK-1 - serum/glucocorticoid regulated kinase-1, SREBP - sterol-regulatory-element-binding protein, PKCα – protein kinase C α.

Compared to mTORC1, the role of mTORC2 is poorly understood. mTORC2 can be activated by growth factors/insulin like mTORC1, but it is not activated by nutrient deprivation (Laplante & Sabatini, 2012). mTORC2 activates its downstream targets, PKCα, RhoA that is important for the organization of the actin cytoskeleton (Jacinto et al., 2004), and Akt and SGK-1 that promote cell survival (Aoyama et al., 2005). As shown in Figure 1.5, insulin stimulation causes mTORC2 activation, which then phosphorylates Akt. The importance of mTORC2 in glucose metabolism has been demonstrated. Insulin failed to phosphorylate Akt at Ser473 and AS160 at Thr642 in skeletal muscle of mice lacking rictor, and these mice showed a 50% reduction of glucose uptake following insulin stimulation compared to wild type mice, and developed glucose intolerance (Kumar et al., 2008). In addition, fat cell-specific rictor knockout mice showed 65% reduction of insulin-stimulated glucose uptake compared to wild type mice (Kumar et al., 2010).

1.5.2 Mechanisms of muscle contraction/exercise stimulated glucose uptake

Muscle contraction or exercise is a physiologically relevant stimulus for increased glucose uptake, and intense exercise is able to increase skeletal muscle glucose uptake as much 50-fold (Katz et al., 1986). The mechanisms by which exercise increases glucose uptake are dependent on the action of GLUT4, and also involve calcium (Ca^{2+}) as a key molecule (Merry & McConell, 2009; Richter & Hargreaves, 2013).

For many years, it was believed that Ca^{2+} released from the sarcoplasmic reticulum (SR) by depolarization of muscle due to contraction, directly stimulated GLUT4 translocation from intracellular vesicles to the cell membrane, thereby increasing glucose uptake. This was based on several studies showing that caffeine treatment (which stimulates Ca^{2+} release from the SR) increased glucose uptake in skeletal muscle (Holloszy & Narahara, 1967; Wright et al., 2005). Ca^{2+} has a significant role in both skeletal and cardiac muscle contraction as follows: (1) muscle depolarization through neuronal stimuli activates L-type Ca^{2+} channels, (2) Ca^{2+} influx into the cells promotes a further increase in cytosolic Ca^{2+} by opening of SR ryanodine receptors, and (3) it subsequently initiates a myosin-actin "cross-bridge muscle cycle", provoking muscle contraction (**Kuo & Ehrlich, 2015**). However, later studies demonstrated that muscle contraction-mediated glucose uptake requires AMP-activated protein kinase (AMPK) since stimulation with caffeine increased AMPK activation both in rat and mouse skeletal muscle (Egawa et al., 2011; Jensen et al.,

2007), and in mouse soleus muscle overexpressing a dominant negative AMPK, the effect of caffeine on glucose uptake was significantly diminished (Jensen et al., 2007).

AMPK is a serine/threonine protein kinase essential for the regulation of energy balance. It is a heterotrimeric protein consisting of one catalytic subunit (α-subunit) and two regulatory subunits (β- and γ-subunits). In mammals, there are 12 isoforms of AMPK present due to the combination of 2 α-subunit isoforms (α1 and α2), 2 β-subunit isoforms (β1 and β2) and 3 γ-isoforms (γ1, γ2 and γ3) (Iseli et al., 2005). All isoforms are differently distributed in tissues, with the α2-subunit expressed predominantly in skeletal and cardiac muscle (Salt et al., 1998). The α-subunit contains a Thr-172 phosphorylation site vital for the Ca^{2+} dependent activation of AMPK, and Ser485/491 phosphorylation sites that limit AMPK activation (Valentine et al., 2014). The β-subunit contains a glycogen-binding domain, which allows AMPK to associate with glycogen (McBride et al., 2009). The γ-subunit contains 3 AMP-binding sites, two of which can bind either AMP or ATP, but a third site is tightly occupied with AMP. In the inactive state, AMPK binds two ATP and one AMP, while in active states three AMP are bound to these sites (Xiao et al., 2007). AMPK can also be activated by two identified upstream kinases: CAMKKβ and LKB1, of which CAMKKβ is activated by Ca^{2+} (Gormand et al., 2011).

AMPK activity is increased in skeletal muscle during exercise/contraction, and can also be activated by hormones (e.g. leptin, ghrelin, adiponectin), as well as a change in AMP/ATP ratio due to metabolic stress. AMPK activation promotes catabolic processes to replenish ATP by inhibiting anabolic processes (**Hutchinson et al., 2008**). There are some studies in transgenic mouse models indicating a pivotal role of AMPK in glucose uptake: Muscle specific dominant-negative kinase-dead α2 AMPK overexpressing mice showed reduced contraction- stimulated glucose uptake compared with wild type mice (Lefort et al., 2008; Mu et al., 2001; Sylow et al., 2017b). The proposed mechanism of contraction-stimulated glucose uptake in muscle is summarised in Figure 1.7.
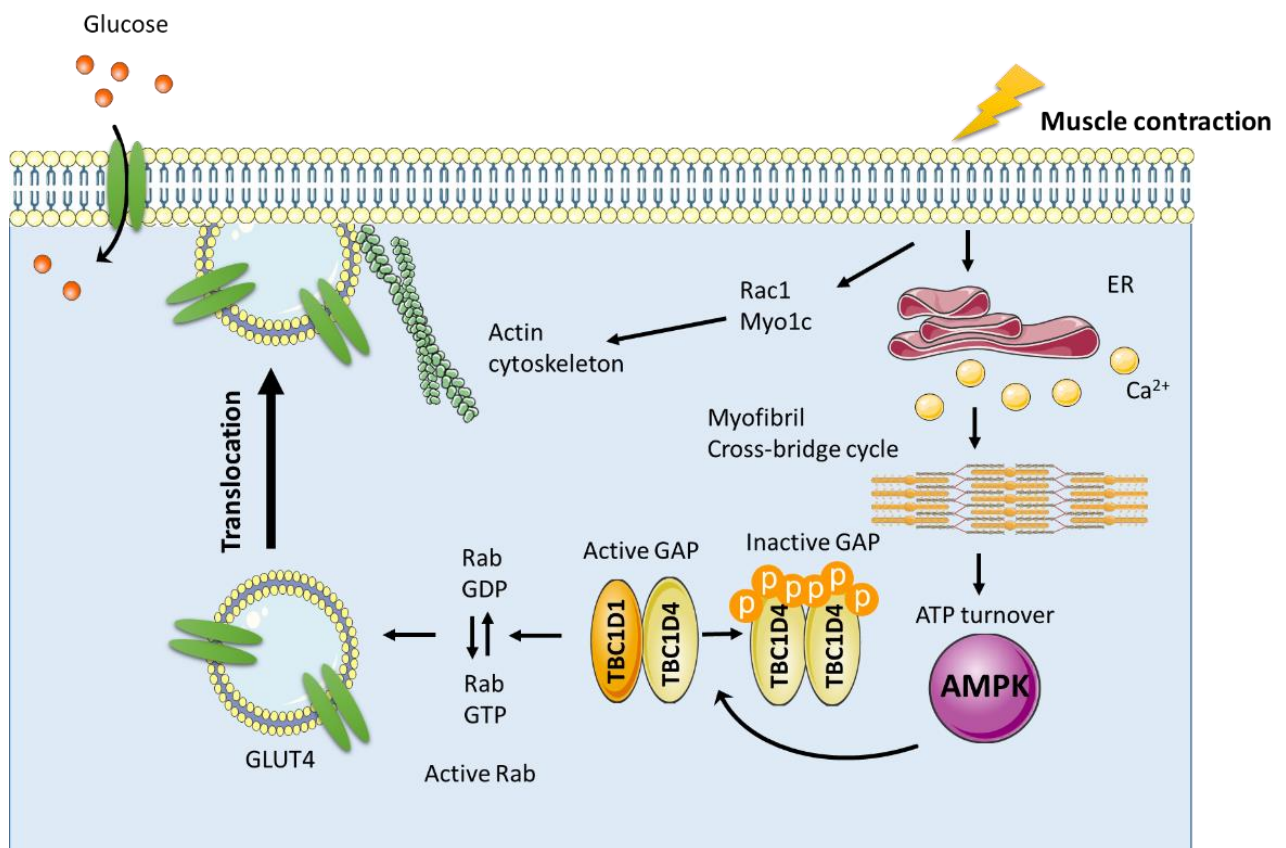
Figure 1.7: Signalling pathways involved in muscle contraction mediated glucose uptake

During muscle contraction, intracellular Ca^{2+} released from the sarcoplasmic reticulum (SR) activates so called "cross-bridge muscle cycle". This metabolic stress increases the AMP–ATP ratio, which leads to activation of AMPK (**Sylow et al., 2017a**). Phosphorylation of the Rab GTPase-activating proteins TBC1D1 and TBC1D4 (also called AS160, Akt substrate of 160 kDa) follows activation of AMPK (**Cartee, 2015**; Vichaiwong et al., 2010). Rab activation then promotes GLUT4 translocation/glucose uptake in muscle (**Richter & Hargreaves, 2013**; **Sylow et al., 2017a**). In addition, activation of Rac1 and Myo1c by mechanical stress may elicit GLUT4 translocation (Sylow et al., 2013). Images of ER, membrane, actin cytoskeleton and calcium were obtained from www.servier.com. Figure was adapted from (**Richter & Hargreaves, 2013**).

Abbreviations: AMPK - AMP-activated protein kinase, ER - endoplasmic reticulum, GAP - GTPase activating protein, TBC - Tre2/Bub2/Cdc16, TBC1D1 – TBC1 domain 1, TBC14D – TBC domain 4, Myo1c – myocin 1C

1.5.3 G protein-coupled receptors involved in glucose metabolism

In metabolic disease research, it is of particular interest to identify pathways that can stimulate GLUT4 translocation without depending on proteins involved in the insulin signalling pathway that are down-regulated in T2D. Over 30 G protein-coupled receptors (GPCRs) including GLP-1 receptors, free fatty acid receptors (FFAR1-4), cannabinoid (CB1) receptors, and adrenoceptors (ARs) are involved in glucose metabolism (**Riddy et al., 2018**). For example, GLP-1 receptors are highly expressed in pancreatic β cells, and their activation leads to an increase in insulin secretion (Drucker et al., 1987; Kebede et al., 2008). As such, there are several GLP-1 receptor agonists (including exenatide, liraglutide, semaglutide etc) that are used clinically for the management of T2D. Activation of ARs can increase glucose uptake independently of insulin, implicating ARs as alternative targets for the treatment of T2D (Sato et al., 2014a; Sato et al., 2018). The detailed AR mediated glucose uptake mechanism is discussed in Section 1.7.

1.6 G protein-coupled receptors

1.6.1 Structure of G protein coupled receptor

GPCRs are activated by a variety of stimuli including hormones, neurotransmitters, ions, photons, organic odorants, amines, peptides, proteins, lipids, and nucleotides (Fredriksson et al., 2003; **Rosenbaum et al., 2009**). They are the largest family of membrane receptors in the human genome, with more than 800 human GPCRs identified. Based on sequence, structural similarity and ligand binding criteria, they are divided into 5 main classes: rhodopsin-like receptors (class A), secretin receptors (class B), metabotropic glutamate (class C), adhesion, and Frizzled/Taste2 (class F) receptors (Fredriksson et al., 2003), but they all share a common structure of 7 transmembrane (TM) spanning α-helices linked by 3 extracellular loops (ECL1-3) and 3 intracellular loops (ICL1-3), an extracellular N-terminus, and an intracellular C-terminal region (Fredriksson et al., 2003; Kroeze et al., 2003; **Palczewski et al., 2000**). Different classes of GPCRs show remarkable structural diversity in the ECL, ICL, N-terminal and C-terminal regions (**Basith et al., 2018**). The N-terminus is considered important for receptor trafficking, cell surface expression in general, and ligand binding (Class B and C receptors, and some Class A receptors) (Couvineau et al., 1996; Kochl et al., 2002; Nechamen & Dias, 2000). The 7TM bundle region is the structural core, forming a ligand binding pocket, that undergoes conformational changes upon ligand binding. The cytoplasmic ends of TM helices and the ICL regions interact with effector proteins such as G proteins (**Zhang et al., 2015**).

1.6.2 G protein-coupled receptor mediated signalling

GPCRs couple to 4 main heterotrimeric G protein families (Gs, Gi/o, Gq/11, G12/13), which result in the regulation of several effectors that include second messenger producing enzymes or ion channels. Gs activates adenylate cyclase (AC), increases cyclic AMP (cAMP) production and activates PKA, while Gi/o inhibits AC activation. Gq/11 activates phospholipase C (PLC), and the resultant cleavage of phosphatidylinositol (4, 5)-bisphosphate (PIP2) produces inositol trisphosphate (IP3) and diacylglycerol (DAG), which release Ca^{2+} and activate protein kinase C (PKC), respectively. G12/13 interacts with RhoGTPase nucleotide exchange factors (RhoGEFs) and regulates cellular proliferation, contraction and morphology (**Kelly et al., 2007**; **Siehler, 2009**; **Worzfeld et al., 2008**). While most GPCRs couple to predominately one G protein, promiscuous coupling to other G proteins can occur. For example, the β_2-AR mainly mediates effects via Gs, but can also couple to Gi/o in some cellular systems (Daaka et al., 1997) as evidenced mainly through the use of pertussis toxin that catalyses the ADP-ribosylation of Gi/o, preventing GDP displacement by GTP, thereby blocking inhibition of AC by Gi/o.

1.6.3 Desensitisation and internalisation of GPCRs as exemplified by the β_2-AR

GPCRs (such as the β_2-AR) can be desensitised and subsequently internalised (Figure 1.8) through a mechanism involving phosphorylation of the receptor at specific sites in intracellular regions. The β_2-AR is phosphorylated on serine and threonine residues within the cytoplasmic loops and C-terminal tail domains by G protein coupled receptor kinases (GRKs) and by PKA (Emorine et al., 1989; Granneman et al., 1991; Muzzin et al., 1991). Phosphorylation of these residues by PKA in the β_2-AR results in uncoupling of the receptor from Gαs (Bouvier et al., 1989). GRKs play a major role in the desensitisation of agonist occupied β_2-ARs (homologous desensitisation). GRKs are serine/threonine protein kinases that specifically recognize and phosphorylate agonist-occupied GPCRs. To date, there are 7 GRK isoforms (GRK1 to GRK7) identified (Weiss et al., 1998). These GRK isoforms are grouped into 3 different families; (1) GRK1 subfamily (GRK1 and GRK7) are the selective kinases responsible for the regulation of rhodopsin photoreceptors, (2) GRK4 subfamily (GRK4, GRK5 and GRK6) are the G-protein $\beta\gamma$-subunit-insensitive kinases, and (3) GRK2 subfamily (GRK2 and GRK3) are $\beta\gamma$-subunit-regulated kinases, (also known as the β-AR kinase 1 and 2) (Erdtmann-Vourliotis et al., 2001; **Ribas et al., 2007**). GRKs 2 and 3 are recruited to the plasma membrane by direct interaction with free G$\beta\gamma$ subunits released upon activation of heterotrimeric G proteins (Pitcher et al., 1992). The receptor is subsequently phosphorylated on serine and threonine residues in the

intracellular (e.g. C terminal) domains, which in turn, increases receptor binding affinity for β-arrestins (Krasel et al., 2005). There are 4 different arrestin isoforms, named arrestin 1 to 4. Of those, arrestin-2 (β-arrestin1) and arrestin-3 (β-arrestin2) are ubiquitously expressed, and appear to act on multiple GPCRs (Bychkov et al., 2012). Of note, these two arrestins are detected in different cellular locations: β-arrestin1 is found in both the cytoplasm and nucleus, whereas β-arrestin2 is only present in cytoplasm (Scott et al., 2002). Following the binding of β-arrestin, agonist-promotedinternalisation of the receptor occurs. β-arrestin also functions as an adapter protein, which allows receptors to associate with components of the clathrin-coated pit, and promotes the dynamin (Dyn)-dependent sequestration of receptors and the formation of intracellular vesicles (Laporte et al., 2000). Upon internalisation, those receptors are trafficked to an acidified endosomal pool, where the ligand is released. Subsequently, the receptor is dephosphorylated by a GPCR-specific protein phosphatase PP2A isoform, and is then either degraded or recycled to the plasma membrane (Luttrell & Lefkowitz, 2002; Zhang et al., 1999).

1.6.4 Scaffolding function of GRK and β-arrestin

Along with the well documented role of GRKs to phosphorylate GPCRs resulting in receptor desensitisation, GRKs have additional phosphorylation substrates, and also exhibit scaffolding functions via direct interactions with signalling proteins and direct downstream signalling cascades without eliciting their kinase activity (**Gurevich et al., 2012**). It has been reported that GRKs can associate with multiple binding partners (**Ribas et al., 2007**; **Watari et al., 2014**). Some important binding partners include (1) caveolin1 (Schutzer et al., 2005), (2) clathrin (Shiina et al., 2001), (3) PI3K (Naga Prasad et al., 2002), and (4) Akt (Liu et al., 2005) (see Chapter 4 for further discussion). Binding of β-arrestin to the receptor can also act as a scaffold for cellular signalling partners which include (1) c-Src, which affects ERK1/2 phosphorylation (Luttrell et al., 1999), (2) ERK1/2, which is involved in activation of the mitogen-activated protein kinase (MAPK) (Shenoy et al., 2006), and (3) phosphodiesterase 4, which affects the rate of cAMP turnover (Perry et al., 2002). As such, both GRKs and β-arrestin acting as scaffolding proteins and can interact with several cellular proteins independent from their kinase activity.

1.6.5 Biased agonism

Traditionally, development of GPCR therapeutics has focused on the effects of conventional agonists and antagonists. One current trend of GPCR drug development, however, focuses on biased

ligands that offer the opportunity in drug design to selectively activate one or more desired signalling pathways which mediate favourable responses, over other signalling pathways that may mediate adverse effects (**Luttrell et al., 2015**; **Violin et al., 2014**). Biased agonism refers to the ability of ligands to preferentially activate one or more intracellular signalling pathways (**Gundry et al., 2017**). The most prominent mechanism to explain bias involves the ligands stabilising functionally distinct receptor conformations. There are many GPCRs that have shown to have biased ligands (**Bologna et al., 2017**; Rominger et al., 2014), which include α_{1A}-ARs (da Silva Junior et al., 2017; Evans et al., 2011) and β-ARs (Ghanouni et al., 2001a; Ghanouni et al., 2001b).

There are some considerations which can affect the identification of biased agonists, including system bias and observation bias. System bias is the contribution of cell/tissue specific effect which arises from differential coupling of the system (for example, receptor expression level can affect both agonist potency and maximal response). Observation bias is the reflection of the experimental conditions such as time, temperature and buffer conditions unique to the assay (da Silva Junior et al., 2017; **Gundry et al., 2017**; **Smith et al., 2018**). In order to assess true ligand bias, test ligands should be compared with a reference ligand, which can cancel out the influence of system and observation bias (Evans et al., 2011; Klein Herenbrink et al., 2016). For example, the Black and Leff operational model describes agonism by two parameters dependent on agonist properties: (1) K_A, the functional equilibrium dissociation constant of the agonist and (2) K_E, the concentration of agonist occupied receptor that elicits the half maximal tissue response; the model also incorporates (3) R_t, receptor density and (4) the maximum response of the system, Emax. Usually K_E is not fitted directly, but instead the transduction coefficient τ (=R_t/K_E) is obtained from concentration response data. When comparing pathways and ligands, bias factors related to the τ / K_A ratio may be quantified in comparison to a reference ligand (Black & Leff, 1983; Black et al., 1985). Appropriate choice of the reference agonist is an important factor. Although endogenous ligands are often used as a reference ligand, they may cause off-target activities by binding to other endogenous receptor subtypes (van der Westhuizen et al., 2014). Absence of off-target effects should be confirmed by sensitivity to antagonism (van der Westhuizen et al., 2014) or assays in non-transfected cells (da Silva Junior et al., 2017). Also, the use of endogenous ligands to determine the measurement time
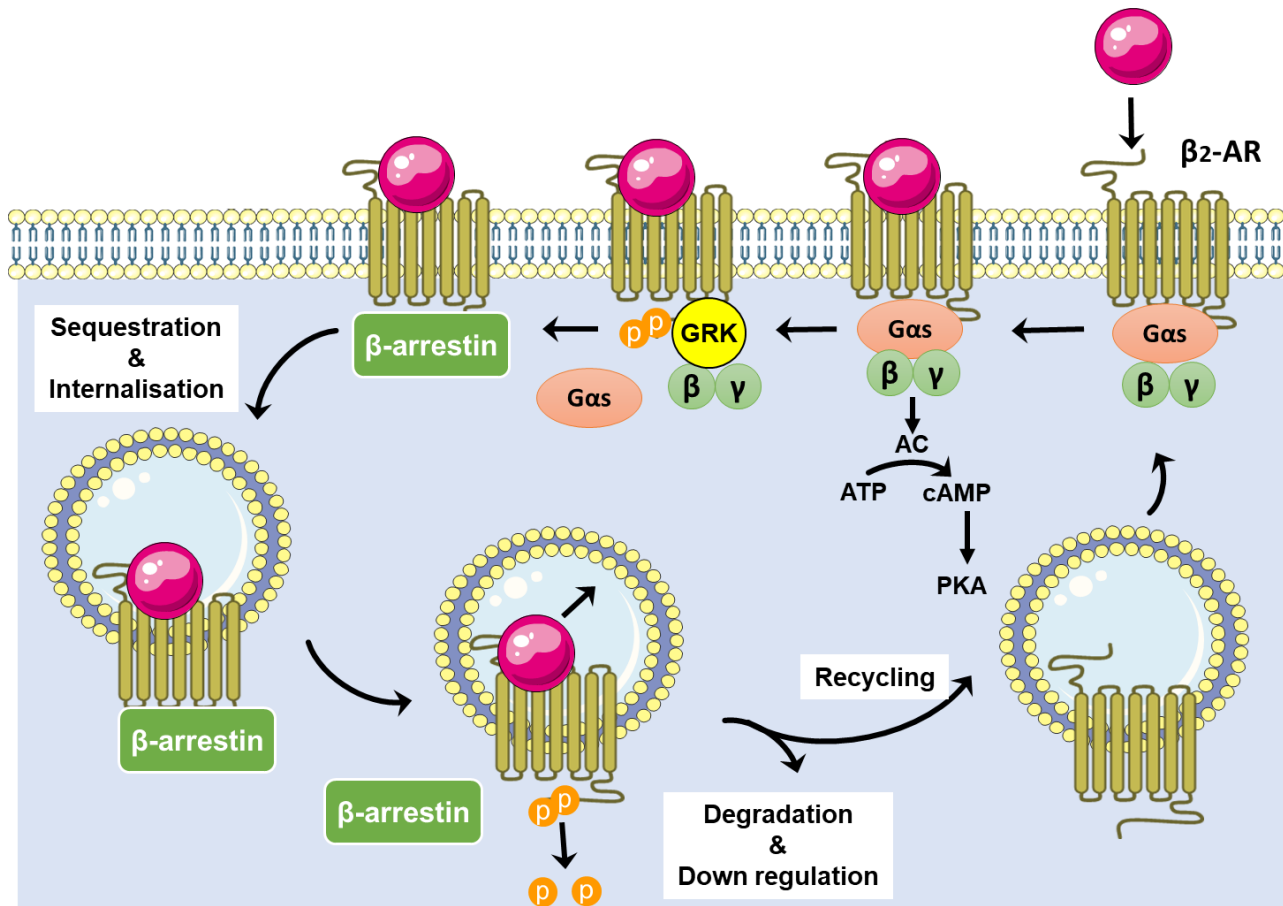
Figure 1.8: Regulation of the β₂-AR

Ligand bound β₂-AR produces functional responses via Gαs. Receptor desensitisation is elicited by GRK mediated receptor phosphorylation. β-arrestin bound receptor causes clathrin-mediated receptor endocytosis. In an endosomal compartment, β-arrestin and ligand are dissociated from receptor, after which receptor is dephosphorylated by protein phosphatase. Receptor is then recycled to the plasma membrane or degraded (Luttrell & Lefkowitz, 2002). Images of receptors and membrane were obtained from www.servier.com.

Abbreviations: AC - adenylyl cyclase, cAMP – cyclic AMP, GRK – G protein receptor kinase, PKA – protein kinase A.

in assays could be problematic if test ligands show different kinetic profile compared to the endogenous ligand, since the operational model is derived on the assumption of equilibrium conditions (Klein Herenbrink et al., 2016). In addition, biased signalling should be examined in *ex vivo*, *in vivo* and in human cells if possible (Broad et al., 2016).

1.7 Adrenoceptors

Activation of the sympathetic system through the release of adrenaline (from adrenal gland) and noradrenaline (from nerve terminals) causes a "fight-or-flight" response. This initiates a variety of responses, such as increased heart rate and cardiac output, and increased energy expenditure by up-regulating the delivery of well-oxygenated, nutrient-rich blood to skeletal muscle and other tissues (**Gordan et al., 2015**; **McCorry, 2007**). ARs are subdivided into 3 main families: α_1-ARs (α_{1A}-, α_{1B}-, α_{1D}-AR), α_2-ARs (α_{2A}-, α_{2B}-, α_{2C}-), and β-AR subtypes (β_1-, β_2-, β_3-) (Brede et al., 2004; Saunders & Limbird, 1999). α_1-AR, α_2-AR and β-ARs are primarily coupled to Gq/11, Gi/o and Gs respectively (Figure 1.9). These AR subtypes are distributed differently in a variety of tissues or cell types, and are involved in the regulation of many physiological responses (Figure 1.10). Specifically, several studies have revealed that the activation of α_{1A}-AR (expressed in cardiomyocytes) and β_2-ARs (expressed in skeletal muscle) have roles in glucose uptake. This thesis focuses on the signalling mechanisms of α_{1A}-AR and β_2-AR mediated glucose uptake.

1.7.1 Adrenoceptors in skeletal muscle

β-ARs are expressed in skeletal muscle, with a 3-fold greater density of β-ARs in slow-twitch muscles compared to fast twitch muscles (Martin et al., 1989). The β-AR subtypes detected in skeletal muscle are predominantly the β_2-AR (both in fast and slow twitch muscles), with a minor population of β_1–ARs detected (in slow twitch muscles) (Jensen et al., 1995; Watson-Wright & Wilkinson, 1986). β_3-ARs are not detected in skeletal muscle (Evans et al., 1996). In diabetes, β-AR expression level in skeletal muscle remains unchanged or increases (Xavier et al., 2012; Yang et al., 2002). Several cell lines are used to study skeletal muscle function including rat L6 and mouse C2C12 skeletal muscle cells. L6 cells are a good model to investigate the mechanism of β_2-AR mediated glucose uptake since they express high levels of the β_2-AR (but not β_1- or β_3-ARs) and GLUTs (mainly GLUT4) during

α₁-AR   β-AR   α₂-AR

Gαq/11   PLC   PIP₂   Gαs   AC   Gαi

β γ   DAG   IP₃   β γ   ATP   cAMP   β γ

PKC   Ca²⁺   PKA

Downstream effects
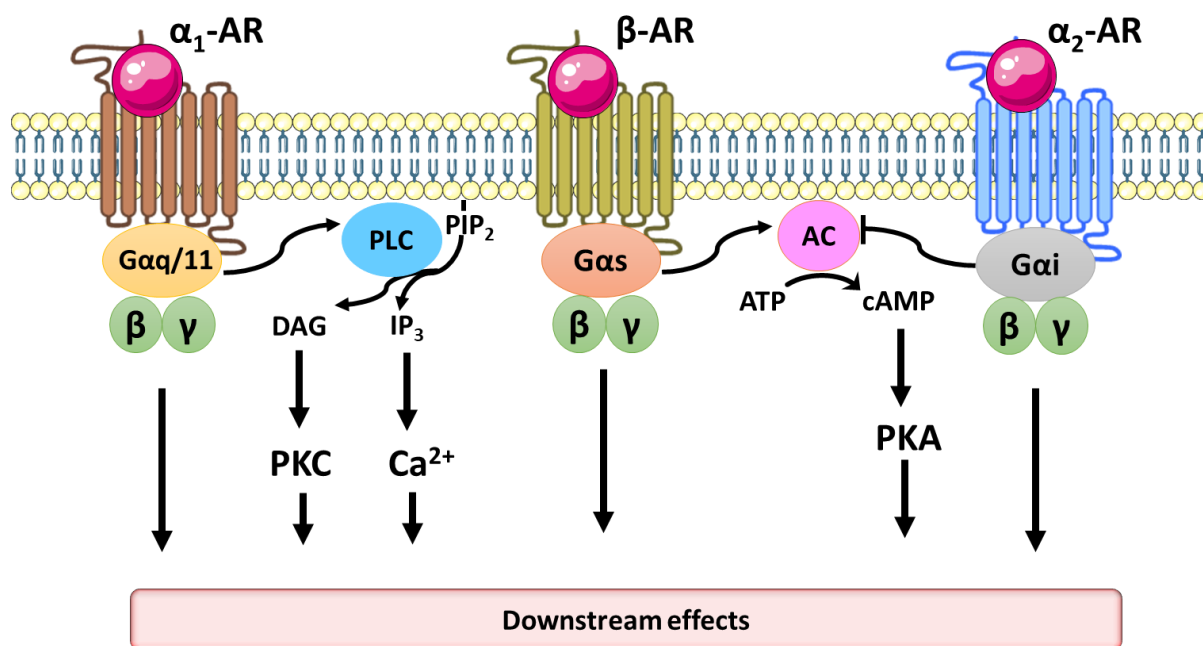
Figure 1.9: Distinct intracellular pathways activated by adrenoceptors coupling to different G proteins

α_1-ARs (α_{1A}-, α_{1B}-, α_{1D}-) are Gαq coupled-receptors. They activate PLC, which causes the hydrolysis of membrane lipid, PIP2 into IP3 and DAG. This results in the release of Ca^{2+} from the endoplasmic reticulum and activation of PKC. β-ARs (β_1-, β_2-, β_3-) are Gαs coupled-receptors, that stimulate cAMP accumulation through AC, whereas α_2-ARs (α_{2A}-, α_{2B}-, α_{2C}-) couple to Gαi to inhibit AC activation. Note that this figure shows the predominant signalling mechanisms of each AR subtype, but adrenoceptors can couple to more than one G protein. Images of receptors and membrane were obtained from www.servier.com.

Abbreviations: AC - adenylyl cyclase, cAMP – cyclic AMP, DAG – diacylglycerol, IP3 - inositol trisphosphate, PIP2 - phosphatidylinositol (4, 5)-bisphosphate, PKA – protein kinase A, protein kinase C – PKC, PLC - phospholipase C.

Central nervous system
Subtypes; α_1, α_2, β_1,

Lung
Subtype; β_1,

Brown adipose tissue
Subtypes; α_1, α_2, β_1, β_3

Liver
Subtypes; α_1, α_2

Heart
Subtypes; α_1, β_1, β_2

Pancreas
Subtypes; α_2

Vascular smooth muscle
Subtypes; α_1, α_2, β_2

White adipose tissue
Subtypes; α_2, β_1

Gastro intestinal tract
Subtypes; α_2, β_2

Bladder
Subtypes; β_3

Prostate
Subtypes; α_1

Skeletal muscle
Subtypes; α_1, β_2
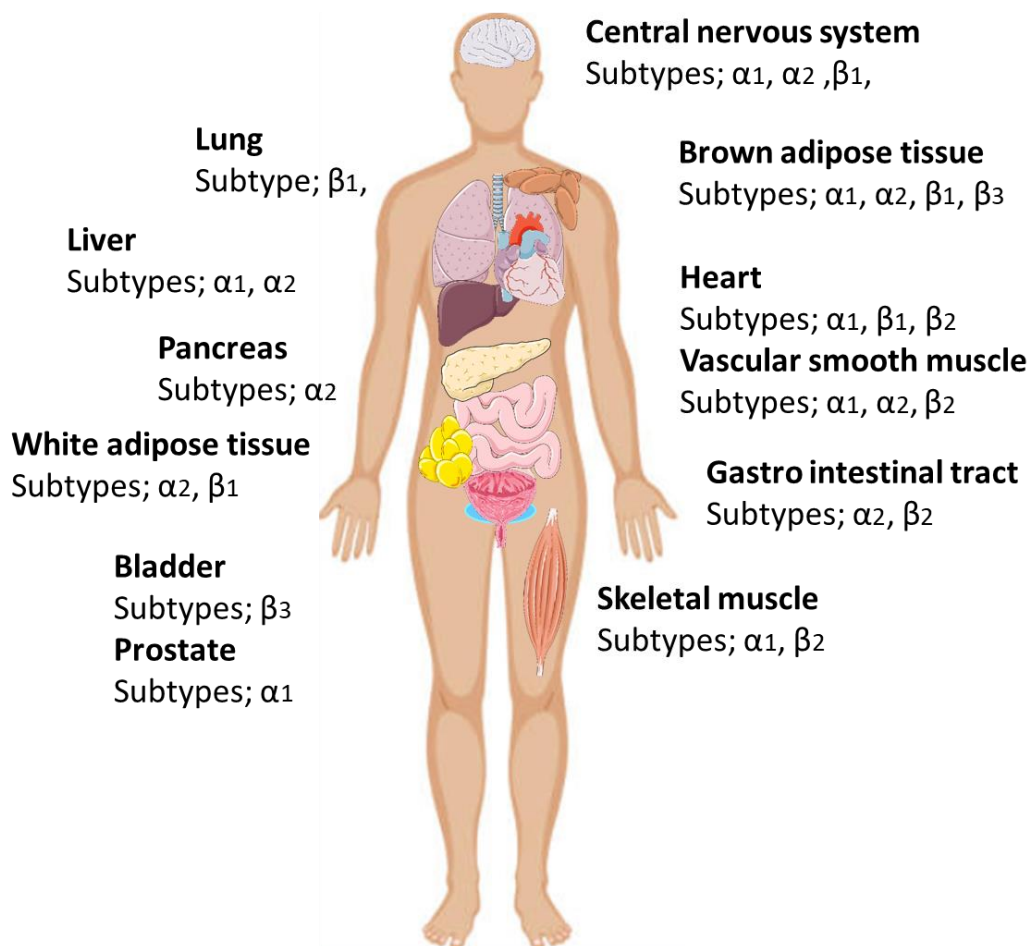
Figure 1.10: Adrenoceptor distribution in the body

Adrenoceptors are located throughout the body including the central nervous system, lung, vascular smooth muscle, pancreas, adipocyte, liver, brain, gastrointestinal tract, heart, skeletal muscle, bladder and prostate (Berkowitz et al., 1994; Colciago et al., 2016; **Davis et al., 2008**; Furukawa et al., 1995; **Giovannitti et al., 2015**; Gordan et al., 2015; Gros et al., 1999; Hutchinson et al., 2008; Kenny et al., 1996; Lepor et al., 1993; **Madamanchi, 2007**; **Michel et al., 2010**; **Mutlu & Factor, 2008**; **O'Connell et al., 2014**; **Piascik & Perez, 2001**; Price et al., 1994). Images of organs were obtained from www.servier.com.

their differentiation (Mitsumoto et al., 1991). They also increase glucose uptake in response to insulin and β-AR stimulation (Antonescu et al., 2005; Haney et al., 1995; Nevzorova et al., 2002; Nevzorova et al., 2006; Sato et al., 2014a; Walker et al., 1989). While C2C12 cells express β_2-ARs and GLUT1/4 (Kotliar & Pilch, 1992; Ngala et al., 2008), both insulin and β_2-AR stimulation fail to increase glucose uptake in these cells, thought to be due to an inability of GLUTs to integrate into the cell surface upon stimulation (Tortorella & Pilch, 2002). In addition to β-ARs, low expression of α_1- and α_2-ARs are restricted to vascular smooth muscle, and mediate vasoconstriction of skeletal muscle blood vessels (Lambert & Thomas, 2005). However, whether their expression/function is altered in diabetes is unknown.

1.7.1.1 Effect of β_2-ARs on glucose metabolism

β_2-ARs are the major AR subtype responsible for AR mediated increases in glucose uptake in skeletal muscle (Figure 1.11). Activation of β-ARs by either isoprenaline (non-selective β-AR agonist) or specific β_2-AR ligands (for example, clenbuterol or zinterol) increases glucose uptake in L6 cells (both myoblasts and myotubes) as well as in intact skeletal muscle *in vitro* and *in vivo* (Liu & Stock, 1995; Nevzorova et al., 2002; Nevzorova et al., 2006; Ngala et al., 2008; Ngala et al., 2009; Sato et al., 2014a). The stimulatory effect of isoprenaline on skeletal muscle glucose uptake is abolished in β_1/β_2-AR knockout mice (Sato et al., 2014a).

Activation of β-ARs increases the production of cAMP. In rat soleus muscle, isoprenaline stimulation increased cAMP levels, which was antagonised by the selective β_2-AR antagonist ICI118551 (Roberts & Summers, 1998). Another study in L6 myotubes also showed an increase in cAMP accumulation in response to isoprenaline and zinterol (Dehvari et al., 2012; Nevzorova et al., 2006). Also, this cAMP response was enhanced following inhibition of phosphodiesterase 4 (which catalyses the hydrolysis of cAMP into AMP) with rolipram (Nevzorova et al., 2006). In addition, isoprenaline increased mTORC2 phosphorylation at Ser2481 but not mTORC1 phosphorylation at Ser 2448 in L6 myotubes. Isoprenaline increased GLUT4 translocation in both L6 myotubes and human primary skeletal muscle cells (Sato et al., 2014a).
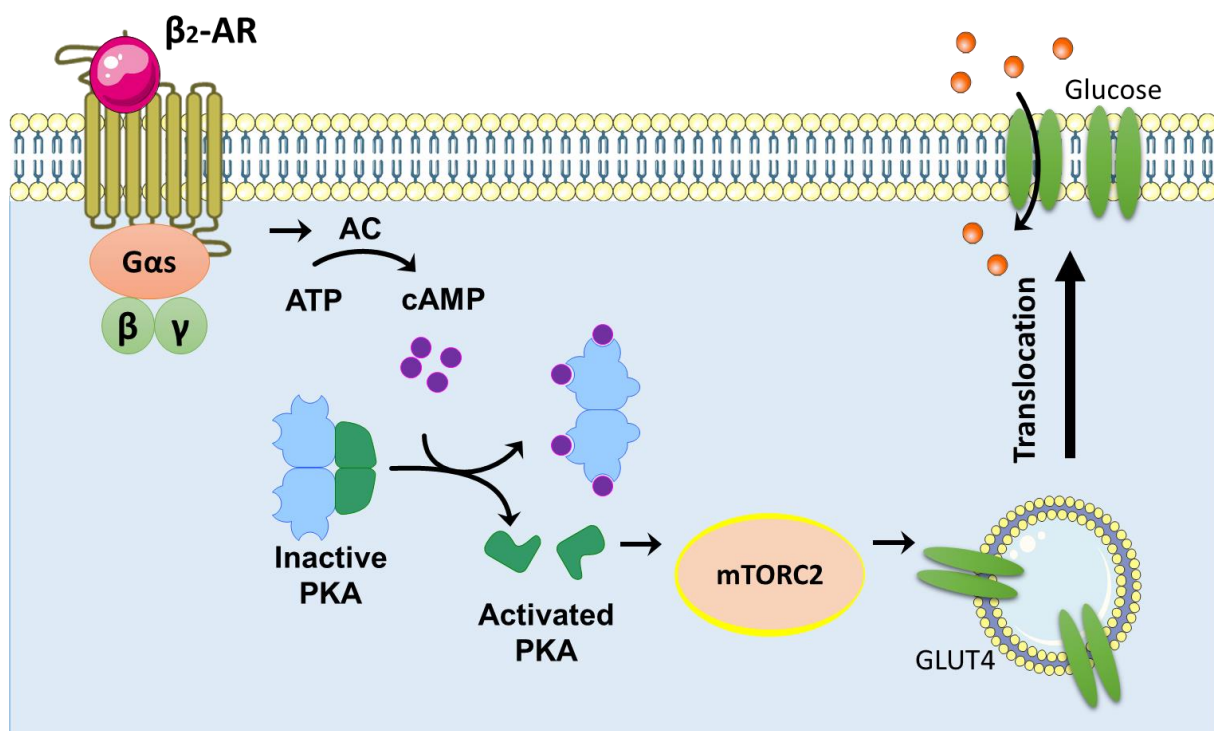
Figure 1. 11: β₂-Adrenoceptor mediated glucose uptake signalling pathway

β_2-ARs are predominantly Gαs coupled receptors. When β_2-AR agonists bind to the receptor, they activate AC, leading to the synthesis of cAMP from ATP. cAMP then activates its downstream target, PKA. In its inactive state, PKA exists as a tetramer of two dimers R- and C-subunits. Binding of cAMP to R-subunits, liberates C-subunits to phosphorylate target proteins. PKA catalyses phosphorylation of various proteins including mTORC2, resulting in stimulation of GLUT4 translocation and glucose uptake (Sato et al., 2014a). Images of receptor, membrane, glucose and PKA were obtained from www.servier.com.

Abbreviations: AC - adenylyl cyclase, C – catalytic, cAMP – cyclic AMP, mTORC2 – mammalian target of rapamycin complex 2, PKA – protein kinase A, R – regulatory.

The β_2-AR system may also affect insulin release since both isoprenaline and terbutaline (a β_2-AR agonist) increased insulin secretion *in vivo* (Ahren & Lundquist, 1981), and β-AR knock out mice (lacking all β-AR subtypes) have impaired glucose-induced insulin release, increased gluconeogenesis and are glucose intolerant (Asensio et al., 2005). β_2-AR knock out mice also developed glucose intolerance, and impaired glucose-induced insulin secretion, signifying an important role of β_2-AR in glucose metabolism (Santulli et al., 2012). Overexpression of β_2-AR in aged mice increased insulin release and protected from glucose intolerance both *in vivo* and *ex vivo* unlike wild type mice which exhibited glucose intolerance (Santulli et al., 2012). Furthermore, mice lacking β-ARs failed to display weight loss following a ketogenic diet (causing elevation of energy expenditure) as opposed to wild type mice (Douris et al., 2017). In obese or T2D animal models including obese Zucker rats, Goto-Kakizaki rats and high fat diet–fed C57BL/6J mice, administration of β_2-AR agonists significantly improved glucose tolerance (Sato et al., 2014a; Torgan et al., 1993). All these studies indicate the potential anti-diabetic effects of β_2-AR agonists.

1.7.1.2 Effects of BRL37344 on skeletal muscle glucose uptake

BRL35135 and BRL37344 (its active de-esterified metabolite) (Figure 1.12) were originally developed as β_3-AR agonists (Arch et al., 1984), with BRL37344 highly specific in mediating adipose tissue lipolysis (a β_3-AR effect) over mediating β_1- or β_2-AR mediated responses in the atria/trachea respectively. In female C57BL/6 (ob/ob) mice, a single dose of BRL37344 increased metabolic rate, and 4-week daily treatment with BRL37344 reduced body lipid content as well as body weight (Arch et al., 1984). In obese Zucker rats, 3-week treatment with BRL37344 reduced weight gain and plasma insulin levels (Santti et al., 1994). Hence, BRL37344 was developed as a potential anti-obesity drug. Unexpectedly, no effect was observed in human studies, with a 10-day BRL37344 treatment of obese patients failing to show any significant changes in body weight (Mitchell et al., 1989), although this short time of treatment may not be sufficient to observe significant weight loss in humans. However this study did demonstrate favourable effects on glucose storage and glucose tolerance (Mitchell et al., 1989) which may be due to actions at β_2-ARs in skeletal muscle rather than β_3-ARs in adipose tissues. The reduction in body weight reported in rodents was due to improved thermogenesis and lipolysis through the activation of β_3-ARs in BAT and WAT. In contrast, it was found that effects on glucose utilization were due to activation of β_2-ARs located in skeletal muscle, in studies utilizing receptor selective antagonists (Liu et al., 1996; Liu & Stock, 1995; Nevzorova et al., 2002; Ngala et al., 2008). In rodents, BRL37344 increased glucose uptake in different types of rat

BRL35135
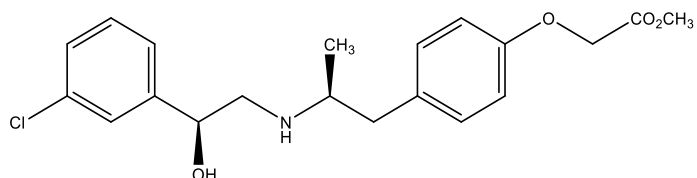
BRL37344
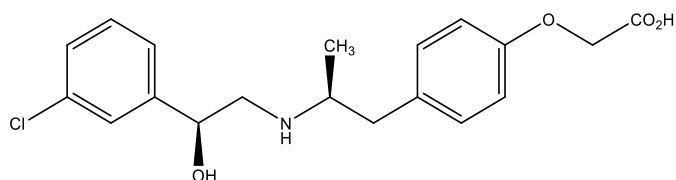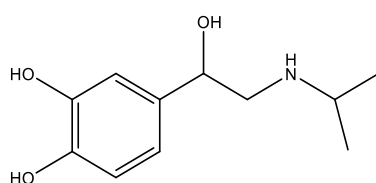
Isoprenaline

Clenbuterol
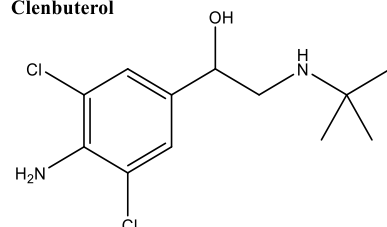
Figure 1.12: Chemical structures of BRL35135/BRL37344, isoprenaline and clenbuterol

In vivo, BRL35135 is de-esterified to BRL37344 (its active metabolite) within 15 min of administration (Arch et al., 1984). Chemical structures were created with ChemDraw Professional 17.1.

skeletal muscles such as slow and fast twitch muscles independently from insulin (Abe et al., 1993). Also, BRL37344 demonstrated an ability to increase glucose uptake in skeletal muscle both *in vitro* and *in vivo* equal to other β_2-AR agonists such as clenbuterol (Abe et al., 1993; Board et al., 2000; Nevzorova et al., 2002; Nevzorova et al., 2006; Ngala et al., 2008). While these results show that BRL37344 is a β_2-AR agonist in skeletal muscle, BRL37344 agonist activity at the cloned β_2-AR has also been demonstrated (Baker, 2010b) (see Chapter 3 for further discussion).

1.7.1.3 The mechanism of β_2-AR mediated glucose uptake

1.7.1.3.1 Role of AC, cAMP and PKA

Many studies suggest a significant role of cAMP in glucose uptake since stimulation with the cAMP analogues (8-Bromoadenosine 3',5'-cyclic monophosphate or dibutyryl cAMP) caused a significant elevation of glucose uptake in rat L6 cells (Nevzorova et al., 2002; Nevzorova et al., 2006; Sato et al., 2014a). Elevation of cAMP levels by inhibiting phosphodiesterase 4 with rolipram potentiated zinterol mediated glucose uptake in L6 cells (Nevzorova et al., 2006). In addition, inhibition of either AC with 2',5'-dideoxyadenosine (DDA) or PKA with PKI reduced zinterol-or isoprenaline-stimulated glucose uptake in L6 cells, respectively (Nevzorova et al., 2006; Sato et al., 2014a).

1.7.1.3.2 Role of Akt/mTOR

PI3K and Akt are considered important for insulin-stimulated glucose uptake, but are not involved in β_2-AR mediated glucose uptake (Sato et al., 2014a). While originally it was thought that β_2-ARs increased glucose uptake via PI3K due to inhibition of responses by PI3K inhibitors such as LY294002 and wortmannin, β_2-ARs in skeletal muscle fail to increase Akt phosphorylation and glucose uptake is not affected by selective Akt inhibitors (Nevzorova et al., 2006; Sato et al., 2014a). This discrepancy is thought to be due to wortmannin and LY294002 inhibiting other kinases such as mTOR, which is involved in β_2-AR mediated glucose uptake (Gharbi et al., 2007).

Recent studies have shown a specific role for mTORC2 in β_2-AR mediated glucose uptake. This is based on studies performed in L6 cells showing that β_2-ARs phosphorylate mTORC2, pharmacological inhibition of mTORC2 reduces β_2-AR mediated glucose uptake, and that siRNA against rictor (and not raptor) inhibits β_2-AR mediated glucose uptake (Sato et al., 2014b). Furthermore, a role for mTOR in β_2-AR mediated glucose uptake was shown *in vivo* and *ex vivo,* with the mTOR inhibitor KU0063794 inhibiting isoprenaline-mediated glucose uptake in isolated rat

soleus muscle *ex vivo*, and in soleus muscle *in vivo* (Sato et al., 2014b). The mechanism whereby β_2-ARs activate mTOR is not completely understood but may involve cAMP/PKA (Sato et al., 2014b) .

1.7.1.3.3 Role of GRKs

GRKs have been suggested to be involved in β_2-AR mediated glucose uptake in studies using a simple recombinant system (CHOGLUT4myc cells). Truncation of the β_2-AR C-terminal tail at T349 (removing all GRK phosphorylation sites) decreases isoprenaline-stimulated glucose uptake compared with wild type cells (Dehvari et al., 2012). Also, isoprenaline stimulation of cells expressing a β_2-AR (–)GRK mutant significantly reduces the activity of GLUT4 translocation to the cell surface compared to the β_2-AR wild type cells (Dehvari et al., 2012). In addition, isoprenaline treatment of cells overexpressing kinase-dead GRK2 (K220R) fails to increase GLUT4 translocation (Dehvari et al., 2012). As such, these studies indicate the potential role of GRKs in glucose uptake following activation of β_2-AR (see Chapter 4 for further discussion).

1.7.2 Adrenoceptors in the heart

1.7.2.1 β-ARs

The human heart expresses predominately β-ARs, with approximately 70% of these the β_1-AR subtype and 30% the β_2-AR subtype (Bristow et al., 1986). Both subtypes contribute to the regulation of heart rate and cardiac contractility but through different mechanisms. β_1-ARs are Gαs coupled receptors and their activation increases contractility via PKA mediated phosphorylation of several proteins including troponin I (modulation of myofilament Ca^{2+} sensitivity), the L-type Ca^{2+} channel (Ca^{2+} influx), and phospholamban (Ca^{2+} reuptake into the SR) (**Lohse et al., 2003**). In contrast, β_2-ARs reduce cardiac contractility by Gαi mediated activation of the cytosolic effector molecule phospholipase A2 (cPLA2) (Madamanchi, 2007).

In human heart failure, there is an elevation of catecholamine levels through up-regulation of the sympathetic nervous system. This prolonged catecholamine stimulation elicits chronic activation of β-ARs, resulting in decreasing cardiac contractile behaviour by significantly desensitising the β_1-AR, and by increasing β_2-AR-Gαi mediated activity, leading to sustained cardiac hypertrophy (Freedman & Lefkowitz, 2004; Katz, 1998). Furthermore, prolonged activation of β-ARs negatively affects oxidative stress, cardiac remodelling and apoptosis (Teerlink et al., 1994; Zhu et al., 2003). This

decreased cardiac function due to prolonged catecholamine stimulation can be rescued by administration of β-AR antagonists including (1) non-selective $\beta_{1/2}$-AR blockers (e.g propranolol) (Armstrong et al., 1977; Talwar et al., 1996), (2) β_1-AR selective blockers (e.g metoprolol and bisoprolol) (Poole-Wilson, 1999; Tepper, 1999) and (3) α_1-AR and $\beta_{1/2}$-AR blockers (e.g carvedilol) (Poole-Wilson et al., 2003).

1.7.2.2 α_1-ARs

In the human heart, α_{1A}- and α_{1B}-ARs are expressed in cardiomyocytes while α_{1D}-ARs are only expressed in coronary smooth muscle cells (Jensen et al., 2009a; Jensen et al., 2009b). There is substantial evidence that indicates the beneficial effects of α_1-AR activation in myocardium (Jensen et al., 2014; Jensen et al., 2009b). In the failing heart, it increases expression of α_1-AR in myocardium by 2-fold compared to normal heart, which accounts for up to 40% of all AR in myocardium (Jensen et al., 2009a). Therefore, in human heart failure, the AR profile in the cardiomyocyte changes from a predominant β_1-AR expression to a more mixed expression of β_1-AR, β_2-AR and α_1-AR due to a marked reduction of β_1-AR but a substantial increase in α_1-AR (Bristow, 1993). Additionally, desensitisation of β_1-AR in heart failure is promoted by up-regulation of GRK2 and GRK5 while the regulation of GRK3, the main GRK isoform mediating α_1-AR activity, is not changed (Aguero et al., 2012; Vinge et al., 2001).

It has been shown that activity of α_1-ARs is necessary for developmental cardiac survival and function. Phenylephrine, a nonselective α_1-AR agonist, inhibits apoptosis in neonatal rat ventricular myocytes (NRVM), and this effect is diminished by addition of the α_1-AR antagonist phentolamine (Iwai-Kanai et al., 1999). Noradrenaline increases glucose uptake and developmental cardiac hypertrophy in NRVM, important for maintaining normal heart function (Sato et al., 2018). Furthermore, ablation of α_1-AR impairs physiological cardiac hypertrophy and reduces stroke volume, heart rate, and cardiac output in double α_{1A}-AR and α_{1B}-AR KO mice (O'Connell et al., 2003). In heart failure, up-regulation of α_1-AR expression level produces cardioprotective effects such as adaptive hypertrophy, positive inotropy, improved contractile function, protein synthesis, cell survival and glucose metabolism (Jensen et al., 2011a; O'Connell et al., 2014), and these positive effects are mainly due to α_{1A}-AR. A study in transgenic mice expressing a constitutively active α_{1A}-AR but not α_{1B}-AR exhibited enhanced contractile function following ischemic injury (Rorabaugh et al., 2005). Following chronic myocardial infarction, transgenic mice with cardiomyocyte-specific α_{1A}-

AR overexpression showed less fibrosis and decreased cardiac remodelling compared to non-transgenic mice (Du et al., 2006; Zhao et al., 2015). Also, the highly selective α_{1A}-AR agonists, A61603 and dabuzalgron (originally known as Ro 115-1240) (Figure 1.13) are protective against doxorubicin-induced cardiotoxicity both *in vitro* and *in vivo* (Beak et al., 2017; Cowley et al., 2015; Vakhrusheva et al., 2008). Importantly, both A61603 and dabuzalgron induce these beneficial effects without affecting blood pressure through vascular α_1-AR activation (Beak et al., 2017; Jensen et al., 2011a).

Activation of α_{1A}-ARs involves key signalling molecules including Ca^{2+}, AMPK, mTOR2, mTORC1 and S6RP (Figure 1.14). α_{1A}-AR agonists increase Ca^{2+} mobilization both in a recombinant system, CHOGLUT4myc cells stably expressing the human α_{1A}-AR, and in NRVM (Sato et al., 2018). Also, agonists increase phosphorylation of AMPK (Thr 172), mTORC2 (Ser 2481), mTORC1 (Ser 2448) and S6RP (Ser 235/236) (Sato et al., 2018). Their activation is considered important for different cardiac functions; Ca^{2+} mobilization (contractility) (Capogrossi et al., 1991), p-mTORC1/p-S6RP (hypertrophy) (Sato et al., 2018), p-mTORC2 (cell survival and glucose uptake) (Hung et al., 2012; Sato et al., 2018) and p-Erk1/2 (cell survival) (Huang et al., 2007; Lu & Xu, 2006).

1.7.2.3 The mechanism of α_{1A}-AR mediated glucose uptake and protein synthesis

Increased Ca^{2+} mobilization is an important step in promoting glucose uptake since A23187 (a Ca^{2+} ionophore) significantly increased glucose uptake in NRVM (Sato et al., 2018). However, intracellular, but not extracellular Ca^{2+} mediates a critical role in glucose uptake as BAPTA-AM (the membrane-permeable Ca^{2+} chelator) abolished A23187-stimulated glucose uptake while BAPTA (not cell permeable Ca^{2+} chelator) showed no effect on glucose uptake (Hutchinson & Bengtsson, 2005). AMPK and mTORC2 but not mTORC1 are involved in α_{1A}-AR mediated glucose uptake in NRVM because (1) inhibition of AMPK with compound C reduced both GLUT4 translocation and glucose uptake, (2) inhibition of mTOR with KU0063794 blocked α_{1A}-AR mediated glucose uptake and (3) inhibition of mTORC1 with acute rapamycin did not reduce glucose uptake (Sato et al., 2018). However, activation of mTORC2 occurs independently from Ca^{2+} and AMPK because A23187 did not increase mTORC2 phosphorylation, and mTORC2 phosphorylation was not decreased by inhibiting AMPK. Hence, there is no cross-talk between the mTORC2 and Ca^{2+}-AMPK pathways (Sato et al., 2018). Unlike insulin signalling, Akt is not activated in α_{1A}-AR mediated glucose uptake. In NRVM, A61603 stimulation failed to increase AKT phosphorylation at Ser473/Thr308. Also, the Akt inhibitor X did not reduce α_{1A}-AR mediated glucose uptake (Sato et al., 2018). mTORC1 and Ca^{2+} are involved in α_{1A}-AR mediated protein synthesis/hypertrophy in NRVM since (1) inhibition of mTOR with

A61603   Dabuzalgron
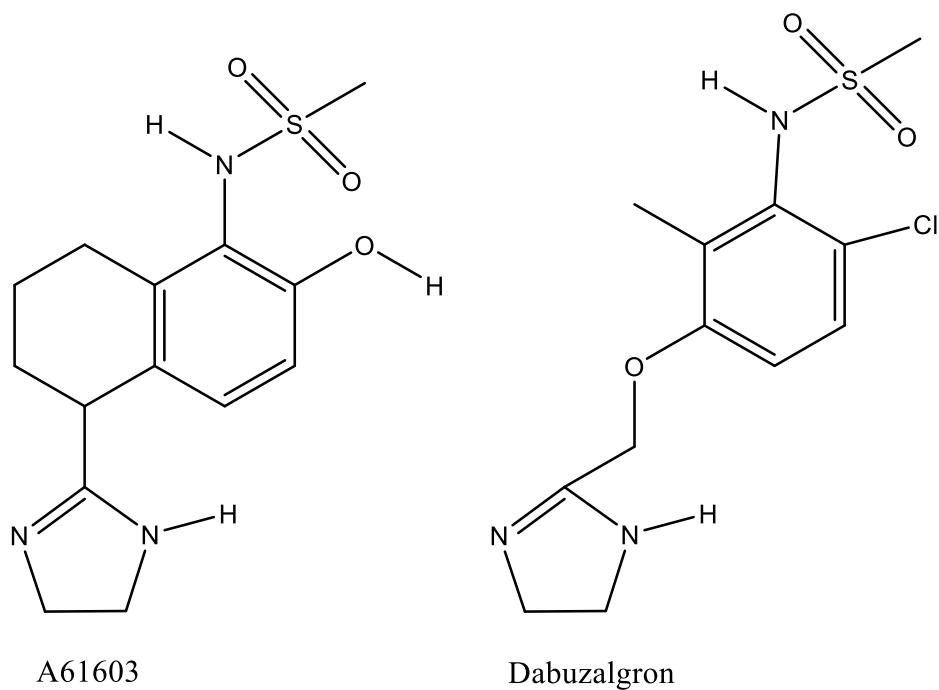
Figure 1.13: Chemical structures of A61603 and dabuzalgron

A61603 and dabuzalgron (formerly known as Ro 115-1240) are the highly selective α_{1A}-AR agonists.

Chemical structures were created from ChemDraw Professional 17.1.
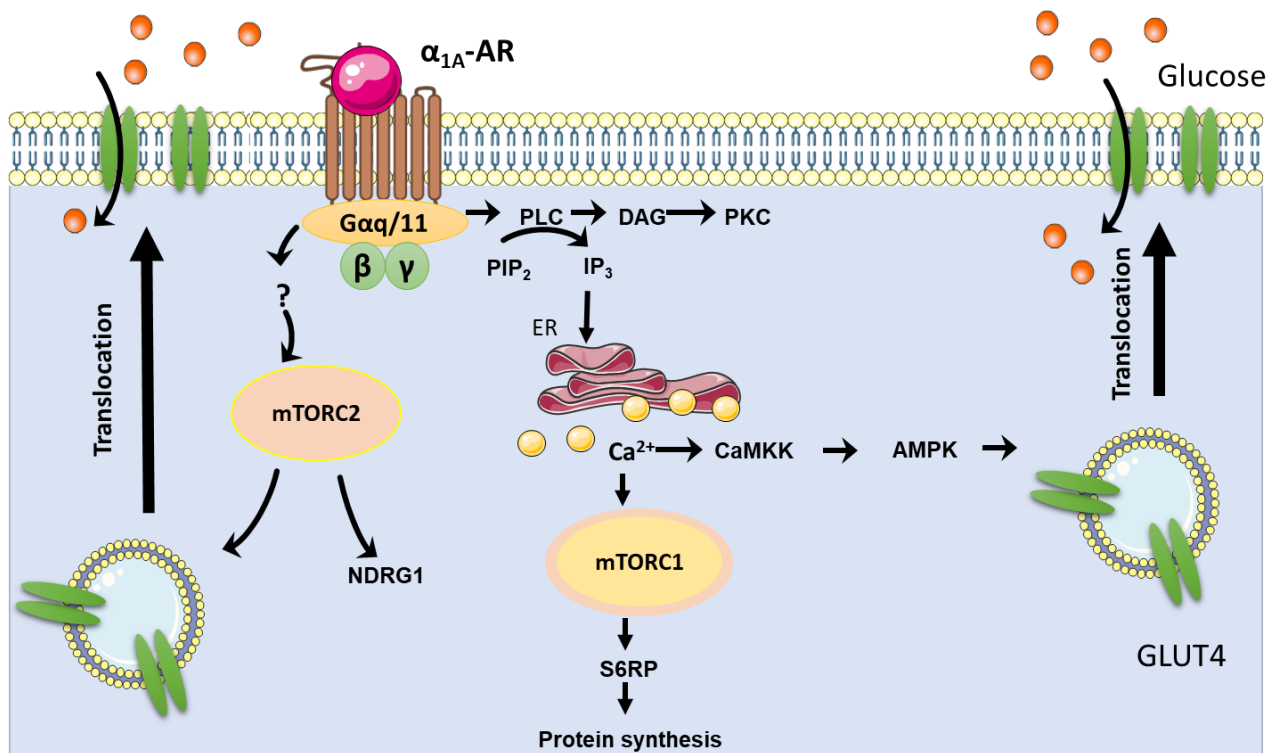
Figure 1.14: α_{1A}-Adrenoceptor mediated glucose uptake and protein synthesis signalling pathway

Activation of α_{1A}-AR promotes both glucose uptake and protein synthesis via distinct pathways. Their activation causes PIP2 hydrolysis by PLC at the plasma membrane, releasing IP3 and DAG (Hutchinson & Bengtsson, 2006; O'Connell et al., 2014). The mechanism underlying increased glucose uptake is as follows; IP3 binding to the IP3 receptor on the sarcoplasmic reticulum stimulates Ca^{2+}release, which in turn activates CaMKK and AMPK. mTORC2 is also activated via an AMPK-independent pathway. NDRG1 is directly activated by mTORC2, and serves as a downstream marker of mTORC2 activation (Weiler et al., 2014). Activation of AMPK and mTORC2 stimulates GLUT4 translocation to the plasma membrane and increases glucose uptake (Hutchinson & Bengtsson, 2006; Sato et al., 2018). DAG at the plasma membrane activates PKC (O'Connell et al., 2014). It has been suggested that the PLC-PKC pathway is also linked to glucose uptake, but there is little evidence for the mechanisms involved. In contrast, protein synthesis pathway involves mTORC1 – S6RP following Ca^{2+}release from the ER. Images of receptor, membrane, glucose and ER were obtained from www.servier.com.

Abbreviations: AC - adenylyl cyclase, AMPK – AMP-activated protein kinase, CaMKK - Calcium/Calmodulin-dependent Protein Kinase Kinase, cAMP – cyclic AMP, DAG – diacylglycerol, ER - endoplasmic reticulum, IP3 - inositol trisphosphate, mTORC1 – mammalian target of rapamycin complex 1, mTORC2 – mammalian target of rapamycin complex 2, NDRG1 - N-myc downstream regulated gene 1, PIP2 - phosphatidylinositol (4, 5)-bisphosphate, PKA – protein kinase A, protein kinase C – PKC, PLC - phospholipase C, S6RP - S6 ribosomal protein.

KU0063794 inhibited growth of cells, (2) Increased phosphorylation of S6RP (downstream target of mTORC1) was totally abolished by rapamycin treatment and (3) A23187 increased mTORC1 phosphorylation (Sato et al., 2018). Therefore, α_{1A}-AR mediated glucose uptake occurs via two distinct pathways involving Ca^{2+}-AMPK or mTORC2. In contrast, protein translation occurs via a Ca^{2+} and mTORC1-dependent pathway.

1.8 Aims and scope of the thesis

Insulin plays a major role in the regulation of glucose homeostasis and increases peripheral glucose uptake into insulin-sensitive tissues by a mechanism involving PI3K, Akt, and translocation of GLUT4 from the cytosol to the plasma membrane. In insulin resistance states, insulin-stimulated glucose uptake is significantly impaired (Abdul-Ghani & DeFronzo, 2010), mainly at the level of IRS1, PI3K and Akt. Recent studies have shown that activation of ARs increases peripheral glucose uptake independently of insulin (Sato et al., 2014a; Sato et al., 2018). This includes activation of α_{1A}-ARs in cardiomyocytes, β_2-ARs in skeletal muscle, and β_3-ARs in brown adipocytes (Liu & Stock, 1995; Merlin et al., 2018; Nevzorova et al., 2002; Nevzorova et al., 2006; Ngala et al., 2008; Ngala et al., 2009; Olsen et al., 2014; Sato et al., 2014a; Sato et al., 2018). Our previous and current studies indicate that AR mediated glucose uptake occurs via activation of signalling pathways that are distinct from that of insulin, in that they occur independently of PI3K or Akt, but share some common signalling effectors such as mTOR (Sato et al., 2014a; Sato et al., 2018). However, the mechanism whereby ARs promote glucose uptake is still not clear. This thesis therefore focuses on filling our knowledge gaps in which signalling pathways/mediators are activated following α_{1A}-AR and β_2-AR activation, and whether they are involved in increased glucose uptake. This will lead to a deeper understanding of the role of ARs in glucose metabolism. We have utilised three different model systems to address this goal. To investigate signalling pathways involved in β_2-AR mediated glucose uptake, we have firstly utilised L6 skeletal muscle cells that endogenously express the β_2-AR (Chapter 3) as well as recombinant cells expressing the cloned human β_2-AR (Chapter 4). This allows us to mechanistically explore regions of the receptor that may contribute to increased glucose uptake that can not be performed in cells endogenously expressing the receptor. To investigate signalling pathways involved in α_{1A}-AR mediated glucose uptake, we have utilised recombinant cells expressing the cloned human α_{1A}-AR (Chapter 5), and also cardiomyocytes that endogenously express the α_{1A}-AR (Sato et al., 2018).

Chapter 3: BRL37344 stimulates GLUT4 translocation and glucose uptake in skeletal muscle via β₂-adrenoceptors without causing classical receptor desensitisation

Activation of β₂-ARs in response to isoprenaline or zinterol increases glucose uptake in skeletal muscle, however it is also associated with elevation of cAMP level (Nevzorova et al., 2006; Sato et al., 2014a), which can elicit adverse effects including altered vasoreactivity and cardiac hypertrophy *in vivo* (Berdeaux & Stewart, 2012; El-Armouche & Eschenhagen, 2009; Sutherland & Robison, 1969). It was suggested that BRL37344, a dual β₂/β₃-AR agonist originally developed for the treatment of obesity, is different from those classical β-AR agonists as it increases glucose uptake in skeletal muscle via β₂-ARs without increasing global cAMP levels (Roberts & Summers, 1998). This could be of importance as targeting the β₂-AR therapeutically to promote skeletal muscle glucose uptake may result in adverse on-target effects in other tissues expressing β₂-AR. However, the mechanism of BRL37344-stimulated glucose uptake has not been rigorously investigated. We therefore examined the mechanism of isoprenaline- and BRL37344-stimulated glucose uptake in L6 cells.

Chapter 4: GRK and PKA phosphorylation sites in the β₂-AR tail are not involved in β₂-AR mediated glucose uptake

β₂-AR mediated glucose uptake in response to conventional agonists such as isoprenaline occurs via cAMP, PKA and mTORC2 in skeletal muscle (Sato et al., 2014a). However, since inhibition of AC/PKA only partially inhibited β₂-AR mediated glucose uptake (Nevzorova et al., 2002; Nevzorova et al., 2006; Sato et al., 2014a), this may suggest the involvement of more than one pathway. One possible signalling molecule is GRK (Mayor et al., 2018), which has a role in β₂-AR mediated glucose uptake in transfected CHOGLUT4myc cells since (1) truncation of the β₂-AR C-terminus (lacking GRK mediated receptor phosphorylation sites) reduced isoprenaline-stimulated glucose uptake, (2) isoprenaline-stimulated glucose uptake in cells expressing a β₂-AR (-)GRK mutant was reduced and (3) isoprenaline did not increase GLUT4 translocation in cells overexpressing a kinase-dead GRK2 (K220R) mutant (Dehvari et al., 2012). Therefore, we produced CHOGLUT4myc cells stably expressing the human wild type β₂-AR and a series of mutant β₂-ARs lacking different serine or threonine residues in GRK phosphorylation sites, and determined the relative contribution of these sites in β₂-AR mediated cAMP production and GLUT4 translocation/glucose uptake in response to isoprenaline and BRL37344.

Chapter 5: Cellular signalling in response to A61603 and dabuzalgron in CHOGLUT4 cells expressing human α_{1A}-adrenoceptors

Stimulation of cardiomyocyte α_{1A}-ARs prevents pathologic remodelling in heart failure by activating canonical survival pathways as well as metabolic pathways (Jensen et al., 2014; Sato et al., 2018). The α_{1A}-AR selective agonist A61603 increases glucose uptake, protein translation, and cell growth in both CHOGLUT4myc cells stably expressing the human α_{1A}-AR and in neonatal rat cardiomyocytes (Sato et al., 2018). Glucose uptake requires two parallel pathways involving Ca^{2+} - AMPK, and mTORC2 for glucose uptake, whereas activation of mTORC1-S6RP is required for protein translation. Dabuzalgron is novel α_{1A}-AR selective agonist, originally developed for the treatment of urinary incontinence (Blue et al., 2004; Musselman et al., 2004), and both A61603 and dabuzalgron protect against doxorubicin mediated cardiotoxicity without affecting blood pressure in animal models (Beak et al., 2017; Cowley et al., 2015; Jensen et al., 2011a; Vakhrusheva et al., 2008). In this study, we therefore further examined the signalling pathways activated by both A61603 and dabuzalgron in CHOGLUT4myc cells stably expressing the human α_{1A}-AR, with a focus on examining whether (1) dabuzalgron displayed biased agonism across a range of signalling pathways that are important in cellular metabolism and survival (2) whether glucose uptake mediated by α_{1A}-ARs is associated with production of cAMP which is known to activate mTOR in β-AR systems.

CHAPTER 2

General methods

2.1 Materials

Drugs and reagents were purchased as follows: 2-deoxy-[^{3}H] deoxy glucose (8 Ci/mmol), [^{3}H]-CGP12177A (either 30 ci/mmol or 37.7 ci/mmol), [^{3}H]-prazosin (78 Ci/mmol), (PerkinElmer, MA, USA); N^6- Benzoyladenosine- 3', 5'- cyclic monophosphate (6-Benz-cAMP), 8-Bromoadenosine 3',5'-cyclic monophosphate (8-Br-cAMP), A23187, A61603, BAPTA AM, BRL37344, Fluo-4-AM, forskolin, hoechst 33342 (H33342), 3-isobutyl-1-methylxanthine (IBMX), insulin, (-)-isoprenaline, KU0063794, (-)-noradrenaline, (−)-phentolamine, prazosin, protein kinase A inhibitor, rapamycin, U0126 and U73122 (Sigma-Aldrich, MO, USA); PKCζ pseudosubstrate, (S)-(-)-propranolol, tamsulosin and UBO-QIC (Tocris Bioscience, Bristol, UK); Myc-Tag (71D10) Rabbit mAb #2278 and phospho-NDRG1 (Thr346) (D98G11) XP® Rabbit mAb #5482 (Cell Signalling, MA, USA); IRDye® 800CW Goat anti-Rabbit IgG (Li-Cor®, NE, USA); Anti-NDRG1 antibody [EPR5593] (ab124689) and pitstop (Abcam, Cambridge, UK); SNAP-Surface Alexa Fluor 488 (New England Biolabs, Ipswich, MA, USA); AlexaFluor^{TM}488 Goat anti-Rabbit IgG (Thermo Fisher Scientific, MA, USA). Dabuzalgron was synthesized by Prof Jonathan Baell (Monash University, Australia). Other drugs and reagents are stated in Methods section, otherwise, they were of analytical grade.

Generally, compounds were diluted in either MilliQ purified water or dimethyl suphoxide (DMSO) and stored as single-use aliquots at -20°C, except for prazosin and noradrenaline which were freshly prepared before use.

All cell culture media, reagents and supplements were obtained as follows;

In The University of Nottingham
Dulbecco's Modified Eagle Media-Ham's, DMEM F12 (1:1), phosphate buffered saline (PBS), trypsin ethylenediaminetetraacetic acid (EDTA) solution, L-glutamine , G418, Blasticidin, clear 96 well plates (Sigma-Aldrich, MO, USA or Thermo Fisher Scientific, MA, USA); pcDNA 3.1(+) zeo vector, optiMEM, lipofectamine and zeocin (Invitrogen, Paisley, UK); foetal calf serum (FCS) (PAA laboratories, Pasching, Austria). Tissue culture flasks were from Thermo Fisher Scientific, MA, USA. Black side clear bottom cell culture 96-well microplates (655090), white side clear bottom cell culture 96-well microplates were from Greiner Bio-one, Stonehouse, UK.

In Monash University

Foetal bovine serum, Dulbecco's Modified Eagle Media (1x) (DMEM), Dulbecco's Modified Eagle Media (1x) (DMEM) F12 (1:1), phenol red-free DMEM, 2.5% trypsin, optiMEM, Hank's Balanced Salt Solution, HBSS, HEPES (Greiner Bio-one, Stonehouse, UK). G418, Lipofectamine (Thermo Fisher Scientific, MA, USA). Tissue culture flasks, clear 96 well plates, clear 24 well plates, clear 6 well plates were from Corning Incorporated, NY, USA. Black side clear bottom cell culture 96-well microplates, white ProxiPlate-384 microplates and white OptiPlate-384 microplates were from PerkinElmer, MA, USA. White side clear bottom cell culture 96-well microplates were from Greiner Bio-one, Stonehouse, UK.

2.2 Generation of β_2-adrenoceptor mutant constructs

2.2.1 Overview

The human β_2-AR cDNA including β_2-AR wild type (Figure 2.1), β_2-AR (-)GRKct or β_2-AR (-) GRK/PKA containing both start and stop codons was placed into pDONR201 (Thermo Fisher Scientific, MA, USA) by Dr. Peter Keov and Dr. Alaa Adbul-Ridha (Monash University). Mutation of specific β_2-AR sites was performed using site-directed mutagenesis. Mutated β_2-AR plasmids (Figure 2.2; Table 2.1) were then transformed into *E.coli* DH5α, and DNA was extracted for confirmation of point mutations in the β_2-AR coding region by DNA sequencing. Afterwards, the mutated β_2-AR inserts were transferred to the mammalian vector, pcDNA6.2/C-EMGFP-DEST (Thermo Fisher Scientific, MA, USA) by linear recombination (LR) reaction (gateway reaction), and the resulting plasmid was then transformed into *E.coli*. The extracted DNA by Miniprep was analysed by full sequencing of the insert. Sequence of DNA amplified by Maxipreps was again confirmed by sequencing.

2.2.2 Site-directed mutagenesis

This used an *in vitro* mutagenesis approach that promotes oligo-mediated introduction of specific changes in double stranded plasmid DNA. The mutant strand is synthesized by denaturation of DNA templates, annealing of mutagenic primers and extension of primers. The enzyme DpnI is then used to digest methylated and hemimethylated template DNA, so the only DNA remaining is the non-methylated mutated plasmid DNA generated during thermal cycling.
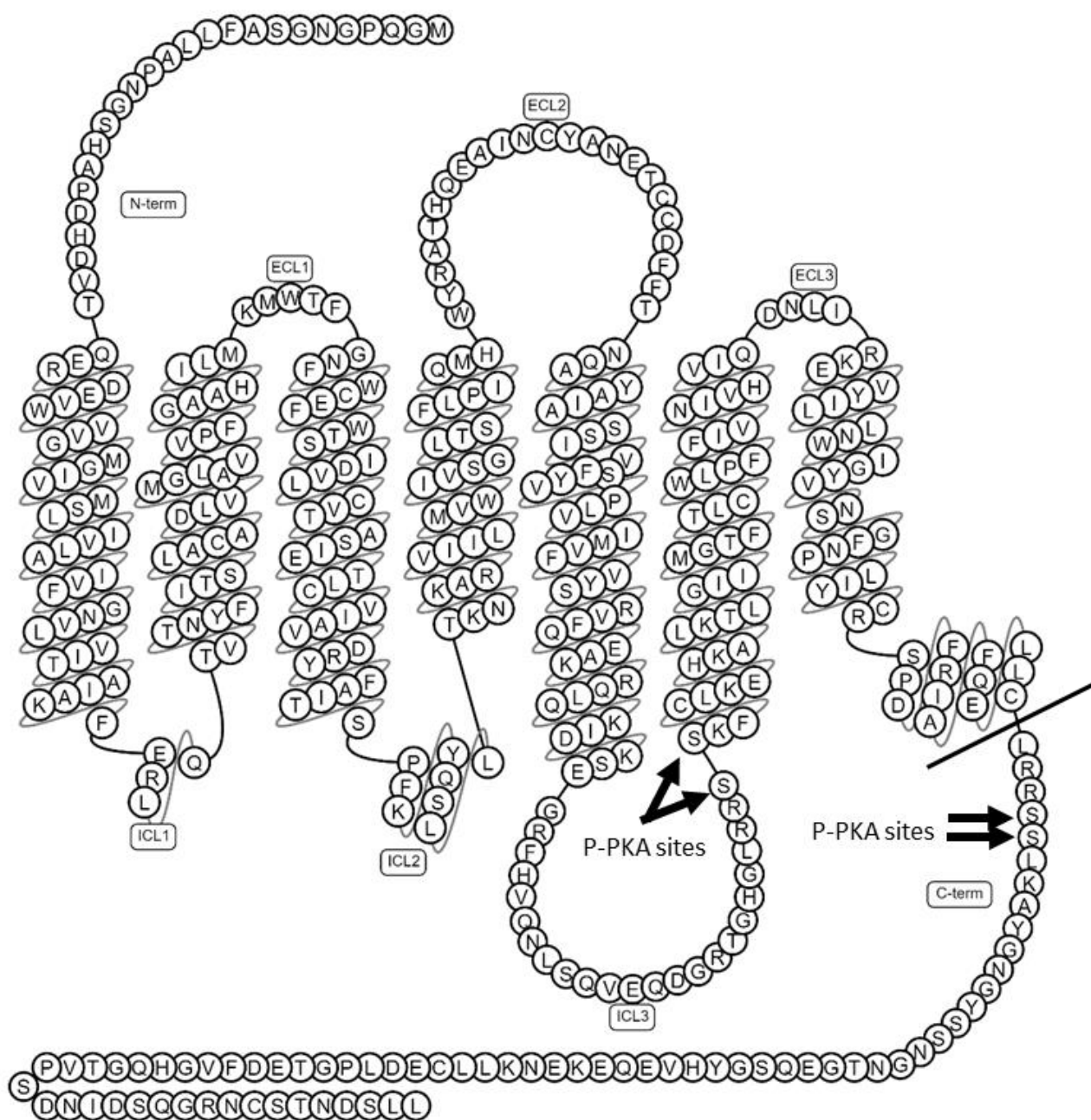
Figure 2.1: Topological model of the human β₂-AR

The topological model of β₂-AR (Genbank ref NM_000024) with PKA phosphorylation sites. This figure was adapted from http://gpcrdb.org/protein/adrb2_human/.

Figure 2.2: The sequences of β$_2$-AR wild type or mutant C termini, following the Cys palmitoylation site

The sequences of β$_2$-AR wild type or mutant receptors after the black line indicated in figure 2.1. Blue or yellow shows the amino acids mutated to alanine at potential GRK phosphorylation sites or PKA phosphorylation sites, respectively (Fredericks et al., 1996; Nobles et al., 2011). To note, PKA phosphorylation sites at the boundary of transmembrane domain 6 and intracellular loop 3 were also mutated to alanine in the β$_2$-AR (-) GRK/PKA construct.

Table 2.1: β$_2$-AR constructs

(A) β$_2$-AR wild type. β$_2$-AR mutants carrying mutations in which GRK and/or PKA phosphorylation sites are replaced by alanine residues, as follows; (B) β$_2$-AR (-) GRKprox 4 GRK site mutations in a proximal cassette, (C) β$_2$-AR (-) GRKct 7 GRK site mutations in distal cassette, (D) β$_2$-AR (-) GRKcom complete 11 GRK site mutations, (E) β$_2$-AR (-) GRK/PKA Complete 15 GRK/PKA site mutations, (F) β$_2$-AR DSLL 10 GRK site mutations except C-terminus PDZ motif (DSLL) and (G) β$_2$-AR DALL 1 mutation in the C-terminal PDZ motif.

Constructs	Description	Mutations	Figure 2.2
β$_2$-AR Wild type	None	0	(A)
β$_2$-AR (-) GRKprox	GRK site mutations in a proximal C-terminal cassette	4	(B)
β$_2$-AR (-) GRKct	GRK site mutations in distal C-terminal cassette	7	(C)
β$_2$-AR (-) GRKcom	Complete mutation of all GRK sites	11	(D)
β$_2$-AR DSLL	GRK site mutations except C-terminus PDZ motif (DSLL)	10	(E)
β$_2$-AR (-) GRK/PKA	Complete mutation of all GRK/PKA sites	15	(F)
β$_2$-AR DALL	Mutation in a C-terminus PDZ motif	1	(G)

To generate mutant β$_2$-AR constructs in pDONR201, the QuikChange Multi Site-Directed Mutagenesis kit (Agilent Technologies, Santa Clara, CA, USA) was used according to the manufacturer's instructions. In PCR tubes, the following materials were added; 100 ng template DNA (pDONR201 carrying β$_2$-AR wild type insert, β$_2$-AR (-)GRKct insert or β$_2$-AR (-) GRK/PKA insert) (Dehvari et al., 2012), 100 ng of both forward and reverse primers (Table 2.2), 1 µl of QuikChange Multi enzyme blend (Pfu turbo DNA polymerase) (2.5 U µl^{-1}), 1 µl of dNTP mix (10 U µl^{-1}), 0.5 µl of quick solution (which improves amplification efficiencies), 2.5 µl of 10 x QuikChange Multi reaction buffer made up to total 25 µl with double distilled water (ddH$_2$O). Reactions were initiated by heating at 95°C for 2 min. Denaturation, annealing and extension of target DNA fragments was at 95°C for 1 min, 55°C for 1 min and 65°C for 12 min (2 min/kb), respectively and this cycle was repeated 30 times. After the last cycle, tubes were heated at 65°C for 14 min prior to cooling down at 4°C. When reactions were completed, they were treated with 1 µl DpnI (Thermo Fisher, MA, USA) overnight at 37°C to degrade methylated template DNA.

2.2.3 Transformation

Chemically competent *E. coli* DH5α, made by Mr. George Christopoulos or Dr. Ann Stewart (Monash University, Australia), were defrosted on ice, and 50 µl was transferred into 15 ml tubes on ice. 3 µl of mutated/DpnI-treated plasmid DNA was added and incubated for 30 min on ice. Bacteria were heat-shocked at 42°C for 45 sec, and then placed on ice for 2 min to facilitate cellular DNA uptake. 300 µl of sterile super optimal broth with catabolite repression (SOC) media made by Dr. Ann Stewart was added to the tubes, then they were placed in a shaking incubator for 1 h at 37°C. Following the incubation, 200 µl of cell suspension was evenly spread onto Luria-Bertani (LB) agar plates containing 50 µg ml^{-1} kanamycin (Sigma-Aldrich, MO, USA), and the plates incubated overnight at 37°C. Next day, five individual colonies from each plate were picked using a 200 µl sterile pipette tip and inoculated into a 15 ml tube containing 5 ml LB broth (10 mg ml^{-1} NaCl (high salt), 10 mg ml^{-1} tryptone and 5 mg ml^{-1} yeast extract) and 50 µg ml^{-1} kanamycin, and the cells grown in a shaking incubator overnight at 37°C.

Table 2.2: Oligonucleotides used for QuikChange mutagenesis and sequencing

The β_2-AR WT or β_2-AR (-) GRKct was used for the template of generating of β_2-AR (-) GRKprox /β_2-AR DALL or β_2-AR (-) GRKcom, respectively. Following the generation of β_2-AR (-) GRKcom, it was used for the template of β_2-AR DSLL. **Bold** indicates the mutated nucleotides. Primers used for sequencing were also included in this table.

Primers	Strand	Length	Sequence (5→3)
β_2-AR (-) GRKprox β_2-AR (-) GRKcom	Forward	51	GGAATGGCTAC**GCCGGC**AACGGCAAC**GCA**GGGGAGCAG**GGT**GGATATCACG
	Reverse	51	CGTGATATCC**ACC**CTGCTCCCC**TGC**GTTGCCGTT**GCCGGC**GTAGCCATTCC
β_2-AR DALL	Forward	31	GTAGTACAAATGAC**GCA**CTGCTGTAATCTAG
	Reverse	31	CTAGATTACAGCAGTG**CGT**CATTTGTACTAC
β_2-AR DSLL	Forward	31	GTGGTGCAAATGAC**TCA**CTGCTGTAATCTAG
	Reverse	31	CTAGATTACAGCAGTG**AGT**CATTTGCACCAC
pDONR seq5 (external)	Forward	25	TCGCGTTAACGCTAGCATGGATCTC
ICL3 (internal)	Forward	30	CGCAGGGGATCCAGGGTCTTTCAGGAGGCC
pDONR seq3 (external)	Reverse	24	GTAACATCAGAGATTTTGAGACAC
T7 promoter (external)	Forward	20	TAATACGACTCACTATAGGG
GFP (external)	Reverse	22	CGTCGCCGTCCAGCTCGACCAG

2.2.4 Miniprep

DNA was extracted following the instruction of Wizard® Plus SV Minipreps DNA Purification System (Promega, WI, USA). This isolation of plasmid DNA is based on the alkaline- sodium dodecyl sulfate (SDS) lysis procedure. The bacteria carrying the plasmid DNA of interest is lysed with alkaline-SDS solution. SDS also releases cell content by solubilizing cell membrane proteins and phospholipids. Addition of potassium acetate neutralizes the alkaline solution, and leads to the formation of a precipitant containing cell debris, proteins, lipids, small chromosomal DNA and SDS. Plasmid DNA floating in supernatant is captured onto silica in the presence of high salt. The bound DNA is released in water following the removal of contamination by a spin-wash.

5 ml of the overnight bacterial culture was centrifuged for 5 min at 4000 rpm to form a pellet, which was thoroughly resuspended in 250 µl of cell resuspension solution (50 mM Tris-HCl pH 7.5, 10 mM EDTA 100 µg ml^{-1} RNase A). The resuspended cells were lysed by mixing in 250 µl of the lysis solution (0.2 M NaOH, 1% SDS). 350 µl of the neutralization solution (4.09 M guanidine hydrochloride, 0.8 M potassium acetate, 2.1 M glacial acetic acid) was added and the suspension centrifuged for 10 min at 13000 rpm. A spin column was inserted into a provided collection tube, and the supernatant containing plasmid DNA from the centrifugation step was then transferred and centrifuged for 1 min at 12000 rpm. After discarding the eluate, the column was centrifuged with 750 µl of wash solution (60% ethanol, 60 mM potassium acetate, 8.3 mM Tris-HCl, 0.04 mM EDTA) for 1 min at 12000 rpm, and this wash step was repeated with 250 µl of wash solution. To remove any remaining ethanol, the column was centrifuged again for 2 min at 12000 rpm following discarding the eluate. 100 µl sterile ddH$_2$O was added to the spin column inserted to a sterile 1.5 ml microcentrifuge tube, and centrifuged for 1 min at 12000 rpm to elute the plasmid DNA. Mutations in β$_2$-AR were assessed by Sanger DNA sequencing on both strands using pDONR seq5 (forward) primer, β$_2$-AR ICL3 (forward) primer and pDONR seq3 (reverse) primer (AGRF, Vic, Australia).

2.2.5 DNA purification

The purity and yield of plasmid DNA was quantified using a Nanodrop™ 2000 Spectrophotometer (Thermo Fisher Scientific, MA, USA). Nucleic acids or proteins reach a peak absorbance at absorbance 260 nm or 280 nm, respectively. Quality of cDNA was assessed by ratio of absorbance at 260 nm and 280 nm (A$_{260/280}$). The ratio of 1.8 was considered as pure cDNA, and ratio of 1.7 − 1.9 was accepted as clean cDNA. Additionally, If the ratio is less than 1.7 or greater than 1.9 it

indicates high contamination with protein or RNA, respectively. Concentration of cDNA was calculated based on Beer-Lambert equation as follows;

$$C = \frac{A * \varepsilon}{b}$$

Where C is the nucleic acid concentration (ng μl^{-1}), A is the absorbance in AU (1AU = 50 ng μl^{-1} for double-stranded DNA), ε is the extinction coefficient of DNA (ng μl^{-1}) and b is the pathlength (0.1 cm for the Nanodrop).

2.2.6 Gateway reaction

Gateway technology uses the bacteriophage lambda recombination system to facilitate exchange of DNA sequences flanked by site-specific attachment (att) sites between vectors (Figure 2.3). The ccdB gene is a lethal gene which inhibits growth of *E. coli* strains by the interference with *E. coli* DNA gyrase. After recombination reactions therefore, cells that have taken up the empty destination vector containing a ccdB gene, or by-product molecules retaining the ccdB gene, fail to grow. Also, *E. coli* transformed with kanamycin resistant but not ampicillin resistant pDONR entry clones are unable to grow. Colonies which grow on ampicillin resistant plates are the positive colonies containing the DNA of interest in the destination vector pcDNA6.2.

DNA inserts encoding wild type and mutant β_2-ARs were transferred from the pDONR201 entry vector (Figure 2.4A) into the Gateway destination vector, pcDNA6.2/C-EMGFP-DEST (Figure 2.4B), using the LR Clonase kit (Thermo Fisher Scientific, MA, USA) in accordance with manufacturer's instructions. 150 ng of destination vector, 150 ng of β_2-AR pDONR plasmid, 2 μl of gateway LR cloning enzyme (Thermo Fisher Scientific, MA, USA), made up to 12 μl with ddH$_2$O, were added in 1.5 ml tubes on ice. Reactions were incubated overnight at room temperature (RT). The recombinant vector was transformed into *E. coli* strain DH5α as in Section2.2.3. Then, 200 μl of cells spread onto 100 μg ml^{-1} ampicillin (Sigma-Aldrich, MO, USA) resistant LB agar (35 mg ml^{-1}) plates were incubated overnight at 37°C. Next day, two individual colonies from the plates were picked using a 200 μl sterile pipette tip and dropped into a 15 ml tube containing 5 ml LB broth and 100 μg ml^{-1} ampicillin and grown in a shaking incubator overnight at 37°C. The following day, DNA was eluted by miniprep as in Section 2.2.4. Identification of correct insertion of β_2-AR DNA was confirmed by Sanger DNA sequencing on both strands using T7 promoter (forward) primer, ICL3 (forward) primer and GFP (reverse) primer (AGRF, Vic, Australia).
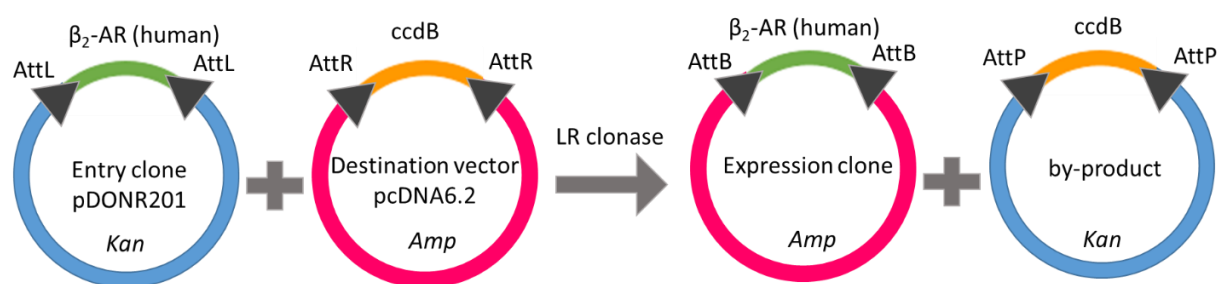
Figure 2.3: LR Reaction

It is a recombinant reaction between the attL-containing entry clone and attR-containing destination vectors to generate an attB-containing expression clone by LR Clonase enzyme mix
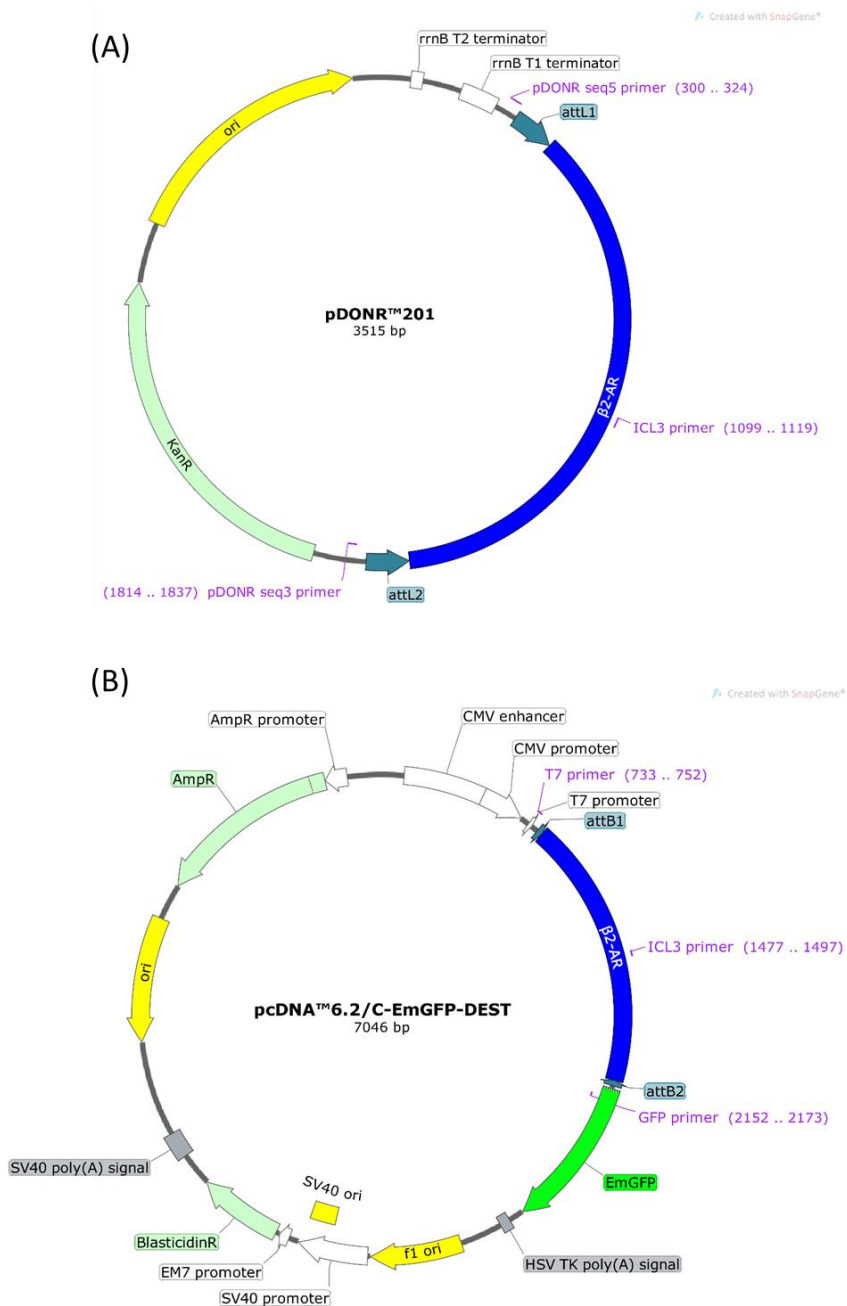
Figure 2.4: Plasmid map of pDONR201 and pcDNA6.2/C-EMGFP-DEST

(A) β$_2$-AR was originally placed in the entry clone pDONR201, (B) β$_2$-AR was placed between the attB1 and attB2 sites of a Destination vector, pcDNA6.2/C-EMGFP-DEST through LR reaction. These vectors also encodes resistance (R) genes for the antibiotics, Kanamycin (Kan) or Blasticidin (light green). Figures were created with SnapGene®.

Abbreviations/Descriptions: CMV - cytomegalovirus, EM7 - synthetic bacterial promoter, EmGFP - Emerald GFP, f1 - f1 bacteriophage, HSV TK - herpesvirus thymidine kinase, ori - origin of replication, rrnB T1 - transcription terminator T1 from the *E. coli* rrnB gene, rrnB T2 - transcription terminator T2 from the *E. coli* rrnB gene, poly (A) – polyadenylation.

2.2.7 Maxiprep

An individual colony picked using a 200 μl sterile pipette tip was dropped into a conical flask containing 250 ml LB broth and 250 μg ml^{-1} ampicillin, and grown in a shaking incubator overnight at 37°C.

HiSpeed Plasmid Maxi Kit (QIAGEN, Hilden, Germany) was used to isolate plasmid DNA according to the manufacturer's instructions. The bacterial culture was centrifuged (4000 rpm; 20 min), and the pellet formed was air dried. The pellet was completely dissolved in 10 ml of the chilled buffer P1 (Resuspension buffer; 50 mM Tris·Cl pH 8.0, 10 mM EDTA, 100 μg ml^{-1} RNase A). 10 ml of the buffer P2 (lysis buffer; 200 mM NaOH, 1% SDS (w/v)) was added to the resuspended cells and mixed by inversion. Addition of 10 ml of chilled buffer P3 (neutralization buffer; 3.0 M potassium acetate pH 5.5) to the lysed cells formed a white aggregate (cell debris, proteins, lipids, bacterial genomic DNA and SDS), which was centrifuged (4000 rpm; 5 min) to separate plasmid DNA from other material. During this centrifugation, HiSpeed Maxi Tips were prepared to use for filtration with 10 ml of buffer QBT (equilibration buffer; 750 mM NaCl, 50 mM MOPS pH 7.0, 15% isopropanol (v/v), 0.15% Triton® X-100 (v/v)). The lysate following centrifugation was transferred to a QIA filter cartridge and incubated for 10 min at RT. The cell lysate, followed by 2 x 30 ml of buffer QC (wash buffer; 1.0 M NaCl, 50 mM MOPS pH 7.0, 15% isopropanol (v/v)) was then filtered through HiSpeed Maxi Tips. DNA bound to the filter was eluted with 15 ml of buffer QF (elution buffer; 1.25 M NaCl, 50 mM Tris·Cl pH 8.5, 15% isopropanol (v/v)). 10.5 ml of isopropanol was added and incubated for 5 min at RT to precipitate DNA. It was applied to the QIA precipitator Maxi modules using a 30 ml syringe. The DNA bound in the QIAprecipitator was washed with 2 ml of 70% ethanol, in turn air dried to remove remaining ethanol. Finally, DNA was eluted into a sterile 1.5 ml microcentrifuge tube with TE buffer (10 mM Tris base pH 8.0, 1 mM EDTA). The purity and yield of plasmid DNA was quantified using Nanodrop^{TM} 2000 Spectrophotometer as described in Section 2.2.5.

2.3 Generation of SNAP-tagged β$_2$-adrenoceptor constructs

2.3.1 Overview

The SNAP tag lacking both start and stop codons, following a Kozak consensus site (GCCACC) for translation and 5HT3 receptor signal sequence (MRLCIPQVLLALFLSMLTGPGEGSRKLT), was placed into the multiple cloning site of the pcDNA3.1 (+) zeo vector (Figure 2.5) between the KpnI and

BamHI restriction sites by Dr Nick Holliday (The University of Nottingham) (Watson et al., 2012). Native and mutant human β_2-AR cDNAs lacking a start codon, but including a stop codon were then PCR amplified to introduce flanking restriction sequences, and placed in frame downstream of SNAP-tag in this vector between BamHI and XbaI restriction sites.

PCR β_2-AR products were amplified from the relevant pcDNA6.2/C-EMGFP-DEST construct. Both PCR products and the pcDNA3.1 (+) zeo SNAP vector was also digested with BamHI and XbaI restriction enzymes; and the vector was afterwards treated with thermosensitive alkaline phosphatase to remove phosphate groups at DNA ends and prevent ligation. The inserts and SNAP vector were purified, and ligated. The recombinant vector was transformed into competent XL-1 *E.coli*, and DNA was extracted by miniprep. Insertion of the insert was confirmed by loading on the gel and sequencing. A midiprep was then performed and the insert DNA sequence was again confirmed by sequencing.

2.3.2 Amplification of DNA of SNAP tagged β_2-AR

Using selected β_2-AR-pcDNA6.2/C-EMGFP-DEST constructs, the coding regions of wild type and mutated human β_2-AR (β_2-AR (-) GRKCom, β_2-AR (-) GRK/PKA, β_2-AR DALL) were amplified by PCR. Forward and reverse primers (Sigma-Aldrich, MO, USA, listed in Table 2.3) incorporated a flanking BamHI or XbaI site respectively. 50 ng of β_2-AR template, 3 µl of forward and reverse primers (600 nM final concentration), 2 µl of dNTP (400 µM), 5 µl of 10 x Pwo buffer (with 2.5 mM final concentration $MgSO_4$) made up to 50 µl with ddH_2O were placed in a sterile PCR tube. In a thermal cycler, tubes were heated at 95°C for 2 min, then held at 58°C. After the addition of 0.5 µl of Pwo proof reading polymerase (Roche, Basel, Switzerland), tubes were again heated at 72°C for 1 min 45 s. Denaturation, annealing and extension of target DNA fragments was set up at 95°C for 30 sec, 58°C for 1 min and 72°C for 1 min 45 s, respectively and this cycle was repeated 25 times. Reactions were then heated at 72°C for 7 min prior to cooling down at 4°C.
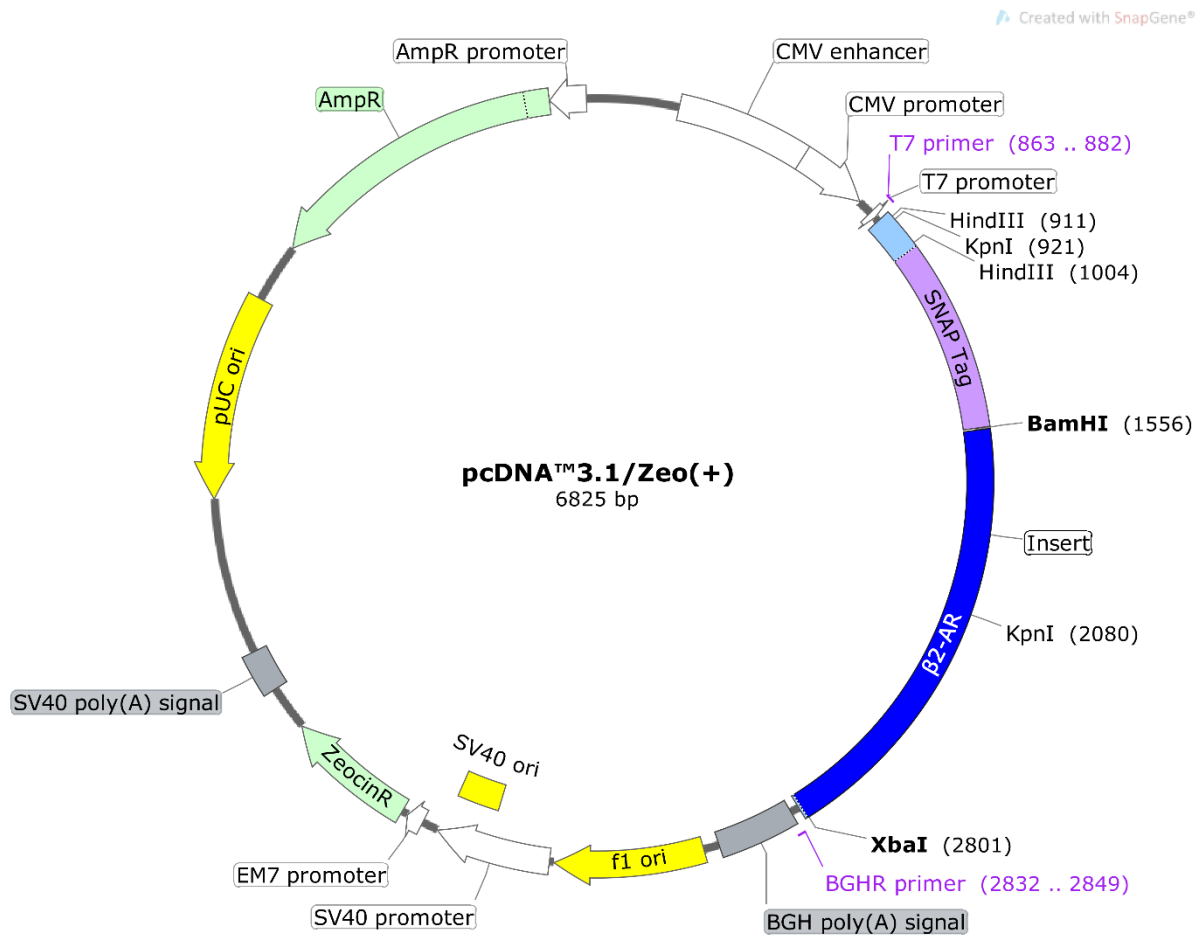
Figure 2.5: Plasmid map of pcDNA3.1 (+) zeo SNAP- β₂-AR vector

The signal sequence / SNAP tag (light blue / purple) and the β₂-AR (blue) was placed into the multiple cloning site of this vector between KpnI / BamHI and BamHI / XbaI restriction sites, respectively. This open reading frame starts from a start codon with 5HT3 receptor signal sequence following KpnI site and Kozak consensus site as indicated in light blue. The stop codon was encoded at the end of β₂-AR sequence. This vector also encodes resistance (R) genes for the antibiotics including ampicillin and zeocin (light green). Figure was created with SnapGene®.

Abbreviations/Descriptions; BGH - bovine growth hormone, CMV - cytomegalovirus, EM7 - synthetic bacterial promoter, f1 - f1 bacteriophage, ori - origin of replication, poly (A) – polyadenylation, pUC - high-copy-number ColE1/pMB1/pBR322/pUC origin of replication.

Table 2.3: Oligonucleotides used as PCR primers for SNAP β₂-AR cloning and for sequencing

The same forward primer including BamHI site (underlined) was used for PCR based amplification of all the constructs, and includes β₂-AR sequence starting at codon 2 in frame with the SNAP tag and BamHI site. The different reverse primers including XbaI site (underlined) were used for different constructs based on the mutated nucleotides at the C-termini. **Bold** indicates STOP codon. ***Bold and Italic*** indicates sites mutated from wild type β₂-AR sequence. Primes used for sequencing were also included in this table.

Primers	Strand	Length	Sequence (5→3)
β₂-AR Wild type (SNAP)	Forward	34	AATAAT<u>GGATCC</u>GGGCAACCCGGGAACGGCAGCG
	Reverse	35	ATAAGG<u>TCTAGA</u>**TTA**CAGCAGTGAGTCATTTGTAC
β₂-AR (-) GRKcom (SNAP)	Forward	34	AATAAT<u>GGATCC</u>GGGCAACCCGGGAACGGCAGCG
	Reverse	35	ATAAGG<u>TCTAGA</u>**TTA**CAGCAG***TGC***GTCATT***TGCAG***
β₂-AR GRKneg/PKAneg (SNAP)	Forward	34	AATAAT<u>GGATCC</u>GGGCAACCCGGGAACGGCAGCG
	Reverse	35	ATAAGG<u>TCTAGA</u>**TTA**CAGCAG***TGC***GTCATT***TGCAC***
β₂-AR DALL (SNAP)	Forward	34	AATAAT<u>GGATCC</u>GGGCAACCCGGGAACGGCAGCG
	Reverse	35	ATAAGG<u>TCTAGA</u>**TTA**CAGCAG***TGC***GTCATTTGTAC
T7 promoter (external)	Forward	20	TAATACGACTCACTATAGGG
BGHR (external)	Reverse	18	TAGAAGGCACAGTCGAGG

2.3.3 Separation of PCR DNA fragments by agarose gel electrophoresis

Agarose gel electrophoresis separates DNA fragments according to their size. When placed in an electric field, the negatively charged DNA fragments migrate to the positively charged electrode, and migration rate through the agarose gel is dependent on fragment size.

To prepare a 1% agarose gel, 500 mg of agarose was dissolved in 50 ml TBE buffer (89 mM Tris base, 89 mM boric acid, 2 mM EDTA; pH 7.6) by heating in a microwave for 2 min. It was then cooled down for 5-10 min, prior to addition of ethidium bromide (final concentration 100 µg ml^{-1}) to visualize DNA bands under ultraviolet (UV) light, and pouring the agarose into the gel tray and allowing it to set. Once the gel was formed, it was transferred into an electrophoresis tank containing TBE buffer. DNA samples in glycerol loading buffer and 1 kb DNA ladder (Promega, WI, USA) were loaded onto the gel and electrophoresed for 45 min at 80 V. The DNA bands were visualized using UV light, and the appropriate bands judged from the DNA ladder were immediately cut from the gel to prevent UV damage, then placed into a sterile 1.5 ml microcentrifuge tube.

Extraction of DNA from the gel was performed using the GenElute™ Gel Extraction Kit (Sigma-Aldrich, MO, USA) following the manufacturer's instructions. Briefly, the gel slice was completely dissolved in gel solubilisation solution (3 x gel volumes) for 10 min at 60°C, then isopropanol (1 x gel volume was added. This solution was transferred to the binding column inserted to a 2 ml collection tube, which was prepared for use by centrifugation of 500 µl of column preparation solution (1 min; 12,000 rpm). The DNA fragments bind to the membrane during centrifugation (1 min; 12,000 rpm), and 500 µl diluted wash solution (80% v/v ethanol) was added to the column and centrifuged (1 min; 12,000 rpm) to wash the column. After the eluate was discarded, tubes were centrifuged (1 min; 12,000 rpm) again to remove any remaining ethanol. The binding column was inserted into a new collection tube and centrifuged (1 min; 12,000 rpm) with 50 µl ddH$_2$O to elute the DNA fragments.

2.3.4 Restriction digestion of DNA

The amplified inserts encoding wild type human β_2-AR or mutated β_2-AR, and the SNAP-tagged pcDNA 3.1(+)zeo vector (Figure 2.5) were all double-digested at BamHI and XbaI sites (Thermo Fisher Scientific, MA, USA). Specifically, 400 ng of β_2-AR insert DNA, 1 µl of each restriction enzyme, and 2 µl FastDigest buffer (Thermo Fisher, Paisley, UK) made up to 20 µl with ddH$_2$O were placed in sterile

0.5 ml microcentrifuge tubes and incubated for 3 h at 37°C. The vector (2 μg) was digested by incubation (1 h at 37°C, 5 min at 80°C, 15 min at 65°C) in a tube containing 1 μl of each restriction enzyme, 2 μl FastDigest buffer, 2 μg DNA made up to 20 μl with ddH$_2$O. Vector was further treated with FastAP thermosensitive alkaline phosphatase (Thermo Fisher Scientific, MA, USA) to remove phosphate groups at DNA ends (1 h at 37°C, 10 min at 75°C). This dephosphorylation leads to reduced background colonies by preventing re-ligation of the empty vector.

The inserts and SNAP tagged vector were purified from other reaction components using GenElute™ PCR Clean-Up Kit (Sigma-Aldrich, MO, USA) according to the manufacturer's instructions. Briefly, 20 μl of enzyme digested product, 80 μl of ddH$_2$O, 500 μl of binding solution were mixed and then added to plasmid mini spin column inserted into a 2 ml collection tube, which was ready to use after addition and centrifugation of 500 μl of column preparation solution (30 sec; 12,000 rpm). It was centrifuged (1 min; 12,000 rpm), and the eluate was discarded. 500 μl of wash solution (80% v/v ethanol) was added and centrifuged (1 min; 12,000 rpm). To remove excess ethanol, it was centrifuged again (1 min; 12,000 rpm) after the eluate was discarded. The collection tube was replaced to a new collection tube, and 50 μl ddH2O was added and centrifuged (1 min; 12,000 rpm) to elute the DNA.

2.3.5 Ligation
After the purification of vector and insert DNA, inserts were ligated into the SNAP vector with the molar ratio of insert (1.2 kb): vector (5.7 kb) = 3:1.
Positive ligations (containing the insert DNA) were set up alongside negative ligations (containing ddH$_2$O instead of the insert DNA). 50 ng of vector and 30 ng of insert were incubated with 1 μl 10 x ligase buffer (final concentration: 40 mM Tris-HCl, 10 mM MgCl$_2$, 10 mM dithiothreitol, 0.5 mM ATP; pH 7.8), 1 μl T4 DNA ligase (Thermo Fisher Scientific, MA, USA), and appropriate volume of ddH$_2$O (total 10 μl), overnight at 16°C.

2.3.6 Bacterial transformation
Competent cells from *E. Coli* strain XL-1, made by Ms. Marleen Groenen (The university of Nottingham), were defrosted on ice, and 100 μl was placed to the sterile 1.5 ml microcentrifuge tubes on ice. 1.5 μl β-mercaptoethanol solution was added (20 mM) for 10 min on ice before incubation with 5 μl of ligated products (either positive and negative reactions) for 30 min on ice.

Afterwards, cellular DNA uptake was promoted by heat-shock reaction (45 sec at 42°C and 2 min on ice). 400 µl of sterile LB broth (20 g l^{-1}) was subsequently added to tubes, which were placed in a shaking incubator for 1 h at 37°C. Following the incubation, 150 µl of cells were spread onto 75 µg ml^{-1} ampicillin LB agar plates and incubated overnight at 37°C. Next day, the ratio of positive colonies containing the vector with the antibiotic resistance gene to negative colonies was determined by the direct comparison of colonies appeared on the agar plates. For each construct, individual positive colonies picked up using a 200 µl sterile pipette tip was dropped into a 30 ml tube containing 5 ml LB broth and 100 µg ml^{-1} ampicillin, and grown in a shaking incubator overnight at 37°C.

2.3.7 Miniprep

DNA was extracted following the instructions of GenElute™ Plasmid Miniprep Kit (Sigma-Aldrich, MO, USA). 3 ml of the overnight bacterial culture was centrifuged for 5 min at 3000 rpm to form a pellet, which was completely resuspended in 200 µl of chilled resuspension solution containing RNase to remove any RNA. The resuspended cells were lysed by mixing 200 µl of the lysis solution (NaOH / SDS). 350 µl of the neutralization/binding solution (potassium acetate) was added and centrifuged for 10 min at 13,000 rpm, resulting in separation of cell debris, chromosomal DNA, proteins, lipids and SDS in the pellet and the plasmid DNA in the supernatant. A GenElute Miniprep Binding column was inserted into the provided microcentrifuge tube, and 500 µl of the column preparation solution was added and centrifuged for 30 sec at 12,000 rpm to prepare columns. The supernatant containing plasmid DNA was then transferred and centrifuged for 30 sec at 12,000 rpm. After discarding the eluate, it was centrifuged with 750 µl of diluted wash solution (80% v/v ethanol) for 30 sec at 13,000 rpm to wash away residual salt and other contaminants. To remove any remaining ethanol, columns were centrifuged again for 2 min at 12,000 rpm after discarding the eluate. 100 µl sterile ddH$_2$O was added to the binding column inserted to a new microcentrifuge tube, and centrifuged for 1 min at 12,000 rpm to elute the plasmid DNA.

Identification of correct insertion of β$_2$-AR DNA was confirmed by gel analysis and DNA sequencing (The University of Nottingham, United Kingdom) on both strands using T7 promoter (forward) and BGHR (reverse) primers (Table 2.3).

2.3.8 Midiprep

An individual colony picked using a 200 μl sterile pipette tip was dropped into a 30 ml tube containing 50 ml LB broth and 100 μg ml^{-1} ampicillin, and grown in a shaking incubator overnight at 37°C.

QIAFilter™ Plasmid Midiprep Kit (QIAGEN, Hilden, Germany) was used to purify plasmid DNA according to the manufacturer's instructions. The principles of Midiprep procedure are the same as the one described under Maxiprep (Section 2. 2. 7). Bacterial culture was centrifuged (4000 rpm; 10 min), and the pellet formed was air dried. It was completely resuspended in 4 ml of buffer P1. 4 ml of the alkaline lysis buffer P2 was then added to the resuspended cells and mixed by inversion. Addition of 4 ml of chilled neutralization buffer P3 to the lysed cells, the lysate was left to stand for 10 min at RT as a white aggregate (cell debris, proteins, genomic DNA) was formed. In the meantime, QIAGEN-tips were prepared for use by filtration with 10 ml of buffer QBT. Then the lysate was filtered through a QIAFilter syringe into the primed QIAGENtip column, and allowed to elute via gravity flow. In turn 2 x 10 ml wash buffer QC was then filtered through QIAGEN-tips. DNA bound to the filter was eluted with 5 ml of buffer QF. 3.5 ml of isopropanol was added and centrifuged for 10 min at 4000 rpm. To wash the DNA pellet, 2 ml of 70% ethanol was added and centrifuged for 10 min at 4 000 rpm. A further ethanol purification step was made by adding 2.2 x volume of 100% ethanol and 0.1 x volume of 3 M sodium acetate (pH 5.2) to this DNA pellet. It was centrifuged (10 min; 4000 rpm), and the formed pellet was then washed by 2 ml of 70% ethanol. Following centrifuge (5 min; 4000 g), the ethanol was removed, and the pellet was air-dried for 10 min. It was then dissolved in TE buffer (1 μg μl^{-1}).

Sample DNA was sequenced on both strands using T7 and BGHR primers at The University of Nottingham, United Kingdom. The purity and yield of plasmid DNA was quantified using NanodropTM 2000 Spectrophotometer as described in Section 2.2.5.

2.4 Cell culture

2.4.1 Growing and splitting cells
CHOβ$_2$GLUT4myc cells (CHO-K1 cells stably expressing different human β$_2$-AR constructs and myc tagged GLUT4) were grown in DMEM F12 (1:1) supplemented with 2 mM L-glutamine and 5%

(vol/vol) FCS in 75cm^2 tissue culture flasks (T75). The cells were grown at 37°C, in 5% CO$_2$. CHOα$_{1A}$GLUT4myc cells (CHO-K1 cells stably expressing human α$_{1A}$-AR and myc tagged GLUT4) were grown in DMEM F12 (1:1) containing 5% (vol/vol) FBS in 175 cm^2 tissue culture flasks (T175) at 37°C, 5% CO$_2$. G418 at 0.2 mg ml^{-1} was used for the maintenance of CHO cell lines. Rat L6 cells were grown as a monolayer in DMEM containing 10% (vol/vol) FBS, and 10 mM HEPES in 175 cm^2 tissue culture flasks.

Cells were split at 80-100% confluency. Media was removed and sterile phosphate buffered saline (PBS) was added to remove the remaining media in the flask. To detach the cells from flasks, 1 ml of 0.25% trypsin-EDTA solution was applied and incubated for 3-5 min at 37°C. 10 ml of media was added to terminate the trypsin reaction, and DMEM containing the detached cells was transferred to a 30 ml universal tube. Cells were centrifuged for 5 min (1000 rpm), then the resulting pellet was fully resuspended in 10 ml of media, from which 500 μl – 1 ml was split to the new flasks.

2.4.2 Freezing and thawing of cells

Cells grown in T75 flasks were collected in 30 ml tube following the centrifuge as described in Section 2.4.1. The pellet was resuspended with freezing media (FCS or FBS containing 10% (v/v) DMSO) 1 ml per stock/cryovial. The number of aliquots was 3 to 5, depending on the confluency of the cells. Stocks were then placed in -80°C or liquid nitrogen for long-term storage.

Cells were defrosted in a water bath, and immediately transferred into a T75 flask containing growth media. This was placed in the incubator at 37°C for 15 – 20 min until the cells attached to the flask. The media was then removed to wash away DMSO and replaced with flesh media for the cells to grow.

2.5 Generation of stable cell lines

2.5.1 Transfection

Human GLUT4 tagged with extracellular human c-myc epitope was placed into Mammalian expression vector, pDOL (neomycin resistant, selected by G418), and it was stably transfected to CHO-K1 cell line. This stable CHOGLUT4myc cell line was provided by Dr Kazuhiro Kishi (University of Tokushima, Tokushima, Japan) (Kanai et al., 1993). CHOGLUT4myc cells were placed in 25 cm^2

flasks (T25) and grown to 50% confluency in normal growth media (Section 2.4.1). Next day, transfection of the β_2-AR constructs was performed using lipofectamine according to manufacturer's instructions. Briefly, 2 µg of β_2-AR DNA (SNAP tagged or SNAP untagged) and 18 µl of lipofectamine were separately mixed with 200 µl optiMEM in sterile 1.5 ml microcentrifuge tubes. These two solutions were combined in one tube, and incubated for 30 min at RT to promote formation of lipofectamine/DNA complexes. While incubating, T25 flasks were washed with 1 ml of optiMEM and 1.2 ml of optiMEM was added. After incubation, the lipofectamine/DNA reactant was mixed with 800 µl of optiMEM, and transferred to the T25 flasks. Cells were then incubated overnight at 37°C and in 5% CO_2 to deliver DNA lipid complexes to cells.

2.5.2 Positive selection

The next day, cells were split into a T75 flask. They were maintained in growth media containing the selection antibiotics, blasticidin, zeocin or G418 (for untagged receptor expressing cells; 20 µg ml^{-1} blasticidin and 0.8 mg ml^{-1} G418, or for SNAP tagged receptor transfectants; 200 µg ml^{-1} zeocin and 0.8 mg ml^{-1} G418) for selection in cells containing pcDNA6.2, pcDNA3.1(+) or pDOL, respectively for two weeks. Media was replaced every three to four days with media still containing the selection antibiotics.

2.5.3 Dilution cloning

Dilution cloning was performed following two weeks of positive cell selection. Cells were trypsinised and counted using a haemocytometer. Two different sets of dilution cloning including 10 cells/ml (20 ml x 2) and 1 cell/ml (20 ml x 2) were prepared, 200 µl of which was added per well in clear bottomed 96 well plates (two plates each). Following one week, single colonies growing in the wells were marked, and wells were replaced with fresh media to promote further cell growth. When grown enough, wells containing single individual colonies were washed with PBS and treated with 50 µl trypsin-EDTA solution. Cells were then transferred to 24 well plates containing 2 ml of media. Cells were well suspended, and 200 µl x 2 samples from each well were added to white opaque tissue culture treated 96-well microplates (SNAP untagged) or 96-well microplates (SNAP tagged). Once confluent, cells were screened to identify positive clones using [^{3}H]-CGP12177A binding (untagged receptor transfections) or SNAP-surface labelling (SNAP β_2-AR transfectants).

2.5.4 Screening for the untagged β₂-adrenoceptor transfected cells

Media was removed, and replaced with 100 µl of serum free DMEM:F12 without or with 20 µM propranolol to determine total binding or non-specific binding, respectively. 100 µl of 2 nM [³H]-CGP12177A (calculation in Section 2.10.2) was added to all the wells and incubated for 2 h at 37°C, 5% CO_2. Incubations were terminated by washing in cold PBS twice, after which, 100 µl of Microscint 20 was added to each well. White plate back and top seals (Perkin Elmer, MA, USA) were applied to the bottom or the top of the plate, respectively. The radioactivity was measured on a Topcount NXT (Perkin Elmer, MA, USA) at 21°C for 2 min per well after overnight incubation at RT. The clones which showed more than 2-fold difference between total and non-specific binding were selected and grown in T75 flasks. Those candidate clones were again screened with whole cell [³H]-CGP12177A competition binding assays to select the clone for use in further functional assays.

2.5.5 Screening for the SNAP-β₂-AR transfected cells

The principle of fluorescent labelling by SNAP tag is summarised in Figure 2.6. Cells were labelled with 0.2 µM membrane impermeant SNAP-surface benzyl guanine-AF 488 (New England Biolabs, Hitchin, UK) in DMEM:F12 containing 10 % FCS for 30 min at 37°C, 5% CO_2, prior to treatment with vehicle or 10 µM isoprenaline for 1 h at 37°C, 0% CO_2. The reaction was terminated by aspirating the HBSS and adding 100 µl of 3% paraformaldehyde (Thermo Fisher Scientific, MA, USA) in PBS for 10 min at RT. Cells were washed with 100 µl PBS for 5 min, after which nuclei were stained with 100 µl of 2 µg ml⁻¹ Hoechst 33342 (H33342) for 15 min at RT. Cells were washed with 100 µl PBS once before imaging. Plates were scanned using an IX Ultra confocal plate reader (Molecular Devices, San Diego, CA, U.S.A.), using a Plan Fluor 40 x NA0.6 extra-long working distance objective. Two channels, DAPI (405 nm excitation) and FITC (488 nm excitation) were used to observe nuclei stained with H33342 and labelled receptors with SNAP-AF 488, respectively. After imaging, cells with appropriate morphology as well as positive SNAP labelling were picked and grown in T75 flasks. The selected clones were re-screened using the full internalisation assay to select cell lines for further experiments.
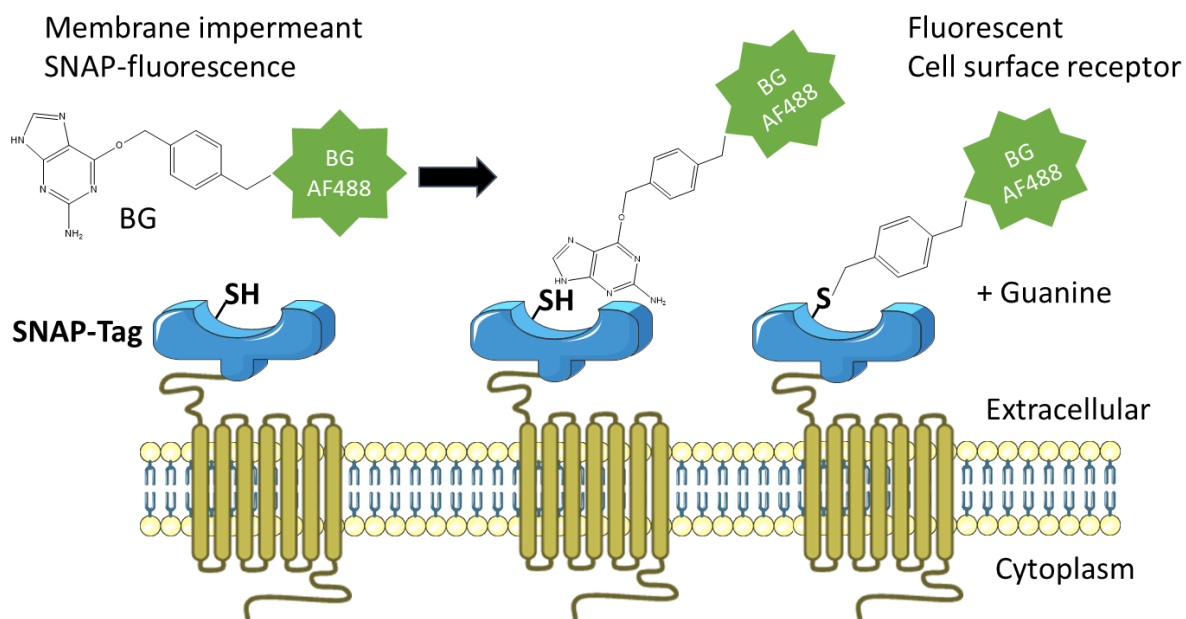
Figure 2.6: Fluorescent labelling of receptor at SNAP-tag

The SNAP-tag is fused to the N-terminal of receptor. When O6-benzylguanine (BG) derivatives bearing a fluorophore such as AlexaFluor 488 are added to the system, they release guanine and the fluorophore modified benzyl group is covalently bound to the SNAP tag via an irreversible reaction. This enables cell surface receptors to be visualized by selective fluorescent labelling (Keppler et al., 2003; Keppler et al., 2004).

2.6 Radioligand assays

2.6.1 2-deoxy-[^{3}H] D-glucose uptake

Cells were plated at 5×10^4 cells per well in 24-well plates. Cells were serum starved in DMEM F12 (1:1) supplemented with 2 mM L-glutamine or DMEM (starvation media) for 2 nights before an experiment. On the day of experiment, media incubated for 2 nights was replaced with flesh starvation media, and cells were exposed to agonists for 2 h at 37°C, 5% CO_2. Following incubation, media was removed and replaced with glucose-free media. Agonists were re-added and incubated for 15 min at 37°C, 5% CO_2. 2-Deoxy-[^{3}H]-D-glucose (8 Ci/mmol, final concentration 50 nM) was then placed for 15 min at 37°C, 5% CO_2 to allow the cells to take up glucose. The reactions were terminated by washing with PBS/DMEM (1:1) twice, after which, cells were lysed (0.4 M NaOH, 1 h, 60°C). Samples were transferred to scintillation vials (Sarstedt, Nümbrecht, Germany) containing 2.5 ml of Microscint 20 (PerkinElmer, MA, USA), and incubated for 1 h at RT. Radioactivity was counted on a β counter TriCarb 2910TR (PerkinElmer, MA, USA) for 3 min per vial at 21°C.

2.6.2 Whole cell [^{3}H]-CGP12177A saturation binding assays

Cells were plated at 1×10^4 cells / well in white side clear bottom tissue culture treated 96-well microplates. Next day, the media was removed from the plates. Cells were incubated with 100 µl of serum free DMEM F12 (1:1) supplemented with 2 mM L-glutamine in the absence (total binding) or presence of 20 µM (S)-(-)-propranolol (non-specific binding, final assay concentration 10 µM). 100 µl of 0.01 - 7nM [^{3}H]-CGP12177A in the same media was immediately added and the plates incubated for 2 h at 37°C, 5% CO_2. The assay was terminated by washing in cold PBS twice to remove free radioligand, after which 100 µl of Microscint 20 (PerkinElmer, MA, USA) was added to each well. White plate back and top seals (PerkinElmer, MA, USA) were applied to the bottom or the top of the plate, respectively. The plates were counted on a Topcount NXT at 21°C for 2 min per well after overnight incubation at RT. The actual concentration of [^{3}H]-CGP12177A used was also determined by counting 50 µl stock sample [^{3}H]-CGP12177A with 6 ml Microscint 20 (PerkinElmer, MA, USA) and 500 µl of 0.1 M imidazole (to prevent count variation due to different brands of Microsint 20) scintillation vials (Sarstedt, Nümbrecht, Germany) on a β counter TriCarb 2910TR (PerkinElmer, MA, USA) at 21°C for 3 min. Concentration of cellular protein was determined following cell lysis in 100 µl 0.4 M NaOH, using the Pierce™ bicinchoninic acid (BCA) Protein Assay Kit (Thermo Fisher Scientific, MA, USA) and bovine serum albumin as standard as in Section 2.6.4.

2.6.3 Whole cell [^{3}H]-CGP12177A competition binding assays

Cells were seeded at 1×10^4 cells / well in white side clear bottom tissue culture treated 96-well microplates and grown overnight. Next day, media was replaced with 80 µl of serum free DMEM F12 (1:1) supplemented with 2 mM L-glutamine. Serial dilutions of ligands were made up in the same serum free media at 10 × required final concentration (in a total assay volume of 200 µl), and 20 µl of each dilution was added to the plate in triplicate. Non-specific binding wells contained (S)-propranolol (10 µM). The incubation was started by addition of 100 µl of ~ 2 nM [^{3}H]-CGP12177A in the same media, for 2 h at 37°C, 5% CO_2. The radio ligand binding assay was terminated by washing in cold PBS twice and adding 100 µl of Microscint 20 (PerkinElmer, MA, USA). Radioactivities were counted as described in Section 2.6.2. Cellular protein concentration was determined as in Section 2.6.4.

2.6.4 Protein concentration determination

Protein concentration was determined using Pierce™ BCA Protein Assay Kit (Thermo Fisher Scientific, MA, USA) following the manufacturer's instructions. The BCA assay combines two reactions; (i) the reduction of Cu^{2+} to Cu^{1+} in complex with the peptide backbone under alkaline conditions (the biuret reaction), and (ii) a development reaction by which the two molecules of BCA react with one Cu^{1+} to produce a purple chelated complex. The amount of BCA/copper complex, measured by absorbance at 562 nm, is linearly proportional to protein concentration over the range investigated in the experiment. A series of BSA concentrations (0.125 mg ml^{-1} – 2 mg ml^{-1}) were prepared to generate the standard curve. 25 µl of each standard and samples were added in duplicate to a clear 96 well plate. 200 µl of BCA working reagent, made up with Reagent A containing sodium carbonate, sodium bicarbonate, bicinchoninic acid and sodium tartrate in 0.1 M sodium hydroxide and Reagent B containing 4% cupric sulfate in the ratio of 50 to 1, was added to each well. The plate was incubated for 30 min at 37°C and scanned on a MRX plate reader (Dynatech Labs, Chantilly, VA) to measure absorbance at 562 nm. The BSA absorbance values were plotted for a standard curve, and concentrations of samples were interpolated from their absorbance values.

2.7 Functional assays

2.7.1 LANCE cAMP assays

TR-FRET is a technology of fluorescence resonance energy transfer (FRET) combined with time-resolved measurement (TR). In this assay, when a donor (long-lived fluorescence) and an acceptor (short-lived fluorescence) are in close proximity, the energy is transferred between those two fluorophores, leading to the generation of a signal after the decay of background autofluorescence, which is proportional to the degree of product formation. Here, this technology describes a principle of detecting and quantifying cAMP produced upon the activation of the target receptors (Figure 2.7A, 2.7B). LANCE cAMP assay is based on the competition between sample cAMP and a europium-labelled cAMP tracer complex (Biotin-cAMP and streptavidin labelled with Europium-W8044 chelate, Eu-SA) for binding sites on AlexaFluor®647 labelled cAMP specific antibodies. In the absence of sample cAMP, the cAMP tracer complex bound to antibodies brings the cAMP donor Eu-chelate and antibody AF647 acceptor fluorophores into close enough proximity for FRET to take place. A light pulse at 340 nm excites the Eu-chelate of the cAMP tracer complex, leading to transfer the energy emitted by the Eu-chelate to AlexaFluor®647 on the antibodies. This emits light at 665 nm as an indicator of binding. The presence of unlabelled sample cAMP, however, competes for the interaction between cAMP tracer complex and antibodies so that intensity of the fluorescent measured at 665 nm is decreased. The sample cAMP concentration is therefore inversely proportional to the FRET signal.

Cells were plated at $1x10^4$ cells per well in 96-well plates. Cells were serum-starved overnight before each experiment. Next day, cells were treated with agonists in the stimulation buffer (0.1% BSA (w/v), 5 mM HEPES, 1 x HBSS pH 7.4) in the presence or absence of 0.5 mM IBMX for 30 min or 2 h at 37°C, 5% CO_2. For the time course study, agonists were added at decreasing time points prior to the lysis of cells. Media was removed by aspiration and the reactions were terminated by the addition of 100% ice cold ethanol. Ethanol was completely evaporated at RT and the lysis buffer (0.1% BSA (w/v), 0.3% tween-20 (w/v), 5 mM HEPES, H_2O, pH 7.4) was added to the plates. In each experiment, 100 µM forskolin was used as a positive control and all experiments were performed in duplicate.
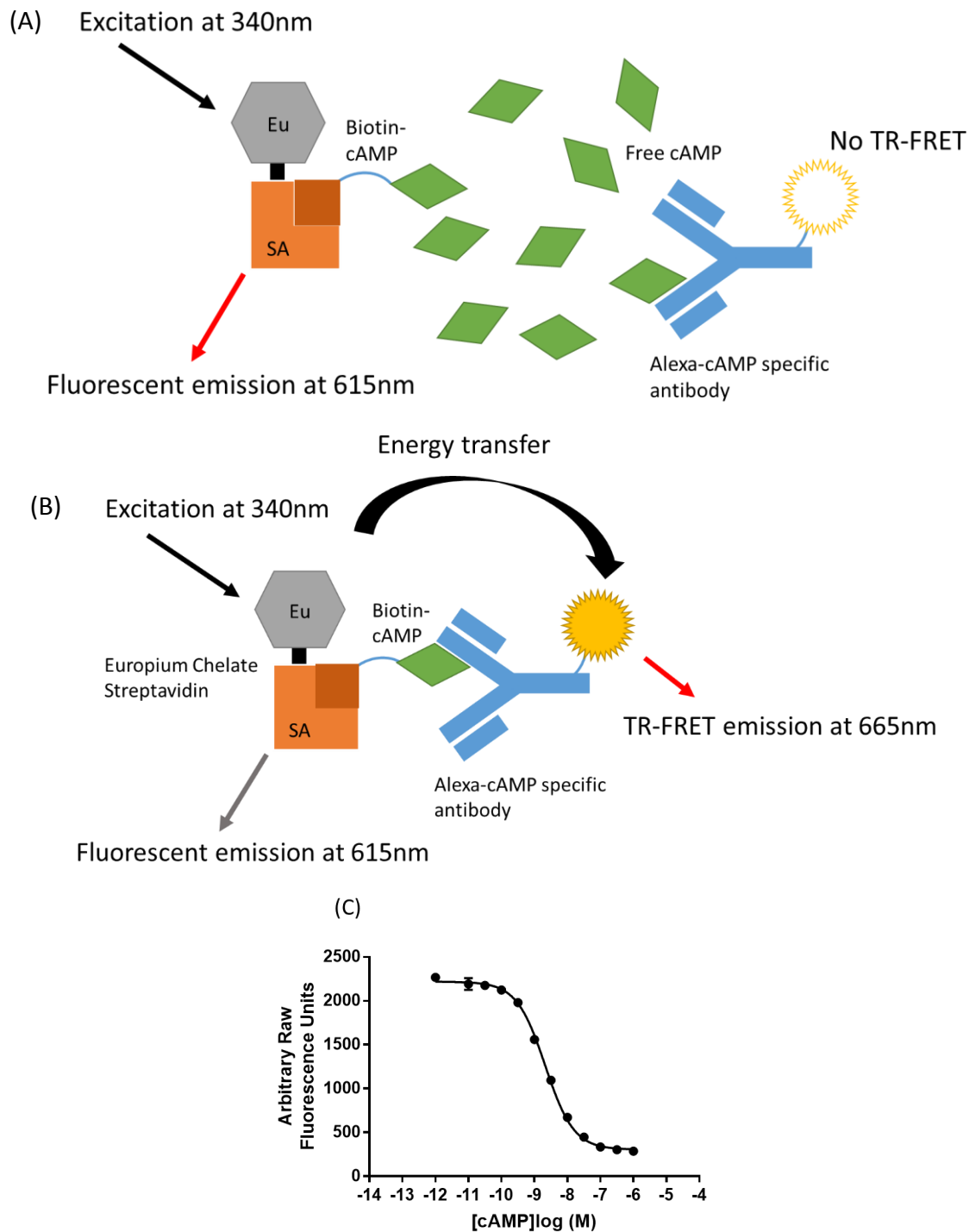
Figure 2.7: Principle of the LANCE cAMP Assay

In (A), without sample cAMP, the energy emitted from Eu-SA/bcAMP tracer is transferred to the cAMP antibodies, leading to generate a TR-FRET signal at 665 nm. In (B), the presence of cAMP interferes with the binding of Eu-SA/b-cAMP tracer to cAMP antibodies, leading to produce light at 615 nm. (C) An example of cAMP standard carve following 1 h incubation at RT.

cAMP was measured using LANCE assay (PerkinElmer, MA, USA) following manufacture's protocol. A series of cAMP concentrations ranging from 1 µM to 10 pM were prepared to generate the standard curve (Figure 2.7C). 5 µl of each standard and samples were added in white OptiPlate-384 microplates. 5 µl of antibody solution (Alexa Fluor® 647-anti cAMP antibody diluted at 1:100 in detection buffer composed of 50 mmol/l HEPES, 10 mmol/l calcium chloride, and 0.35% Triton X-100[1] pH 7.4) was also transferred to the plate and incubated for 30 min at RT. 10 µl of detection mix containing 0.02% LANCE Eu-W8044 labelled streptavidin (Eu-SA) and 0.07% Biotin cAMP (b-cAMP) in detection buffer was incubated for 1 h at RT. Production of cAMP was measured by time resolved fluorescence (dual emission at 665 nm and 620 nm, excitation at 337 nm), using a PHERAstar FS (BMG Labtech, Germany). Sample cAMP levels were extrapolated from standards (Figure 2.7C), and data were shown as pmol cAMP/well or were normalized with 100 µM forskolin.

2.7.2 Ca^{2+} mobilization assays

Cells were seeded at 5×10^4 cells per well in 96-well plates one day before an experiment. On the day of the experiment, cells were washed three times in a Ca^{2+} buffer containing 150 mM NaCl, 2.6 mM KCl, 1.18 mM $MgCl_2.2H_2O$, 10 mM D-glucose, 10 mM HEPES, 2.2 mM $CaCl_2.2H_2O$, and 2 mM probenecid, 0.5% (w/v) BSA in 1 x HBSS, pH 7.4. Under dim light condition, cells were incubated with membrane permeable 0.1% (v/v) Fluo-4 AM in Ca^{2+} buffer for 1 h at 37°C. Cells were washed with Ca^{2+} buffer twice to remove excess Fluo-4 AM, then incubated with 90 µl/well of Ca^{2+} buffer for a further 30 min at 37°C prior to transfer a plate to a FlexStation (Molecular Devices, Sunnyvale, CA). Ca^{2+} accumulation was measured by real time fluorescence (emission at 520 nm, excitation at 485 nm), and recorded every 1.7 s over 200 s with drug additions (10 µl/well, 1:10 dilution) occurring at 17 s. In each experiment, 1 µM A23187 was used as a positive control and all experiments were performed in duplicate. The data represents average agonist response obtained from peak [Ca^{2+}] measurements following subtraction of basal [Ca^{2+}] measurements, normalised to 1 µM A23187.

2.8 Phosphorylated protein assays

2.8.1 Amplified Luminescent Proximity Homogeneous (Alpha) screen assays
This is a bead-based technology to assess biomolecular interactions (Figure 2.8), and the phosphorylation of endogenous ERK1/2 (at T202/Y204) and S6RP (at S235/S236) were measured using this system. Donor bead labels containing a photosensitizer, phthalocyanine converts ambient

oxygen to singlet oxygen at 680 nm excitation. When analyte is captured by donor and acceptor beads in close proximity, energy transfer occurs from the singlet oxygen to thioxene derivatives within the acceptor bead, in turn emits light at 520-620 nm.

Cells were plated at $1x10^4$ cells per well in 96-well plates, and serum-starved overnight before an experiment. Cells were stimulated by agonists for 2 h at 37°C, 5% CO_2. For the time course study, agonists were added at decreasing time points prior to the lysis of cells. The reactions were terminated by the addition of 100 μl of 1 x lysis buffer. In each experiment, 10% (w/v) FBS was used as a positive control and all experiments were performed in duplicate. The activity of ERK1/2 and S6RP was measured using AlphaScreen SureFire pERK1/2 or pS6RP assay kit (PerkinElmer, MA, USA) according to the manufacturer's instructions. 4 μl of samples were transferred to white ProxiPlate-384 microplates. 5 μl of acceptor mix (acceptor beads, reaction buffer and activation buffer in the ration of 1:10:40) was added to the plate and incubated for 2 h at 37°C on the shaker. 2 μl of donor mix (donor beads and dilution buffer in the ration of 1:20) was placed and incubated for 2 h at 37°C on the shaker. The plate was then scanned using EnVision™ Multilabel Plate Reader (PerkinElmer Life and Analytical Sciences, Shelton, CT, USA), and Phospho-protein was measured by excitation wavelength; 680 nm and emission wavelength; 520–620 nm. Data in relative fluorescence units (RFU) obtained from the EnVision reader were normalised to basal.

2.8.2 InCell Western (Li-Cor) assays

Cells were plated at $1x10^4$ cells per well in black side clear bottom cell culture 96-well microplates and serum-starved over 2 nights. On the day of experiment, cells were stimulated with agonists for 2 h at 37°C. For the 2 h time course study, agonists were added at decreasing time points prior to the termination of the reaction. The reaction was terminated by aspiration of the media and fixation with 100 μl of 4% paraformaldehyde in PBS for 15 min at RT, and washed with PBS once. Quenching and permeabilisation of cells were accomplished by incubating with 100 μl of quench buffer (0.15 M Tris in PBS pH 8.0) with 0.01% Triton X for 10 mins at RT. Cells were washed with PBS three times, and this was then replaced to 100 μl of Odyssey® Blocking Buffer (Li-Cor®, NE, USA) and incubated for 1 h at RT.

$^1O_2$

Excitation 680nm

Emission 520nm-620nm

Biotinylated antibody

p

Streptavidin-coated
Alpha Donor Bead

Protein A conjugated
Acceptor Bead
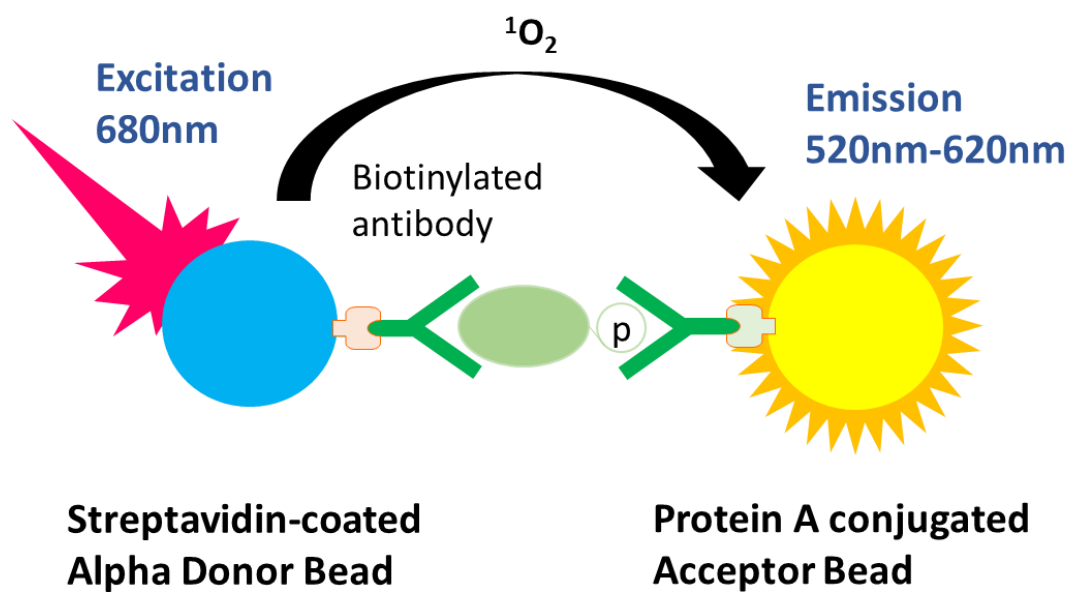
Figure 2.8: Principle of Alpha screen assay

In the presence of phosphorylated protein, for example ERK1/2, a sandwich antibody complex is formed between total and phosphor-specific antibodies linked to the donor beads and acceptor beads, using biotin-strepavidin, or protein A interactions. The release of singlet oxygen from the 680 nm excited donor beads transfers a cascade of energy to the acceptor beads in close proximity, which then emit light at 520-620 nm.

Next day, the blocking buffer was removed and 50 μl of primary antibodies, phospho- N-Myc Downstream Regulated 1 (p-NDRG1) rabbit monoclonal antibody, (#5482, Cell Signalling, NA, USA) and total NDRG1 rabbit monoclonal antibody, (ab124689, Abcam, Cambridge, UK) for control, diluted at 1:500 dilution in blocking buffer were added and incubated on the shaker 70 rpm overnight at 4°C. To note, these 2 primary antibodies were derived from the same host, therefore added in the separate plates seeded at the same number of cells at the same time. Cells were gently washed with our times with 150 μl/well of TBST (Tris-buffered saline, 0.1% Tween-20), then incubated with 100 μl of IRDye® 800CW Goat anti-Rabbit IgG (LCR-926-32211, Li-Cor®, NE, USA) diluted at 1:5000 in blocking buffer on the shaker 70 rpm for 2 h at RT under dim light condition. Prior to the imaging, cells were washed with 150 μl/well of TBST four times and TBST as completely aspirated. Plate was scanned using Odyssey Infrared Imaging System version 3.0 (Li-Cor®, NE, USA) with scan parameter as follows; scan resolution: 169 μm, quality: medium, focus offset: 3.0 mm, scan area: 13 cm x 9 cm. Channel, 800 was used to detect phosphor-NDRG1 and total NDRG1.

2.9 Microscope based assays

2.9.1 Internalisation assays

Cells expressing SNAP-tagged β_2-ARs were used to perform the internalisation assay (Kilpatrick et al., 2015).

Cells were plated at 1×10^4 cells per well in black side clear bottom cell culture 96-well microplates. Next day, cells were treated with 0.2 μM membrane impermeant SNAP-surface benzyl guanine-AF 488 (New England Biolabs, Ipswich, MA, USA) in growth media, DMEM F12 (1:1) supplemented with 2 mM L-glutamine and 5% (v/v) FCS, and incubated for 30 min at 37°C, 5% CO_2. Cells were then washed with 1 x HBSS, and incubated with required concentration of agonists for 1 h at 37°C, 0% CO_2. For the 1 h time course study, agonists were incubated for a time period as calculated (1 h minus various time points). Following incubation, all the steps including fixation, washing, staining and imaging were accomplished as described in Section 2.5.5.

2.9.2 Myc-GLUT4 translocation assays

Human c-myc epitope was tagged at the extracellular loop of human GLUT4 (GLUT4myc) (Kanai et al., 1993). Therefore, myc epitope was used for a marker of GLUT4 present at the cell surface. In non-permeabilized cells, only GLUT4 translocated to the plasma membrane was labelled with myc primary antibody (Dehvari et al., 2012).

Cells were plated at 1×10^4 cells per well in black side clear bottom cell culture 96-well microplates one day before an experiment. Cells were incubated with agonists in the DMEM F12 (1:1) supplemented with 2 mM L-glutamine for 2 h at 37°C, 5% CO_2. Alternatively, for the 2 h time course study, agonists were added at decreasing time points as indicated prior to termination of the reaction. The reaction was stopped by aspirating the media, and cells were subsequently fixed with 100 µl of 1% paraformaldehyde in PBS for 20 min at RT to limit cell permeabilisation. Cells were then quenched with 100 µl of 1 x quench buffer (0.15 M Tris in PBS, pH 8.0) for 10 min at RT, and blocked with 5% (w/v) of BSA in PBS for 2 h at RT. Cells were washed with PBS once before incubated with 50 µl of myc-tag primary rabbit polyclonal antibodies (#2278 Cell Signalling, MA, USA) (1:200 dilution in 1.5% (w/v) BSA in PBS) overnight at 4°C. Next day, cells were gently washed with PBS three times and incubated with AlexaFluor 488 Goat anti-Rabbit IgG secondary antibodies (Cell Signalling, MA, USA) (1:2000 dilution in PBS) for 2 h at RT under dim light conditions. Nuclei were stained with 100 µl of 2 µg ml^{-1} H33342 in PBS for 15 min at RT. Cells were then washed with PBS three times before observing the reactions by an IX Ultra confocal plate reader (Molecular Devices, San Diego, CA, U.S.A.), fitted with a Plan Fluor 40 x NA0.6 extra-long working distance objective. Nuclei and myc-GLUT4 labelling were imaged using DAPI (405 nm excitation, H33342) and FITC (488 nm excitation, SNAP-AF 488 labelled myc antibody conjugates) channels, respectively.

2.9.3 Fluorescence resonance energy transfer (FRET)

FRET is a technique to detect the generation of second messenger in real time and in live cells by measuring a distance of a pair of fluorophores in overlapping spectra (a donor and an acceptor fluorophore) fused to the peptide containing 'sensor' of the second messenger (Figure 2.9) (Halls & Canals, 2018). Energy transfer from an excited donor fluorophore to an acceptor fluorophore occurs if these two molecules are in their close proximity (less than 10 nm) (Clegg, 1995). If a second

messenger binds to the sensor peptide, it alters the distance between these two molecules following its conformational change, therefore changing the FRET signal (Halls & Canals, 2018).

Cells were plated at a density of 1×10^4 cells per well in black side clear bottom cell culture 96-well microplates (PerkinElmer). Cells were transfected with 40 ng of the FRET biosensors pmEpac2 or cytoEpac2 (Nikolaev et al., 2004; Wachten et al., 2010) using 1 mg ml^{-1} PEI. 24 h following transfection, media was changed to DMEM containing 0.5% FBS overnight. Single live cell FRET experiments were performed using a high-content GE Healthcare INCell 2000 Analyser as described previously (Halls et al., 2015). Briefly, fluorescence imaging was performed with a Nikon Plan Fluor ELWD 40 x (NA, 0.6) objective and FRET module. Cells were sequentially excited with a CFP filter (430/24) with emission measured with YFP (535/30) and CFP (470/24) filters and a polychroic mirror optimised for the CFP/YFP filter pair (Quad3). Cells in Hanks' balanced salt solution (HBSS) at 37 °C were measured every 1 min for 4 min to generate baseline emission ratio values. Cells were stimulated with vehicle or ligand, and images captured every 1 min for 20 min. At the end of every experiment, the same cells were stimulated for 10 min with the positive control (10 µM forskolin and 100 µM IBMX) to generate a maximal FRET change, and the positive emission ratio images were captured for 4 min.

2.10 Kinetic assay

2.10.1 Real time bioluminescence resonance energy transfer (BRET)

Bioluminescence resonance energy transfer (BRET) is a technique to monitor the interaction of one protein of interest (e.g., GPCR) fused to a donor luminophore such as Rluc, hRluc, Rluc2, or Rluc8 and another protein of interest (e.g., β-arrestin) fused to an acceptor fluorophore such as Venus or GFP10 (Figure 2.10) (Kocan & Pfleger, 2011). Oxidation of coelenterazine by the luminescent protein emits light. Under these circumstances, when the distance of luminophore and fluorophore is less than 10 nm in the presence of its substrate resonance energy transfer from the donor emission to the acceptor fluorescent protein can occur, detected as longer wavelength emission (Kocan et al., 2010).
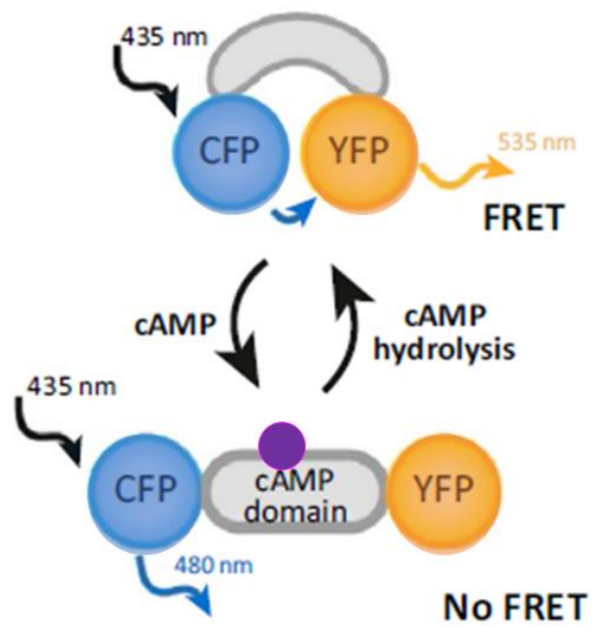
Figure 2.9: Principles of FRET detecting cAMP response

cAMP-binding domain is fused to a complementary pair of fluorophores, cyan fluorescent protein (CFP) and yellow fluorescent protein (YFP). Following binding of a second messenger, cAMP to cAMP-binding domain, FRET biosensors causes a conformational change, which increases the distance between these 2 fluorophores, thus resulting in loss of FRET signal. Figure was adapted from (Halls & Canals, 2018).

Recruitment of β-arrestin 1, β-arrestin 2 or Kras (plasma membrane marker) was measured by real time kinetic BRET assay (Kocan et al., 2008). CHOGLUT4myc cells seeded in 6 well plates at a density of 6×10^5 cells per well were co-transfected with β_2-AR-Rluc8 (100 ng/6-well) and β-arrestin 1-Venus (300 ng/6-well), β-arrestin 2-Venus (300 ng/6-well) or Kras-Venus (300 ng/6-well) using Lipofectamine 2000 (Thermo Fisher Scientific, MO, USA). The next day, cells were re-plated in white tissue culture treated 96-well microplates and grown overnight in phenol red-free DMEM with 5% FBS. 48 h following transfection, cells in each well were assayed in 100 µl final volume with 5 µM coelenterazine-H, and stimulated with 10 µl of 10 × concentration of ligand. BRET was measured at 37 °C by PHERAstar FS microplate reader (BMG LabTech, Germany). Emissions were simultaneously measured from donor Rluc8 (475 ± 15 nm) and acceptor Venus (535 ± 15 nm) were simultaneously recorded in time course. Cells were assayed before and after treatment with ligands or vehicle (5% FBS phenol red-free-DMEM media plus 0.01% (w/v) BSA). Ligand-induced BRET was calculated by subtracting the ratio of emission through the acceptor wavelength window over emission through the donor wavelength window for a vehicle-treated cell sample from the same ratio for a second aliquot of the same cells treated with ligand(s) (Kocan et al., 2008). The final pre-treatment reading is presented at the zero time point (time of ligand/vehicle addition).

2.11 Data analysis

All data were analysed using GraphPad Prism v7.02 (GraphPad software, San Diego CA, U.S.A) using pre-programmed equations. Definition of equation parameters were listed in Table 2.4.

All pooled data are represented as the mean ± standard error of the mean (s.e.mean) from 3 independent experiments performed in duplicate, triplicate or quadruplicate at least (exception was indicated). Independent experiments were individually fit and pooled parameters such as EC_{50} and Emax was expressed as the mean ± s.e.mean.

2.11.1 Agonist concentration response

Concentration response curves were analysed using the following equation

$$Response = \frac{Rmin + Rmax[D]}{[D] + EC_{50}}$$

Where Rmin is the minimal agonist response, Rmax is the maximal agonist response minus Rmin, [D] is the drug concentration, EC_{50} is agonist concentration which produces half maximal response as described in Figure 2.11. Hill slope is constrained to 1.
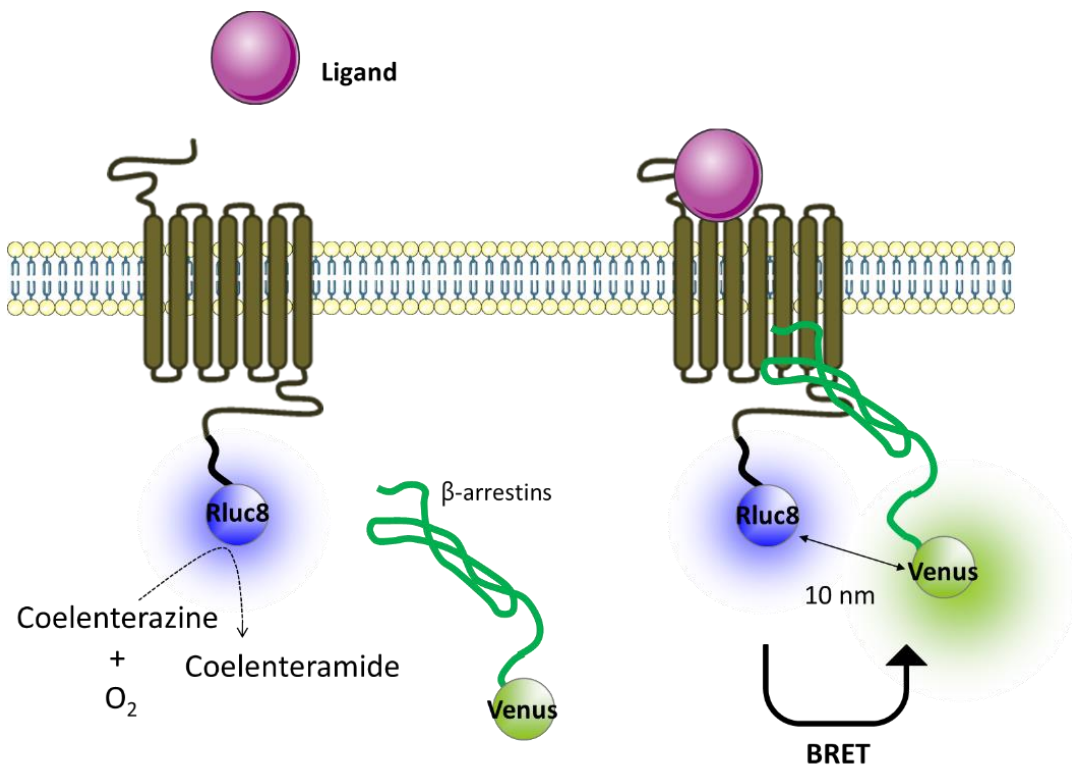
Figure 2.10: Principles of the BRET assay

The β_2-AR is fused to the donor fluorophore Rluc8, whereas the protein of interest such as β-arrestin, is fused to the acceptor fluorophore Venus. Following ligand binding to the β_2-AR, energy transfer occurs only when β_2-AR-Rluc8 and β-arrestin-Venus are in close proximity (< 10 nm apart).

Table 2.4: Definition of equation parameters

Parameter definitions	
[A]	Logarithm of agonist concentration
[AR]	Concentration of agonist occupied receptors
Background/Basal	Response in unstimulated system
Bmax	Maximal specific binding
[D]	Logarithm of drug concentration
EC_{50}	Agonist concentration which produces 50% of maximal response
Emax	Maximal possible response of the system
IC_{50}	Agonist concentration which inhibits 50% of maximal inhibition
K_A	Agonist dissociation constant; concentration of agonist required for occupancy of 50% of the receptors
K_D	Equilibrium binding constant
K_E	Stimulus coupling efficiency; concentration of agonist occupied receptor that elicits the half maximal tissue response
K_i	Affinity of the ligand
n	Slope of the transducer function
NS	Non-specific binding
R	Transduction coefficient (τ / K_A)
Rmax	Maximal agonist response
Rmin	Minimal agonist response
R_T	Total receptor concentration
SA	Specific activity
τ	Transducer ratio
V	Assay volume
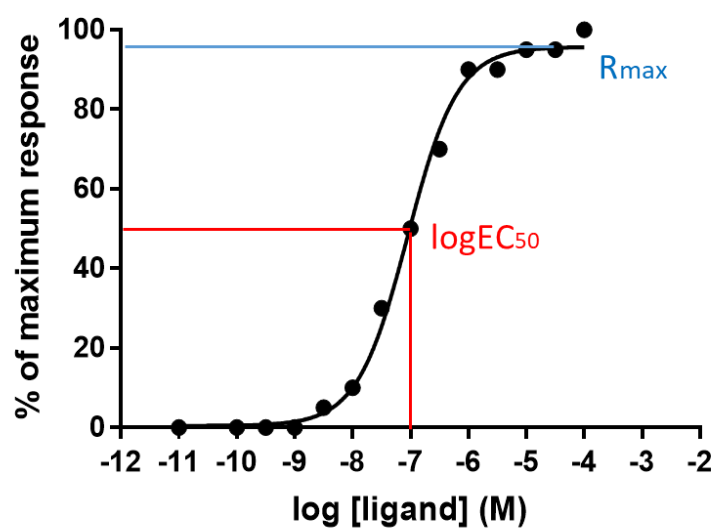
Figure 2.11: Concentration response curve analysis

Ligand maximal response (Rmax) and the logarithm of concentration of ligand that produces a half-maximal response (LogEC$_{50}$) were determined from concentration response curve.

2.11.2 Binding data analysis

2.11.2.1 Saturation binding

The actual free concentration of radioligand was calculated using the equation below relating the specific activity to the amount of radioligand, and conversion factor relating Ci to dpm (1 Ci = 2.22 x 10^{12} dpm)

$$\text{Moles radioligand} = \frac{\text{dpm}/2.22 \text{ x } 10^{12}}{\text{SA}}$$

$$\text{Concentration of radioligand} = \frac{\text{Moles radioligand}}{V}$$

Where dpm is the count in dpm (from the β counter standard sample), SA is the specific activity of [^{3}H]-prazosin (78 ci/mmol) or [^{3}H]-CGP12177A (either 30 ci/mmol or 37.7 ci/mmol) and V is assay volume.

Total binding and non-specific binding were calculated as follows;

$$\text{Non-specific binding} = (\text{NS x [D]}) + \text{Background}$$

$$\text{Total binding} = \frac{\text{Bmax [D]}}{K_D + [D]} + (\text{NS x [D]}) + \text{Background}$$

Where Bmax is the maximal specific binding, D is concentration of radioligand either [^{3}H]- prazosin or [^{3}H]-CGP12177A, K_D is the equilibrium binding constant, NS is the linear slope of the non-specific binding against radioligand concentration and background represents the counts without the addition of radioligand. These 2 equations were globally fit to obtain both total and non-specific binding data.

Specific binding was calculated by subtraction of non-specific binding from total binding using one site binding model as follows;

$$\text{Specific binding} = \frac{\text{Bmax [D]}}{K_D + [D]}$$

This equation was globally fit to obtain specific binding data.

Bmax was converted to fmol mg $^{-1}$ using the conversion factors (1 Ci = 2.22 x 10^{12} dpm and 10^{12} fmol = 1 mmol) and equations as follows;

$$\text{cpm/fmol} = \text{SA (Ci/mmol)} \times [2.22 \times 10^{12} \text{ dpm/Ci}] \times [\text{mmol}/10^{12} \text{ fmol}] \times \text{Efficiency (cpm/dpm)}$$

$$\text{fmol/mg} = \frac{\text{cpm} / (\text{cpm/fmol})}{\text{mg protein}}$$

Where SA is the specific activity of either [^{3}H]-prazosin or [^{3}H]-CGP12177A (either 30 ci/mmol or 37.7 ci/mmol), cpm is the count in cpm (from Top counter), mg protein was determined from protein assay (Section 2.6.4) and Efficiency was 30.7% via the fit of the β-spectrum in the Top counter.

2.11.2.2 Competition binding

Specific [^{3}H]-CGP12177A binding was determined by normalizing counts using non-specific binding in the presence of 10 µM (S)-(-)-propranolol (0%) and total binding (100%). IC$_{50}$ (the sample agonist concentration which inhibits 50% of [^{3}H]-CGP12177A binding) calculated by the equation, log (inhibitor) vs response with Hill slope = -1 was converted to pK$_i$ using the Cheng-Prusoff correction (Cheng & Prusoff, 1973);

$$IC_{50} = \frac{\text{Bottom} + (\text{Top} - \text{Bottom})}{1 + 10^{(\text{LogIC}_{50} - [\text{D1}])\,\text{HillSlope}}}$$

$$K_i = \frac{IC_{50}}{1 + \left(\frac{[\text{D2}]}{K_D}\right)}$$

$$pK_i = -\log K_i$$

Where D1 is the concentration of the sample ligand, top is the maximal agonist response, bottom is the minimal agonist response, K$_i$ is the affinity of the sample ligand, D2 is the concentration of [^{3}H]-CGP12177A and K$_D$ is the affinity of [^{3}H]-CGP12177A as obtained from saturation binding.

2.11.3 InCell western (Li-Cor) assay

Quantification of phosphor-NDRG1 and total NDRG1 was analysed using FIJI ImageJ software (National Institutes of Health, USA). Well was manually encircled and the same surface area was applied to all the wells to measure fluorescent intensity per well. The percentage of NDRG1 phosphorylation was determined by first normalizing phosphor-NDRG1 level to total NDRG1 level in each well, after which normalizing to the average of the vehicle treated wells. The figures

represent average well fluorescent intensity quantified by phospho-NDRG1/total NDRG1, normalized to vehicle.

2.11.4 Internalisation

Quantification of receptor internalisation was analysed using an automated granularity algorithm (MetaXpress 5.01, Molecular Devices). It was set to identify the intracellular receptor labelled compartments of 6–10 µm in diameter and nuclei of 7-11 µm in diameter (Figure 2.12). Grayscale intensity thresholds for identification were selected for each experiment with reference to the positive (10 µM isoprenaline) and negative (vehicle) controls. Each individual experiment collected 6 images per well (3 sites in duplicate) and the figures represent average fluorescent intensity / cell, normalized to vehicle.

2.11.5 GLUT4 translocation

GLUT4 translocation was quantified through automated multi wave scoring algorithm (MetaXpress 5.01, Molecular Devices), which scored cells 5-60 µm in diameter. Graylevel intensity thresholds were set according to the positive (10 µM insulin) and negative (vehicle) controls (Figure 2.13). Each individual experiment collected 6 images per well (3 sites in duplicate) and the figures represents stained integrity intensity, normalized to vehicle.

2.11.6 FRET

Data were analysed with the FIJI distribution of ImageJ (Schindelin et al., 2012). The three emission ratio image stacks (baseline, stimulated and positive) were collated and aligned with the StackCreator script (Halls et al., 2015). Cells were selected with the CellMarkup script (Halls et al., 2015), and fluorescence intensity was measured over the combined stack. Background intensity was subtracted, and then the FRET data were plotted as the change in FRET emission ratio relative to the maximal response for each cell [FRET ratio/maximum FRET ratio (F/Fmax)] using the BatchAnalyse script (Halls et al., 2015). Only cells that showed more than a 3% change relative to baseline after stimulation with the positive control were considered for analysis.

Figure 2.12: Representative granularity analysis images

CHO SNAP- β_2-AR WT cells were SNAP surface AF488-labelled and then treated with either 10 μM isoprenaline or 10 μM BRL37344 for 1 h at 37°C prior to fixation. The panels show nuclei stained with H33342 (left), SNAP- β_2-AR (middle), and granularity analysis (right), with nuclei in green and receptors containing granules of 6-10 μm diameter in white. Images are representative of 5 independent experiments performed in duplicate. For clarity, the images above were cropped to 500 x 500 pixels from the original 1000 x 1000 pixels image used for analysis.
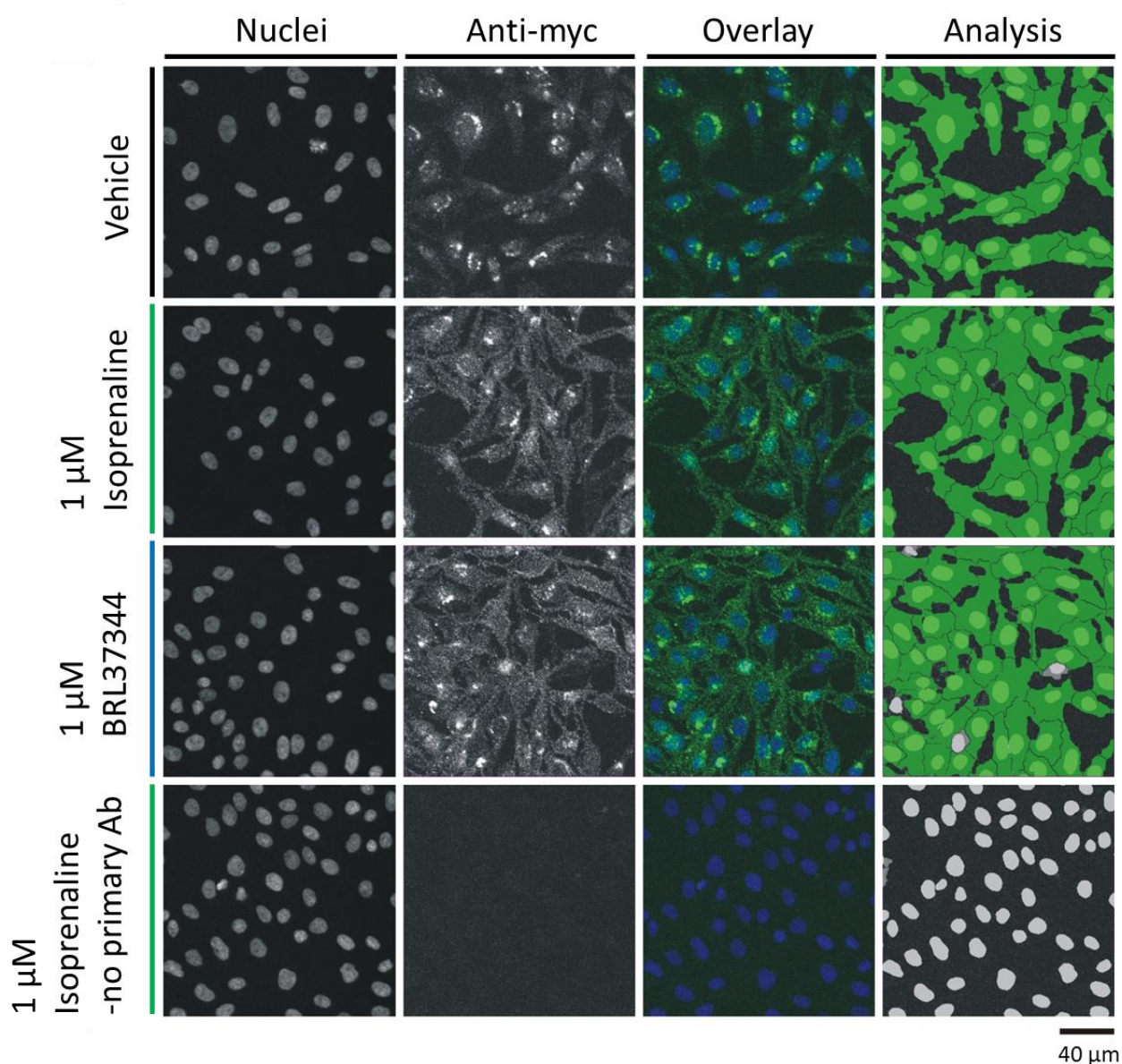
Figure 2.13: Representative multiwave scoring analysis images

Cells tagged at the extracellular human c-myc epitope were treated with either 1 µM isoprenaline or 1 µM BRL37344 for 1 h at 37°C prior to fixation. The panels show nuclei stained with H33342 (left), GLUT4-myc (centre left), overlay (centre right) and multiwave scoring analysis (right), with nuclei in blue and GLUT4-myc in green. Images are representative of 5 independent experiments performed in duplicate. For clarity, the images above were cropped to 400 x 400 pixels from the original 1000 x 1000 pixels image used for analysis.

2.11.7 The Black and Leff operational model

The operational model of Black and Leff (Black & Leff, 1983; Black et al., 1985) describes agonist activity as a function of agonist-receptor interactions and receptor-effector cascades that result in an observed response.

Equation 1 is based on the law of mass action, with receptor occupancy described by 3 parameters including agonist concentration ([A]), the agonist dissociation constant (K_A) and the total receptor concentration (RT).

$$\text{Equation 1,} \quad \text{Concentration of agonist bound receptor} = \frac{R_T[A]}{K_A + [A]}$$

The relationship between an observed agonist response and occupied receptor is described by equation 2;

$$\text{Equation 2,} \quad \text{Effect of the ligand} = \frac{E_{max}[AR]}{K_E + [AR]}$$

Where [AR] is concentration of agonist-bound receptor, Emax is the maximal possible response of the system, and K_E is the concentration of agonist occupied receptor that elicits a half-maximal cellular response. Combining equations 1 and 2 generates the commonly used operational model (equation 3);

$$\text{Equation 3,} \quad \text{Effect of the ligand} = \frac{(E_{max}\tau[A])}{K_A + [A](1 + \tau)}$$

$$\text{Where} \quad \tau = \frac{R_T}{K_E}$$

In this operational model, potency and maximal agonist response are described as follows (Figure 2.14);

$$EC_{50} = \frac{K_A}{\tau + 1}$$

$$R_{max} = \frac{E_{max}\tau}{\tau + 1}$$

Recently the classical Black and Leff operational model has been extended to quantify ligand bias using the 'Transduction coefficient' (R), which is a single parameter representing the effectiveness of the agonist defined by the ratio of τ/K_A. Effect of the ligand is determined differently depending on whether it is a full or partial agonist (van der Westhuizen et al., 2014)

$$R = \frac{\tau}{K_A}$$

Partial agonists

Equation 4, $\text{Effect of the ligand} = \text{Basal} + \dfrac{(E_{max} - \text{Basal})}{1 + \left(\dfrac{\frac{[A]}{10^{LogK_A}} + 1}{10^{LogR} \text{ x } [A]} \right)^{n}}$

Full agonists

Equation 5, $\text{Effect of the ligand} = \text{Basal} + \dfrac{(E_{max} - \text{Basal})}{1 + \left(\dfrac{[A] + 1}{10^{LogR} \text{ x } [A]} \right)^{n}}$

Where Basal is the response in the unstimulated system and n is the slope of the transducer function that links occupancy to response. Values of Emax, basal and n were shared between agonists and these equations were globally fit to obtain the effect of the ligand. For partial agonists $LogK_A$ was fitted (equation 4) whereas for full agonists $LogK_A$ was constrained to 0 (equation 5) (van der Westhuizen et al., 2014). More details about the use of LogR in the determination of bias are described in chapter 4 and 5.

2.11.8 Statistical analysis

All statistical tests were conducted in GraphPad Prism v7.02. The statistical significant difference was analysed by using Student's unpaired or paired t tests (between two groups), One-way ANOVA Dunnett's multiple comparisons test (between multiple groups), or Two-way ANOVA (between two curves) and expressed as follows, $*P < 0.05, **P < 0.01, ***P < 0.001$.
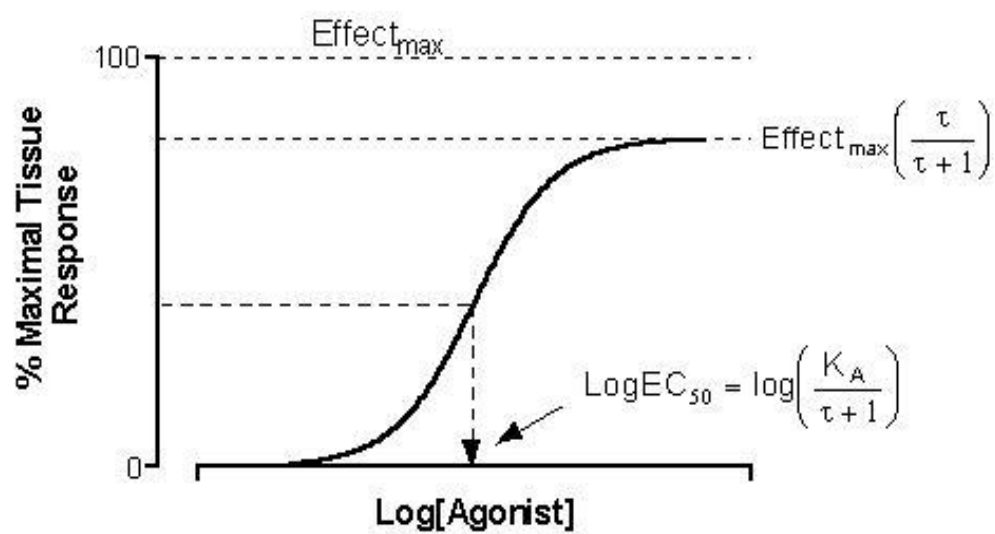
Figure 2.14: Agonist concentration curve in operational model

Agonist potency (EC_{50} value) is determined by $K_A / \tau + 1$ whereas agonist maximal response (Rmax values) is determined by $Emax(\tau / \tau + 1)$

CHAPTER 3

BRL37344 stimulates GLUT4 translocation and glucose uptake in skeletal muscle via β_2-adrenoceptors without causing classical receptor desensitisation

BRL37344 stimulates GLUT4 translocation and glucose uptake in skeletal muscle via β₂-adrenoceptors without causing classical receptor desensitisation

Saori Mukaida[1#], Masaaki Sato[1#], Anette I. Öberg[2], Nodi Dehvari[2], Jessica M. Olsen[2], Martina Kocan[1], Michelle L. Halls[1], Jon Merlin[1], Anna L. Sandström[2], Robert I. Csikasz[2], Bronwyn A. Evans[1], Roger J. Summers[1,3], Dana S. Hutchinson[1,3*], and Tore Bengtsson[2*]

[1]Drug Discovery Biology, Monash Institute of Pharmaceutical Sciences, Monash University, 381 Royal Parade, Parkville, Victoria 3052, Australia

[2]Department of Molecular Biosciences, The Wenner-Gren Institute, The Arrhenius Laboratories F3, Stockholm University, SE-106 91 Stockholm, Sweden

[3]Department of Pharmacology, Monash University, Clayton, Victoria 3800, Australia

[#]Authors contributed equally

*Author for correspondence:

Prof Tore Bengtsson

Department of Molecular Biosciences, The Wenner-Gren Institute, The Arrhenius Laboratories F3, Stockholm University, SE-106 91 Stockholm, Sweden

Email: tore.bengtsson@su.se

Telephone: +46 (0) 8 164126

Fax: + 46 (0) 8 156756

*Co-corresponding author:

Dr Dana Hutchinson

Drug Discover Biology, Monash Institute of Pharmaceutical Sciences, Monash University, 381 Royal Parade, Parkville, Victoria 3052, Australia

Email: dana.hutchinson@monash.edu

Telephone: +61 (0)3 99039077

ORCID: 0000-0001-9947-0106

Running title: Mechanisms of β₂-adrenoceptor mediated glucose uptake

Keywords: Glucose uptake; β₂-adrenoceptor; GLUT4; β-arrestin; skeletal muscle; receptor desensitisation; isoprenaline; BRL37344

Duality of Interest:

TB own stocks in Atrogi AB.

RJS and DSH are scientific advisors to Atrogi AB.

No other potential conflicts of interest relevant to this article were reported.

Abstract

The type 2 diabetes epidemic makes it important to find insulin independent ways to improve glucose homeostasis. This study examines the mechanisms activated by a dual β_2-/β_3-adrenoceptor agonist BRL37344 to increase glucose uptake in skeletal muscle, and its effects on glucose homeostasis *in vivo*. We measured the effect of BRL37344 on glucose uptake, GLUT4 translocation, cAMP levels, β_2-adrenceptor desensitisation, β-arrestin recruitment, Akt and mTOR phosphorylation using L6 skeletal muscle cells as a model. We further tested the ability of BRL37344 on skeletal muscle glucose metabolism in animal models (glucose tolerance tests, *in vivo* and *ex vivo* skeletal muscle glucose uptake). In L6 cells, BRL37344 increased GLUT4 translocation and glucose uptake via activation of only β_2-adrenceptors, with a similar potency and efficacy to that of the non-selective β-adrenoceptor agonist isoprenaline, despite being a partial agonist with respect to cAMP generation. This occurred independently of Akt phosphorylation but was dependent upon mTORC2. Furthermore, BRL37344 did not promote agonist mediated desensitisation of the receptor, since it failed to recruit β-arrestin1/2 to the β_2-adrenoceptor, as compared to isoprenaline. BRL37344 improved glucose tolerance tests and increased glucose uptake into skeletal muscle *in vivo* and *ex vivo* through a β_2-AR mediated mechanism. In conclusion, our results show that BRL37344 stimulates skeletal muscle glucose uptake via β_2-adrencoceptors independently of Akt. BRL37344 is a partial agonist with respect to cAMP, but a full agonist for glucose uptake, and importantly does not result in classical receptor desensitisation or internalisation of the receptor.

3.1 Introduction

There are currently 425 million adults living with type II diabetes (T2D) worldwide, with the incidence to increase by 48% to 629 million by 2045 (https://www.idf.org/about-diabetes/what-is-diabetes.html). The primary defects responsible for the development and progression of T2D are decreased peripheral glucose utilization due to loss of insulin sensitivity, impaired pancreatic insulin secretion, and increased hepatic glucose production. Skeletal muscle is the primary site of insulin-stimulated glucose uptake in the body, accounting for ~80% of insulin-stimulated glucose uptake in the fed state. While current medications such as metformin increase peripheral insulin sensitivity, they are not without side effects, including lactic acidosis, and are not recommended for patients with impaired liver and kidney function. The insulin signalling pathway is impaired in T2D (Frojdo et al., 2009), hence identifying new therapeutic avenues that target peripheral glucose utilization independently of insulin would have considerable merit.

Over 30 G protein-coupled receptors (GPCRs) have been implicated in the development, progression, and treatment of insulin resistance, obesity, and T2D (Riddy et al., 2018), including the β_2-adrenoceptor (β_2-AR) in skeletal muscle. Activation of the β_2-AR either by the endogenous ligands adrenaline and noradrenaline, or by selective β_2-AR agonists, results in an increase in glucose uptake (Abe et al., 1993; Liu & Stock, 1995; Nevzorova et al., 2002; Nevzorova et al., 2006; Sato et al., 2014a). One drawback of this approach is that β_2-ARs are also expressed in many other tissues including lung, heart, blood vessels, kidney, brain, lymphocytes and liver, potentially giving rise to a multitude of side effects. Additionally, glucose homeostasis may also be affected since β_2-AR activation is known to increase the secretion of glucagon and insulin (Ahren & Lundquist, 1981; Lacey et al., 1991) and to stimulate hepatic gluconeogenesis and glycolysis (Exton, 1987; Vardanega-Peicher et al., 2000). Persistent exposure of β_2-ARs to agonists also results in desensitisation, suggesting that any approach attempting to therapeutically target β_2-ARs to promote glucose uptake must minimize on-target effects on tissues other than skeletal muscle, and the loss of efficacy through receptor desensitisation.

In skeletal muscle, almost all β_2-AR mediated effects are thought to be attributable to cAMP, including inhibition of proteolysis (Navegantes et al., 2001), increased ion transport (Flatman & Clausen, 1979), increased force of contraction (Cairns & Dulhunty, 1993), and changes in gene expression (Nagase et al., 1996). However, the signalling pathways contributing to β_2-AR mediated

glucose uptake have until recently been unclear. Initial studies suggesting that phosphoinositide 3-kinase (PI3K), a key mediator of insulin stimulated glucose uptake, was involved were based on pharmacological inhibitors such as wortmannin and LY294002 (Nevzorova et al., 2006; Sato et al., 2014a). However, these PI3K inhibitors were likely mediating their effects via activity at related kinases, since a downstream target of PI3K, Akt, was not stimulated by the β_2-AR (Nevzorova et al., 2006; Sato et al., 2014a). Our recent work has revealed that β_2-AR mediated glucose uptake in skeletal muscle requires mammalian target of rapamycin (mTOR) and subsequent translocation of GLUT4 from intracellular vesicles to the plasma membrane (Sato et al., 2014a). While cAMP analogues do mimic the effects of β_2-AR agonists and also increase mTOR phosphorylation, GLUT4 translocation, and glucose uptake, inhibition of the Gαs-cAMP pathway only partially reduces β_2-AR mediated glucose uptake (Nevzorova et al., 2006; Sato et al., 2014a). As such, the underlying mechanism controlling mTOR activity and GLUT4 translocation is still unclear.

While β_2-ARs classically couple to Gαs proteins leading to increases in intracellular cAMP levels, it is now clear that β_2-AR signalling is pleiotropic, with downstream effects also mediated through Gαi/o proteins, MAP kinases, G protein coupled receptor kinases (GRKs), and β-arrestins (Evans et al., 2010). There is growing evidence to suggest that receptors, including the β_2-AR, that activate pleiotropic signalling may respond to different ligands with preferential activation of pathways giving rise to different signalling profiles, termed biased signalling (Evans et al., 2010). This is important, as while β_2-AR agonists such as clenbuterol increase skeletal muscle glucose uptake *in vitro* and *in vivo* and improve glucose tolerance *in vivo* (Ngala et al., 2008; Ngala et al., 2009; Sato et al., 2014a), its use in humans is problematic due to side effects including skeletal tremor and cardiovascular complications. Therefore, we aimed to determine if there are ligands that activate the β_2-AR and thereby increase glucose uptake but cause minimal cAMP signalling, to minimize on-target side effects in the heart and liver. Here, we suggest that another ligand, BRL37344, may have more potential. BRL37344 was originally developed in rodent models as a β_3-AR agonist (Arch et al., 1984) for the treatment of obesity, but failed to show efficacy in clinical trials. However, studies in humans showed that it did improve glucose tolerance and insulin sensitivity in obese and diabetic patients (Cawthorne et al., 1992). In some tissues it was subsequently shown to be a full β_2-AR agonist, increasing glucose uptake in skeletal muscle solely through actions at β_2- and not β_3-ARs (Liu et al., 1996; Nevzorova et al., 2002; Ngala et al., 2008; Ngala et al., 2009). Here we find that in L6 cells, BRL37344 has little effect on cAMP production but is as effective as isoprenaline and insulin

in promoting GLUT4 translocation and glucose uptake, suggesting that BRL37344 may have beneficial signalling properties at the β_2-AR compared to classical β_2-AR agonists such as isoprenaline. In addition, BRL37344, unlike classical β_2-AR agonists, increased glucose uptake without causing β_2-AR desensitisation. Finally, activation of β_2-ARs by BRL37344 had beneficial effects *in vivo* on glucose tolerance in glucose intolerant mice.

3.2 Materials and Methods

3.2.1 Cell culture

L6 cells from American Type Culture Collection (Manassas, VA, USA) were grown in DMEM supplemented with 4 mM L-glutamine, 10% (v/v) FBS, 100 Units/ml penicillin, 100 µg/ml streptomycin, and 10 mM HEPES, in a 37 $^{\circ}$C incubator with 5% CO_2. Cells were grown as myoblasts by ensuring cells were kept at less than 70% confluency. Upon confluency (90%), differentiation was induced by lowering the FBS concentration to 2% (v/v) for 7 days, with media changes every 2 days. Prior to experiment, L6 cells were serum starved overnight. Human primary skeletal muscle cells (SKMC) were purchased from Karocell AB (Stockholm, Sweden), Lonza (Basel, Switzerland), and Promocell GmbH (Heidelberg, Germany), and grown in Hams F-10 media containing 20% (v/v) heat-inactivated FBS, 2 mM L-glutamine, 50 Units/ml penicillin and 50 µg/ml streptomycin. Differentiation was initiated by reducing FBS levels to 4% (v/v) for 3 days followed by 2% (v/v) for 4 days. Prior to experiment, SKMC cells were serum starved overnight.

3.2.2 cAMP assays

Agonist-stimulated cAMP accumulation in L6 cells was measured using the LANCE cAMP detection kit (PerkinElmer) with 384-well white Optiplates (PerkinElmer) and a 2103 EnVision plate reader (PerkinElmer). L6 cells were plated at 1×10^4 cells per well in 96-well plates and differentiated as described above. Cells were stimulated with BRL37344 or isoprenaline in stimulation buffer (Hanks' Balanced Salt Solution (HBSS) containing 0.1% (w/v) bovine serum albumin (BSA), 5 mM HEPES, 1.3 mM $CaCl_2$, 5.6 mM glucose, pH 7.4) for indicated times at 37 °C. The assay was terminated by addition of 50 µl per well of 99.8% ethanol, and samples evaporated overnight. Lysis buffer (0.1% (w/v) BSA, 0.3% (v/v) Tween-20, 5 mM HEPES, pH 7.4; 100 µl/well) was added to each well. cAMP levels were quantified by mixing 10 µl of cell lysate with 5 µl cAMP antibodies labelled with Alexa Fluor 647 (ThermoFisher Scientific) and incubating for 30 minutes at room temperature. 10 µl of detection solution containing biotin-cAMP and europium-labelled streptavidin was added, and incubated overnight. Time-resolved fluorescence resonance energy transfer signals were acquired in a 2103 EnVision plate reader (PerkinElmer) using excitation at 340 nm, with emission measured at 615 and 665 nm wavelengths.

3.2.3 Förster resonance energy transfer (FRET) assays L6 myoblasts were plated at a density of 1×10^4 cells per well in black optically clear 96-well microplates (PerkinElmer) as described above. Cells were transfected with 40 ng of the FRET biosensors pmEpac2 or cytoEpac2 (Nikolaev et al., 2004; Wachten et al., 2010) using 1 mg/ml PEI. 24 h following transfection, media was changed to DMEM containing 0.5% FBS (v/v) overnight.

Single live cell FRET experiments were performed using a high-content GE Healthcare INCell 2000 Analyser as described previously (Halls et al., 2015). Briefly, fluorescence imaging was performed with a Nikon Plan Fluor ELWD 40 x (NA, 0.6) objective and FRET module. Cells were sequentially excited with a CFP filter (430/24) with emission measured with YFP (535/30) and CFP (470/24) filters and a polychroic mirror optimized for the CFP/YFP filter pair (Quad3). L6 cells in HBSS at 37 °C were measured every 1 min for 4 min to generate baseline emission ratio values. Cells were stimulated with vehicle or ligand, and images captured every 1 min for 20 min. To note, 1 μM of ligands were used to prevent saturation of the FRET cAMP sensors. At the end of every experiment, the same cells were stimulated for 10 min with the positive control (10 μM forskolin and 100 μM IBMX) to generate a maximal FRET change, and the positive emission ratio images were captured for 4 min. Data were analysed with the FIJI distribution of ImageJ (Schindelin et al., 2012). The three emission ratio image stacks (baseline, stimulated and positive) were collated and aligned with the StackCreator script (Halls et al., 2015). Cells were selected with the CellMarkup script (Halls et al., 2015), and fluorescence intensity was measured over the combined stack. Background intensity was subtracted, and then the FRET data were plotted as the change in FRET emission ratio relative to the maximal response for each cell [FRET ratio/maximum FRET ratio (F/Fmax)] using the BatchAnalyse script (Halls et al., 2015). Only cells that showed more than a 3% change relative to baseline after stimulation with the positive control were considered for analysis.

3.2.4 Real-time kinetic bioluminescence resonance energy transfer (BRET) assays

CHOGLUT4myc cells seeded in 6 well plates at a density of 6×10^5 cells per well were co-transfected with β_2-AR-Rluc8 (100 ng/6-well) and β-arrestin 1-Venus (300 ng/6-well), β-arrestin 2-Venus (300 ng/6-well) or Kras-Venus (300 ng/6-well) using Lipofectamine 2000 (Invitrogen). The next day, cells were re-plated in white tissue culture treated 96-well microplates and grown overnight in phenol red-free DMEM with 5% FBS. 48 h following transfection, cells in each well were assayed in 100 μl final volume with 5 μM coelenterazine-H, and stimulated with 10 μl of 10 × concentration of ligand. BRET was measured at 37 °C by PHERAstar FS microplate reader from BMG LabTech (Germany).

Emissions were simultaneously measured from donor Rluc8 (475 ± 15 nm) and acceptor Venus (535 ± 15 nm) were simultaneously recorded in time course. Cells were assayed before and after treatment with ligands or vehicle (5% FBS phenol red-free-DMEM media plus 0.01% (w/v) BSA). Ligand-induced BRET was calculated by subtracting the ratio of emission through the acceptor wavelength window over emission through the donor wavelength window for a vehicle-treated cell sample from the same ratio for a second aliquot of the same cells treated with ligand(s) (Kocan et al., 2008). The final pre-treatment reading is presented at the zero time point (time of ligand/vehicle addition).

3.2.5 Glucose uptake in L6 and SKMC cells

Glucose uptake was measured as previously described (Nevzorova et al., 2002). Briefly, cells were plated at $1x10^5$ cells per well in 12-well plates and differentiated as described above. Cell stimulation was performed with antagonists or inhibitors added 30 min ahead of agonists that were then incubated for 2 h at 37 °C. Media was then changed to glucose-free media, drugs re-added, and plates incubated for a further 15 min before 2-deoxy-^{3}H-D-glucose (50 nM) was added and the plates incubated for a further 15 min. Reactions were terminated by washing twice in ice-cold PBS. Cells were digested (0.2 M NaOH, 1 h, 60 °C), and samples transferred to vials with scintillation liquid and radioactivity measured by liquid scintillation counting.

3.2.6 Western Blotting

Differentiated myotubes in 12 well plates were serum-starved overnight prior to the experiment. Immunoblotting was performed as previously described (Lindquist et al., 2000). Primary antibodies (total AKT, phospho-CREB Ser 133, and mTOR Ser2481 diluted 1:1000) were all from Cell Signalling and were detected using a secondary antibody (horseradish peroxidase-linked anti-rabbit IgG, Cell Signalling) diluted 1:2000 and enhanced chemiluminescence (ECL, Amersham Biosciences).

3.2.7 αScreen assays for protein phosphorylation

Phosphorylation of Akt1,2,3 (Thr308/Ser473) and S6RP (Ser235/236) was measured using αScreen SureFire® kits (PerkinElmer). L6 cells were seeded in 96 well plates at a density of $1x10^4$ cells per well, differentiated as described above, serum-starved overnight and then stimulated with BRL37344, isoprenaline, and insulin for the indicated time periods. Protein phosphorylation was measured and detected according to the manufacturer's instructions.

3.2.8 Immunocytochemistry and immunofluorescence

L6 cells were plated at 1×10^4 cells per well in 8 well culture chamber slides (BD Biosciences, Franklin Lakes, BJ) and differentiated as described above. After serum starved overnight in DMEM (supplemented with 4 mM L-glutamine, 100 Units/ml penicillin, 100 µg/ml streptomycin, and 10 mM HEPES), cells were treated with BRL37344 (10 µM), isoprenaline (1 µM) or insulin (1 µM) for 2 h. Media was discarded, and fixed with 2% (w/v) formaldehyde in PBS for 15 mins and wash with PBS 3 times. Then cells were quenched with 150 mM Tris (pH 8.0) for 10 min, and washed with PBS 3 times. Cells were then blocked with 5% (w/v) BSA in PBS for 1 h, washed with PBS 3 times, and incubated with Myc-tag primary antibody (Cell Signalling Technology (Danvers, MA)) solution (1:500 dilution in 1.5% (w/v) BSA in PBS) overnight at 4 °C. Cells were then washed with PBS and incubated with Alexa Fluor 488-conjugated goat anti-rabbit IgG secondary antibody (1:1000 dilution, 1.5% BSA in PBS) for 1 h. Nuclei were stained by DAPI (5 µg/mL) for 3 mins. Images were observed in a Leica DMLB epifluorescence microscope. Images were acquired using a DC350F camera with IM500 software (Leica Microsystems AB).

3.2.9 Animals

β_3-Adrenoceptor knockout (β_3 KO) mice on FVB/N background (Susulic et al., 1995) were bred at Stockholm University, Sweden. For *in vivo* and *ex vivo* glucose uptake experiments, 12-16 week old female β_3-AR KO mice fed a chow diet were used. For the *in vivo* glucose tolerance tests, female β_3-AR KO mice were fed high fat diet at 12 weeks of age (45% kcal fat, 35% kcal carbohydrates, 20% kcal proteins; 4.7 kcal/g; Research Diets Inc Catalogue number D12451) for 14 weeks at 30 ºC, and were kindly provided by Dr. Natasa Petrovic (Stockholm University, Sweden).

3.2.10 *In Vivo* Glucose Uptake

In vivo glucose uptake was measured using the 2-deoxy-^{3}H-D-glucose method (Liu & Stock, 1995) with some modifications. Mice were fasted for 5 h and anesthetized with 67 mg/kg pentobarbital i.p. and once anesthetized, were injected with BRL37344 (1 mg/kg i.p.) or saline. After 20 min, 2-deoxy-^{3}H-D-glucose (130 µCi/kg) (Perkin Elmer, Waltham MA USA; 8 Ci/mmol) was injected i.p. and mice killed by CO_2 1 h later. Skeletal muscle was dissected and lysed in 0.5 M NaOH for 1 h and radioactivity measured by liquid scintillation counting.

3.2.11 *Ex vivo* Glucose Uptake in gastrocnemius and soleus Muscle

Gastrocnemius or soleus muscles were dissected from β_3-KO mice and suspended in Krebs-Henseleit bicarbonate (KHB) buffer (118.5 mM NaCl, 4.7 mM KCl, 1.2 mM KH_2PO_4, 25 mM $NaHCO_3$, 2.5 mM $CaCl_2$, 1.2 mM $MgSO_4$, 5 mM HEPES) in organ baths containing 30 ml KHB buffer with 5 mM glucose and 15 mM mannitol, bubbled with 95% O_2/5% CO_2 (pH 7.4) and maintained at 37 °C. Muscle was incubated with BRL37344 for 1 h, before rinsing with KHB buffer (containing 20 mM mannitol) for 10 min, followed by incubation in KHB buffer (containing 8 mM 3-O-methylglucose, 12 mM mannitol, 438 µCi/mmol 3-O-methyl[^{3}H]glucose (80.2 Ci/mmol; PerkinElmer), and 42 µCi/mmol [^{14}C]-mannitol (58.8 mCi/mmol; PerkinElmer, USA) for 12 min. Muscles were rinsed with PBS and frozen in liquid nitrogen, before being weighed and digested in 1 ml of 0.5 M NaOH at 60°C. ^{3}H and ^{14}C were measured by liquid scintillation counting. Total muscle 3-O-methylglucose and extracellular space were measured as described previously (Zierath, 1995). Intracellular 3-O-methylglucose accumulation was calculated by: Total muscle 3-O-methylglucose – extracellular 3-O-methylglucose = intracellular 3-O-methylglucose. This is then expressed as a rate of 3-O-methylglucose transport per ml of intracellular water per hour.

3.2.12 *In vivo* glucose tolerance test

Mice were treated with 1 mg/kg BRL37344 i.p. twice a day for four days before *in vivo* glucose tolerance tests were performed. On the fifth day, mice were starved for 6 h prior to glucose (2 g/kg i.p.) administration. Blood glucose was measured using a glucometer (Accu-Check Aviva) before glucose injection and following 15, 30, 60 and 90 min after glucose addition. Prior to treatment with BRL37344, a glucose tolerance test was performed on the same animals treated with saline (0.5 mL i.p.) 30 min prior to glucose administration.

3.2.13 Data analysis

All measurements were taken in duplicate–quadruplicate with n referring to the number of independent experiments performed, and the results are expressed as the mean ± s.e.mean. The statistical significance of differences between groups was analysed by one- or two-way analysis of variance (ANOVA), followed by post-hoc Dunnett or Tukey multiple comparison tests when appropriate. Statistical significance was set at $P<0.05$.

3.3 Results

3.3.1 Glucose uptake in skeletal muscle in response to isoprenaline and BRL37344 is mediated by β₂-adrenoceptors

In L6 myotubes, the prototypical β-AR agonist isoprenaline (pEC_{50} 7.3 ± 0.2; maximal response 175 ± 3.5%; basal response defined as 100 %), the dual β₂-/β₃-AR agonist BRL37344 (pEC_{50} 6.9 ± 0.1; maximal response 162 ± 3.2%), and insulin (pEC_{50} 7.3 ± 0.2; maximal response 170 ± 3.7%), all increased glucose uptake in a concentration-dependent manner (Figure 3.1A). This was associated with significant increases of GLUT4 localization at the cell surface in response to BRL37344, isoprenaline, and insulin (Figure 3.1B, C). BRL37344, isoprenaline, and insulin also significantly increased glucose uptake in human SkMC myotubes (Figure 3.1D). In L6 cells, the selective β₃-AR agonist CL316243 (0.1-10 μM) had no effect on glucose uptake (Figure 3.1E), and the effects of BRL37344, isoprenaline, and insulin were not inhibited by the β₃-AR antagonist SR59230A (Figure 3.1F). The concentration of SR59230A used in this study (1 μM) is appropriate for antagonism of β₃-AR mediated responses (Manara et al., 1996; Nisoli et al., 1996). This suggests that BRL37344 stimulation of glucose uptake in L6 cells does not involve β₃-ARs, which are not expressed in L6 cells (Nevzorova et al., 2002). In contrast, responses to BRL37344 and isoprenaline (but not insulin) were blocked by the β₂-AR selective antagonist ICI118551 (Figure 3.1G), indicating that glucose uptake requires the β₂-AR.

3.3.2 Effect of BRL37344 on glucose uptake in skeletal muscle *ex vivo* and *in vivo*, and on glucose tolerance *in vivo*

The effect of BRL37344 on glucose uptake in skeletal muscle *ex vivo* and *in vivo* was assessed in β₃-AR KO mice to remove any possible contribution of β₃-ARs to the BRL37344 response. BRL37344 significantly increased glucose uptake into isolated gastrocnemius and soleus muscle obtained from β₃-AR KO mice *ex vivo* (Figure 3.2A). Acute administration of BRL37344 *in vivo* also significantly increased glucose uptake into gastrocnemius and soleus muscle in β₃-AR KO mice (Figure 3.2B). To assess whether this effect of BRL37344 was retained in a diabetic model, we used β₃-AR KO mice fed a high fat diet at thermoneutrality (30 °C) for 14 weeks, then treated twice a day for 4 days with either saline or BRL37344 (1 mg/kg i.p.). Significant improvements in glucose tolerance were observed in mice treated with BRL37344 (Figure 3.2C).
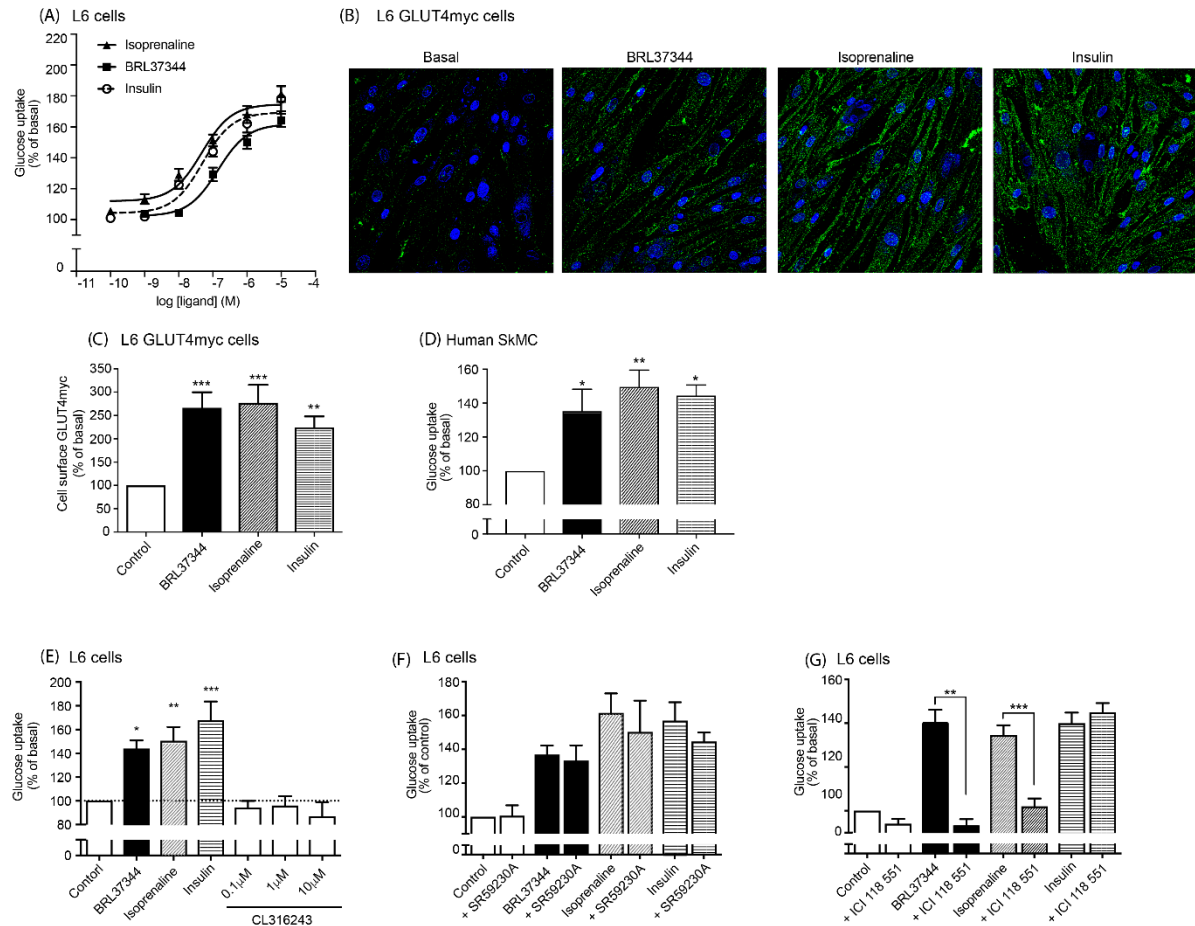
Figure 3.1: (A) Isoprenaline, BRL37344, and insulin increase glucose uptake in a concentration-dependent manner in rat L6 myotubes (n=17). (B, C) Treatment with BRL37344 (10 µM), isoprenaline (1 µM) or insulin (1 µM) increases GLUT4 at the cell surface in rat skeletal muscle L6 cells stably expressing GLUT4myc (n=4). Green is myc antibody staining, while blue is DAPI nuclei staining. (D) In human SkMC myotubes, BRL37344 (10 µM), isoprenaline (1 µM), and insulin (1 µM) all significantly increased glucose uptake (n=5). (E) The selective β_3-AR agonist CL316243 failed to increase glucose uptake in L6 myotubes in contrast to BRL37344 (10 µM), isoprenaline (1 µM), or insulin (1 µM) (n=5). (F) The β_3-AR antagonist SR59230A (1 µM) failed to affect glucose uptake in response to BRL37344 (10 µM), isoprenaline (1 µM), or insulin (1 µM) in L6 myotubes (n=5-7). (G) The β_2-AR antagonist ICI118551 (1 µM) significantly inhibited glucose uptake in response to BRL37344 (10 µM) and isoprenaline (1 µM), but not that to insulin (1 µM), in L6 myotubes (n=6-10). Asterisks represent statistical difference as analysed by one-way ANOVA between control and treated samples (**$P < 0.01$, ***$P < 0.001$).
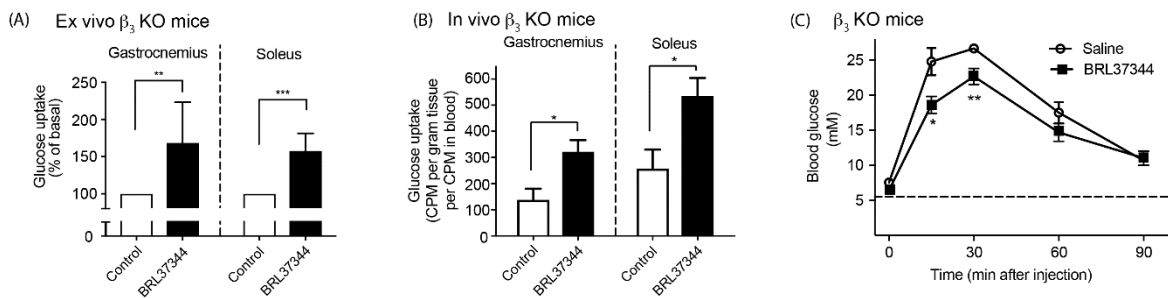
Figure 3.2: (A) In gastrocnemius and soleus muscle from β_3-AR knockout (KO) mice *ex vivo*, BRL37344 (10 µM) significantly increased basal glucose uptake (n=6). (B) BRL37344 (1 mg/kg i.p.) also significantly increased glucose uptake in gastrocnemius and soleus muscle from β_3-AR KO mice *in vivo* (n=6). (C) Effect of BRL37344 (1 mg/kg i.p. twice daily for 4 days) on blood glucose levels after glucose (2 g/kg i.p.) in glucose intolerant β_3-AR KO mice (high fat diet for 14 weeks at 30 °C) (n=5). Asterisks represent statistical differences as analysed by Student's paired *t*-test (A, C) or Student's unpaired t-test (C) between control and treated samples (**$P < 0.01$, ***$P < 0.001$).

3.3.3 Isoprenaline but not BRL37344 produces robust increases in cAMP levels in rat skeletal muscle L6 cells

cAMP accumulation was measured following stimulation of L6 cells with isoprenaline or BRL37344 in the absence of phosphodiesterase inhibitors. Examination of the time course of cAMP accumulation showed a peak cAMP response after 5 min of stimulation with isoprenaline (1 µM), and BRL37344 (10 µM); however, the maximal response to isoprenaline was ~3.3-fold higher ($P<0.001$) compared to that of BRL37344 (Figure 3.3A). BRL37344 was also significantly less potent than isoprenaline (pEC_{50} 6.7 ± 0.1 and 8.4 ± 0.2 respectively; $P<0.001$) (Figure 3.3B). A downstream target of cAMP is phosphorylation of CREB. Whereas isoprenaline (1 µM) increased CREB phosphorylation levels by ~ 3-fold, with levels maximally increased after 30 min of stimulation (Figure 3.3C), BRL37344 (10 µM) failed to produce a significant increase in CREB phosphorylation (Fiureg 3.3C). To examine whether BRL37344 and isoprenaline caused localized production of cAMP in different regions of the cell, L6 myoblasts were transfected with either the cAMP biosensor pmEpac2 that detects cAMP at the cell membrane, or with cytoEpac2 to detect cAMP in the cytoplasm (Halls et al., 2015). Both isoprenaline (1 µM) and BRL37344 (10 µM) increased cAMP levels at the plasma membrane and in the cytoplasm, with the response to isoprenaline significantly higher ($P<0.001$) than that to BRL37344 (Figure 3.3D, 3.3E).

3.3.4 Increased glucose uptake in rat skeletal muscle L6 cells in response to isoprenaline and BRL37344 involves mTORC2 but not Akt activation

Insulin increases glucose uptake via a well characterized pathway. Following activation of the insulin receptor and insulin receptor substrate (IRS) proteins, increased PI3K activity promotes phosphatidylinositol (3,4,5)-trisphosphate (PIP_3) formation at the inner plasma membrane, that in turn recruits inactive Akt and 3-Phosphoinositide-dependent protein kinase-1 (PDK1) to the plasma membrane. This facilitates PDK1-mediated phosphorylation of Akt at Thr308, causing a conformational change in Akt that is required for subsequent phosphorylation at Ser473 and full activation, leading to phosphorylation of AS160 and translocation of GLUT4 to the plasma membrane. In contrast, glucose uptake in response to β-AR activation in skeletal muscle involves mTORC2 and GLUT4 translocation without activation of Akt (Sato et al., 2014a).
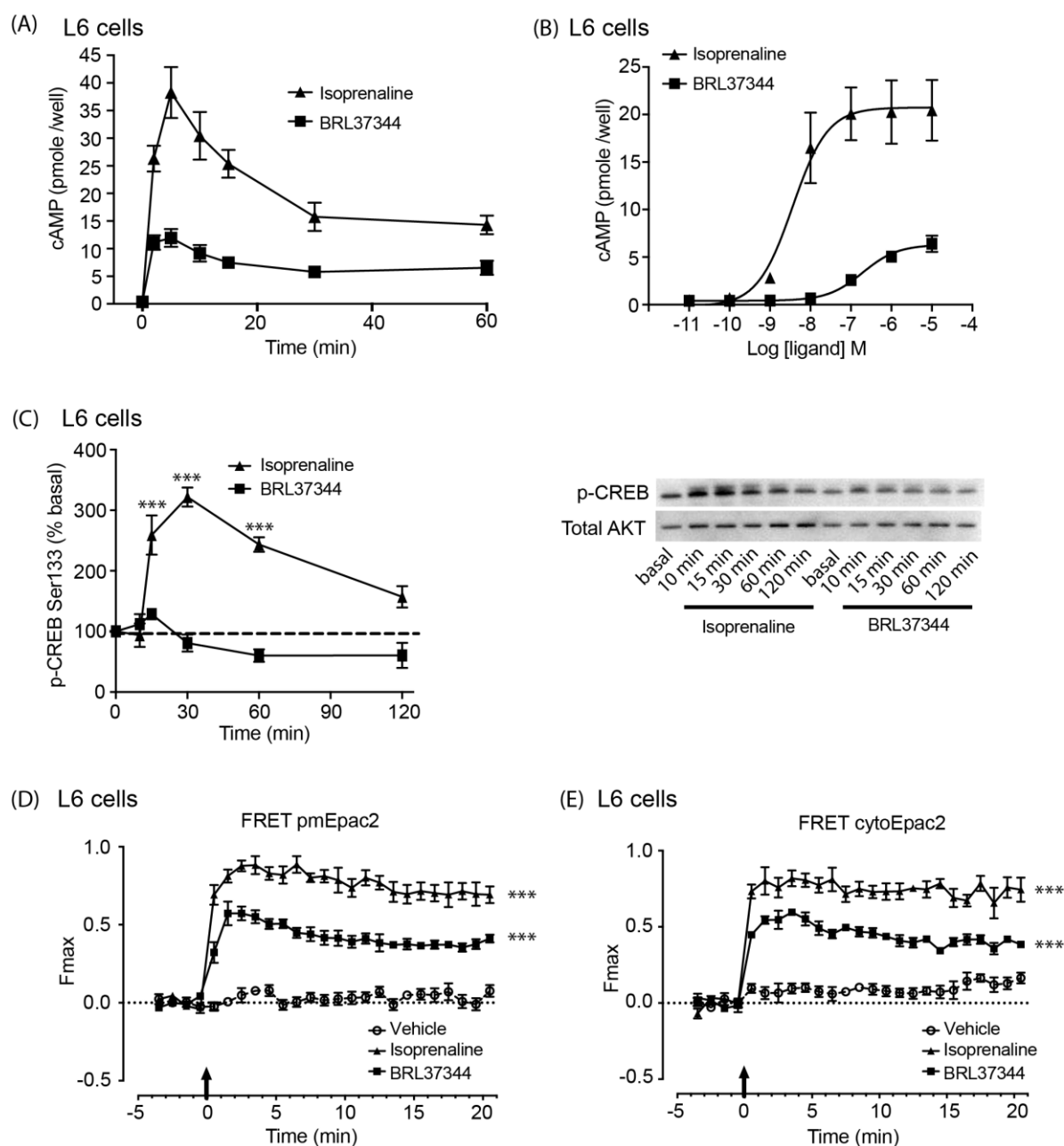
Figure 3.3: (A) Time course of cAMP production in response to isoprenaline (1 μM) and BRL37344 (10 μM) in rat L6 myotubes (n=6-8) (Basal = 0.47 pmol cAMP/well). Experiments were performed in the absence of IBMX. (B) Isoprenaline and BRL37344 increased intracellular cAMP levels in a concentration-dependent manner in rat L6 myotubes (n=7). Experiments were performed in the absence of IBMX following 30 min of stimulation with either isoprenaline or BRL37344. (C) Effect of isoprenaline (1 μM) or BRL37344 (10 μM) on CREB phosphorylation levels in rat L6 myotubes. Blot is representative image from 3 experiments. (D) Effect of isoprenaline (1 μM) or BRL37344 (1 μM) on cAMP levels in L6 myoblasts transfected with the cAMP biosensor pmEpac2 to detect cAMP at the cell membrane, or (E) cytoEpac2 to detect cAMP in the cytoplasm (n= 5). Asterisks represent statistical difference as analysed by two-way ANOVA between control and treated samples (*$P<0.05$, **$P < 0.01$, ***$P < 0.001$).
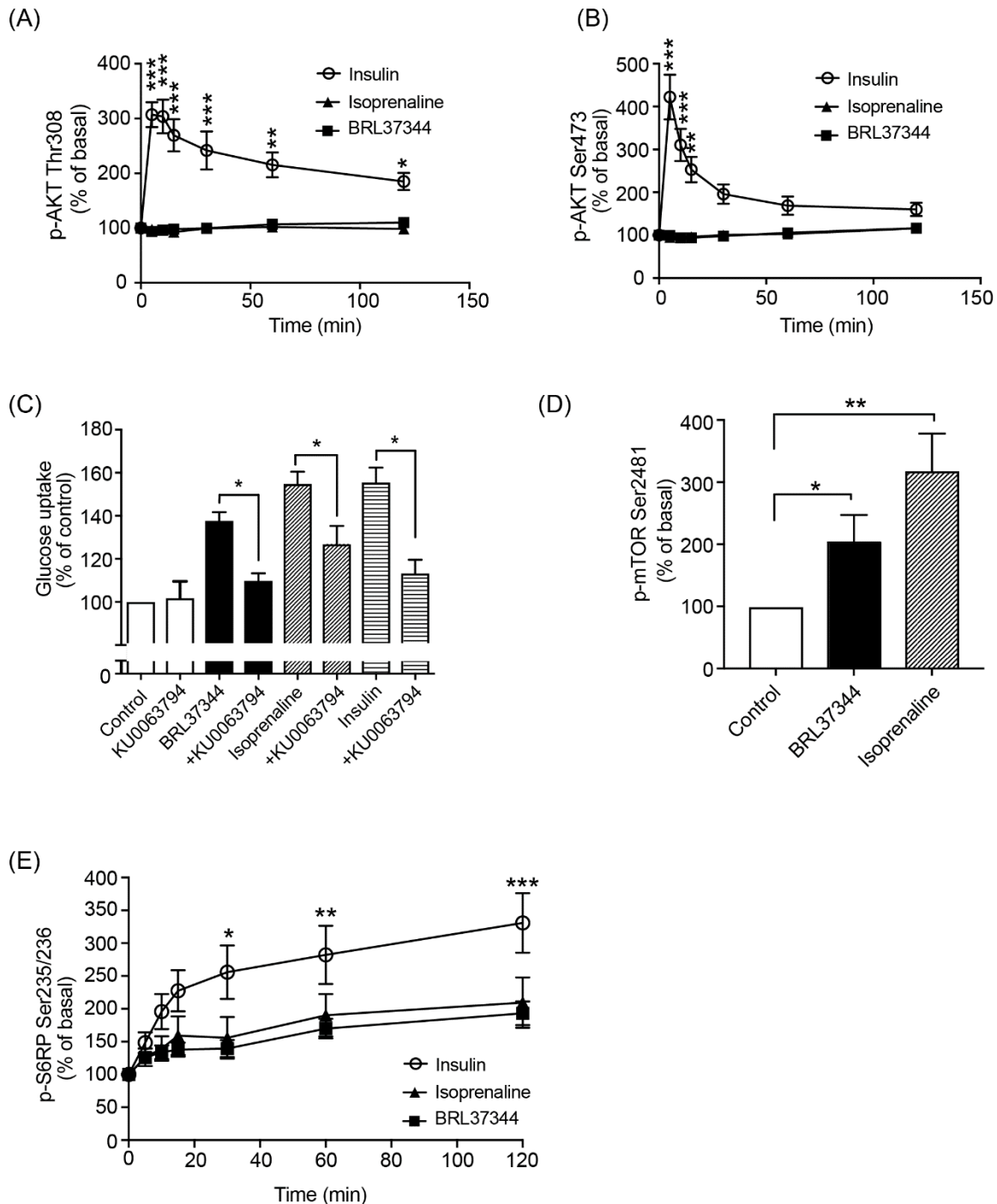
Figure 3.4: Insulin (1 μM), but not isoprenaline (1 μM) or BRL37344 (10 μM), increased phosphorylation of Akt at (A) Thr308 and (B) Ser473 in rat L6 myotubes (n=4-6). (C) Glucose uptake in response to isoprenaline (1 μM), BRL37344 (10 μM), and insulin (1 μM) was significantly reduced by the mTOR inhibitor KU0063794 (1 μM) in rat L6 myotubes (n=5-11). (D) Increased mTOR phosphorylation at Ser2481 following 2h exposure to isoprenaline (1 μM) and BRL37344 (10 μM) in rat L6 myotubes (n=5). (E) Insulin (1 μM), but not isoprenaline (1 μM) or BRL37344 (10 μM), significantly increased S6RP phosphorylation at Ser235/Ser236 compared to basal levels in rat L6 myotubes (n=5-6). Asterisks represent statistical difference as analysed by one-way ANOVA (C, D) or two-way ANOVA (A, B, E) between control and treated samples (*$P < 0.05$, **$P < 0.01$, ***$P < 0.001$).

Here we confirm that insulin (1 μM) phosphorylates Akt at Thr308 and Ser473, with neither isoprenaline (1 μM) nor BRL37344 (10 μM) causing any change relative to basal Akt phosphorylation (Figure 3.4A, 3.4B). Instead, glucose uptake in response to BRL37344 as well as insulin and isoprenaline involved mTOR, since glucose uptake was inhibited by the selective mTOR inhibitor KU0063794 (1 μM) (Figure 3.4C). It is likely that mTORC2 rather than mTORC1 is involved since BRL37344 and isoprenaline both caused phosphorylation of mTOR at Ser2481 (known to be associated with mTORC2 activation; Figure 3.4D), whereas neither isoprenaline nor BRL37344 caused phosphorylation of the mTORC1 downstream target S6RP (Figure 3.4E).

3.3.5 Isoprenaline, but not BRL37344, recruits β-arrestin to the receptor, resulting in receptor desensitisation

To determine whether isoprenaline or BRL37344 result in desensitisation of β_2-AR-mediated responses, we measured cAMP accumulation following pre-exposure of L6 cells to either BRL37344 (10 μM) or isoprenaline (1 μM). Pre-exposure to BRL37344 did not desensitise subsequent cAMP responses to either BRL37344 or isoprenaline, whereas pre-exposure to isoprenaline desensitised subsequent responses to both agonists (Figure 3.5A-D). In addition, L6 cells were exposed to either isoprenaline or BRL37344 for periods of up to 20 h then tested to determine glucose uptake after a 15 min incubation with ^{3}H 2-DG. Glucose uptake was only slightly inhibited after prolonged exposure to isoprenaline but not BRL37344 (Figure 3.5E). The marked desensitisation of the cAMP response but only slight desensitisation of glucose uptake after isoprenaline exposure suggests that the small amount of cAMP generated either by isoprenaline after desensitisation or by BRL37344 is sufficient to promote GLUT4 translocation and resulting glucose uptake.

We next examined the effect of β_2-AR activation by isoprenaline and BRL37344 on BRET between β_2-AR Rluc-8 and β-arrestin-1-Venus, or β-arrestin-2-Venus, and the plasma membrane marker KRas-Venus in L6 cells. Isoprenaline (1 μM), but not BRL37344 (10 μM), caused an increase in the BRET signal between β_2-AR Rluc-8 and both β-arrestin-1-Venus and β-arrestin-2-Venus (Figure 3.5 F, 3.5G). There was also a decrease in the BRET signal between β_2-AR Rluc-8 and the plasma membrane marker KRas-Venus (Figure 3.5H) following isoprenaline but not BRL37344 treatment, indicating that there was movement of the receptor away from the cell membrane only in response to isoprenaline. This suggests that only isoprenaline promotes an interaction between the β_2-AR and β-arrestins and consequent movement of the receptor away from the cell membrane.
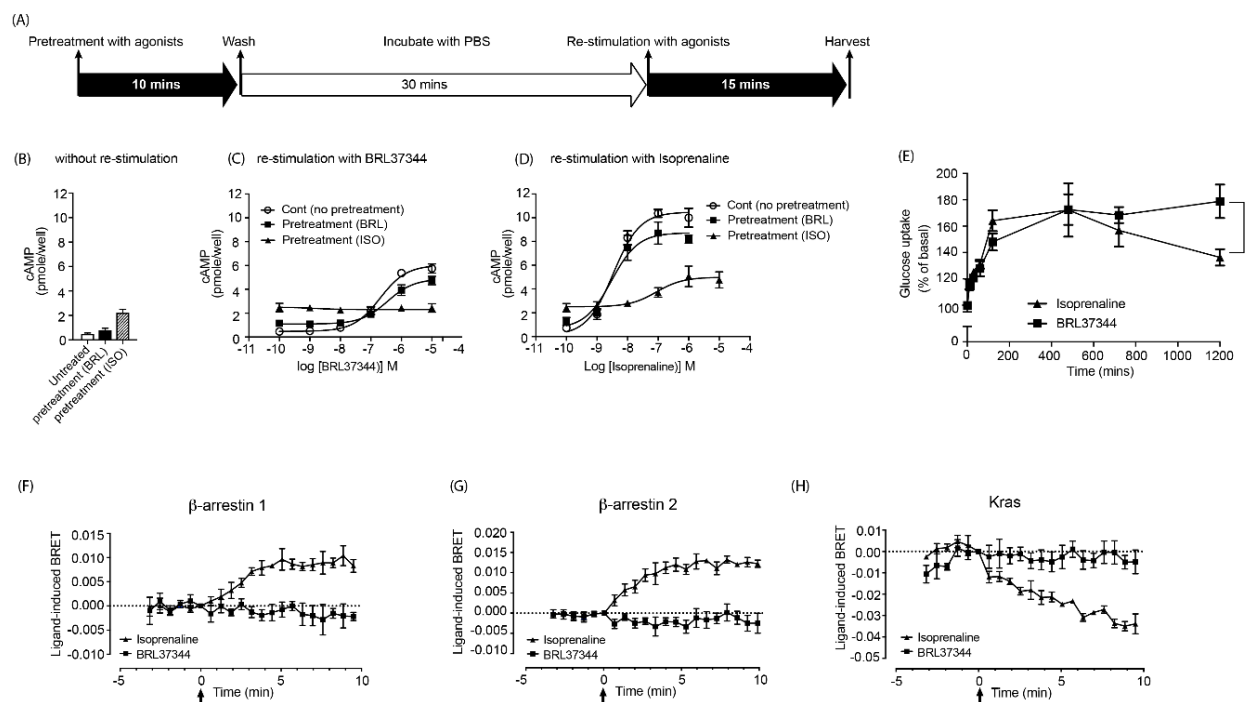
Figure 3.5: (A) Schematic of the desensitisation protocol used to assess the effect of BRL37344 or isoprenaline on cAMP levels. Cells were pre-treated with either BRL37344 (10 μM) or isoprenaline (1 μM) for 10 min, cells washed with PBS for 30 min, before cells were then stimulated with either BRL37344 or isoprenaline for 15 min. (B) cAMP levels following PBS washout period (n=4). (C) cAMP accumulation in response to BRL37344 or (D) isoprenaline following pretreatment of cells with either BRL37344 (10 μM) or isoprenaline (1 μM) (n=4). (E) Glucose uptake (15 min exposure) after exposure of cells to isoprenaline or BRL37344 for periods up to 20 hrs. Interaction of (F) β-arrestin 1, (G) β-arrestin 2, and (H) K-Ras with the $β_2$-AR following stimulation with either isoprenaline (1 μM) or BRL37344 (10 μM) in CHO-GLUT4myc cells (n=3-4). Asterisks represent statistical difference as analysed by one-way ANOVA between control and treated samples (**$P < 0.01$, ***$P < 0.001$).

3.4 Discussion

BRL35135 and BRL37344 (its active de-esterified metabolite) were originally developed as anti-obesity drugs targeting the β_3-AR (Arch et al., 1984). Studies in mice showed that BRL35135 was an effective anti-obesity agent, decreasing body weight and whole body fat composition in female *ob/ob* mice treated daily for 4 weeks independently of changes in food intake (Arch et al., 1984; Cawthorne et al., 1992), an effect that was not evident in non-obese mice (Cawthorne et al., 1992). β_3-AR activation also decreased weight gain in genetically obese male Zucker rats treated daily for 3 weeks independently of effects on food intake (Santti et al., 1994). These improvements in body weight with BRL35135 did not translate into humans, with BRL35135 treatment having no effect on body weight when administered to obese subjects for 10 days (Cawthorne et al., 1992; Mitchell et al., 1989). However, BRL35135 and BRL37344 did have favorable effects on glucose homeostasis both in humans and rodents. In humans, BRL35135 (10 days administration to obese subjects) improved glucose tolerance, and increased insulin-stimulated glucose disposal, with no effects on fasting blood glucose or plasma insulin levels (Cawthorne et al., 1992; Mitchell et al., 1989). In rodents, chronic BRL35135 administration improved glucose tolerance and lowered plasma insulin levels in obese rats (Cawthorne et al., 1992; Santti et al., 1994), and increased glucose uptake into skeletal muscle in lean rats (Liu & Stock, 1995). Acute BRL35135 administration also increased glucose uptake into skeletal muscle (Abe et al., 1993; Liu & Stock, 1995). This collective data clearly shows that BRL35135 improves glucose homeostasis in both rodents and humans.

This discrepancy between the ability of BRL35135/BRL37344 to improve glucose homeostasis but have no effect on body weight in humans could be explained by BRL35135/BRL37344 acting as agonists at both β_2- and β_3-ARs. Responses to BRL37344 in rodent adipocytes are mediated by actions at β_3-ARs since these responses are resistant to antagonism by conventional $\beta_{1/2}$-AR antagonists (Hollenga & Zaagsma, 1989; Langin et al., 1991; Wilson et al., 1984) and are absent in brown adipocytes obtained from β_3-AR knockout mice (Chernogubova et al., 2005). Additionally, BRL37344 is ineffective in human white adipocytes that do not express the β_3-AR (Langin et al., 1991). However, responses to BRL37344 in skeletal muscle are mediated through β_2-AR, based on studies in L6 skeletal muscle cells that show that β_2- but not β_3-AR are expressed, pharmacological studies using receptor specific antagonists (Nevzorova et al., 2002), and on glucose uptake responses *in vivo* (Liu & Stock, 1995). Our study here utilized L6 cells and also β_3-AR knockout mice

to exclude any actions BRL37344 may have on β_3-ARs. In L6 cells, isoprenaline, BRL37344 and insulin had similar efficacy in promoting glucose uptake and in promoting GLUT4 translocation to the cell surface. All three drugs also promoted glucose uptake in human SkMC cells. Glucose uptake in L6 cells was not due to actions on β_3-AR since there was no response to the selective β_3-AR agonist CI316243, and the effects of isoprenaline and BRL37344 were blocked by the β_2-AR selective antagonist ICI118551 but not the β_3-AR selective antagonist SR59230A. BRL37344 also increased glucose uptake both *ex vivo* and *in vivo* in gastrocnemius and soleus muscles from β_3-AR knockout mice. In addition, chronic treatment with BRL37344 improved glucose tolerance in β_3-AR knockout mice placed on a high fat diet for 14 weeks. Our results clearly show that BRL37344 increases glucose uptake in L6 cells by activating β_2-ARs, and that the effects on glucose tolerance are still evident in β_3-AR knockout mice.

Theoretically on-target actions of BRL37344 at the β_3-AR may not be detrimental to its use *in vivo* since β_3-ARs are predominantly expressed in adipose tissue (in particular brown adipose tissue) and the gastrointestinal tract/urogenital system, with a β_3-AR agonist (mirabegron) currently approved for the treatment of overactive bladder (see (Dehvari et al., 2018) for a recent review). BRL37344 also relaxes human detrusor muscle (Badawi et al., 2007), with similar efficacy and potency to mirabegron (Svalo et al., 2013). With respect to actions in adipose tissue, in healthy adult humans, mirabegron increases brown adipose tissue activity (Cypess et al., 2015), with brown adipose tissue playing a major role in cold-induced glucose clearance in mice (Bartelt et al., 2011). Hence any actions that BRL37344 may have at β_3-ARs in human tissues would be beneficial, especially in the context of individuals with T2D. One of the most frequent complications of diabetes is lower urinary tract dysfunction that occurs in ~80% of diabetic patients, including 50% with bladder dysfunction (Daneshgari & Moore, 2006). This would limit adverse effects of BRL37344 on the bladder, and could theoretically be beneficial in T2D patients with bladder dysfunction. However, it is most likely that any beneficial effects of BRL37344 on glucose homeostasis in humans most likely occurs through interactions at β_2-ARs and not β_3-ARs since only β_2-ARs are found in human skeletal muscle.

A second question is whether BRL37344 activity at β_2-ARs may have adverse effects in cell types other than skeletal myocytes, especially cardiomyocytes. We have shown here, using a variety of techniques, that while BRL37344 is a full agonist for glucose uptake, it is a partial agonist for cAMP accumulation. Direct measurement of cAMP, pCREB activation and the use of cell membrane and

cytoplasmic cAMP biosensors all showed weaker responses to BRL37344 than isoprenaline. Despite these weak cAMP responses, however, cardiac responses to BRL37344/BRL35135 have been observed. In rodents, BRL37344 has partial agonist (~ 80% of the response to isoprenaline) chronotropic effects due to actions at β_1/ β_2-ARs (Arch et al., 1984; Wilson et al., 1984). These effects occur at significantly higher concentrations than that required for lipolysis in white and brown adipocytes (BRL35135 is 33-fold, and BRL37344 more than 400-fold selective for stimulating lipolysis *vs* atria rate (Arch et al., 1984; Wilson et al., 1984)). In human atria, BRL37344 exhibited inotropic partial agonist effects (~ 40% of the maximal response to isoprenaline) that were antagonized by propranolol (Pott et al., 2003). It should be noted that in human atria, responses to BRL37344 were only observed at high concentrations over 1 µM (Pott et al., 2003). When BRL35135 (BRL37344 pro-drug) was administered to healthy male subjects, an increase in heart rate (~9 beats/min) was observed (Cawthorne et al., 1992). However, it should be noted that the individuals who had the greatest improvements in glucose tolerance and decreases in hyperinsulinemia were those that were the most glucose intolerant/diabetic, and that no arrhythmias, tachycardia or changes in blood pressure were noted (Cawthorne et al., 1992). The only visible side effect was a mild tremor in the fingers/hands that was correlated with plasma BRL35135 levels (Cawthorne et al., 1992). Thus, while retaining activity for glucose uptake in skeletal muscle, BRL37344 appears to exhibit relatively weak to no side effects in tissues where the response is mediated primarily by cAMP.

In skeletal muscle, β_2-AR agonists (including BRL37344) increase glucose uptake utilizing a pathway that is independent of the insulin signalling pathway (Sato et al., 2014a). Instead of PI3K and Akt, β_2-AR utilize a pathway involving activation of mTORC2 (Sato et al., 2014a). We were able to confirm this here and to show that in contrast to insulin, neither isoprenaline nor BRL37344 cause phosphorylation of Akt at Thr308 or Ser473 (Figure 3.4) yet both β-AR agonists cause phosphorylation of mTOR at Ser2481. In addition, glucose uptake in response to BRL37344, isoprenaline or insulin was inhibited by the mTOR inhibitor KU0063794. Unlike insulin, both BRL37344 and isoprenaline had only a weak effect on S6RP phosphorylation at Ser235/Ser236, known to be downstream of mTORC1, suggesting together with phosphorylation of mTOR at Ser2481 that the dominant effect is on mTORC2. This is important since in T2D, the insulin signalling pathway is down-regulated mainly at the level of IRS/PI3K/Akt activation (Frojdo et al., 2009), suggesting that increasing glucose uptake through a non PI3K-Akt pathway is attractive therapeutically. While the mechanistic details leading to β_2-AR activation of mTORC2 are not clear,

our previous studies indicate a role for cAMP (Sato et al., 2014a). Both isoprenaline and BRL37344 are full agonists for glucose uptake but BRL37344 is a partial agonist for cAMP. Whether BRL37344 requires cAMP or another unknown effector to activate mTORC2 is not clear at this stage. One possibility is that a small, localized increase in cAMP is sufficient to promote signalling pathways leading to GLUT4 translocation, which can then remain in the plasma membrane for a prolonged period (the protein half-life of GLUT4 is ~48 h (Sargeant & Paquet, 1993), with a single GLUT4 molecule being able to undergo multiple rounds of recycling before being targeted for degradation) to enable maximal glucose uptake. Thus, there may be a difference in the rate of GLUT4 translocation, but at steady-state, the rate of glucose uptake is similar in response to both isoprenaline and BRL37344. This requires further investigation.

Although BRL37344 is a weak partial agonist for cAMP production, and a full agonist with respect to glucose uptake, we cannot with these experiments conclude that BRL37344 is a biased agonist at the β_2-AR. Biased agonists acting at a given receptor produce different efficacies at different signalling outputs (Evans et al, 2010). One explanation is that differences in receptor conformation are produced by structurally distinct ligands, and there is evidence to support this from NMR studies of interactions between the β_2-AR and diverse agonists (Liu et al., 2012). While biased agonism has been demonstrated for several GPCRs including the β_2-AR (Evans et al., 2010), we cannot say that this occurs for BRL37344 based on the evidence presented here. Many studies investigating biased agonism at GPCRs focus on the interaction of a GPCR with β-arrestin proteins, leading to the concept of $G\alpha$- or β-arrestin-biased compounds. Continuous activation of the β_2-AR by a full agonist leads to rapid receptor desensitisation. This occurs through a well-characterized pathway: upon receptor activation, specific residues in the C-terminal tail are phosphorylated by GRKs, leading to β-arrestin recruitment, receptor internalisation, and subsequent loss of β_2-AR responsiveness. In our study, BRL37344 stimulation of the β_2-AR failed to recruit β-arrestin-1 or -2 to the receptor, whereas isoprenaline promoted rapid β-arrestin recruitment. Thus, BRL37344 is certainly not β-arrestin-biased, and further studies are needed to determine whether this agonist promotes interaction of the β_2-AR with alternative signalling proteins or complexes.

Receptor desensitisation is a potential clinical problem associated with the long-term use of β_2-AR agonists. We therefore utilized several experimental paradigms to examine desensitisation following isoprenaline or BRL37344 treatment. We showed that BRET interactions between the

receptor and β-arrestin1 and 2 were increased following isoprenaline treatment, whereas there was decreased interaction between the receptor and the plasma membrane marker K-Ras. In contrast, BRL37344 treatment had no effect on any of the interactions. This is consistent with the ability of isoprenaline, but not BRL37344, to cause receptor internalisation. Direct measurement of cAMP responses after agonist pre-addition showed marked desensitisation in response to isoprenaline but not BRL37344. This difference also translates to glucose uptake where prolonged treatment with isoprenaline for up to 20 h produced desensitisation of glucose uptake to isoprenaline but not BRL37344. This lack of desensitisation produced by BRL37344 may be a desirable property clinically, as improvements in glucose homeostasis would require chronic administration.

In conclusion, we have shown that BRL37344 increases glucose uptake into skeletal muscle through activation of β_2-ARs *in vitro*, *ex vivo*, and *in vivo*. This occurs by increased translocation of GLUT4 to the cell surface through a signalling pathway not involving Akt, clearly distinguishing the pathway from insulin. Importantly, BRL37344 achieves this with minimal increases in cAMP production, and without recruiting β-arrestin to the receptor and does not promote receptor desensitisation. The ability of BRL37344 to promote glucose uptake utilizing pathways distinct from insulin that are desensitised in T2D may offer an alternative therapeutic approach. The results presented here opens up for the usage of β_2-ARs agonists with these beneficial characteristics in the search for novel T2D diabetes drugs.

CHAPTER 4

GRK and PKA phosphorylation sites in the β₂-AR tail are not involved in β₂-AR mediated glucose uptake

4.1 Introduction

cAMP is an important signalling molecule for mediating the cellular and physiological effects of β_2-AR stimulation, including skeletal muscle glucose uptake. β_2-AR mediated glucose uptake in skeletal muscle is attenuated by inhibition of PKA/AC (Nevzorova et al., 2002; Nevzorova et al., 2006; Sato et al., 2014a), and cAMP analogues mimic the effects of β_2-AR stimulation (Nevzorova et al., 2002; Nevzorova et al., 2006; Sato et al., 2014a). In Chapter 3 however, we showed that BRL37344, a dual $\beta_{2/3}$-AR agonist, increases glucose uptake and GLUT4 translocation in skeletal muscle to the same extent as the non-selective β-AR agonist isoprenaline, but was a partial agonist with respect to cAMP. In addition, the kinetics of β_2-AR stimulated cAMP production is significantly different from that of increased glucose uptake: β_2-AR mediated glucose uptake increases slowly and the effect is sustained for up to 20 h (Chapter 3), whereas cAMP levels rise rapidly (within minutes) before transiently returning to basal levels (Nevzorova et al., 2006) (Chapter 3). This may suggest that desensitisation of the β_2-AR cAMP response may occur in parallel with an alternative signalling mechanism that maintains increased glucose uptake.

Following activation, β_2-ARs are rapidly desensitised by receptor phosphorylation, direct receptor interactions with scaffolding proteins such as β-arrestin, and receptor internalisation. β_2-ARs are phosphorylated at serine or threonine residues located within consensus sites in the third intracellular loop and C-terminal tail of the receptor by PKA (Clark et al., 1988; Hausdorff et al., 1989; Yuan et al., 1994) and GPCR kinases (GRKs) (Ferguson et al., 1996; Ferguson et al., 1995; Goodman et al., 1996; Tsuga et al., 1994). GRKs are serine/threonine protein kinases and have an important role in ligand occupied receptor phosphorylation. There are 7 GRK isoforms defined to date (GRK1–GRK7). While GRK2, GRK3, GRK5, and GRK6 are ubiquitously expressed, GRK1, GRK4 and GRK7 have limited tissue expression (Homan & Tesmer, 2014; Watari et al., 2014). GRK2 and GRK5 are the predominant GRK isoforms expressed in skeletal muscle (Garcia-Guerra et al., 2014; Jones et al., 2003; Kunapuli & Benovic, 1993), with GRK2 involved in the modulation of skeletal muscle contractile function and physiology. Skeletal muscle-specific GRK2 knockout (KO) mice display reduced force of contraction in fast twitch muscles but not in slow twitch muscles following electrical stimulation (Woodall et al., 2016). Another study showed that overexpression of GRK2 slowed down skeletal muscle differentiation, while overexpression of a GRK2 kinase dead mutant (K220R) promoted premature differentiation of multinucleated myocytes (Garcia-Guerra et al., 2014). Some studies have suggested that GRK5 is associated with the pathogenesis of

cardiomyocyte hypertrophy, but less is known about its role in skeletal muscle (Hullmann et al., 2014).

There is growing evidence to show that GRK2 is involved in the regulation of glucose metabolism (Mayor et al., 2018). In adult rat ventricular cardiomyocytes, insulin stimulation promoted recruitment of GRK2 to the plasma membrane (Ciccarelli et al., 2011). Up-regulation of GRK2 negatively affected insulin-stimulated membrane translocation of GLUT4, and reduction of GRK2 levels during heart failure improved glucose uptake (Ciccarelli et al., 2011). In C2C12 skeletal muscle cells, overexpression of GRK2 reduced insulin-stimulated phosphorylation of IRS-1, Akt and extracellular signal–regulated kinases1 /2 (Erk1/2), and reduced insulin-stimulated glucose uptake, whereas siRNA knockdown of GRK2 increased insulin-stimulated phosphorylation of IRS-1, Akt and Erk1/2, and increased insulin-stimulated glucose uptake (Garcia-Guerra et al., 2010). This is thought to be independent of the kinase activity of GRK2 as overexpression of a kinase dead GRK2 mutant (K220R) has the same effect as overexpression of wild type GRK2 (Garcia-Guerra et al., 2010). It was postulated that IRS forms a direct interaction with GRK2 to affect insulin signalling (Fu et al., 2015). Also, GRK2 (+/-) mice fed with high fat diet showed an enhanced insulin-stimulated glucose clearance compared to wild type mice under the same diet control (Garcia-Guerra et al., 2010). Collectively these results indicate that GRK2 may have an inhibitory role in insulin-stimulated signalling and glucose uptake.

In contrast, it was found that activation of GRK causes positive effects on β_2-AR mediated glucose uptake, following a study which examined the role of GRK phosphorylation sites in the C-terminal tail of the β_2-AR on glucose uptake using several different approaches in CHOGLUT4myc cells (CHO K1 cells stably expressing human GLUT4 carrying an exofacial human c-myc tag) (Dehvari et al., 2012). Truncation of the C-terminal tail of the β_2-AR following the Cys341 palmitoylation site at position 344 (removing GRK sites and PKA sites in C-terminal tail) and 349 (distal to the PKA consensus sequence, but still lacking GRK sites) resulted in reduced isoprenaline-stimulated glucose uptake, indicating that the C-terminal tail of the β_2-AR is important for this response (Dehvari et al., 2012). This was thought to be due to interactions of the β_2-AR C-terminal tail with GRK as this part of the C-terminus contains Ser/Thr residues required for potential GRK phosphorylation. Further studies revealed that a β_2-AR (-)GRK mutant (where the last 11 Ser/Thr residues in the C-terminal tail were replaced with Ala) abolished isoprenaline-stimulated GLUT4 translocation, although cells expressing a β_2-AR (-)PKA phosphorylation mutant (where Ser261/262 and Ser345/346 were replaced with Ala) retained this effect (Dehvari et al., 2012). In addition, in cells overexpressing a

kinase-dead GRK2 (K220R) mutant, isoprenaline failed to increase GLUT4 translocation (Dehvari et al., 2012). These results indicated that activation of the β_2-AR promotes GLUT4 translocation/glucose uptake through GRK mediated receptor phosphorylation. Also, there is evidence that β_2-ARs exert some of their effects in skeletal muscle through GRK2 mediated mechanisms. However, the activity of GRK2 caused an inhibitory effect on skeletal muscle hypertrophy since the β_2-AR agonist clenbuterol significantly increased muscle size in skeletal muscle-specific GRK2 KO mice. This was postulated to be due to enhanced Akt signalling (Woodall et al., 2016). In some systems such as cardiac myocytes, GRK2 activity or protein interactions contributes to crosstalk between β_2-AR and insulin signalling (Fu et al., 2015).

It has been difficult to identify the relevant GRK phosphorylation sites in β_2-ARs that are associated with receptor desensitisation. Originally it was considered that all 11 Ser/Thr residues in the C-terminal tail of the β_2-AR (Figure 4.1) are involved in GRK mediated desensitisation mechanism (Bouvier et al., 1988). A later study utilizing sequence analysis *in vitro* indicated that the distal portion of the C-terminal tail (T384, T393, S396, S401, S407, and S411) is phosphorylated by GRKs (Fredericks et al., 1996), but mutations in these 6 sites did not cause significant effects on GRK-mediated desensitisation (Seibold et al., 1998). More recently, substitution mutation of S355, S356 and S364 in the proximal portion of the β_2-AR C-terminal tail suggested that these 3 residues are the critical residues responsible for β_2-AR phosphorylation as well as desensitisation in human embryonic kidney (HEK) 293 cells (Seibold et al., 2000). Also, mass spectrometry, phospho-specific antibodies and phospho-amino acid analysis have shown that different GRK isoforms can be specifically phosphorylated at different Ser/Thr residues in the β_2-AR: GRK2 (T360, S364, S396, S401, S407 and S411), GRK5 (T384, T393, S396, S401, S407 and S411) and GRK6 (S355 and S356) (Fredericks et al., 1996; Nobles et al., 2011; Yang et al., 2017). It is noteworthy that T360 and S364, both GRK2 phosphorylation sites, demonstrated the greatest fold increases in phosphorylation in response to isoprenaline in HEK293 cells, compared to other Ser/Thr residues in β_2-AR C-terminal tail (Nobles et al., 2011). There is no evidence to date that T408 is phosphorylated by any of the GRK isoforms.

The aim of this study was to examine the role of GRK and PKA phosphorylation sites in the C-terminal tail on β_2-AR mediated cAMP production, glucose uptake and GLUT4 translocation, as well as agonist-promoted β_2-AR internalisation. We generated CHOGLUT4myc cells that stably expressed the wild type (WT) human β_2-AR (Figure 4.1) or mutant β_2-ARs (Figure 4.2). In the 6 different β_2-AR constructs, we mutated either (1) a proximal Ser/Thr cassette of the C-terminal tail - S355A, S356A,

T360A and S364A, (2) a distal Ser/Thr cassette of the C-terminal tail - T384A, T393A, S396A, S401A, S407A, S411A and T408A (T408 was also mutated despite no evidence to date suggesting it is phosphorylated by any of the GRK isoforms, to ensure all Ser/Thr residues in this portion of the C-terminal tail were mutated), (3) both the proximal and distal cassettes of the C-terminal tail, (4) both the proximal and distal cassette of the C-terminal tail except for S411, (5) both the proximal and distal cassette of β_2-AR C-terminal tail and all PKA phosphorylation sites – S261A, S262A, S345A and S346A or (6) a β_2-AR mutant with just a mutated PSD95–Dlg–ZO1 (PDZ) domain binding motif – S411A. For all the studies conducted, we utilised two distinct β-AR agonists. The first agonist is isoprenaline that causes interaction of the β_2-AR with β-arrestin 1/2 (Srivastava et al., 2015), and subsequent desensitisation of the β_2-AR. Isoprenaline was chosen over more selective β_2-AR agonists (such as clenbuterol for example) as our previous work were performed with isoprenaline (Dehvari et al., 2012; Nevzorova et al., 2002; Nevzorova et al., 2006; Sato et al., 2014a), allowing for easier comparison of results to these previous studies. The second agonist used is BRL37344 that fails to result in β_2-AR desensitisation, yet still increases glucose uptake and GLUT4 translocation to the same extent as isoprenaline (Chapter 3).
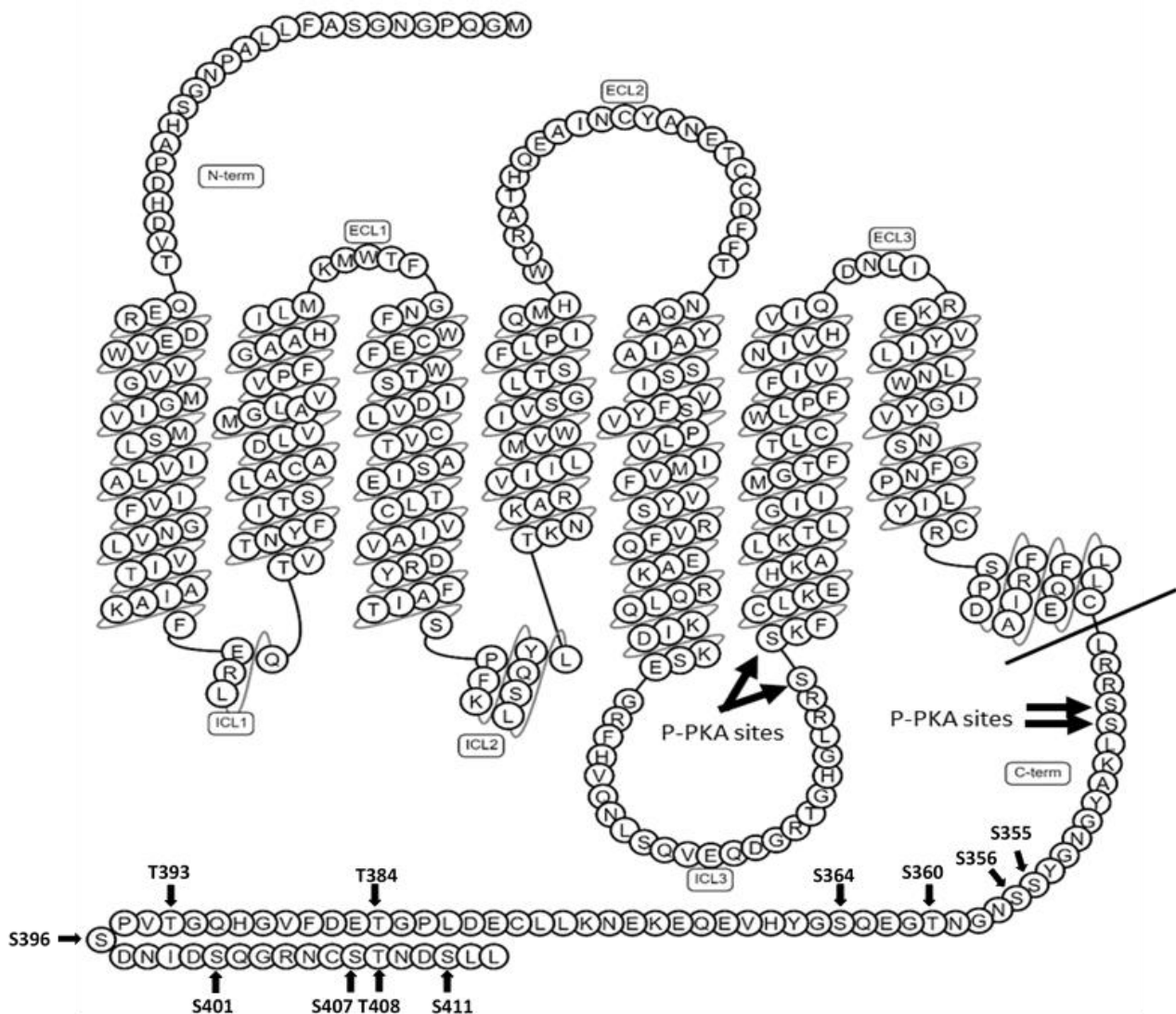
Figure 4.1: Topological model of β₂-AR

The topological model of β$_2$-AR with PKA phosphorylation sites as well as Ser/Thr residues (putative GRK phosphorylation sites) in C-terminal tail. The small black arrows indicate the location of serine or threonine residues in C-terminal tail.
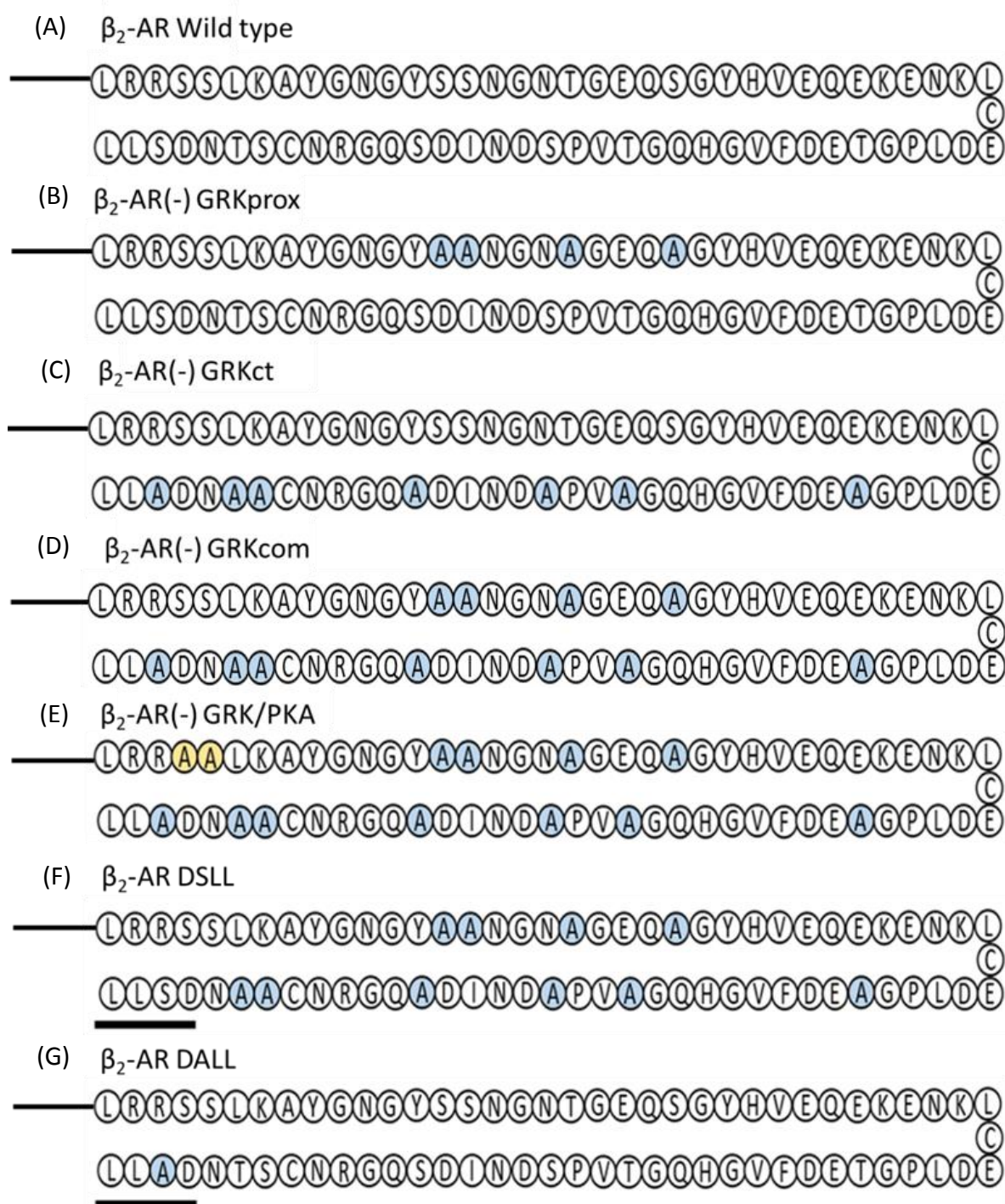
Figure 4.2: The C-terminal sequences of β₂-AR wild type or mutants

The sequences of β₂-AR wild type or mutants after the black line indicated in Figure 4.1. Blue or yellow shows the residues mutated to alanine in GRK phosphorylation sites or PKA phosphorylation sites, respectively. Note that PKA phosphorylation sites in ICL3 were also mutated to alanine in the β₂-AR (-) GRK/PKA construct. (A) β₂-AR wild type. β₂-AR mutants carrying mutations in which GRK and/or PKA phosphorylation sites are replaced by alanine residues, as follows; (B) β₂-AR (-) GRKprox 4 GRK site mutations in a proximal cassette,   (C) β₂-AR (-) GRKct 7 GRK site mutations in distal cassette, (D) β₂-AR (-) GRKcom complete 11 GRK site mutations, (E) β₂-AR (-) GRK/PKA complete 15 GRK/PKA site mutations, (F) β₂-AR DSLL 10 GRK site mutations except C-terminus PDZ motif (DSLL) and (G) β₂-AR DALL 1 mutation in the C-terminal PDZ motif.

4.2 Methods

4.2.1 Expression of the human β₂-AR in CHOGLUT4myc cells and cell culture

The human β_2-AR or mutant β_2-ARs were subcloned into pcDNA6.2/C-EMGFP-DEST (Section 2.2) or pcDNA3.1 (+) zeo vector already encoding SNAP-tag (Section 2.3). CHOGLUT4myc cells were stably transfected with the human β_2-AR or mutant β_2-ARs as described in Section 2.5. Rat L6 cells were grown as a monolayer in Dulbecco's Modified Eagle's Media (DMEM, Invitrogen, Paisley, UK), containing 10% (vol/vol) foetal bovine serum (FBS), and 10 mM HEPES. For differentiation, cells were allowed to reach confluence and the media changed to DMEM containing 2% (vol/vol) FBS for 7 d, with media changes every second day. CHO cells were grown in Dulbecco's Modified Eagle's Media-Ham's, DMEM F12 (1:1) (Sigma-Aldrich, MA, USA or Thermo Fisher Scientific, MA, USA), containing 5% (vol/vol) foetal calf serum, FCS (PAA laboratories, Pasching, Austria). Cells were grown at 37°C, 5% CO_2 in a water jacketed incubator as described in Section 2.4.

4.2.2 siRNA transfection

For transfection, L6 cells were seeded at 1×10^5 cells per well in 12-well plates and grown overnight. 100 pmole of small interfering RNA (siRNA) control (scrambled siRNA) or siRNA GRK (QIAGEN) was transfected using Lipofectamine 2000 (Invitrogen, Paisley, UK) in DMEM containing 5% FBS. Next day, media was replaced with DMEM containing no serum. Glucose uptake assays were performed 48 h after transfection.

4.2.3 [³H]-CGP12177A saturation and competition binding assays

The characteristics of [³H]-CGP12177A binding to whole cells were determined in saturation and competition studies as described in Section 2.6.2 and Section 2.6.3. For saturation studies, cells were incubated with varying concentrations of [³H]-CGP12177A (0 – 7 nM) in the presence or absence of 10 µM (-)-propranolol. In competition studies, cells were incubated with [³H]-CGP12177A (~2 nM) and a range of concentrations of either the β-AR agonist isoprenaline or the $\beta_{2/3}$-AR agonist BRL37344, with non-specific binding determined by 10 µM (-)-propranolol. All experiments were performed at 37°C for 2 h (Baker, 2010a). Analysis of saturation and competition assays is detailed in Section 2.11.2, respectively.

4.2.4 Cyclic AMP accumulation assays

cAMP accumulation assays were performed as described in Section 2.7.1. Cells were treated with varying concentrations of either isoprenaline or BRL37344 for 30 min in the presence or absence of 0.5 mM IBMX. For time course studies, isoprenaline or BRL37344 (1 µM) were added at specific time points in the absence of IBMX. Results are expressed as a percentage of the response to the adenylate cyclase activator forskolin (100 µM) or pmole cAMP per well in each independent experiment. Analysis of data is detailed in Section 2.11.1.

4.2.5 β_2-AR internalisation assays

Internalisation assays were performed in CHOGLUT4myc cells expressing SNAP tagged human β_2-AR as described in Section 2.9.1. Cells were treated with either isoprenaline or BRL37344 (10 µM) at $37^\circ C$ for 1 h. As this assay is driven by receptor occupancy with limited receptor reserve, 10 µM ligand concentrations were chosen. The granularity diameter settings are set on the basis of the perinuclear compartment diameter. Results are expressed as a percentage of the β_2-AR internalisation response in vehicle treated cells (100 %) in each independent experiment. Analysis of data is detailed in Section 2.11.4.

4.2.6 [^{3}H]-2-deoxyglucose uptake assays

[^{3}H]-2-deoxyglucose uptake assays were performed as described in Section 2.6.1. Cells were treated with varying concentrations of either isoprenaline or BRL37344 for 2 h. Insulin (10 µM) was used as a positive control in each experiment performed. 10 µM of BRL37344 was used in L6 cells since 1 µM of BRL37344 was not enough to produce maximal glucose uptake effect in Chapter 3. Results are expressed as a percentage of glucose uptake in vehicle-treated cells in each independent experiment. Analysis of data is detailed in Section 2.11.1.

4.2.7 GLUT4 translocation assays

GLUT4 translocation assays were performed as described in Section 2.9.2. Cells were treated with either isoprenaline or BRL37344 (1 µM) for 2 h. Insulin (10 µM) was used as a positive control in each experiment performed. Results are expressed as a percentage of the amount of GLUT4 at the cell surface in comparison to vehicle-treated cells in each independent experiment. Analysis of data is detailed in Section 2.11.5.

4.2.8 Reverse transcription-PCR

This was performed in CHOGLUT4myc cells (Dehvari et al., 2012) or L6 cells by Dr Dana S Hutchinson.

4.2.9 Data analysis

All results are expressed as mean ± s.e.mean of n independent experiments. Since clonal cells are used, each n number is defined as an experiment performed on different days from cells from different passages. Data was analysed with GraphPad PRISM v7.02. Statistically significant difference was analysed by using (1) Student's paired t tests to make pairwise comparisons of siRNA mediated inhibitory effects where siRNA was used, or to compare the magnitude of the same response at two different time points, (2) Student's unpaired t tests to make pairwise comparisons between two ligands, two pathways or two receptors (3) One-way ANOVA Dunnett's multiple comparisons test to make comparison of effects acted on multiple receptors, (4) Two-way ANOVA Sidak's multiple comparisons test to make comparison of receptor internalisation effect. P values less than 0.05 were considered significant.

The operational model, an analytical approach to quantify agonist bias, (Black & Leff, 1983; Riddy et al., 2017) (Section 2.11.7) was used to determine the transduction ratio R ($=\tau$ /K_A), and to compare the effects of isoprenaline vs BRL37344 in wild type or mutated β_2-AR as below;

Transduction ratio (R) is defined by the ratio of τ /K_A as follows;

$$\text{Equation 1,} \quad R = \frac{\tau}{K_A}$$

Where τ is an index of the coupling efficacy of the agonist, and K_A is the functional equilibrium dissociation constant of the agonist.

The logarithm of the "transduction coefficient" (LogR) was obtained by fitting concentration response curves using equation 2 in GraphPad Prism (v7.0; GraphPad Software, La Jolla, CA).

$$\text{Equation 2,} \quad \text{Effect of the ligand} = \text{Basal} + \frac{(E_m - \text{Basal})}{1 + \left(\dfrac{\dfrac{[A]}{10^{\text{Log}K_A}} + 1}{10^{\text{Log}R} \text{ x } [A]}\right)^n}$$

Where [A] is the concentration of agonist, Em is the maximal possible response of the system, Basal is the response in unstimulated system, logK$_A$ is the logarithm of the functional equilibrium

dissociation constant of the agonist, n is the slope of the transducer function that links occupancy to response. For partial agonists LogK$_A$ was fitted whereas for full agonists LogK$_A$ was constrained to 0 (van der Westhuizen et al., 2014).

Where the response of mutant β$_2$-ARs was compared to that of wild type, the LogR value was corrected for the receptor expression level of mutant to wild type, since τ is defined in the operational model as the ratio of receptor density R$_T$ divided by the stimulus coupling efficiency K$_E$ (the concentration of agonist occupied receptor that elicits the half maximal tissue response) (Black & Leff, 1983).

Equation 3, $\text{Corrected LogR} = \text{LogR} - \text{Log}\left\{\dfrac{\text{Bmax(Mutant)}}{\text{Bmax(Wild type)}}\right\}$

To determine the relative effectiveness of ligands or mutant receptors, (1) the difference between LogR values (ΔLogR) was calculated using equation 4 (for comparing BRL and ISO parameters), or 5 (for comparing ISO measurements in mutant receptor cell lines versus wild type); (2) the estimated standard errors of the mean of equation 4 or 5 were calculated using equation 6 or 7 respectively; (3) the relative effectiveness toward each pathway, relative to ISO, was calculated using equation 8.

Equation 4, $\Delta\text{LogR} = \text{LogR}_{\text{BRL:Wild type}} - \text{LogR}_{\text{ISO:Wild type}}$

Equation 5, $\Delta\text{LogR} = \text{LogR}_{\text{ISO:Mutant}} - \text{LogR}_{\text{ISO:Wild type}}$

Where ISO is isoprenaline, BRL is BRL37344, Wild type is the β$_2$-AR wild type and Mutant is β$_2$-AR mutant.

Equation 6, $\text{s.e.m}_{\Delta\text{LogR}} = \sqrt{\left(\text{s.e. m}_{\text{BRL:Wild type}}\right)^2 + \left(\text{s.e.m}_{\text{ISO:Wild type}}\right)^2}$

Equation 7, $\text{s.e.m}_{\Delta\text{LogR}} = \sqrt{\left(\text{s.e. m}_{\text{ISO:Mutant}}\right)^2 + \left(\text{s.e.m}_{\text{ISO:Wild type}}\right)^2}$

Equation 8, $\text{Relative effectivness} = 10^{\Delta\text{LogR}}$

To determine bias factors, (1) the difference between the ΔlogR values (ΔΔlogR) was calculated using equation 9; (2) the estimated standard error of mean of equation 9 was calculated using equation 10; (3) each bias factor was calculated using equation 11.

Equation 9, $\Delta\Delta LogR_{Path} = \Delta LogR_{Path1} - \Delta LogR_{Path2}$

Equation 10, $s.e.m_{\Delta\Delta LogR_{Path}} = \sqrt{\left(s.e.m_{\Delta LogR_{Path1-Path2}}\right)^2 + \left(s.e.m_{\Delta LogR_{Path1-Path2}}\right)^2}$

Equation 11, $Bias\ factor = 10^{\Delta\Delta LogR_{Path}}$

4.3 Results

4.3.1 Reduction of [³H]-2-deoxyglucose uptake in L6 myoblast lacking GRK2

Isoprenaline (a non-selective β-agonist), and BRL37344 (a dual $\beta_{2/3}$-agonist) stimulated glucose uptake in rat L6 myotubes expressing the β_2-AR (Chapter 3). Both L6 myoblasts and myotubes express GRK2, GRK4, GRK5 and GRK6 (Figure 4.3). To determine whether GRK2 is involved in isoprenaline- or BRL37344-stimulated glucose uptake, siRNA (siRNA control or siRNA GRK2) was transfected into L6 myoblasts to selectively knock down GRK2 48 h prior to glucose uptake assays. GRK2 knockdown significantly reduced isoprenaline- or BRL37344-stimulated glucose uptake but not insulin-stimulated glucose uptake; in contrast the scrambled siRNA control had no effect on isoprenaline or BRL37344 responses (Figure 4.4). The role of GRK was further examined utilizing CHOGLUT4myc cells stably expressing the human β_2-AR wild type or mutant receptors. Note that CHOGLUT4myc cells predominantly express GRK5 and GRK2 isoforms, and express GRK6 at a lower level ((Dehvari et al., 2012), Figure 4.3).

4.3.2 Examination of the radioligand binding characteristics of [³H]-CGP12177A in CHOGLUT4myc cells expressing the wild type or mutant human β_2-ARs

4.3.2.1 Saturation binding

[³H]-CGP12177A binding occurred in a saturable manner to a single binding site in CHOGLUT4myc cells expressing the wild type β_2-AR (Bmax 158.5 ± 10.6 fmol/mg protein; pK_D 9.49 ± 0.08; n=5; Figure 4.5A; Table 4.1). Saturation binding in CHOGLUT4myc cells expressing the mutant β_2-ARs also occurred in a saturable manner to a single binding site (Figure 4.5B–G; Table 4.1). All mutant receptor cell lines showed comparable levels of [³H]-CGP12177A binding to the β_2-AR in relation to the wild type receptor, with the exception of the β_2-AR (-)GRKprox, the β_2-AR (-)GRKcom and β_2-AR (-) GRK/PKA mutant cell line, which showed significantly less binding capacity (**P<0.01 and ***P<0.001, One-way ANOVA Dunnett's multiple comparisons test). There was no difference in the pK_D values for [³H]-CGP12177A between the different cell lines.
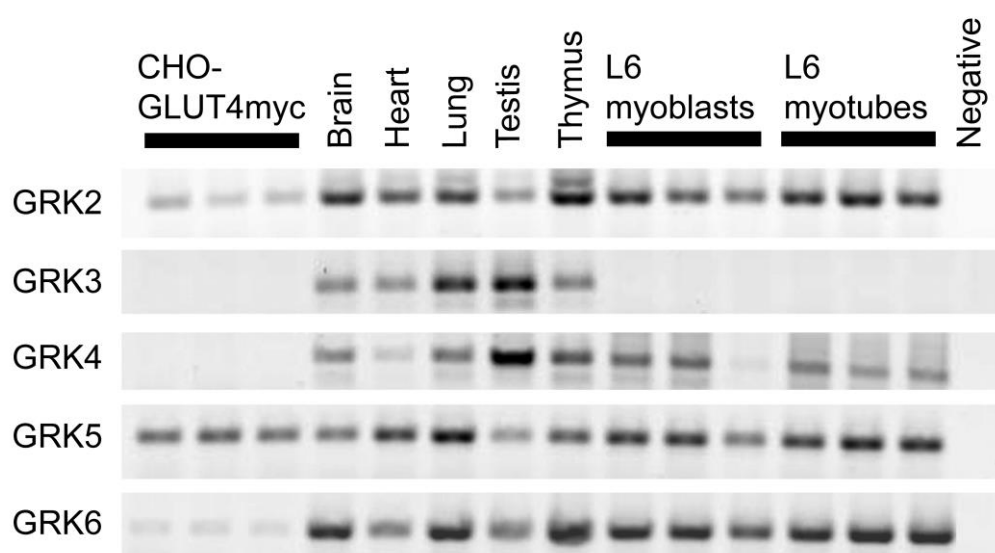
Figure 4.3: Reverse transcription-PCR of GRK isoform mRNAs endogenously expressed in CHOGLUT4myc cells or rat L6 skeletal muscle cells expressing β₂-ARs

Reverse transcription-PCR showing the presence of different GRK isoforms in CHOGLUT4myc cells or L6 cells. The image is representative of 3 independent experiments. Control rat tissues known to express different GRK isoforms are included as positive controls. This was performed in CHOGLUT4myc cells (Dehvari et al., 2012) or L6 cells by Dr Dana S Hutchinson.
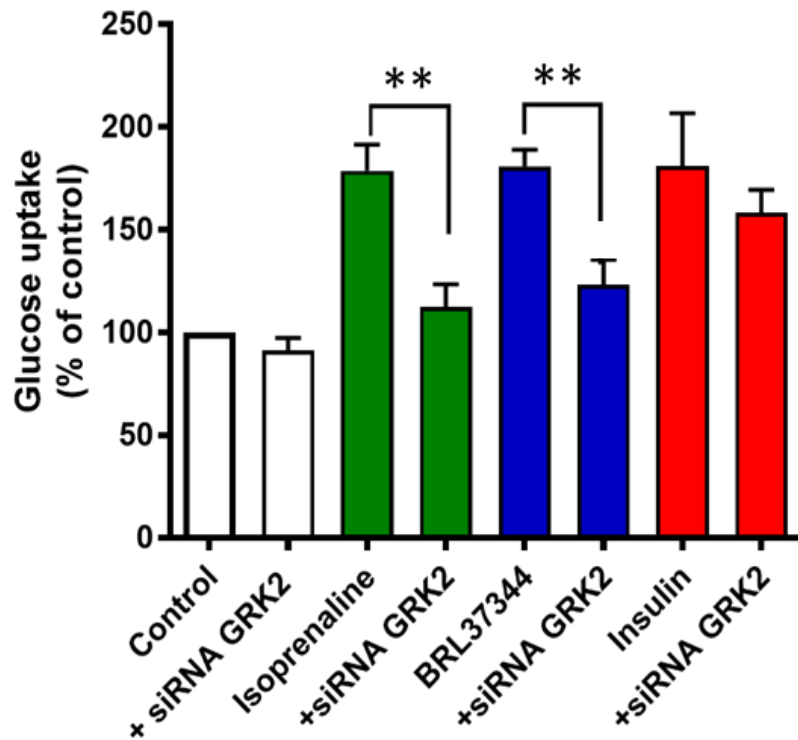
Figure 4.4: Effect of GRK2 ablation on the glucose uptake response to isoprenaline or BRL37344 in rat L6 skeletal muscle cells endogenously expressing β₂-ARs

2-deoxy-[³H]-glucose uptake was measured in L6 myoblasts transfected with siRNA control or siRNA GRK2 following stimulation with either isoprenaline (1 μM), BRL37344 (10 μM) or insulin (1 μM) for 2 h. Values are mean ± s.e.mean of 4-7 independent experiments performed in duplicate. Data are normalized to values in vehicle treated cells at 2 h. Asterisks represent statistical differences as analysed by Student's paired t-test to make pairwise comparisons of siRNA mediated inhibitory effects between two groups (**P < 0.01).
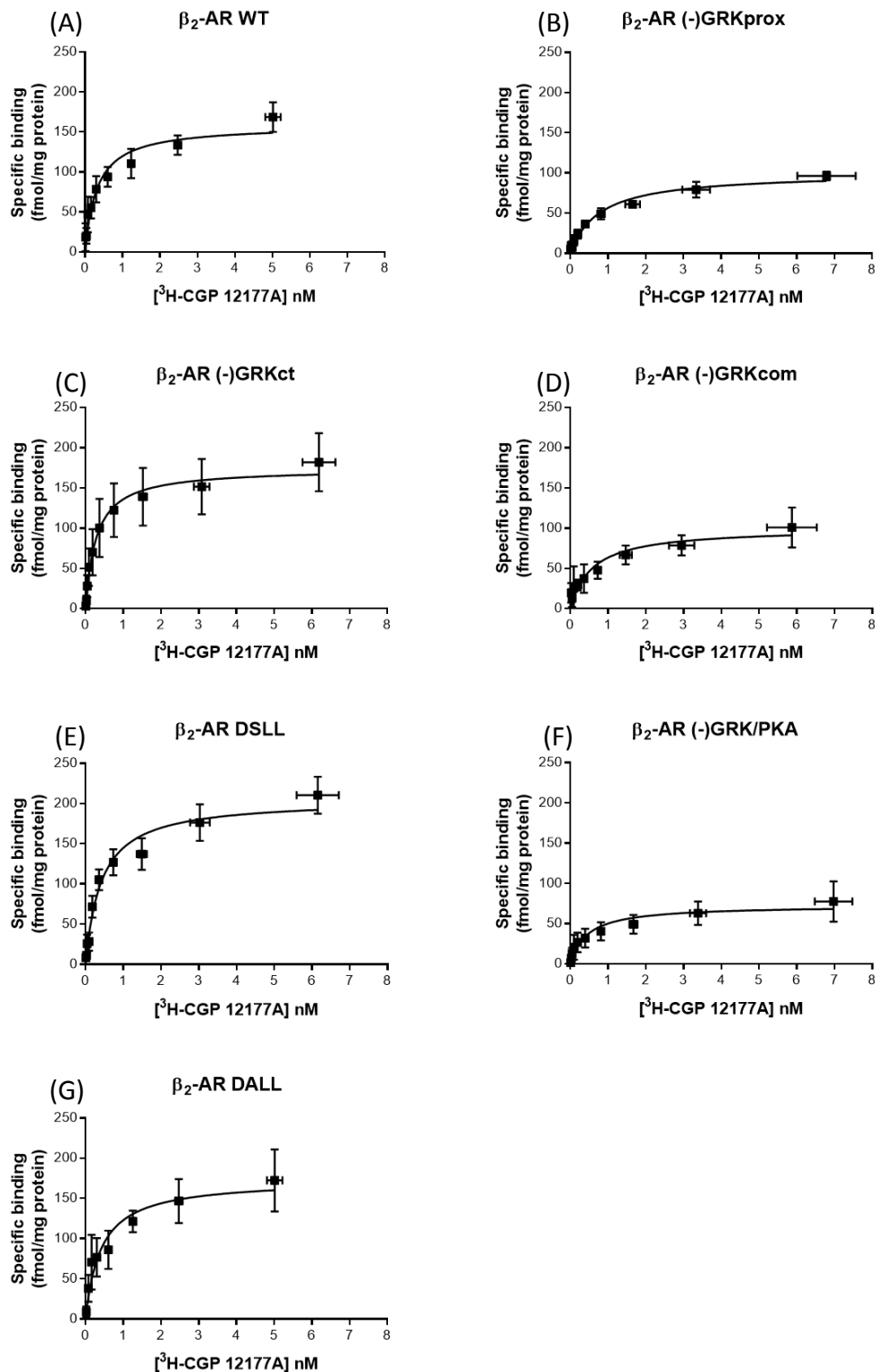
Figure 4.5: Saturation binding of [³H]-CGP12177A in CHOGLUT4myc cells stably expressing wild type or mutant β₂-ARs

Specific binding (expressed as fmol/mg protein) was determined in CHOGLUT4myc cells stably expressing the (A) β₂-AR WT, (B) β₂-AR (-)GRKprox, (C) β₂-AR (-)GRKct, (D) β₂-AR (-)GRKcom, (E) β₂-AR DSLL, (F) β₂-AR (-)GRK/PKA or (G) β₂-AR DALL. Cells were incubated with increasing concentrations of [³H]-CGP12177A for 2 h. Non-specific binding was determined in the presence of 10 µM (-)-propranolol. Points show mean ± s.e.mean of 5 independent experiments performed in quadruplicate.

Table 4.1: Summary of affinity (pK$_D$) and density of binding sites (Bmax) obtained from [^{3}H]-CGP12177A whole cell saturation binding studies in CHOGLUT4myc cells expressing the wild type or mutant β$_2$-ARs.

Data were obtained from saturation binding curves in Figure 4.5. Values represent mean ± s.e.mean of 5 independent experiments performed in quadruplicate. **P<0.01, ***P<0.001 compared to the β$_2$-AR WT Bmax value (One-way ANOVA Dunnett's multiple comparisons test).

CHOβ$_2$ARGLUT4myc	Mutation	pK$_D$	Bmax (fmol/mg protein)
β$_2$-AR WT		9.49 ± 0.08	158.5 ± 10.6
β$_2$-AR (-) GRKprox	GRK site mutations in a proximal cassette	9.11 ± 0.14	100.3 ± 5.6**
β$_2$-AR (-) GRKct	GRK site mutations in distal cassette	9.55 ± 0.04	174.2 ± 6.0
β$_2$-AR (-) GRKcom	Complete GRK site mutations	9.24 ± 0.19	100.1 ± 10.0**
β$_2$-AR DSLL	GRK site mutations except C-terminus PDZ motif	9.38 ± 0.08	205.0 ± 11.1
β$_2$-AR (-) GRK/PKA	Complete GRK/PKA site mutations	9.35 ± 0.13	72.7 ± 5.7 ***
β$_2$-AR DALL	Mutation in the C-terminus PDZ motif	9.39 ± 0.11	173.2 ± 13.9

4.3.2.2 Competition binding

Competition binding studies were performed to determine the affinities (pK_i) of isoprenaline and BRL37344 at the wild type or mutant β_2-ARs expressed in CHOGLUT4myc cells, and to certify that the affinity of those ligands is not affected by the receptor mutations. BRL37344 affinities (pK_i) were similar in all β_2-AR mutant cell lines compared to β_2-AR wild type whereas isoprenaline exhibited very similar pK_i values to β_2-AR wild type and mutant lines except β_2-AR (-) GRKprox and β_2-AR (-) GRKcom ($***P<0.001$, One-way ANOVA Dunnett's multiple comparisons test) (Figure 4.6; Table 4.2).

4.3.3 β_2-AR mediated increases in [^{3}H]-2-deoxyglucose uptake and GLUT4 translocation in CHOGLUT4myc cells expressing the wild type or mutant human β_2-ARs

No glucose uptake in response to either isoprenaline or BRL37344 was observed in cells not expressing the human β_2-AR ((Dehvari et al., 2012), Figure 4.7), and insulin increased glucose uptake in all cell lines used (Figure 4.8B; Table 4.3). Isoprenaline and BRL37344 increased glucose uptake in CHOGLUT4myc cells expressing the wild type human β_2-AR in a concentration specific manner (Figure 4.9A; Table 4.4). This response was retained in all the CHOGLUT4myc cells expressing mutant human β_2-ARs (Figure 4.9B-G; Table 4.4), with no differences in the potency or maximal response to either drug as compared to effects observed at the wild type receptor, with the exception of Rmax values of β_2-AR (-) GRKprox and β_2-AR (-)GRKct for isoprenaline ($**P<0.01$, $*P<0.05$ compared to wild type, One-way ANOVA Dunnett's multiple comparisons test).

GLUT4 translocation to the cell surface in response to isoprenaline or BRL37344 was performed in 4 of the CHOβ_2-AR-GLUT4 cell lines, with the cell lines expressing partial β_2-AR phosphosite-mutations omitted from this study. The human GLUT4 (GLUT4myc) expressed in the transfected cells carries a c-myc epitope within extracellular loop 1. Cells were non-permeabilized during the experiment, therefore, only GLUT4myc at the plasma membrane was selectively labelled with c-myc primary antibody. Isoprenaline or BRL37344 increased the translocation of c-myc tagged GLUT4 to the cell surface in a time (Figure 4.10, 4.15A) in a concentration-dependent manner (Figure 4.14, 4.16A; Table 4.5) in CHOGLUT4myc cells expressing the wild type human β_2-AR. This effect was retained in the mutant β_2-AR cell lines (Figure 4.11-13, 15B-D, 4.16B-D; Table 4.5), with no difference in the potency or maximum response of either drug as compared to effects observed at the wild type receptor. Insulin increased GLUT4 translocation in all cell lines examined, as a positive control (Figure 4.8B).
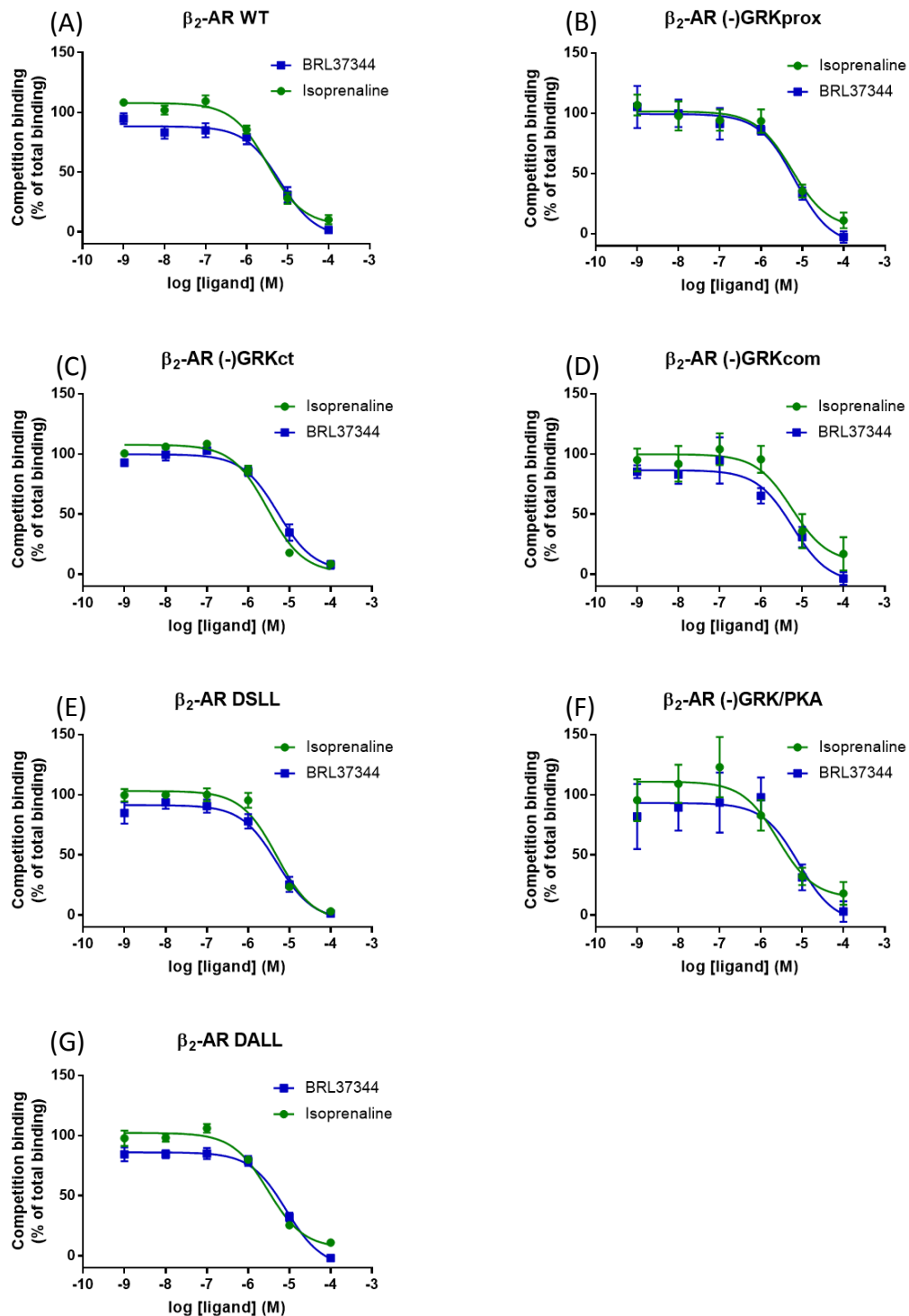
Figure 4.6: Competition binding between [^{3}H]-CGP12177A and the β$_2$-AR agonists, Isoprenaline or BRL37344

Isoprenaline or BRL37344 was incubated with ~ 2 nM [^{3}H]-CGP12177A for 2 h in CHOGLUT4myc cells stably expressing the (A) β$_2$-AR WT, (B) β$_2$-AR (-)GRKprox, (C) β$_2$-AR (-)GRKct, (D) β$_2$-AR (-)GRKcom, (E) β$_2$-AR DSLL, (F) β$_2$-AR R(-)GRK/PKA or (G) β$_2$-AR DALL . Non-specific binding was determined by 10 μM (-)-propranolol. Points show mean ± s.e.mean of 5 independent experiments performed in triplicate, normalised to total binding (100%) and non-specific binding (0%).

Table 4.2: Summary of affinity (pK$_i$) values for isoprenaline and BRL37344 obtained from [^{3}H]-CGP 12177A whole cell competition binding studies in CHOGLUT4myc cells expressing the wild type or mutant β$_2$-ARs.

Data were obtained from competition binding curves in Figure 4.6. Values represent mean ± s.e.mean of 5 independent experiments performed in triplicate. ***P<0.001 compared to the β$_2$-AR WT pK$_i$ value (One-way ANOVA with Dunnett's multiple comparisons test).

	pK$_i$	
	Isoprenaline	BRL37344
β$_2$-AR WT	6.28 ± 0.07	5.87 ± 0.09
β$_2$-AR (-) GRKprox	5.53 ± 0.07***	5.56 ± 0.09
β$_2$-AR (-) GRKct	6.30 ± 0.06	6.02 ± 0.07
β$_2$-AR (-) GRKcom	5.45 ± 0.16***	5.59 ± 0.11
β$_2$-AR DSLL	5.93 ± 0.06	5.88 ± 0.07
β$_2$-AR (-) GRK/PKA	6.29 ± 0.11	5.65 ± 0.07
β$_2$-AR DALL	6.16 ± 0.06	5.69 ± 0.08
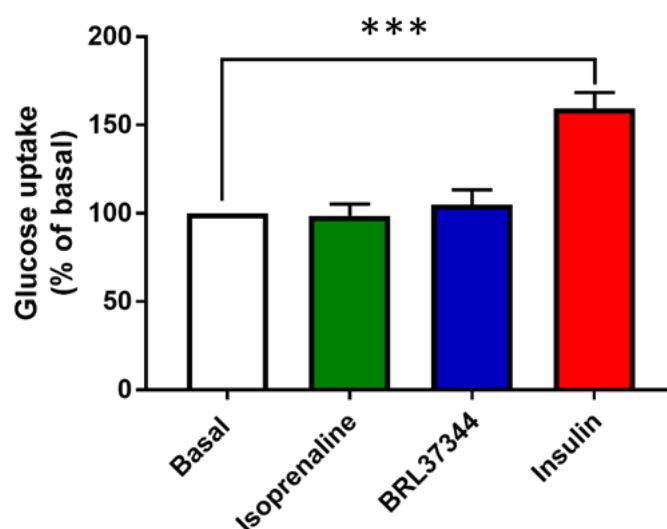
Figure 4.7: Effect of isoprenaline or BRL37344 on glucose uptake in non-transfected CHOGLUT4myc cells

2-deoxy-[^{3}H]-glucose uptake was measured in non-transfected CHOGLUT4myc cells following stimulation with either isoprenaline (1 µM), BRL37344 (1 µM) of insulin (10 µM) for 2 h. Values are mean ± s.e.mean of 4 independent experiments performed in duplicate. Data are normalized to values in basal/vehicle treated cells at 2 h. Asterisks represent statistical differences as analysed by one-way ANOVA and Dunnett's multiple comparisons test for different agonists compared to basal (***$P < 0.001$).
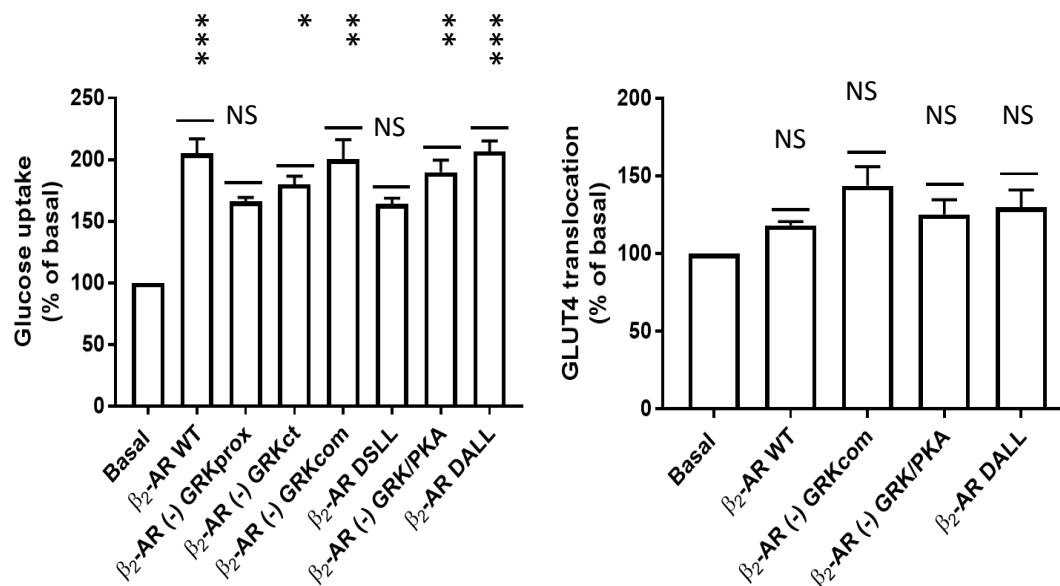
Figure 4.8: Quantification of glucose uptake or GLUT4 translocation in response to insulin in CHOGLUT4myc cells stably expressing the β₂-AR

In (A) glucose uptake following 120 min stimulation with 10 µM insulin either in β₂-AR WT, β₂-AR (-) GRKprox, β₂-AR (-) GRKct, β₂-AR (-) GRKcom, β₂-AR DSLL, β₂-AR (-) GRK/PKA or β₂-AR DALL. In (B), GLUT4 translocation following 120 min stimulation with 10 µM insulin either in β₂-AR WT, β₂-AR DALL, β₂-AR (-) GRKcom or β₂-AR (-) GRK/PKA. Values are mean ± s.e.mean of 5-6 independent experiments performed in duplicate. Data are normalized to values in basal/vehicle treated cells at 120 min. Asterisks represent statistical differences as analysed by one-way ANOVA and Dunnett's multiple comparisons test compared to basal (*$P<0.05$, **$P<0.01$, ***$P < 0.001$). NS = not significant.

Table 4.3: Summary of 10 μM insulin response for [^{3}H]-2-deoxyglucose uptake and GLUT4 translocation in CHOGLUT4myc cells expressing the wild type or mutant β$_2$-ARs

Data were obtained from the bar graphs in Figure 4.8, 4.16. Values represent mean ± s.e.mean from 5-6 experiments performed in duplicate. NA = Not applicable. *P<0.05, **P<0.01, ***P<0.001 compared to the basal (100%) (One-way ANOVA with Dunnett's multiple comparisons test).

	[^{3}H]-2-deoxyglucose uptake (% of basal)	GLUT4 translocation (% of vehicle)
β$_2$-AR WT	205.3 ± 11.6 ***	118.3 ± 2.6
β$_2$-AR (-) GRKprox	166.2 ± 3.3	NA
β$_2$-AR (-) GRKct	180.1 ± 6.7 *	NA
β$_2$-AR (-) GRKcom	200.4 ± 15.2 **	143.8 ± 12.3
β$_2$-AR DSLL	164.0 ± 4.9	NA
β$_2$-AR (-) GRK/PKA	190.0 ± 9.7 **	125.5 ± 9.3
β$_2$-AR DALL	206.7 ± 8.7 ***	129.8 ± 11.2
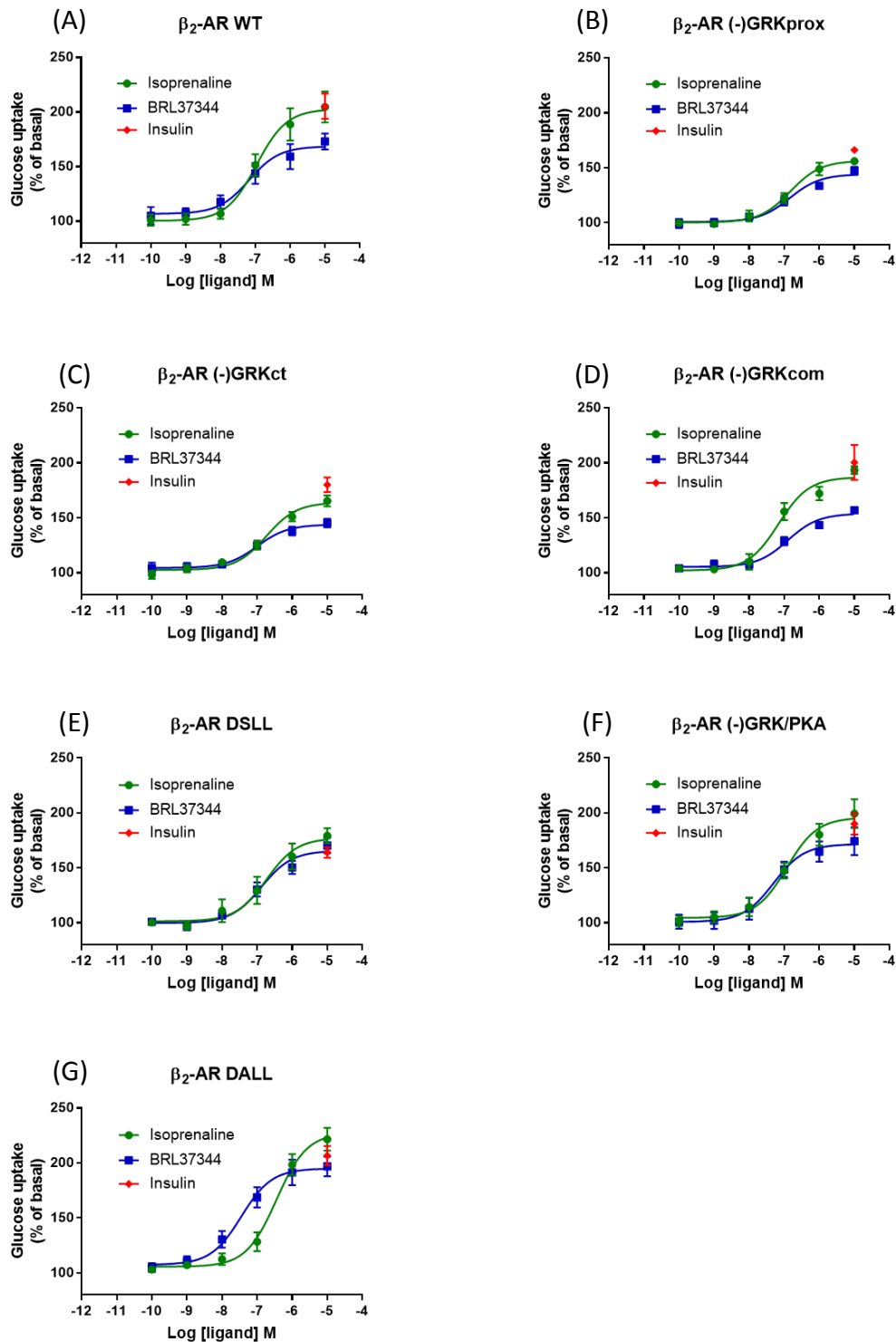
Figure 4.9: Concentration-dependent effect of isoprenaline or BRL37344 on glucose uptake in CHOGLUT4myc cells stably expressing the β₂-AR

2-deoxy-[³H]-glucose uptake was measured in (A) β₂-AR WT, (B) β₂-AR (-) GRKprox, (C) β₂-AR (-) GRKct, (D) β₂-AR (-) GRKcom, (E) β₂-AR DSLL, (F) β₂-AR (-) GRK/PKA or (G) β₂-AR DALL following stimulation with either isoprenaline, BRL37344 or insulin (10 μM) for 2 h. Values are mean ± s.e.mean of 5-6 independent experiments performed in duplicate. Data are normalized to values in vehicle treated cells at 2 h.

Table 4.4: Summary of potency (pEC$_{50}$) and maximal response; Rmax for [^{3}H]-2-deoxyglucose uptake in CHOGLUT4myc cells expressing the wild type or mutant β$_2$-ARs

Data were obtained from the concentration response curves in Figure 4.9. Values represent mean ± s.e.mean from 5-6 experiments performed in duplicate. No pEC$_{50}$ values were significantly different compared to the β$_2$-AR WT pEC$_{50}$. Rmax values for isoprenaline were significantly different for β$_2$-AR (-) GRKprox and β$_2$-AR (-)GRKct as compared to the β$_2$-AR WT response *P<0.05, **P<0.01 (One-way ANOVA Dunnett's multiple comparisons test).

	pEC$_{50}$		Rmax (% of basal)	
	Isoprenaline	BRL37344	Isoprenaline	BRL37344
β$_2$-AR WT	6.98 ± 0.18	7.24 ± 0.26	202.6 ± 7.74	168.1 ± 6.06
β$_2$-AR (-) GRKprox	6.83 ± 0.14	6.84 ± 0.18	156.5 ± 3.32**	144.2 ± 3.27
β$_2$-AR (-) GRKct	6.73 ± 0.15	6.99 ± 0.18	164.1 ± 3.72*	143.9 ± 2.86
β$_2$-AR (-) GRKcom	7.16 ± 0.14	6.95 ± 0.15	186.9 ± 4.45	153.5 ± 3.09
β$_2$-AR DSLL	6.73 ± 0.25	6.87 ± 0.16	177.2 ± 7.89	165.6 ± 4.41
β$_2$-AR (-) GRK/PKA	6.91 ± 0.18	7.28 ± 0.25	196.0 ± 6.87	171.8 ± 6.46
β$_2$-AR DALL	6.44 ± 0.14	7.45 ± 0.20	227.5 ± 7.60	195.0 ± 5.35
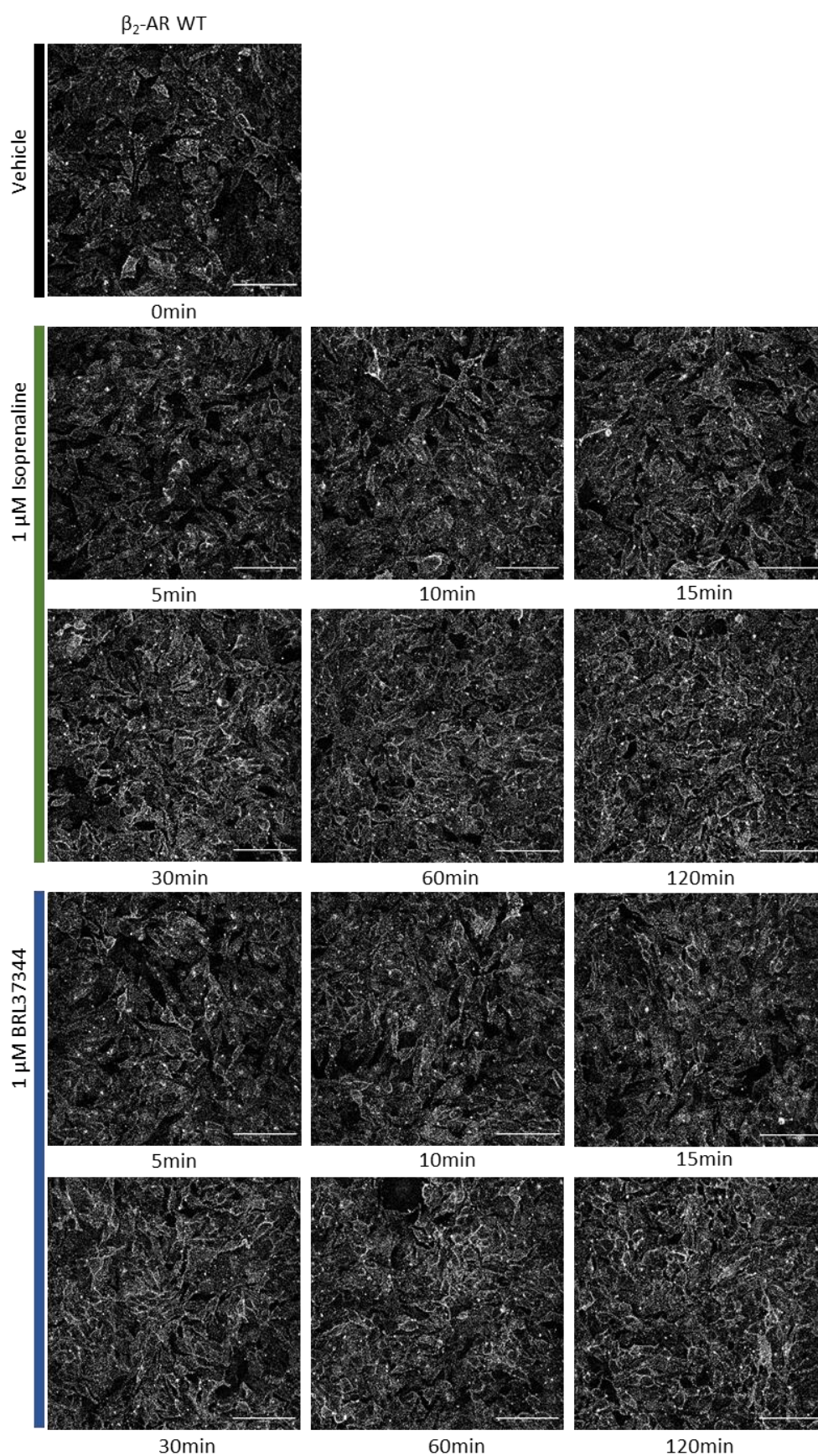
Figure 4.10: Effect of isoprenaline or BRL37344 on GLUT4 translocation in CHOGLUT4myc cells stably expressing the β₂-AR WT receptor

Cells were treated with either 1 μM isoprenaline or 1 μM BRL37344 for 0 – 120 min. Images are representative of 5 independent experiments performed in duplicate. Scale bar is 100 μm.
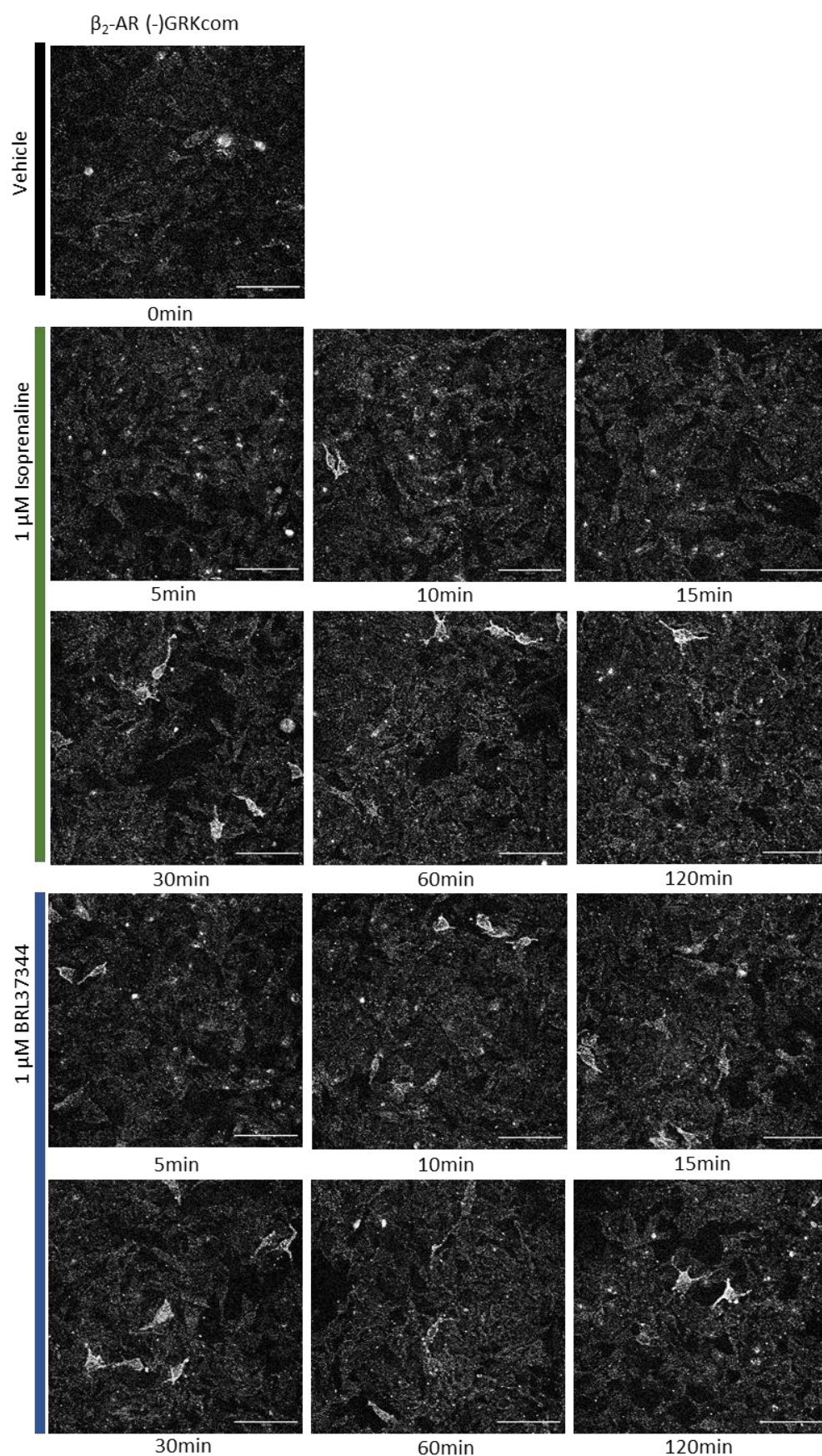
Figure 4.11: Effect of isoprenaline or BRL37344 on GLUT4 translocation in CHOGLUT4myc cells stably expressing the β₂-AR (-) GRKcom receptor

Cells were treated with either 1 μM isoprenaline or 1 μM BRL37344 for 0 – 120 min. Images are representative of 5 independent experiments performed in duplicate. Scale bar is 100 μm.
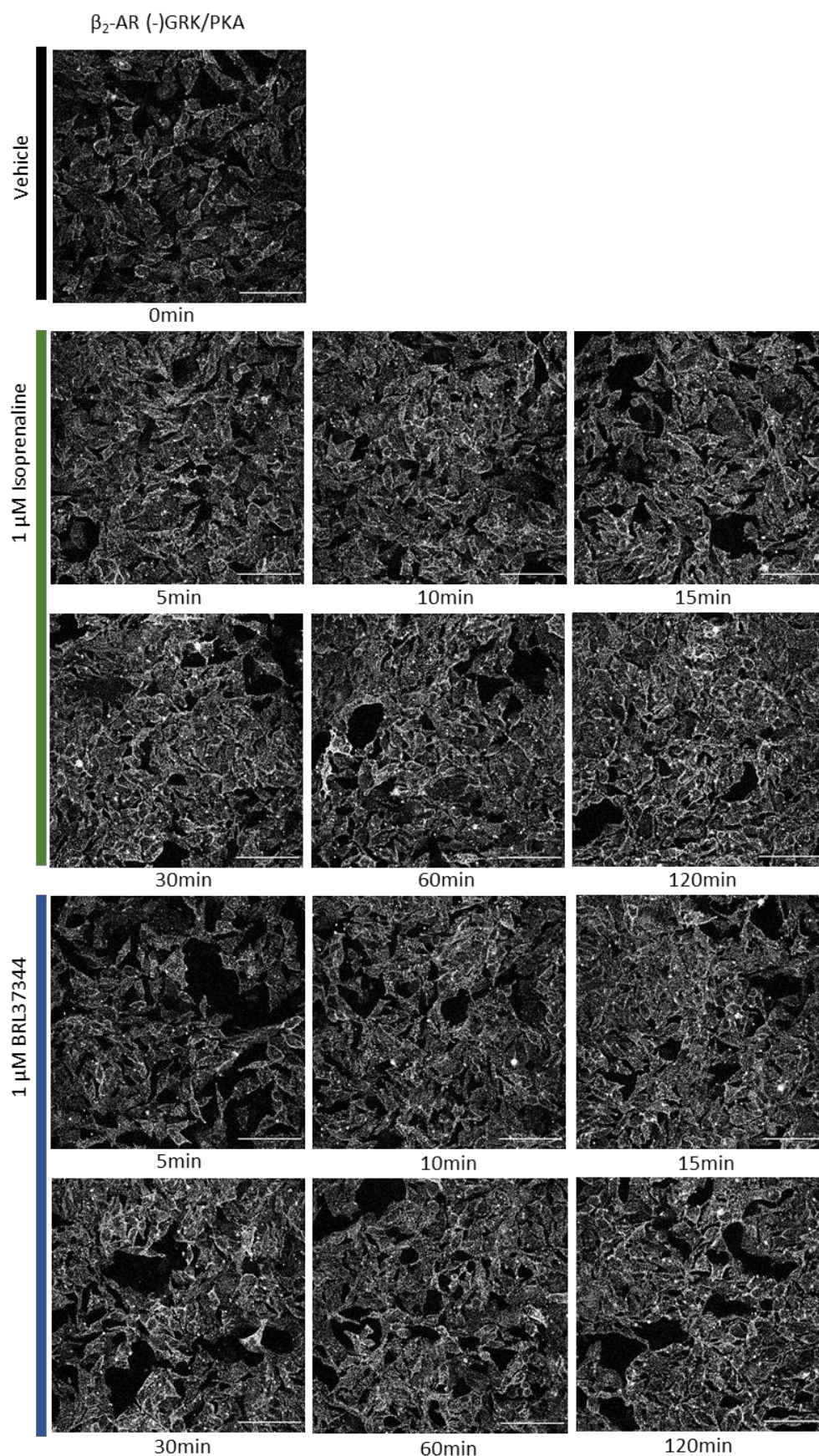
Figure 4.12: Effect of isoprenaline or BRL37344 on GLUT4 translocation in CHOGLUT4myc cells stably expressing the β_2-AR (-) GRK/PKA receptor

Cells were treated with either 1 μM isoprenaline or 1 μM BRL37344 for 0 – 120 min. Images are representative of 5 independent experiments performed in duplicate. Scale bar is 100 μm.
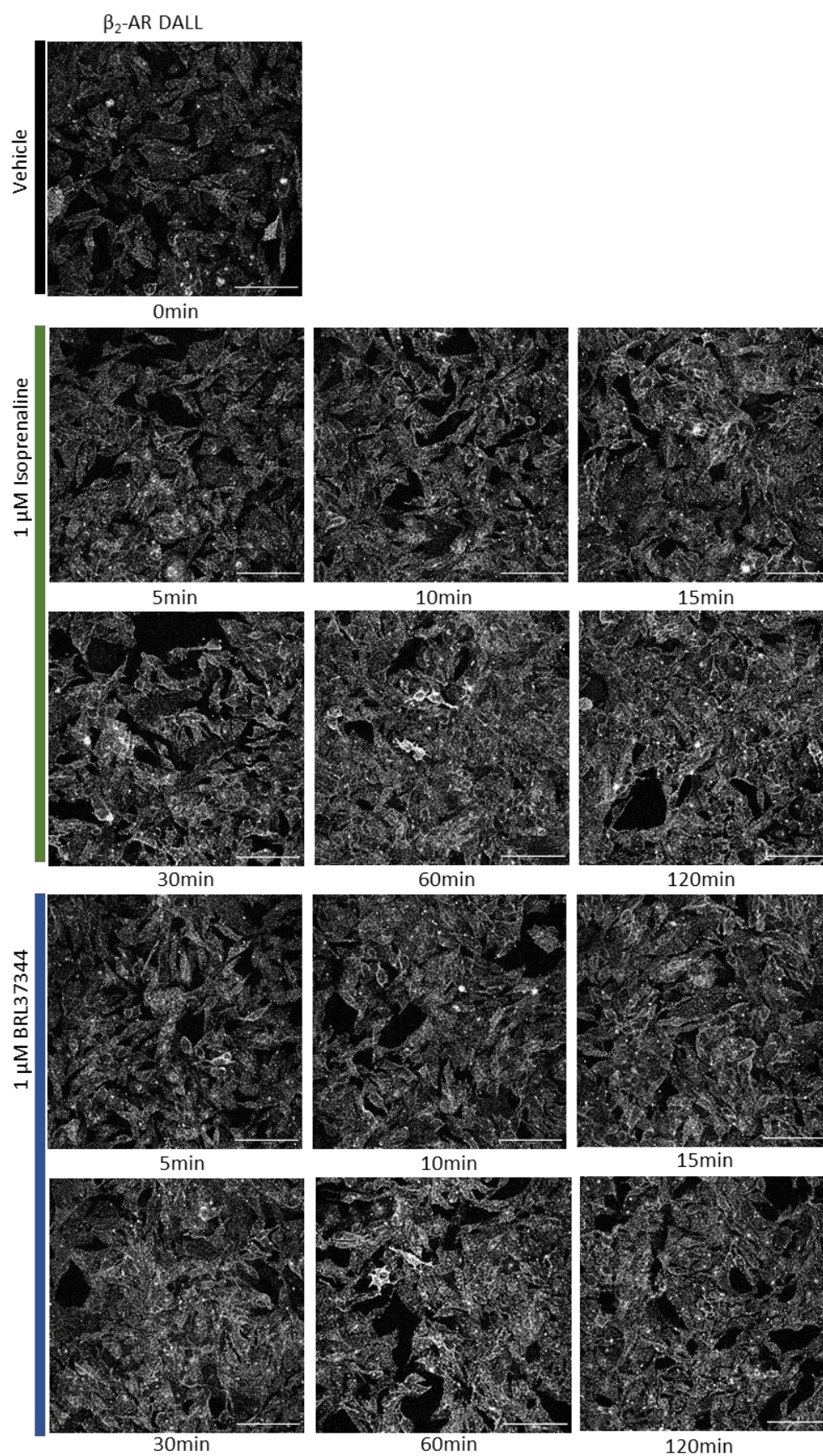
Figure 4.13: Effect of isoprenaline or BRL37344 on GLUT4 translocation in CHOGLUT4myc cells stably expressing the β₂-AR DALL receptor

Cells were treated with either 1 μM isoprenaline or 1 μM BRL37344 for 0 – 120 min. Images are representative of 5 independent experiments performed in duplicate. Scale bar is 100 μm.
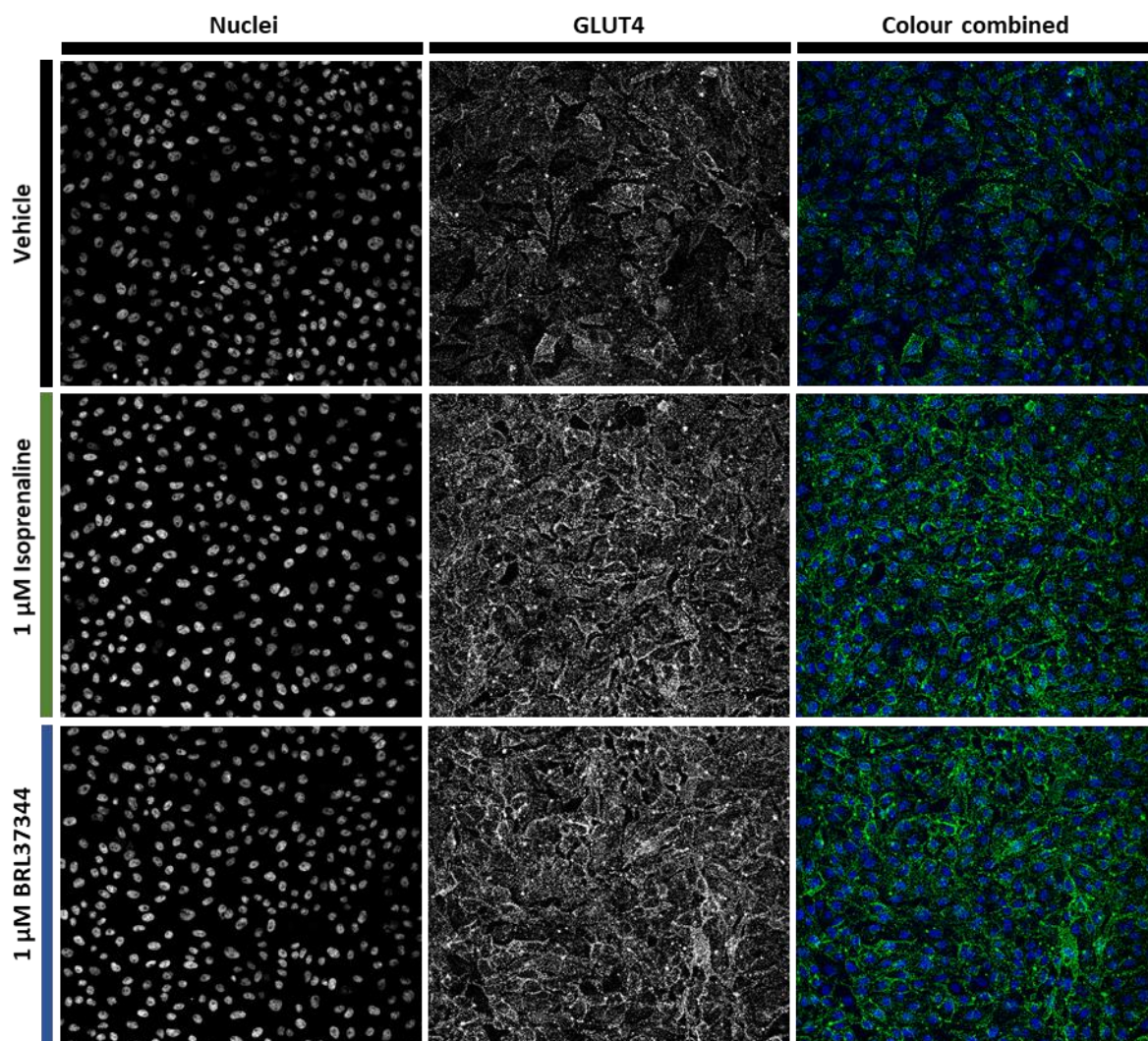
Figure 4.14: GLUT4 translocation in response to Isoprenaline or BRL37344 in CHOGLUT4myc cells stably expressing the β₂-AR WT receptor

Cells were treated with 1 μM isoprenaline or 1 μM BRL37344 for 120 min in prior to fixation. This panel shows nuclei stained with H33342 (left), GLUT4myc captured with myc tag antibody (middle) and the colour combined with nuclei in blue and GLUT4myc in green (right). Images are representative of 5 independent experiments performed in duplicate.
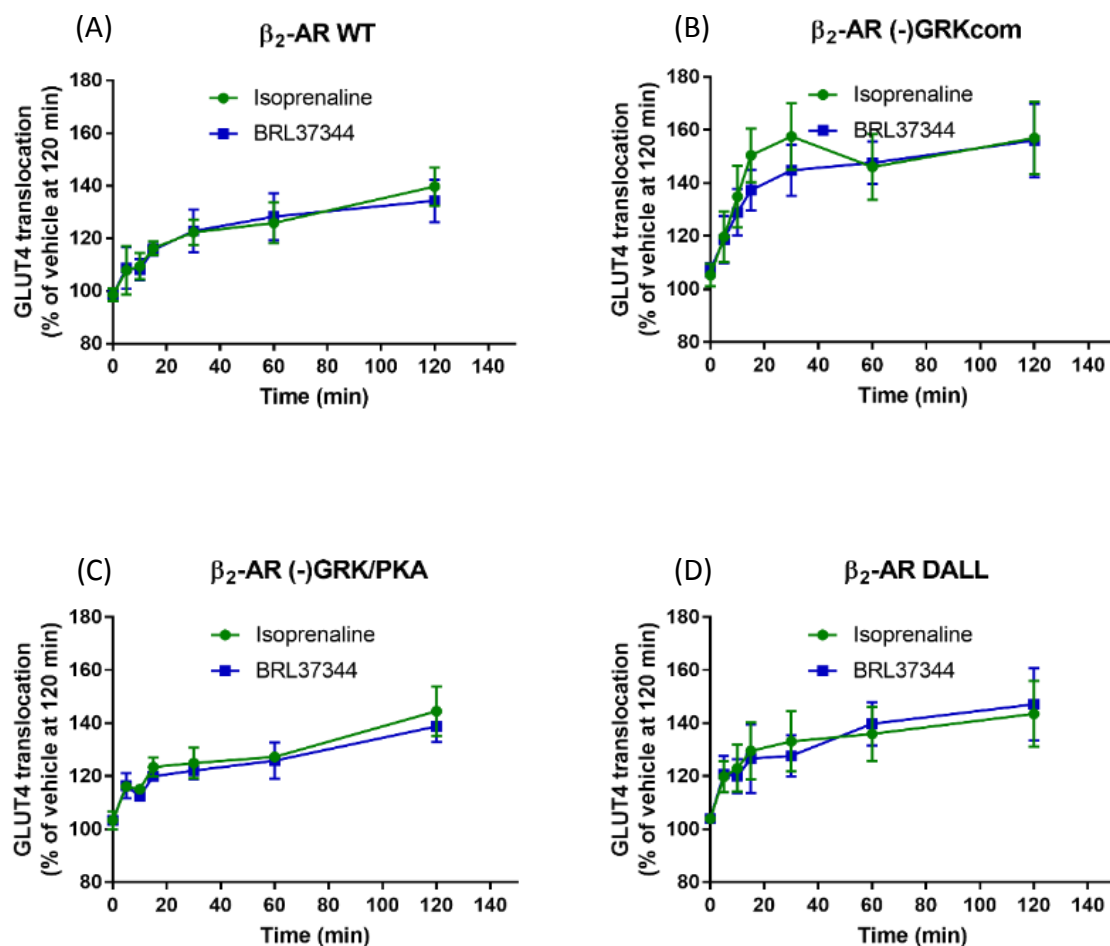
Figure 4.15: Quantification of time course of GLUT4 translocation in response to isoprenaline or BRL37344 in CHOGLUT4myc cells stably expressing the β₂-AR

Time course of GLUT4 translocation following stimulation with either 1 µM isoprenaline or 1 µM BRL37344 in (A) β₂-AR WT, (B) β₂-AR (-) GRKcom, (C) β₂-AR (-) GRK/PKA or (D) β₂-AR DALL. Data was quantified from data obtained from figure 4.10-4.13 using automated multiwave scoring. Values are mean ± s.e.mean of 5 independent experiments performed in duplicate. Data are normalized to values in vehicle treated cells at 120 min.
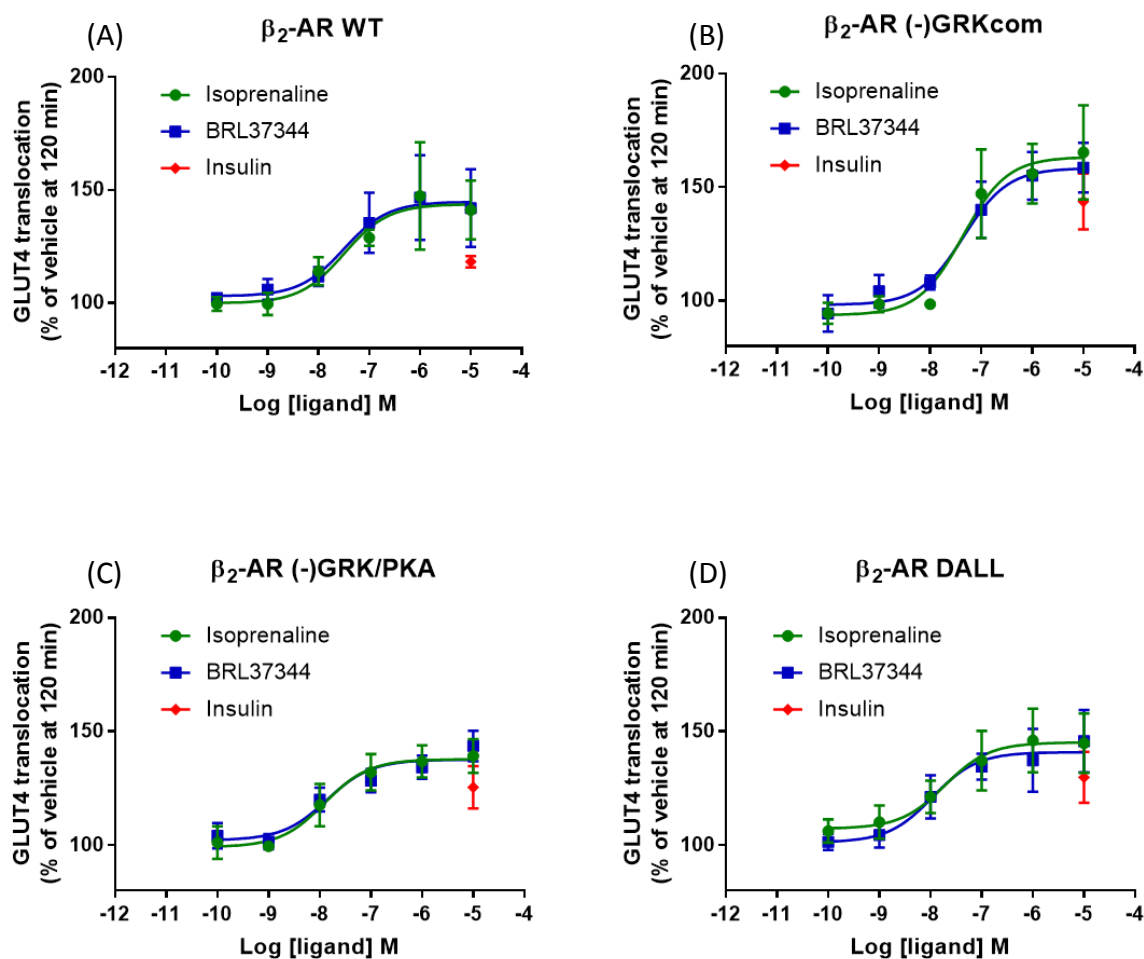
Figure 4.16: Quantification of GLUT4 translocation in response to isoprenaline or BRL37344 in CHOGLUT4myc cells stably expressing the β₂-AR

GLUT4 translocation following 120 min stimulation with either isoprenaline, BRL37344 or insulin (10 μM) in (A) β₂-AR WT, (B) β₂-AR (-) GRKcom, (C) β₂-AR (-) GRK/PKA or (D) β₂-AR DALL. Data was quantified by automated multiwave scoring. Values are mean ± s.e.mean of 5 independent experiments performed in duplicate. Data are normalized to values in vehicle treated cells at 120 min.

Table 4.5: Summary of potency (pEC$_{50}$) and maximal response; Rmax for GLUT4 translocation in CHOGLUT4myc cells expressing the wild type or mutant β$_2$-ARs

Data were obtained from the concentration response curves in Figure 4.16. Values represent mean ± s.e.mean from 5 experiments performed in duplicate. No pEC$_{50}$ values were significantly different compared to the β$_2$-AR WT pEC$_{50}$; No Rmax values were significantly different compared to the β$_2$-AR WT Rmax value (One-way ANOVA Dunnett's multiple comparisons test).

	pEC$_{50}$		Rmax (% of vehicle)	
	Isoprenaline	BRL37344	Isoprenaline	BRL37344
β$_2$-AR WT	7.49 ± 0.57	7.50 ± 0.57	143.7 ± 8.20	144.8 ± 8.12
β$_2$-AR (-) GRKcom	7.36 ± 0.39	7.34 ± 0.32	163.3 ± 9.63	158.4 ± 6.74
β$_2$-AR (-) GRKPKA	7.91 ± 0.37	7.86 ± 0.32	137.8 ± 4.50	137.6 ± 3.53
β$_2$-AR DALL	7.72 ± 0.57	7.96 ± 0.48	145.2 ± 6.85	140.9 ± 5.88

4.3.4 Reduction of β₂-AR mediated [³H]-2-deoxyglucose uptake following inhibition of clathrin mediated endocytosis in CHOGLUT4myc cells expressing the wild type β₂-ARs

Clathrin, which has a major role in receptor internalisation, is a possible GRK binding partner (Shiina et al., 2001). To evaluate whether clathrin may be involved in β₂-AR mediated glucose uptake, experiments were performed in the absence/presence of Pitstop, a pharmacological clathrin inhibitor. Pretreatment of cells with Pitstop for 30 min significantly reduced isoprenaline-or BRL37344- stimulated glucose uptake in the wild type β₂-AR, but also inhibited basal glucose uptake to a similar degree. (**$P < 0.01$,***$P < 0.001$, Two-way ANOVA Dunnett's multiple comparisons test, compared to vehicle) (Figure 4.17).

4.3.5 β₂-AR mediated increases in global cAMP levels in CHOGLUT4myc cells expressing the wild type or mutant human β₂-ARs

In CHOGLUT4myc cells without transfected β₂-ARs, neither isoprenaline nor BRL37344 increased cAMP levels (Figure 4.18). In CHOGLUT4myc cells expressing the wild type human β₂-AR, isoprenaline stimulation produced a robust and sustained cAMP response in the absence of IBMX, while BRL37344 stimulation increased cAMP levels relative to vehicle-treated cells, but this increase was significantly lower than that produced by isoprenaline (Figure 4.19A). 1 µM isoprenaline stimulation caused a transient response in β₂-AR (-) GRKcom and β₂-AR (-) GRK/PKA cell lines (**$P<0.01$ and ***$P<0.001$, respectively, when comparing the 15 min response to 120 min response, paired two-tailed t-test), but it produced a sustained response in β₂-AR DALL, β₂-AR (-) GRKprox, β₂-AR (-) GRKct and β₂-AR DSLL cell lines (Figure 4.19B-G). Concentration-response curves following 30 min incubation with isoprenaline or BRL37344 were conducted in the presence of 0.5 mM IBMX. In comparison to the response in β₂-AR wild type cells, mutation of GRK and/or PKA phosphorylation sites in the β₂-AR did not alter the effect of isoprenaline-stimulated cAMP production (pEC$_{50}$ or Rmax: n.s. $P>0.05$, One-way ANOVA Dunnett's multiple comparisons test) (Figure 4.20; Table 4.6; n=5-6). Also, BRL37344 showed significantly less ability to produce cAMP than isoprenaline in all the cell lines (Figure 4.20). To note, all the mutated receptors retained helix 8, which contributes to Gαs coupling (Liggett et al., 1989; Mouillac et al., 1992; O'Dowd et al., 1989), and the receptors partially or completely lacking GRK phosphorylation sites were functional for Gαs coupled signalling.
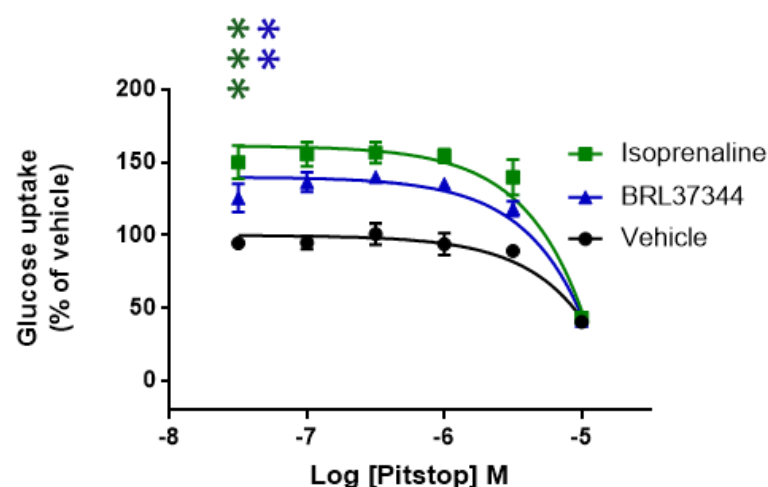
Figure 4.17: Effect of clathrin mediated endocytosis on isoprenaline or BRL37344 stimulated glucose uptake in CHOGLUT4myc cells stably expressing the wild type β$_2$-AR

Cells were pretreated with Pitstop for 30 min. 2-deoxy-[^{3}H]-glucose uptake was measured in β$_2$-AR WT following stimulation with either isoprenaline (1 μM) or BRL37344 (1 μM) for 2 h. Values are mean ± s.e.mean of 5-6 independent experiments performed in duplicate. Data are normalized to values in vehicle treated cells at 2.5 h. Asterisks represent statistical differences as analysed by two-way ANOVA and Dunnett's multiple comparisons test compared to vehicle (**P < 0.01,***P <0.001).
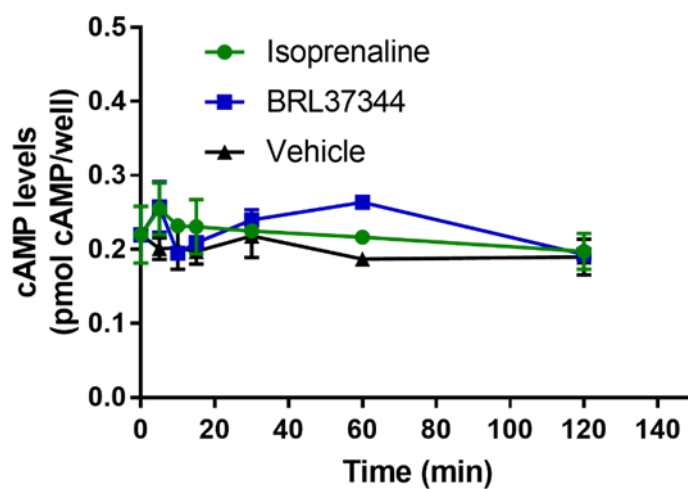
Figure 4.18: Effects of isoprenaline and BRL37344 of cAMP accumulation in CHOGLUT4myc cells

CHOGLUT4myc cells were treated with either 1 µM isoprenaline or 1 µM BRL37344 for different times. The results are expressed as amount of cAMP produced (pmol) per well. Each point shows mean ± s.e.mean of 2 independent experiments performed in duplicate.
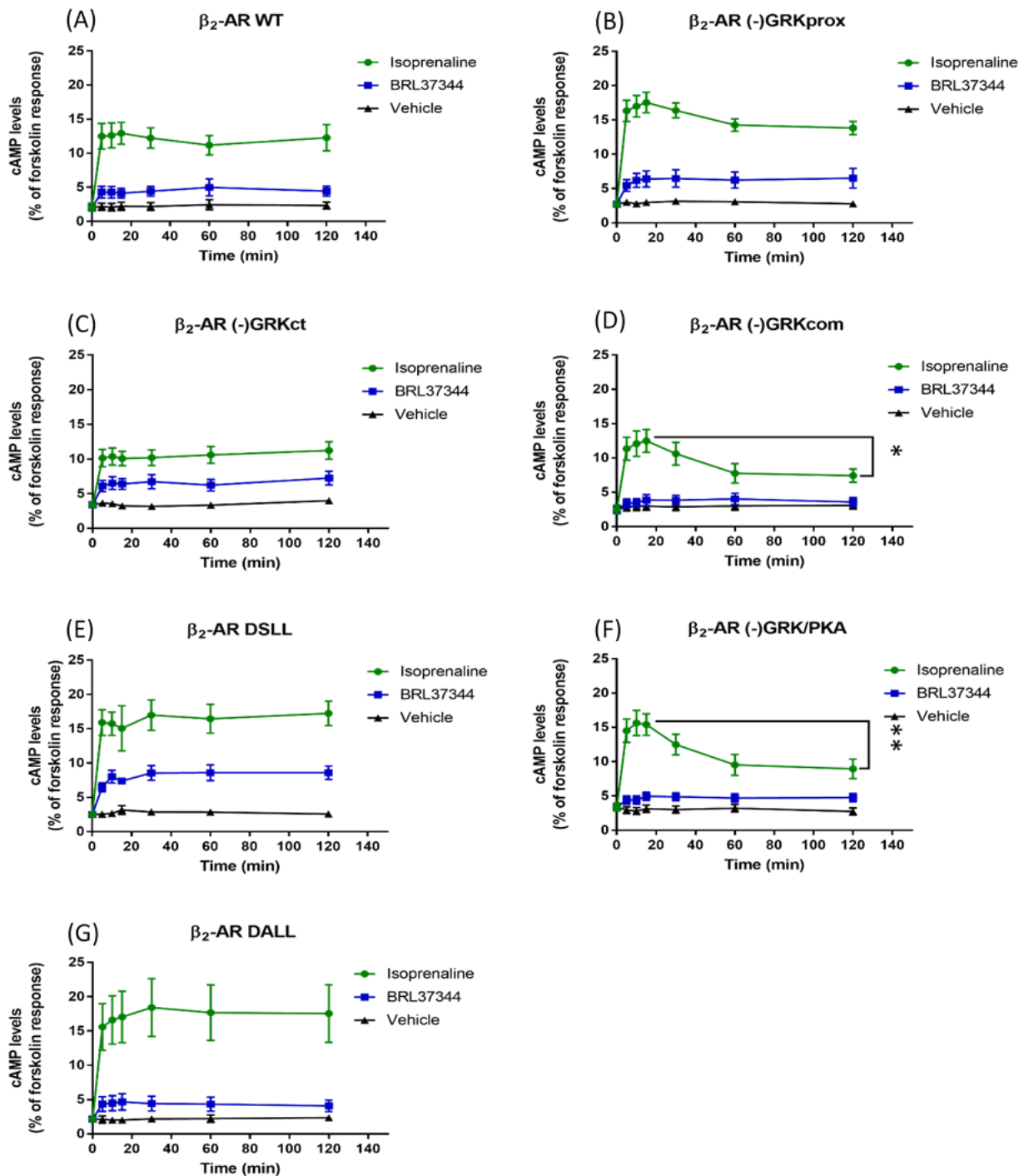
Figure 4.19: Time course of isoprenaline- or BRL37344-stimulated cAMP accumulation in CHOGLUT4myc cells stably expressing the β₂-AR

CHOGLUT4myc cells expressing either (A) β₂-AR WT, (B) β₂-AR (-) GRKprox, (C) β₂-AR (-) GRKct, (D) β₂-AR (-) GRKcom, (E) β₂-AR DSLL, (F) β₂-AR (-) GRK/PKA or (G) β₂-AR DALL were treated with either 1 μM isoprenaline or 1 μM BRL37344 for different times in the absence of IBMX. Results are expressed as percentage of the cAMP produced to the positive control forskolin (100 μM). Each point shows mean ± s.e.mean of 5-6 independent experiments performed in duplicate. Asterisks represent statistical differences as analysed by Student's paired t-test to make comparisons between 15 min (peak point) and 120 min (last point) (*P <0.05) in (D) or between 10 min (peak point) and 120 min (last point) (**P < 0.01) in (F).
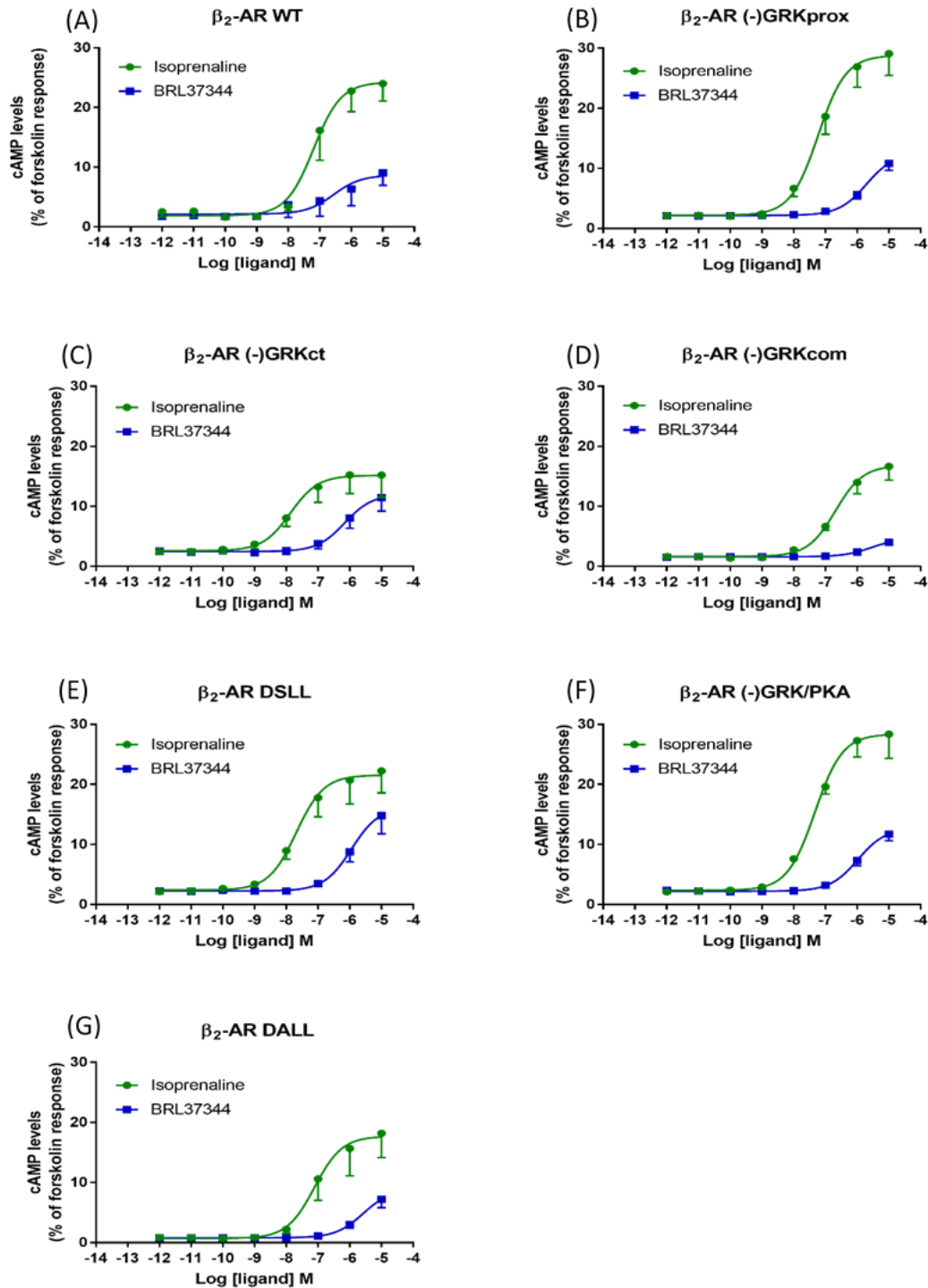
Figure 4.20: Concentration dependent cAMP accumulation in response to isoprenaline or BRL37344 in CHOGLUT4myc cells stably expressing the β2-AR

CHOGLUT4myc cells expressing either (A) β2-AR WT, (B) β2-AR (-) GRKprox, (C) β2-AR (-) GRKct, (D) β2-AR (-) GRKcom, (E) β2-AR DSLL, (F) β2-AR (-) GRK/PKA or (G) β2-AR DALL were treated with isoprenaline or BRL37344 for 30 min in the presence of 0.5 mM IBMX. Results are expressed as percentage of the cAMP produced to the positive control forskolin (100 μM) (30 min). Each point shows mean ± s.e.mean of 5-6 independent experiments performed in duplicate.

Table 4.6: Summary of potency (pEC$_{50}$) and maximal response for cAMP accumulation (30 min) in the presence of 0.5 mM IBMX in CHOGLUT4myc cells expressing the wild type or mutant β$_2$-ARs

Data were obtained from the concentration response curves in Figure 4.20. Values represent mean ± s.e.mean from 5-6 experiments performed in duplicate. No pEC$_{50}$ values were significantly different compared to the β$_2$-AR WT pEC$_{50}$. The maximal cAMP production measured at 10 μM of isoprenaline or BRL37344 in the various β$_2$-AR mutants did not differ significantly compared to β$_2$-AR WT (One-way ANOVA and Dunnett's multiple comparisons test). ND = Not determined.

	pEC$_{50}$		% forskolin response at 10 μM test compound	
	Isoprenaline	BRL37344	Isoprenaline	BRL37344
β$_2$-AR WT	7.19 ± 0.22	6.56 ± 0.57	24.25 ± 1.90	8.66 ± 1.65
β$_2$-AR (-) GRKprox	7.23 ± 0.15	ND	28.80 ± 1.58	12.5 ± 0.96
β$_2$-AR (-) GRKct	7.87 ± 0.30	6.16 ± 0.25	15.16 ± 1.28	12.02 ± 1.32
β$_2$-AR (-) GRKcom	6.68 ± 0.16	ND	16.82 ± 1.03	8.66 ± 1.65
β$_2$-AR DSLL	7.68 ± 0.23	ND	21.54 ± 1.49	16.23 ± 1.74
β$_2$-AR (-) GRK/PKA	7.33 ± 0.14	ND	28.37 ± 1.30	12.7 ± 0.67
β$_2$-AR DALL	7.11 ± 0.29	ND	17.71 ± 1.97	8.91 ± 1.21

To compare cAMP responses under similar experimental conditions to those used for glucose uptake, concentration-response curves were also conducted following 2 h incubation with isoprenaline or BRL37344 in the absence of IBMX. The mutant β_2-ARs showed no difference in the potency or maximum response of isoprenaline or BRL37344 as compared to those of the β_2-AR wild type, with the exception of a greater maximum response of β_2-AR DSLL expressing cells to BRL37344, relative to isoprenaline (**P<0.01, compared to wild type, One-way ANOVA Dunnett's multiple comparisons test) (Figure 4.21; Table 4.7).

4.3.6 β_2-AR mediated receptor internalisation in CHOGLUT4myc cells expressing the wild type or mutant human β_2-ARs

Receptor internalisation in response to isoprenaline or BRL37344 was performed in 4 cell lines expressing SNAP-tagged receptor variants, with the cell lines expressing partial β_2-AR phosphosite-mutations omitted from this study. The SNAP tag is a small 20 kDa protein derived from the DNA repair protein O6-alkylguanine-DNA alkyltransferase, and is covalently labelled with O6-benzylguanine (BG) derivatives bearing a fluorophore such as AlexaFluor 488 in living cells (Keppler et al., 2003). Addition of these membrane impermeant BG-derivatives to N-terminal-fused SNAP tagged GPCRs enables selective fluorescent labelling of cell surface receptors, through irreversible reaction with the SNAP tag active site (Keppler et al., 2003; Keppler et al., 2004). Internalisation of the labelled cell surface receptor population can be subsequently monitored. β_2-ARs were found throughout the cell surface in unstimulated CHOGLUT4myc cells stably expressing the wild type or mutant β_2-AR fusion proteins with an N-terminal SNAP tag. Stimulation with isoprenaline promoted translocation of the β_2-AR wild type from the cell surface to intracellular compartments in a time (Figure 4.22, 4.27A) and concentration-dependent manner (pEC$_{50}$: 6.97 ± 0.31, Rmax: $325.6 \pm 26.7\%$ of vehicle at 100%, n=5) (Figure 4.26, 4.28A). Isoprenaline-stimulated receptor internalisation was also observed in cells expressing the β_2-AR DALL mutant lacking the PDZ motif (pEC$_{50}$: 6.89 ± 0.33, Rmax: $420.3 \pm 43.9\%$ of vehicle at 100%, n=5) (Figure 4.25, 4.27D, 4.28B), and there was no significant difference compared to the wild type (two-way ANOVA Sidak's multiple comparisons test). However, internalisation in response to isoprenaline was not observed for receptors lacking all C-terminal GRK phosphorylation sites, nor for the complete GRK/PKA phosphorylation site receptor mutant (Figure 4.23, 4.24, 4.27B-4.28C). BRL37344 failed to internalise the SNAP β_2-AR in any of the cell lines tested (Figure 4.22-4.28).
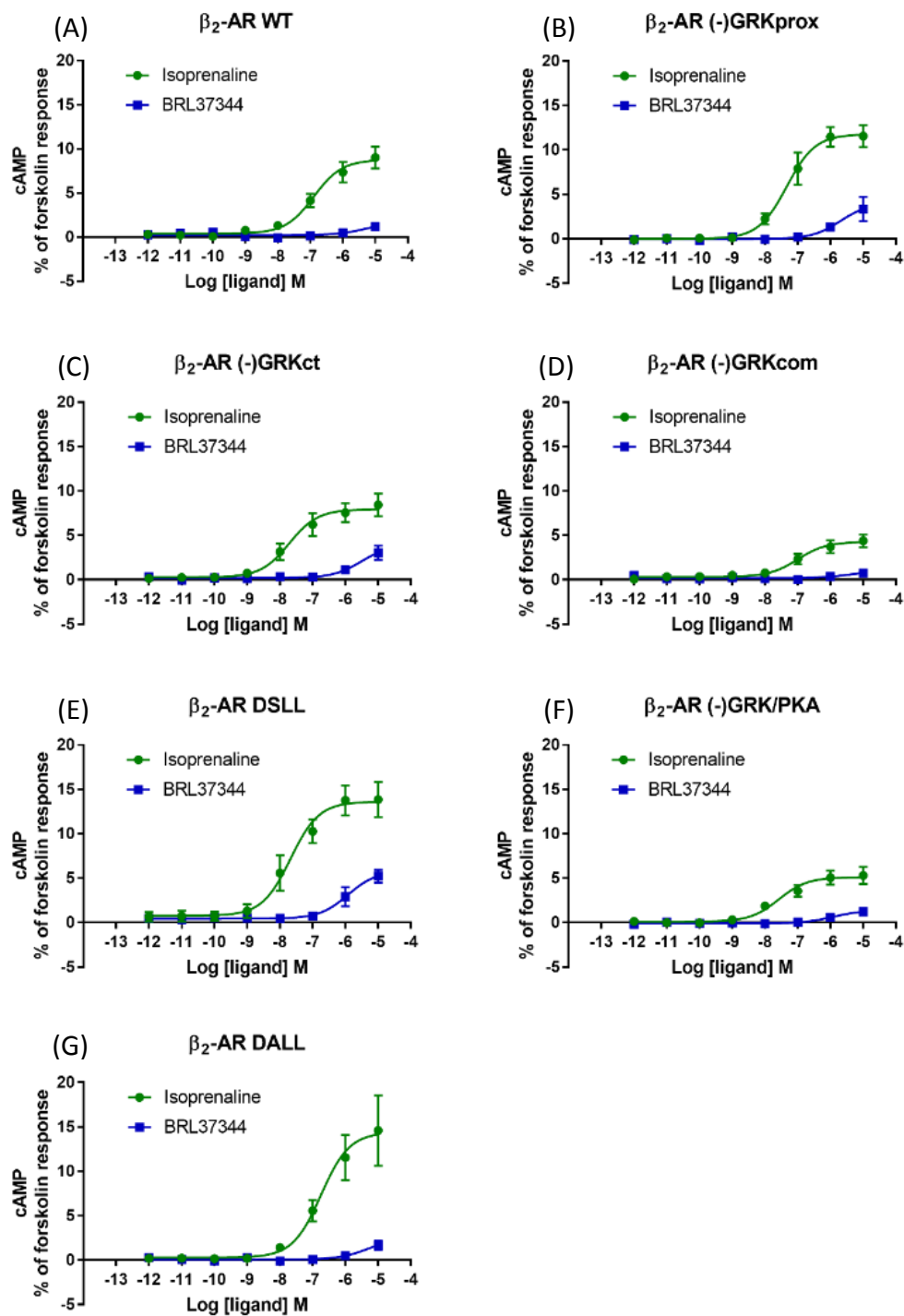
Figure 4.21: Concentration dependent cAMP accumulation in response to isoprenaline or BRL37344 in CHOGLUT4myc cells stably expressing the β₂-AR

CHOGLUT4myc cells expressing either (A) β₂-AR WT, (B) β₂-AR (-) GRKprox, (C) β₂-AR (-) GRKct, (D) β₂-AR (-) GRKcom, (E) β₂-AR DSLL, (F) β₂-AR (-) GRK/PKA or (G) β₂-AR DALL were treated with isoprenaline or BRL37344 for 2 h in the absence of IBMX. Results are expressed as percentage of the cAMP produced to the positive control forskolin (100 μM) (2 h). Each point shows mean ± s.e.mean of 5-6 independent experiments performed in duplicate.

Table 4.7: Summary of potency (pEC$_{50}$) and maximal response for cAMP accumulation (2 h) in the absence of IBMX in CHOGLUT4myc cells expressing the wild type or mutant β$_2$-ARs

Data were obtained from the concentration response curves in Figure 4.21. Values represent mean ± s.e.mean from 5-6 experiments performed in duplicate. No pEC$_{50}$ values were significantly different compared to the β$_2$-AR WT pEC$_{50}$ value; **P<0.01 compared to maximal cAMP production measured at 10 μM of isoprenaline or BRL37344 at β$_2$-AR WT (One-way ANOVA Dunnett's multiple comparisons test). ND = Not determined.

	pEC$_{50}$		% forskolin response at 10 μM test compound	
	Isoprenaline	BRL37344	Isoprenaline	BRL37344
β$_2$-AR WT	6.89 ± 0.15	ND	8.76 ± 0.55	1.69 ± 0.94
β$_2$-AR (-) GRKprox	7.33 ± 0.15	ND	11.76 ± 0.65	4.01 ± 0.95
β$_2$-AR (-) GRKct	7.71 ± 0.21	ND	7.92 ± 0.54	3.93 ± 0.89
β$_2$-AR (-) GRKcom	7.00 ± 0.21	ND	4.27 ± 0.35	0.98 ± 0.54
β$_2$-AR DSLL	7.67 ± 0.20	ND	13.60 ± 0.87	5.80 ± 0.79**
β$_2$-AR (-) GRK/PKA	7.58 ± 0.21	ND	5.10 ± 0.35	1.37 ± 0.32
β$_2$-AR DALL	6.74 ± 0.25	ND	14.39 ± 1.51	2.45 ± 1.06
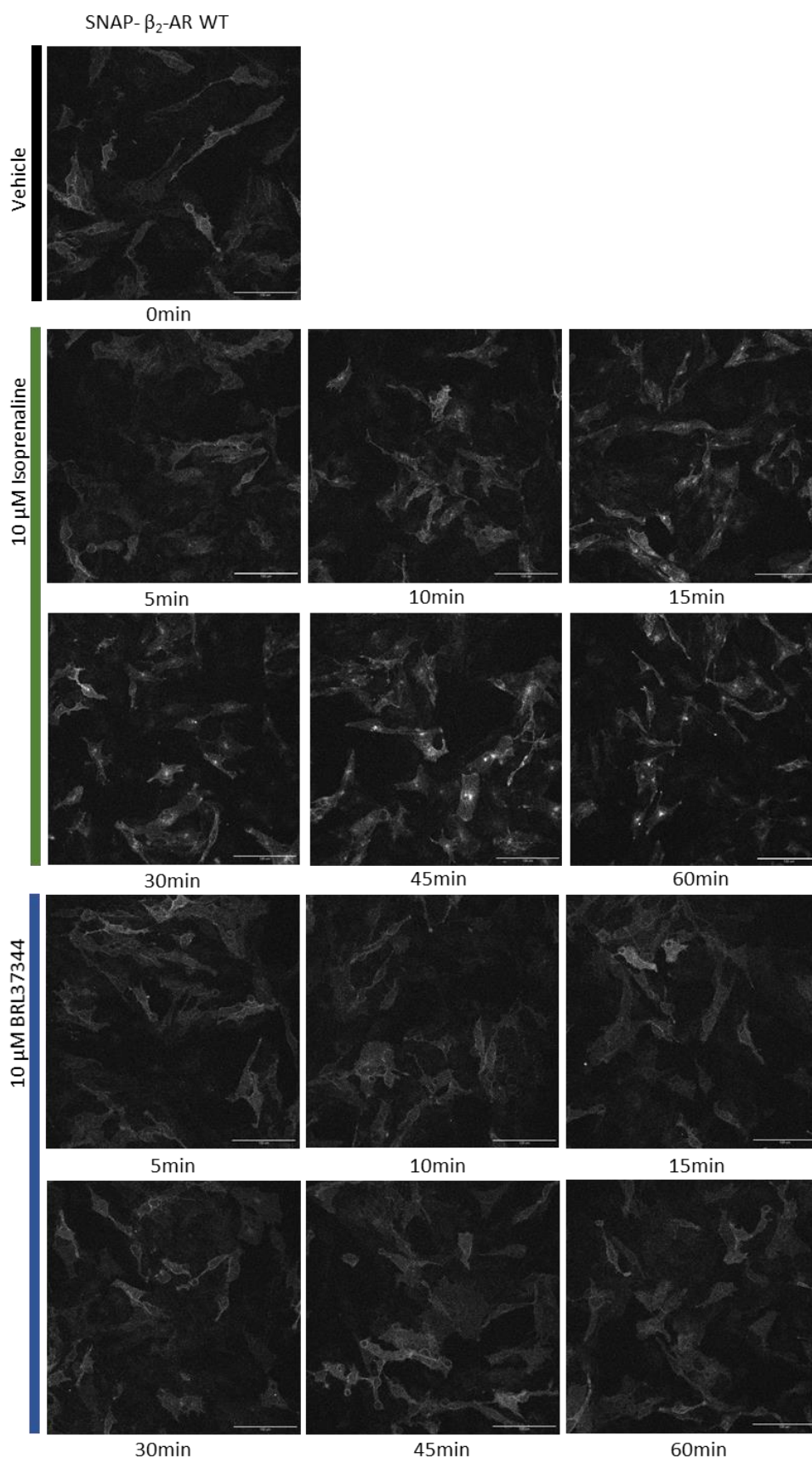
Figure 4.22: Effect of isoprenaline or BRL37344 on the internalisation of the SNAP- β₂-AR WT receptor

Cells were treated with 10 μM isoprenaline or 10 μM BRL37344 for 0 – 60min. Images are representative of 5 independent experiments performed in duplicate. Scale bar is 100 μm.
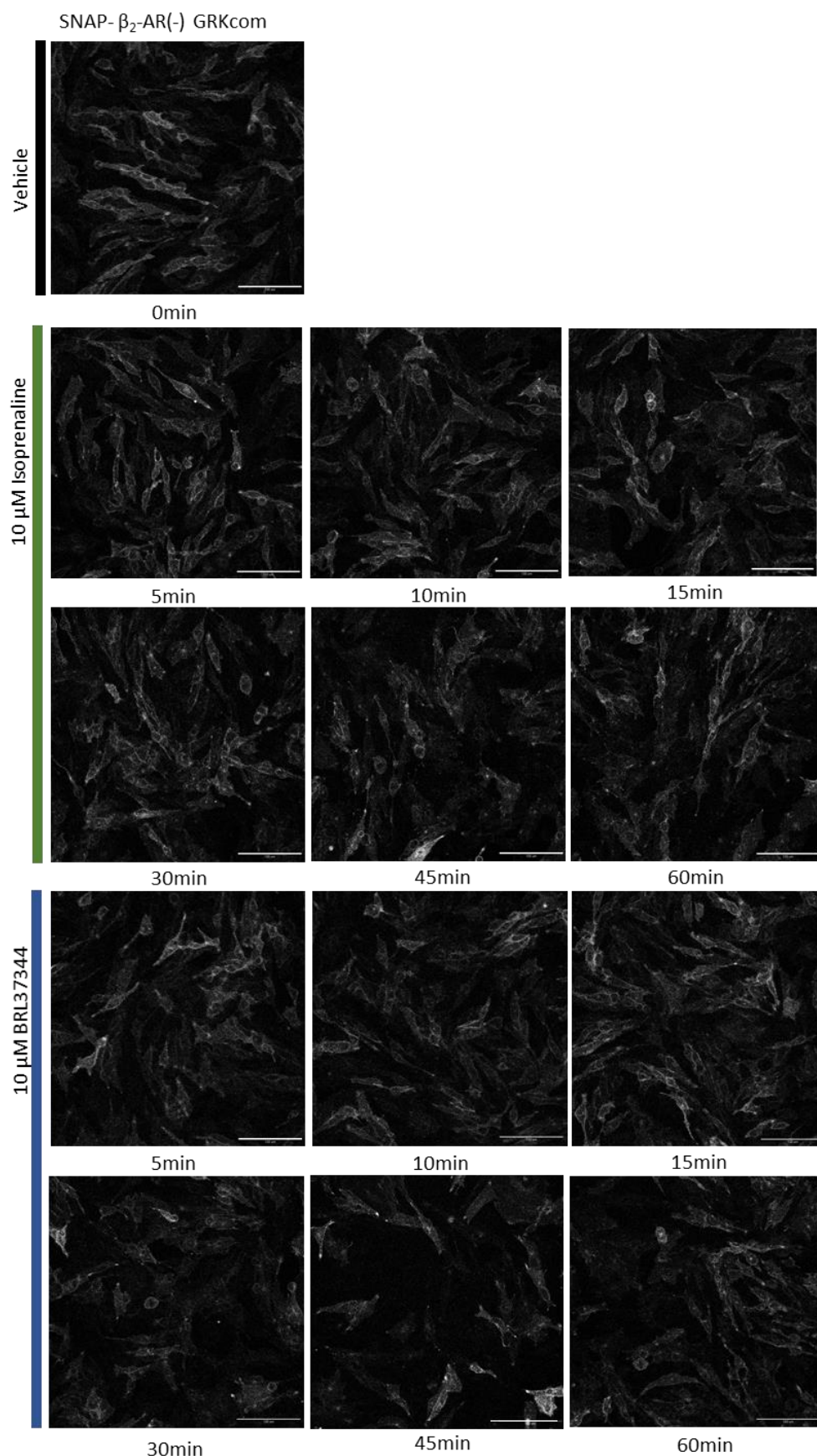
Figure 4.23: Effect of isoprenaline or BRL37344 on the internalisation of the SNAP- β₂-AR (-) GRKcom receptor

Cells were treated with 10 μM isoprenaline or 10 μM BRL37344 for 0 – 60min. Images are representative of 5 independent experiments performed in duplicate. Scale bar is 100 μm.

SNAP β₂-AR(-)GRK/PKA

Vehicle

0min

10 μM Isoprenaline

5min   10min   15min

30min   45min   60min

10 μM BRL37344

5min   10min   15min

30min   45min   60min
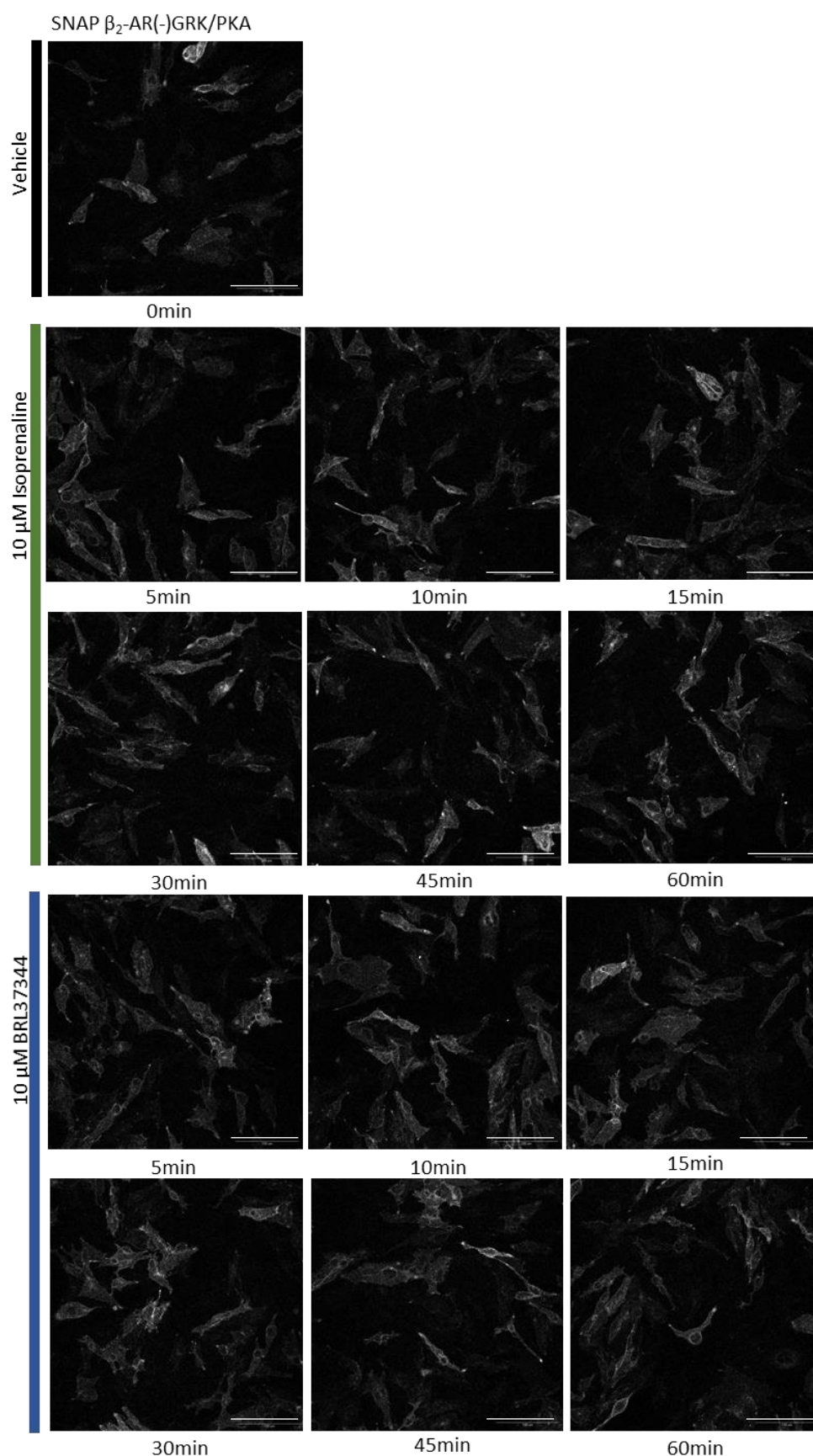
Figure 4.24: Effect of isoprenaline or BRL37344 on the internalisation of the SNAP- β₂-AR (-) GRK/PKA receptor

Cells were treated with 10 μM isoprenaline or 10 μM BRL37344 for 0 – 60min. Images are representative of 5 independent experiments performed in duplicate. Scale bar is 100 μm.
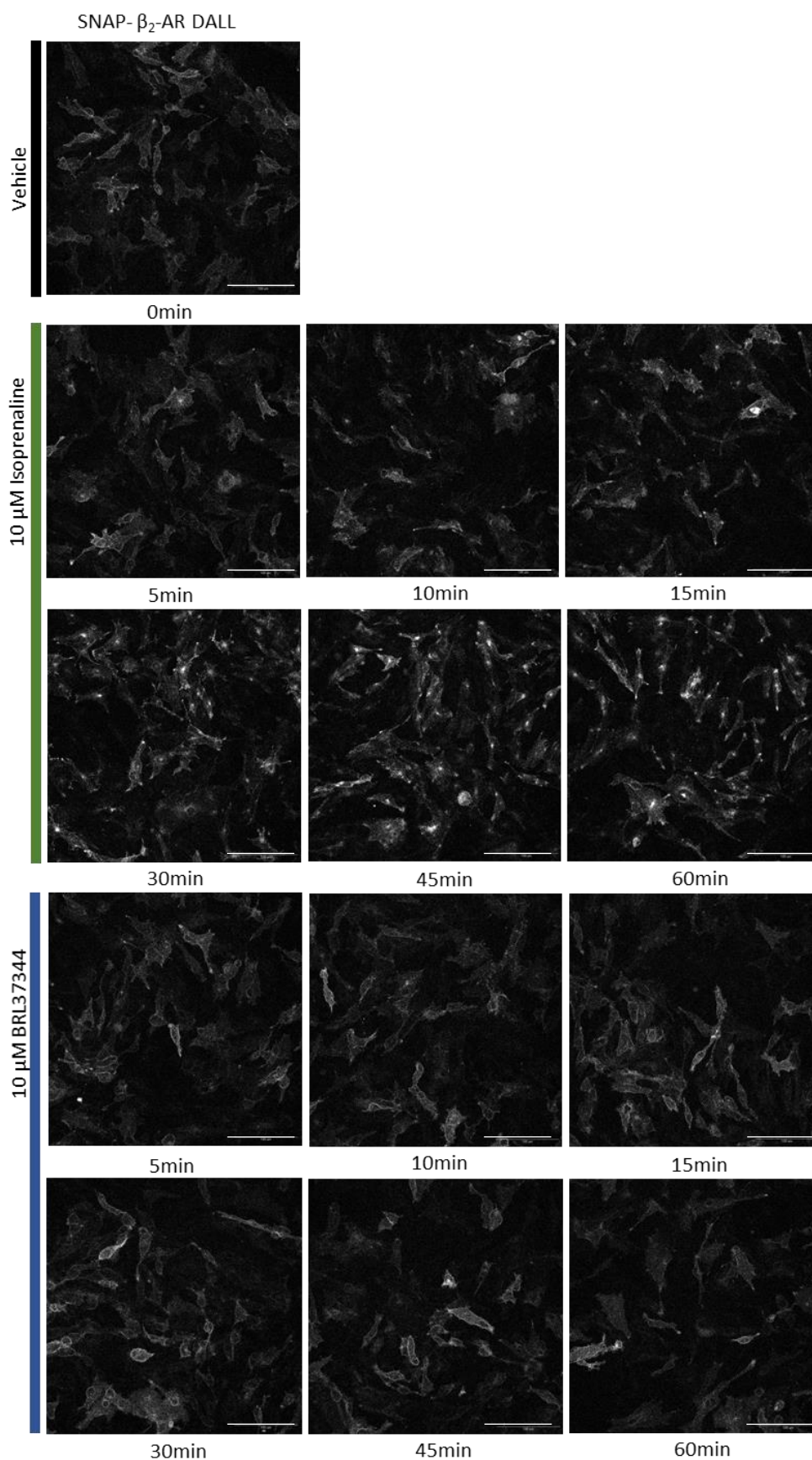
Figure 4.25: Effect of isoprenaline or BRL37344 on the internalisation of the SNAP- β₂-AR DALL receptor

Cells were treated with 10 μM isoprenaline or 10 μM BRL37344 for 0 – 60min. Images are representative of 5 independent experiments performed in duplicate. Scale bar is 100 μm.
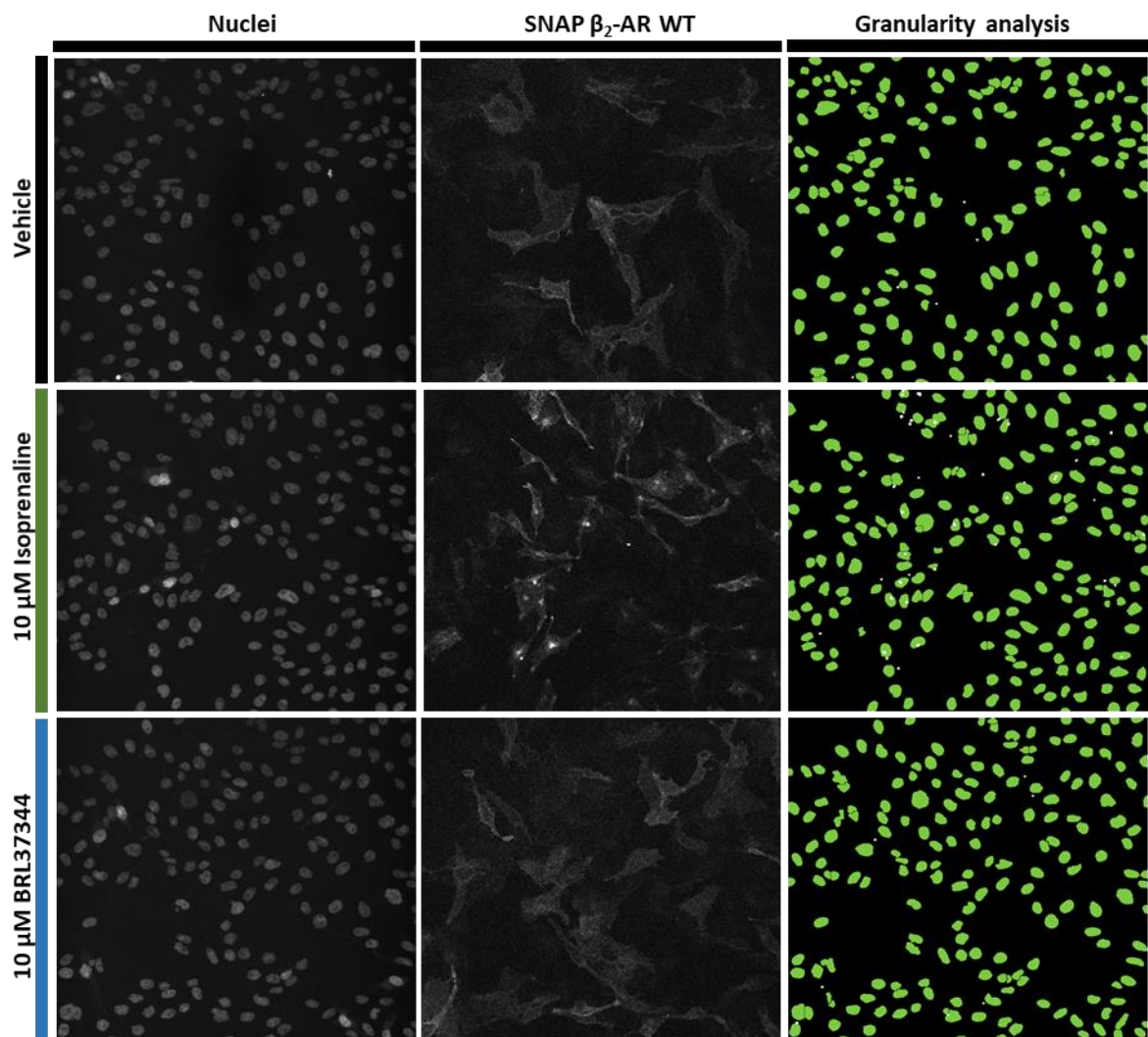
Figure 4.26: Internalisation of the SNAP- β₂-AR WT in response to isoprenaline or BRL37344

Cells were SNAP surface AF488 -labelled and then treated with either 10 µM isoprenaline or 10 µM BRL37344 for 1 h at 37 °C prior to fixation. The panels show nuclei stained with H33342 (left), SNAP- β₂-AR (middle), and granularity analysis (right), with nuclei in green and receptors containing granules of 6-10 µm diameter (corresponding to the diameter of the perinuclear recycling compartments in these cells) in white. Images are representative of 5 independent experiments performed in duplicate.
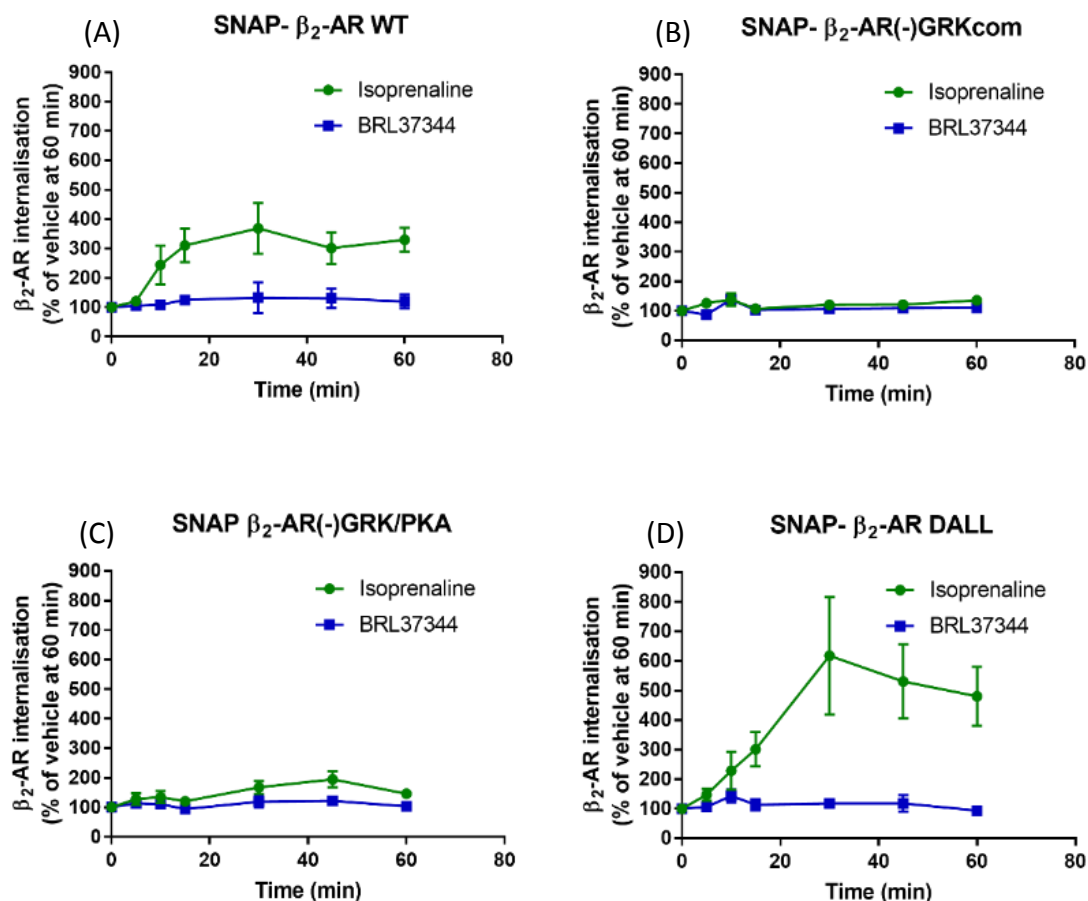
Figure 4.27: Quantification of time course of SNAP- β₂-AR internalisation in response to either isoprenaline or BRL37344

Time course of β_2-AR internalisation following stimulation with either 10 µM isoprenaline or 10 µM BRL37344 in (A) SNAP- β_2-AR WT, (B) SNAP- β_2-AR (-) GRKcom, (C) SNAP β_2-AR (-) GRK/PKA or (D) SNAP- β_2-AR DALL cells. Data was quantified from data obtained from figure 4.22-4.25 using an automated granularity algorithm. Values are mean ± s.e.mean of 5 independent experiments performed in duplicate. Data are normalized to values in vehicle treated cells at 60 min. No significant difference of isoprenaline stimulated receptor internalisation of between SNAP- β_2-AR WT cells and SNAP- β_2-AR DALL cells (two-way ANOVA Sidak's multiple comparisons test).
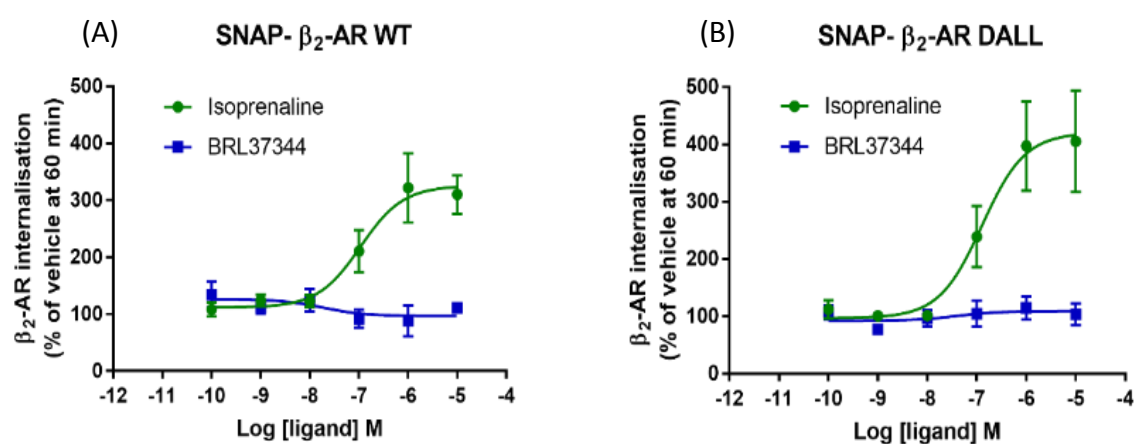
Figure 4.28: Quantification of concentration dependent SNAP- β₂-AR internalisation in response to either isoprenaline or BRL37344

β_2-AR internalisation following 1 h stimulation with either isoprenaline or BRL37344 in (A) SNAP-β_2-AR WT or (B) SNAP- β_2-AR DALL cells. Data were quantified by an automated granularity algorithm. Values are mean ± s.e.mean of 5 independent experiments performed in duplicate. Data are normalized to values in vehicle treated cells at 60 min.

4.3.7 Agonist bias in CHOGLUT4myc cells expressing the wild type or mutant human β₂-ARs

β₂-AR signalling through different pathways was quantified in response to isoprenaline or BRL37344 in CHOGLUT4myc cells expressing the wild type β₂-ARs, using a transduction co-efficient approach (van der Westhuizen et al., 2014). Transduction ratios R ($=\tau/K_A$) were derived from operational model fitting of the concentration-response relationships (van der Westhuizen et al., 2014) for each agonist at each pathway. First the effect of BRL37344 relative to isoprenaline within glucose uptake, GLUT4 translocation and cAMP pathways was expressed as ΔLogR, and then ΔΔLogR was calculated between pathway pairs. (Table 4.8). The ΔΔlogR of glucose uptake and GLUT4 translocation pathways was not significantly different from 0 in wild type cells, indicating little if any bias; however the relative effectiveness of BRL37344 in both pathways was greater than for the cAMP signalling pathway (Table 4.9).

Transduction ratios were also used to compare the effectiveness of Isoprenaline at wild type and mutant receptors, considering cAMP accumulation, glucose uptake and GLUT4 translocation pathways. Expressing the isoprenaline effect as log $[\tau/K_A]$ enabled correction for receptor expression level, which varied approximately 3 fold between the different β₂-AR cell lines (Riddy et al., 2017). Log R was adjusted for the expression level ratio compared to β₂-AR wild type (Table 4.10) and ΔLogR calculated to represent the effect of the mutation on isoprenaline-stimulated cAMP coupling, glucose uptake and GLUT4 translocation (Table 4.10). On this basis, β₂-AR (-) GRKprox and β₂-AR (-) GRK/PKA showed a significant increase in ΔLogR compared to β₂-AR wild type in cAMP pathway whereas it showed no significant difference between wild type and mutants in the other 2 pathways (Figure 4.30; Table 4.10).

Table 4.8: Transduction ratios for Isoprenaline and BRL37344 towards cAMP, glucose uptake and GLUT4 translocation in CHOGLUT4myc cells expressing the wild type β₂-AR

Values of $LogK_A$ (BRL37344 only) and LogR were obtained from by non-linear regression curves using the Operational Model equation 2. ΔlogR ratios were calculated from the logR ratios, considering isoprenaline as the reference ligand using equation 4. The standard error of mean was estimated using equation 6. The relative effectiveness (RE) of the ligands toward cAMP (30 min), glucose uptake or GLUT4 translocation pathway, relative to isoprenaline, was determined by equation 8. Values represent mean ± s.e.mean of 5-6 independent experiments in duplicate. cAMP; Data were analysed in using a two-tailed unpaired Student's t-test on the ΔlogR ratios to make pairwise comparisons between isoprenaline and BRL37344, *P<0.05. ND = Not determined.

	Glucose uptake					
Ligand	$LogK_A$	LogR	ΔLogR	RE		
Isoprenaline	ND	6.42 ± 0.10	0 ± 0.15	1		
BRL37344	-6.57 ± 0.54	6.60 ± 0.19	0.18 ± 0.22	1.51		
	GLUT4 translocation					
Ligand	$LogK_A$	LogR	ΔLogR	RE		
Isoprenaline	ND	6.98 ± 0.42	0 ± 0.60	1		
BRL37344	-6.77 ± 0.62	7.15 ± 0.42	0.17 ± 0.60	1.48		
	cAMP (30 min)				cAMP (2 h)	
Ligand	$LogK_A$	LogR	ΔLogR	RE	$LogK_A$	LogR
Isoprenaline	ND	6.09 ± 0.16	0 ± 0.22	1	ND	5.60 ± 0.19
BRL37344	-5.77 ± 0.88	4.58 ± 0.61	-1.52 ± 0.63*	0.03	ND	ND

Table 4.9: ΔΔlogR ratios and bias factors for BRL37344 in CHOGLUT4myc cells expressing the wild type β₂-ARs

ΔΔlogR ratios were calculated from the ΔlogR ratios (Table 4.8) using equation 9. The standard error of mean was estimated using equation 10. The ligand bias factors (BF), relative to isoprenaline, were determined using equation 11. Values represent the mean ± s.e.mean of 5-6 independent experiments with repeats in duplicate. Data were analysed in using a two-tailed unpaired Student's t-test on the ΔlogR ratios to make pairwise comparisons between two pathways, *P<0.05.

	cAMP (30 min) - Glucose uptake		cAMP (30 min) - GLUT4 translocation		GLUT4 translocation - Glucose uptake	
Ligand	ΔΔLogR	BF	ΔΔLogR	BF	ΔΔLogR	BF
BRL37344	-1.69 ± 0.67*	0.02	-1.68 ± 0.87	0.02	0.01 ± 0.63	0.98

Table 4.10: Transduction ratios for Isoprenaline towards cAMP, glucose uptake and GLUT4 translocation in CHOGLUT4myc cells expressing the wild type or mutant β_2-ARs

LogR values were obtained from by non-linear regression curves using the Operational Model equation 2. LogR values of each mutant were normalized to the receptor expression level of wild type using equation 3. ΔlogR ratios were calculated from the logR ratios, considering isoprenaline (Wild type) as the reference ligand using equation 5. The standard error of mean was estimated using equation 7. The relative effectiveness (RE) of the ligands toward cAMP, glucose uptake or GLUT4 translocation pathway, relative to isoprenaline (wild type), was determined by equation 8. Values represent mean ± s.e.mean of 5-6 independent experiments in duplicate. Data were analysed in using a two-tailed unpaired Student's t-test on the ΔlogR ratios to make pairwise comparisons between β_2-AR WT and each mutant, *P<0.05, **P<0.01.

Construct	cAMP			Glucose uptake			GLUT4 translocation		
	LogR	ΔLogR	RE	LogR	ΔLogR	RE	LogR	ΔLogR	RE
β_2-AR WT	6.09 ± 0.16	0.00 ± 0.22	1.00	6.42 ± 0.10	0.00 ± 0.15	1.00	6.99 ± 0.42	0.00 ± 0.60	1.00
β_2-AR (-) GRKprox	7.01 ± 0.15	0.93 ± 0.22*	8.43	6.12 ± 0.24	-0.31 ± 0.26	0.49			
β_2-AR (-) GRKct	6.60 ± 0.33	0.51 ± 0.33	3.27	5.92 ± 0.23	-0.49 ± 0.23	0.32			
β_2-AR (-) GRKcom	5.65 ± 0.31	-0.44 ± 0.34	0.36	6.82 ± 0.18	0.40 ± 0.20	2.50	7.23 ± 0.30	0.25 ± 0.52	1.77
β_2-AR DSLL	6.21 ± 0.14	0.12 ± 0.21	1.32	5.96 ± 0.19	-0.46 ± 0.22	0.35			
β_2-AR (-) GRK/PKA	7.51 ± 0.16	1.42 ± 0.23**	26.39	6.87 ± 0.17	0.45 ± 0.20	2.81	7.57 ± 0.49	0.59 ± 0.65	3.89
β_2-AR DALL	5.81 ± 0.28	-0.28 ± 0.32	0.53	6.37 ± 0.10	-0.05 ± 0.15	0.90	7.54 ± 0.42	0.55 ± 0.59	3.58

4.4 Discussion

It has been suggested that β_2-AR mediated glucose uptake might occur through both cAMP dependent and cAMP independent mechanisms, as (i) β_2-AR mediated glucose uptake is only partially blocked by pharmacological inhibition of PKA (Nevzorova et al., 2002; Nevzorova et al., 2006; Sato et al., 2014a), and (ii) certain β_2-AR ligands such as BRL37344 increase glucose uptake and GLUT4 translocation to the same degree as isoprenaline with minimal production of cAMP (Chapter 3). One potential mechanism may be through interactions of the β_2-AR with GRK2, since isoprenaline treatment of cells overexpressing a kinase-dead GRK2 (K220R) mutant failed to increase GLUT4 translocation (Dehvari et al., 2012), and other studies have shown a role for GRK in the regulation of glucose metabolism (Ciccarelli et al., 2011; Fu et al., 2015; Usui et al., 2005). Hence, the aim of this study was to examine the role of GRK phosphorylation sites in the β_2-AR C-terminal tail in β_2-AR mediated signalling (glucose uptake, GLUT4 translocation cAMP production, receptor internalisation) in response to isoprenaline and BRL37344.

We used CHOGLUT4myc cells stably expressing the wild type human β_2-AR, or stably expressing 6 different β_2-AR constructs in which combinations of serine and threonine residues comprising potential GRK/PKA phosphorylation sites were mutated to alanine (Figure 4.1-4.2). These included (1) a β_2-AR (-) GRKprox mutant with 4 GRK phosphorylation sites in a proximal cassette mutated (S355A, S356A, S364A and T360A), (2) a β_2-AR (-) GRKct mutant with 7 GRK phosphorylation sites in a distal cassette mutated (T384A, T393A, S396A, S401A, S407A, T408A and S411A), (3) a β_2-AR (-) GRKcom mutant with all 11 GRK phosphorylation sites in both the proximal and distal cassettes mutated, (4) a β_2-AR (-) GRK/PKA mutant with all 11 GRK phosphorylation sites in the proximal and distal cassette mutated, along with 4 PKA phosphorylation sites mutated (S261A, S262A, S345A and S346A). Two other mutants were also constructed: a β_2-AR DSLL mutant that has 10 GRK phosphorylation sites mutated but not S411, and a β_2-AR DALL mutant with 1 mutation (S411A) in the C-terminus PDZ binding motif. PDZ proteins are cytoplasmic adaptor proteins, which can affect GPCR signalling by diverse mechanisms (eg, receptor internalisation, trafficking, recycling, and intracellular sorting) (Romero et al., 2011), with the PDZ-binding motif of the β_2-AR associated with receptor recycling in mouse cardiac myocytes (Xiang & Kobilka, 2003). It has been suggested that the PDZ binding sites critical in β_2-AR are the 4 C-terminal residues including D410, S411, L412 and L413 (Gage et al., 2001), and S411 is also part of a GRK phosphorylation site (Nobles et al., 2011;

Romero et al., 2011). Hence, these 2 mutants, β_2-AR DSLL and β_2-AR DALL have been added in this study to clarify whether any alterations in β_2-AR signalling were due to PDZ motif interactions. Finally, we have applied the operational model to determine whether mutations alter isoprenaline as well as BRL37344 responses in cAMP production, glucose uptake and GLUT4 translocation using a standardized comparison to attempt to correct for differences in receptor expression (Black & Leff, 1983; van der Westhuizen et al., 2014).

Clonal cell lines expressing each mutant receptor were made and evaluated for receptor expression. The receptor expression levels in the wild type cells was 158.5 ± 10.6 fmol/mg protein, which is higher than that reported for β_2-ARs in human skeletal muscle (Elfellah et al., 1989). We chose single cell dilution clones with the lowest receptor expression available since cells that express high β_2-AR protein levels can promiscuously couple to other signalling pathways which may not be relevant in physiological settings (Evans et al., 2010). Some of the mutant cell lines (β_2-AR (-) GRKprox, β_2-AR (-) GRKcom and β_2-AR (-) GRK/PKA) had significantly different levels of expression as compared to the wild type β_2-AR cell line (varying by up to 2-fold from wild type; Table 4.1). However, there were not many positive clones for these mutants and we chose the clones showing closest to wild type β_2-AR expression level. The affinity of isoprenaline but not BRL37344 (measured as pK$_i$) was somewhat lower in β_2-AR (-) GRKprox and β_2-AR (-) GRKcom mutants compared to the wild type β_2-AR, however it is possible that those pK$_i$ values might be determined on an artefact of the fit by GraphPad Prism, which may be improved in the future by using half log concentrations. The Lower pK$_i$ values might have an impact on the agonist potency (Log R values) but not maximal response in the functional assays carried out.

Our previous research in L6 myotubes showed that BRL37344 is a full agonist for glucose uptake with similar potency to that of isoprenaline, but is only a low potency partial agonist for cAMP accumulation (Chapter 3). In this study, in CHOGLUT4myc cells stably transfected with the human β_2-AR wild type, BRL37344 also stimulated GLUT4 translocation and glucose uptake similar to isoprenaline, but only caused a minor effect on cAMP production compared to isoprenaline (Figure 4.19A, 4.20A, 4.21A). The operational model using isoprenaline as a reference ligand, indicated that BRL37344 is a biased agonist for stimulation of glucose uptake and GLUT4 translocation over cAMP signalling (Table 4.9). Functional affinity estimates of BRL37344 pK$_A$ derived from operational modelling of cAMP and glucose uptake pathways were not significantly different from radioligand

binding pK_i, but were also characterized by a high standard error and limited confidence in the mean value.

In the current study, we also observed that isoprenaline but not BRL37344 caused internalisation of the receptor in a time and concentration dependent manner in SNAP tagged CHOGLUT4myc cells stably expressing wild type β_2-AR (Figure 4.27A, 4.28A). This result was consistent with our previous work in which we examined receptor desensitisation using bioluminescence resonance energy transfer (BRET) technology (Chapter 3). In CHOGLUT4myc cells transiently transfected with β_2-AR and BRET sensors, isoprenaline increased the BRET ratio between β-arrestin1/2 and the β_2-AR, and decreased the BRET ratio between the plasma membrane marker Kras and the β_2-AR. BRL37344 caused no significant effects on BRET ratios between the β_2-AR and β-arrestin1/2 or Kras (Chapter 3, Figure 3.5). This was associated with isoprenaline (and not BRL37344) causing functional desensitisation of cAMP responses. Taken together, these studies indicate that BRL37344 preferentially increases glucose uptake and GLUT4 translocation over cAMP production, and does not stimulate receptor internalisation.

Surprisingly neither glucose uptake nor GLUT4 translocation was reduced in response to isoprenaline or BRL37344 stimulation in CHOGLUT4myc cells expressing β_2-AR lacking complete GRK or GRK/PKA phosphorylation sites, compared to cells expressing the wild type β_2-AR (Table 4.10). This indicated that isoprenaline-stimulated glucose uptake/GLUT4 translocation occurs independently from GRK mediated receptor phosphorylation. This result was unexpected, as the original study indicated a critical role of GRK in β_2-AR mediated glucose uptake (Dehvari et al., 2012), based on (1) an approximate 50% reduction in isoprenaline-stimulated glucose uptake in CHOGLUT4myc cells expressing a truncated β_2-AR tail that lacks many of the phosphorylation sites for GRK, (2) near abolishment of isoprenaline-stimulated glucose uptake following transfection of βARKct (which sequesters G$\beta\gamma$ and thereby prevents activation of G$\beta\gamma$-dependent effectors, but also inhibits recruitment of GRK2 and GRK3 to activated receptors (Koch et al., 1993; Pitcher et al., 1995)), and (3) impaired isoprenaline-stimulated GLUT4 translocation in cells overexpressing GRK2 DN (K220R) (Dehvari et al., 2012).

In the current study, receptor mutants lacking complete GRK or GRK/PKA phosphorylation sites showed a clear phenotype since isoprenaline-stimulated β_2-AR internalisation was completely abolished, though these experiments were performed using SNAP-tagged receptors, rather than the cell lines expressing untagged β_2-AR used for signalling. Nonetheless, they retained GLUT4

translocation following stimulation with either isoprenaline or BRL37344, unlike earlier results observed in cells overexpressing the truncated β_2-AR (Dehvari et al., 2012). This could be due to several differences in the experimental system, namely the receptor expression level, assay protocols and analysis. (1) We performed the GLUT4 translocation assay using CHOGLUT4myc cells stably expressing human β_2-AR whereas the previous study utilized CHOGLUT4myc cells transiently transfected with human β_2-AR. (2) Cells were post-fixed, then we used the same concentration of myc-tag primary antibody, however, the incubation length was much longer in this current study (overnight incubation) than previous study (1 h incubation), which might affect the level of surface labelling as well as background staining. (3) It was possible that quantification of GLUT4myc by multi-wave scoring algorithm included the GLUT4 not only expressed at the cell surface but also inside of the cells, though clearly agonist stimulated plasma membrane translocation was observed and quantified using this technique. However, $[^3H]$-2deoxyglucose uptake also demonstrated that stimulation with isoprenaline or BRL37344 increased glucose uptake without depending on the presence of GRK phosphorylation sites in the β_2-AR C-terminal tail. An additional concern in the current study was the unknown expression level of GLUT4 and receptor regulatory proteins such as GRK and β-arrestins in CHOGLUT4myc cells stably expressing β_2-AR mutants, and the potential for this to change as a result of the dilution cloning process. Differences in the expression levels of those proteins in cell lines expressing mutant receptors compared to β_2-AR wild type might affect the results of GLUT4 translocation and glucose uptake assays. Therefore, it is necessary to confirm GRK mRNA and/or protein levels by real time PCR and/or immunoblotting respectively, to determine the genuine effect of mutating GRK phosphorylation sites in β_2-AR on GLUT4 translocation and glucose uptake.

While the primary role of GRK phosphorylation in promoting receptor internalisation (Pitcher et al., 1992; Seibold et al., 2000; Summers et al., 1997) appears to have been lost by our receptor mutants, the activation of β_2-AR could also increase glucose uptake via cAMP mediated mechanisms (Sato et al., 2014a). In fact, β_2-AR lacking complete GRK or GRK/PKA phosphorylation sites increased cAMP production similar to wild type β_2-AR (Figure 4.20). It is possible that the balance between underlying GRK mediated and cAMP mediated mechanisms for glucose uptake could alter following the receptor phosphosite mutations, without this being apparent as a change in potency or maximum effect in the measured endpoint response. Additionally, whether these receptor mutants desensitise or interact with GRK/β-arrestin proteins to the same extent as the wild type receptors would be worthwhile in the future to investigate.

Thus, glucose uptake and cAMP production in response to isoprenaline or BRL37344 were not affected by the β_2-AR mutants lacking partial GRK phosphorylation sites as observed in β_2-AR (-) GRKprox, β_2-AR (-) GRKct or β_2-AR (-) DSLL cell lines either. Therefore, GRK phosphorylation sites in β_2-AR did not exhibit a dramatic effect on receptor function except for an outstanding effect on receptor internalisation.

Although both wild type and mutant β_2-AR clearly increased cAMP production following 30 min incubation with isoprenaline, it was difficult to assess the effect of mutations on isoprenaline-stimulated cAMP production based simply on the concentration response curve parameters. For example, comparison of the EC_{50} values for isoprenaline in the cAMP assay and lower pK_i values determined by competition binding in whole cells under similar conditions indicates the potential for receptor reserve in this assay – i.e. the maximal cAMP receptor response is generated by less than full receptor occupancy by the agonist. Comparisons between wild type and mutant receptors were further complicated by differing receptor expression levels. Therefore, we determined LogR values using the operational model and made adjustments to these values based on the relative receptor expression levels of each mutant compared to wild type (Black et al., 1985; Riddy et al., 2017). ΔLogR, representing the corrected isoprenaline relative effectiveness at mutant receptors compared to wild type receptor, showed significantly increased values for β_2-AR(-) GRKprox and β_2-AR (-) GRK/PKA (Table 4.10), representing an increased efficacy. This could be explained by a lack of the 2 major GRK proximal C tail phosphorylation sites, T360 and S364, in these mutants leading to more limited Gαs protein desensitisation (Nobles et al., 2011). A deficiency of receptor internalisation in β_2-AR (-) GRK/PKA might affect increasing cAMP level. However, ΔLogR of β_2-AR (-) GRKcom was not different from that of wild type β_2-AR. One limitation of the operational model analysis is the assumption that the maximum response of the system (Emax, expressed as a % forskolin response) is assumed to be the same across all the cell lines; however there are reasons why this may in fact vary (e.g. the proportion of cells responsive to β_2-AR might be different between clones). A shared Emax value in the fit may mean that clonal differences unrelated to the receptor function could also influence the estimated logR and $LogK_A$ values.

Furthermore, advances in understanding the complexity of GPCR phosphorylation effects support the possibility that different combinations of phosphosite mutations might show different effects, even when incorporating common Ser / Thr mutations. There is a study which examined the role of potential GRK phosphorylation sites of β_2-AR in the functional desensitisation process in intact cells

(Hausdorff et al., 1989; Hausdorff et al., 1991). In that study, β_2-AR lacking Ser/Thr sites in a proximal portion of the C-terminal tail, corresponding to our β_2-AR (-) GRKprox mutant, showed loss of desensitisation of adenylyl cyclase response in response to isoprenaline, unlike the wild type β_2-AR. However, β_2-AR lacking all the Ser/Thr residues in the proximal and distal portion of the C-terminal tail, corresponding to our β_2-AR (-) GRKcom mutant, displayed an increased desensitisation of adenylyl cyclase response similar to the effect observed at wild type β_2-AR. These results were similar to those observed in our current study, which demonstrated significant difference of cAMP production (Table 4.10), although we still need to determine the cMAP desensitisation responses between those two mutants. The authors suggested two possible interpretations of these findings, that the mutations in the distal portion of the C-terminal tail of the β_2-AR prevented the change in the receptor conformation occurring as a consequence of the mutations in the proximal portion, or alternatively counteracted the effects induced by the conformation change in the proximal portion (Hausdorff et al., 1991). As such, GRK site-specific phosphorylation would be correlated with the determination of receptor conformation, and thereby the effects on signalling.

Furthermore, we now know that GRK kinase phosphorylation patterns can also affect the β-arrestin conformation when bound to the receptor, and potentially direct distinct downstream signalling events (Cahill et al., 2017; Lee et al., 2016; Nuber et al., 2016). A defect in GRK induced receptor phosphorylation attenuates β-arrestin recruitment and conformation, which eventually influences signalling output (Yang et al., 2015). A BRET study showed a significantly reduced intramolecular BRET following activation of β_2-AR in response to isoprenaline in HEK 293 cells with selective knockdown of either GRK2 or GRK6 by siRNA, indicating that GRK phosphorylation events mediate the β-arrestin-1 conformational change (Yang et al., 2015). Also, this study demonstrated that GRK2-phophorylated β_2-AR affects clathrin recruitment by β-arrestins whereas GRK6-phophorylated β_2-AR affects Src activation (Yang et al., 2015). Another study indicated that GRK6-phophorylated β_2-AR is crucial for β-arrestin mediated ERK1/2 activation (Nobles et al., 2011). As such, different patterns of receptor phosphorylation are associated with distinct signalling functions of β-arrestins in a complex manner.

Interestingly, a recent study identified that two additional β_2-AR target residues for phosphorylation , S407 and T408, have a critical capacity to enhance the binding affinity of PDZ domain of sorting nexin 27 (SNX27) to the PDZ binding motif (Clairfeuille et al., 2016). Hence, the PDZ motif (and Ser411) alone is not sufficient to promote receptor sorting following internalisation, and additionally these 2 residues are more likely involved in promoting receptor trafficking. Unlike this finding, our

study showed that the β₂-AR DALL mutant containing S407 and T408 but lacking the PDZ binding site, was still able to undergo agonist-mediated internalisation. However, the β₂-AR DSLL mutant lacking both S407 and T408 phosphorylation sites but containing the PDZ binding sites, might not be sufficient to alter the interaction of β₂-AR with sorting proteins, thus prevent receptor internalisation. Importance of S407 and T408 sites in receptor internalisation should be examined using the β₂-AR DSLL mutant in the future.

Finally, β₂-AR (-) GRKcom and β₂-AR (-) GRK/PKA stimulated more transient changes in global cAMP level following isoprenaline stimulation over time in the absence of IBMX, unlike the sustained response to β₂-AR wild type (Figure 4.19). This finding is not consistent with previous studies, which have all shown increased cAMP accumulation in cells with knockdown of GRK isoforms. For example, in HEK293 cells expressing the human β₂-AR, the β₂-AR mediated cAMP response following isoprenaline stimulation was promoted by GRK6 silencing but not GRK2, GRK3, or GRK5 silencing (Violin et al., 2008). Another study in rat aortic smooth muscle cells showed that isoprenaline significantly increased β₂-AR mediated cAMP accumulation following siRNA-treated depletion of GRK2 or GRK5 but not GRK6. In the same study, double depletion of GRK2 and GRK5 further enhanced cAMP accumulation in response to isoprenaline (Nash et al., 2018).

It is possible that the sustained cAMP response mediated by wild type and most of the mutant β₂-ARs seen in our study arises from endosomal signalling, as has been reported for other Gαs coupled receptors (Pavlos & Friedman, 2017). In turn, observation of endosomal signalling may depend on the cell type examined, and also on receptor abundance. Our future studies should consider whether the absence of receptor internalisation in CHOGLUT4myc cells expressing the β₂-AR (-) GRKcom and β₂-AR (-) GRK/PKA mutants prevents a sustained element of cAMP signalling from endosomal compartments.

Overall, this study did not indicate a significant role of GRK phosphorylation sites in β₂-AR mediated glucose uptake, even when isoprenaline was used as the agonist. Previous studies had shown that (1) overexpression of a GRK2 DN abolished isoprenaline-stimulated GLUT4 translocation in the same CHOGLUT4myc cell line that we used here (Dehvari et al., 2012), and (2) siRNA knockdown of GRK2 did reduce β₂-AR mediated glucose uptake in L6 cells (Figure 4.4). This raises additional possibilities that GRKs are involved in glucose uptake because the kinase activity targets proteins downstream of the β₂-AR, or because of additional GRK functions as scaffolding protein. GRKs are known to

interact directly with various signalling proteins, and modulate downstream signalling cascades (Gurevich et al., 2012). Example binding partners of GRK2 include PI3K (Naga Prasad et al., 2002), the PI3K downstream target, Akt (Liu et al., 2005), and ERK1/2 - mitogen-activated protein kinase kinase (MEK) (Jimenez-Sainz et al., 2006). However, a study which investigated the mechanism of β_2-AR mediated glucose uptake in response to isoprenaline in L6 myotubes, suggested that Akt is not involved (Sato et al., 2014a). In addition, another study demonstrated that inhibition of MKK1 (upstream of Erk1/2) does not reduce BRL37344-stimulated glucose uptake, suggesting that ERK1/2 and MEK are not important (Ngala et al., 2013). Alternative potential GRK binding partners in this system include clathrin (Shiina et al., 2001) and caveolin (Schutzer et al., 2005), which mediate internalisation of β-AR. We did observe that inhibition of clathrin-mediated receptor endocytosis by Pitstop reduced isoprenaline- or BRL37344-stimulated glucose uptake although it also inhibited basal glucose uptake, indicating this effect cannot be interpreted as a selective action on β_2-AR mediated signalling (Figure 4.17). Thus, combined with the lack of β_2-AR internalisation in response to BRL37344, suggests that clathrin may be involved in receptor-independent glucose homeostasis, perhaps involving direct regulation of GLUT4 vesicles (Bogan & Kandror, 2010). The role of caveolin in glucose uptake should be determined by the use of filipin III (an inhibitor which sequesters cholesterol, and thereby disrupts caveolae).

In future studies, we will examine whether kinase or scaffolding properties of GRKs are important for increasing glucose uptake. We need to assess which GRK isoforms are recruited to the wild type and mutant β_2-ARs in CHOGLUT4myc cells using BRET technology (as described for recruitment of β-arrestin 1/2 in Chapter 3), in conjunction with measuring the effect of specific GRK inhibitors or siRNAs that selectively knock down GRK2, GRK5 or GRK6. If we demonstrate involvement of GRK2 by these approaches, we would then reassess the effects of the kinase-dead GRK2 mutant K220R on GLUT4 translocation and glucose uptake in CHOGLUT4myc cells expressing the wild type or mutated β_2-ARs lacking the GRK phosphorylation sites. This would provide key information on whether the kinase activity of GRK2 acts on an effector downstream of the β_2-AR itself.

Conclusion

Our findings indicated that the GRK phosphorylation sites in β_2-AR are not associated with isoprenaline- or BRL37344-stimulated glucose uptake. In the absence of GRK phosphorylation sites in mutant β_2-ARs, isoprenaline increased glucose uptake although it failed to promote receptor

internalisation. GRK phosphorylation sites had no crucial roles in neither BRL37344-stimulated glucose uptake nor receptor internalisation. However, GRKs are considered important for glucose uptake as siRNA knock down of GRK2 dramatically decreased isoprenaline- or BRL37344-stimulated glucose uptake. Therefore, further investigation is required to determine the role of GRK2 in glucose uptake, and also the signalling mechanisms underlying BRL37344-stimulated glucose uptake.

CHAPTER 5

Cellular signalling in response to A61603 and dabuzalgron in CHOGLUT4 cells expressing human α_{1A}-adrenoceptors

5.1 Introduction

α_1-Adrenoceptors (α_1-ARs) have roles in the heart, including α_{1A}- and α_{1B}-ARs that are expressed in cardiac myocytes, and α_{1D}-ARs that are expressed in smooth muscle cells of coronary blood vessels (Jensen et al., 2009a; Jensen et al., 2009b; Rokosh et al., 1994). Myocardial α_1-ARs are required for the normal development of the heart, and substantial evidence indicates beneficial effects of α_1-AR activation (in particular the α_{1A}-AR subtype) in the adult heart, where they have an adaptive and protective role in stress conditions that include heart failure. α_1-AR expression can be increased 2-fold in human heart failure compared to normal hearts (Jensen et al., 2009a), and their activation in rodents results in adaptive hypertrophy, and prevention of cardiomyocyte death (O'Connell et al., 2003; O'Connell et al., 2014; O'Connell et al., 2006; Papay et al., 2013; Zhu et al., 2000). This differs to what occurs in human cardiac failure with β_1-adrenoceptors (β_1-ARs), which are desensitised and down-regulated (Bristow et al., 1982). This cardioprotective role of α_1-ARs is mainly due to the activity of the α_{1A}-AR. Transgenic mice expressing a constitutively active α_{1A}-AR, show enhanced contractile function following ischemic injury, whereas this effect is not observed in transgenic mice expressing a constitutively active α_{1B}-AR (Rorabaugh et al., 2005). Double α_{1A}-AR and α_{1B}-AR knockout mice show reduced cardiovascular parameters (stroke volume, heart rate, cardiac output) compared to wild type mice (O'Connell et al., 2003). In addition, cell death observed in ventricular cardiac myocytes from α_{1A}-AR and α_{1B}-AR double knockout mice caused by oxidative stress or noradrenaline stimulation (activation of β-ARs) was reversed following adenoviral infection of the α_{1A}-AR but not the α_{1B}-AR (Huang et al., 2007). It should be noted that the abundance of cardiac α_1-AR and the subtype distribution are very similar between human and mouse (Jensen et al., 2009a).

A61603, (N-[5-(4,5-dihydro-1H-imidazol-2-yl)-2-hydroxy-5,6,7,8-tetrahydronaphthalen-1-yl]methanesulfonamide hydrobromide), and dabuzalgron, (N-[6-chloro-3-(4,5-dihydro-1H-imidazol-2-ylmethoxy)-2-methylphenyl]methanesulfonamide, formerly called Ro 115-1240), are highly selective α_{1A}-AR agonists (Blue et al., 2004; Knepper et al., 1995), both with reported cardioprotective effects. Although dabuzalgron was originally developed for the treatment of urinary incontinence, it failed in clinical trials (Musselman et al., 2004), and is now in development for the treatment of heart failure. Administration of A61603 produced positive inotropic responses and prevented doxorubicin-induced cardiomyopathy and cardiomyocyte death in a mouse model of heart failure (Cowley et al., 2015; Vakhrusheva et al., 2008). Dabuzalgron treated mice were also protected against doxorubicin mediated cardiotoxicity (Beak et al., 2017). Importantly, both A61603 and dabuzalgron caused these beneficial effects without stimulating vascular α_{1B}- or α_{1D}-ARs, hence

there was no significant elevation of blood pressure (Beak et al., 2017; Jensen et al., 2011a). The basis for α_{1A}-AR mediated cardioprotection is unclear. Therefore, it is important to understand the signalling mechanisms underlying α_{1A}-AR mediated cardioprotection. One important mechanism of cardioprotection has been thought to be increased glucose uptake into cardiomyocytes (Domenighetti et al., 2010; Liao et al., 2002). In heart failure, cardiomyocytes are exposed to hypoxic conditions due to a reduction of coronary blood flow (Essop, 2007). While the healthy heart predominantly uses fatty acids as a main energy substrate by consuming a large amount of oxygen to generate ATP via β-oxidation pathways (Nagoshi et al., 2011), the reduction of oxygen supply in the failing heart leads to a switch in energy substrate utilization from fatty acids to glucose in order to generate ATP (Doenst et al., 2013; Kolwicz & Tian, 2011; Lionetti et al., 2011; Lopaschuk et al., 2010; Nagoshi et al., 2011). Thus, up-regulation of glucose uptake becomes a more important factor to meet the energy demands in heart failure.

In skeletal muscle, α_{1A}-ARs increase glucose uptake through a phospholipase C (PLC)-Ca^{2+}-calcium/calmodulin-dependent protein kinase kinase β (CAMKKβ)–AMP-activated protein kinase (AMPK) mediated mechanism (Hutchinson & Bengtsson, 2005). However, in cardiomyocytes, compound C (an AMPK inhibitor) only partially inhibited α_{1A}-AR mediated glucose uptake (Sato et al., 2018). A second pathway involving the mechanistic target of rapamycin (mTOR) complex 2 was also found to mediate α_{1A}-AR mediated glucose uptake (Sato et al., 2018). mTOR is a 289kDa serine/threonine kinase that assembles into two functionally and structurally distinct multiprotein complexes, the rapamycin sensitive mTOR complex1 (mTORC1), and rapamycin insensitive mTOR complex2 (mTORC2) (Sciarretta et al., 2014). mTORC2 is a central regulator of β-AR mediated glucose uptake in brown adipocytes (Olsen et al., 2014) and skeletal muscle (Sato et al., 2014a), and activation of α_{1A}-ARs increases glucose uptake via mTORC2 in parallel with an AMPK dependent pathway in cardiomyocytes (Sato et al., 2018). α_{1A}-AR and β_2-AR activation of mTORC2 occurs independently of phosphoinositide 3-kinase (PI3K)/Akt, which contrasts to insulin-stimulated glucose uptake (Gan et al., 2011). This is important since PI3K/Akt signalling is down-regulated in certain diseases such as diabetes (Cozzone et al., 2008; Meyer et al., 2002; Sasaoka et al., 2006). In addition, insulin-stimulated Akt phosphorylation is impaired in a mouse model of diabetic cardiomyopathy (Battiprolu et al., 2012). This reduction of Akt phosphorylation in response to insulin is also observed in patients with heart failure complicated with type 2 diabetes (Chokshi et al., 2012). The mechanism of α_{1A}-AR mediated activation of mTORC2 is independent of Ca^{2+} and independent of AMPK signalling (Kamimura et al., 2008), whereas β_2-AR activation of mTORC2

occurs partially through a cAMP/PKA mediated mechanism (Sato et al., 2014a). Thus, cAMP might be a potential mechanism of α_{1A}-AR mediated mTORC2 activation since stimulation of α_{1A}-ARs can increase cAMP levels at least in recombinant systems (Sato et al., 2018).

Cardiac hypertrophy is a myocardial structural alteration, resulting from expansion of muscle mass and increased protein synthesis under conditions of increased workload (Selvetella et al., 2004; Selvetella & Lembo, 2005). Although hypertrophy begins as an adaptive mechanism, myocardial enlargement and additional inflammatory processes place extra demand on the heart, and cause remodelling and fibrosis that ultimately lead to heart failure (McMullen & Jennings, 2007). Activation of α_{1A}-ARs in response to A61603 showed a substantial increase in myocardial cell size and the rate of protein synthesis in neonatal rat cardiomyocytes (Autelitano & Woodcock, 1998). The non-selective α_1-AR agonist phenylephrine increased protein synthesis in rat adult cardiomyocytes, thought to be dependent on the activation of both extracellular signal–regulated kinase (Erk1/2) and mTORC1 (Wang & Proud, 2002). Furthermore, our previous study in neonatal rat cardiomyocytes demonstrated that A61603 stimulated cardiac hypertrophy presumably via mTORC1 and its downstream target S6 ribosomal protein (S6RP) dependent pathway (Sato et al., 2018). Despite increasing hypertrophy, agonists acting at the α_{1A}-AR may be protective due to beneficial effects on survival pathways and on glucose uptake.

Here, we have undertaken a systematic analysis of signalling pathways activated by the α_{1A}-AR, and examined the role of cAMP in glucose uptake in response to noradrenaline, A61603 or dabuzalgron in CHO-GLUT4myc cells stably expressing the human α_{1A}-AR. We also assessed the signalling bias of these ligands (noradrenaline, A61603, and dabuzalgron) across 6 different signalling pathways including Ca^{2+} mobilization, cAMP production, glucose uptake, N-Myc downstream regulated 1 (NDRG1) phosphorylation, S6RP phosphorylation and Erk1/2 phosphorylation.

5.2 Methods

5.2.1 Cell culture

CHOGLUT4myc cells stably expressing the human α_{1A}-AR were a gift from Dr. Kazuhiro Kishi (University of Tokushima, Tokushima, Japan). Cells were grown in 50:50 Dulbecco's modified Eagle's media (DMEM)/Ham's F12 media (Thermo Fisher Scientific, MA, USA) supplemented with 5% (v/v) foetal bovine serum (FBS) (Thermo Fisher Scientific, MA, USA) at 37°C, 5% CO_2 in a water jacketed incubator as described in Section 2.4.

5.2.2 [^{3}H]-prazosin saturation binding assay

Cells were seeded at 5×10^3 cells per well in 24 well plates, and serum starved for 2 days. Cells were washed once with HEPES buffer (NaCl, D-glucose, KCl, $MgSO_4$-$7H_2O$, HEPES, $CaCl_2$-$2H_2O$ and $NaHCO_3$), and then incubated with [^{3}H]-prazosin (100 pM to 10000 pM) for 1 h at 37°C. Non-specific binding was determined in the presence of phentolamine (final concentration, 40 µM). Reactions were terminated by washing twice in HEPES buffer, and samples lysed by the addition of 0.2 M NaOH (30 min, 50°C). Samples were transferred to scintillation vials (Sarstedt, Nümbrecht, Germany) containing 4 ml of Microscint 20 (PerkinElmer, MA, USA) and incubated for 1 h at RT before radioactivity was measured (Sato et al., 2018). The actual concentration of [^{3}H]-prazosin used was also determined by counting 100 µl stock sample [^{3}H]-prazosin with 4 ml Microscint 20 (PerkinElmer, MA, USA) in scintillation vials (Sarstedt, Nümbrecht, Germany) on a β counter TriCarb 2910TR (PerkinElmer, MA, USA) at 21°C for 3 min. Determination of cellular protein concentration was carried out with Pierce™ bicinchoninic acid (BCA) Protein Assay Kit (Thermo Fisher Scientific, MA, USA), using bovine serum albumin as standard as described in Section 2.6.4. Analysis of data is detailed in Section 2.11.2.1.

5.2.3 Ca^{2+} mobilization assays

Ca^{2+} mobilization assays were performed as described in Section 2.7.2. Cells were seeded at 1.0×10^4 cells per well in 96-well plates and grown overnight. Cells were treated with varying concentrations of either noradrenaline, A61603 or dabuzalgron for 1 min (peak response) for the generation of concentration response curves. In each experiment, 1 µM A23187 was used as a positive control and all experiments were performed in duplicate. Results are expressed as percentage of Ca^{2+}mobilization normalized to 1 µM A23187 in each independent experiment. Analysis of data is detailed in Section 2.11.1.

5.2.4 Cyclic AMP accumulation assays

cAMP accumulation assays were performed as described in Section 2.7.1. Cells were seeded at 1.0×10^4 cells per well in 96-well plates. Cells were serum-starved overnight, then treated with varying concentrations of either noradrenaline, A61603 or dabuzalgron for 30 min for the generation of concentration response curves. For time course studies, noradrenaline (100 μM), A61603 (1 μM) or dabuzalgron (10 μM) were added at specific time points. These concentrations of agonists were chosen to give a response equivalent to a pEC_{80} value based on the cAMP concentration response curves. Where indicated, inhibitors of Gαq/11 (UBO-QIC; 100 nM), PLC (U73122; 10 μM), PKCζ (PKCζ pseudosubstrate; 1 μM), or the cell-permeable Ca^{2+} chelator BAPTA AM (10 μM) were added 30 min prior to addition of noradrenaline (1 μM) or A61603 (100 nM). These agonist concentrations were chosen to produce approximately half of the maximal cAMP levels obtained in Fig 5.6A to ensure that the receptors were not maximally occupied. Results are expressed as pmole cAMP per well in each independent experiment. Analysis of data is detailed in Section 2.11.1.

5.2.5 Fluorescence resonance energy transfer (FRET)

FRET was performed as described in Section 2.9.3. CHOGLUT4myc cells were seeded at 1×10^4 cells per well in black side clear bottom cell culture 96-well microplates, and the next day transfected with the α_{1A}-AR (55 ng) and either the FRET biosensor pmEpac2 or cytoEpac2 (40 ng) using 1 mg ml^{-1} polyethylenimine (PEI). Cells were incubated in DMEM containing 0.5% FBS one day prior to an experiment. Cells were assayed with 20 μl of ligand, either noradrenaline (final concentration, 10 nM) or A61603 (final concentration, 1 nM), or 20 μl of positive control (final concentration, 10 μM forskolin and 100 μM IBMX) in 160 μl of HBSS at 37 °C. These concentrations of noradrenaline and A61603 were chosen to prevent saturation of the FRET cAMP sensors. Results are expressed as F/Fmax, the ratio of FRET (ligand)/maximum FRET (positive control) in each independent experiment. Analysis of data is detailed in Section 2.11.6.

5.2.6 Amplified Luminescent Proximity Homogeneous (Alpha) screen assays

Alpha screen assays were performed as described in Section 2.8.1. Cells were seeded at 1.0×10^4 cells per well in 96-well plates. Cells were serum starved overnight, then treated with varying concentrations of either noradrenaline, A61603 or dabuzalgron to determine the phosphorylation of Erk1/2 at T202/Y204 or S6RP at S235/S236 for 10 min or 2 h, respectively. For time course studies, noradrenaline (1 μM), A61603 (100 μM) or dabuzalgron (10 μM) was added at specific time points.

These concentrations of agonists were chosen to give a response equivalent to a pEC_{80} value based on the Erk1/2 or S6RP concentration response curves. Results are expressed as a percentage of phospho-Erk1/2 or phospho-S6RP in vehicle treated cells in each independent experiment. Analysis of data is detailed in Section 2.11.1.

5.2.7 InCell Western (Li-Cor) assays

InCell Western (Li-Cor) assays were performed as described in Section 2.8.2. Cells were seeded at 1.0×10^4 cells per well in black side clear bottom cell culture 96-well microplates. Cells were serum starved for 2 days, then treated with varying concentrations of either noradrenaline, A61603 or dabuzalgron to determine the phosphorylation of NDRG1 for 2 h. For time course studies, noradrenaline (1 μM), A61603 (100 nM) or dabuzalgron (10 μM) were added at specific time points. These concentrations of agonists were chosen to give a response equivalent to a pEC_{80} value based on the NDRG1 concentration response curves. Results are expressed as a percentage of phospho-NDRG1 in vehicle treated cells in each independent experiment. Analysis of data is detailed in Section 2.11.3.

5.2.8 [^{3}H]-2-deoxyglucose uptake assays

[^{3}H]-2-deoxyglucose uptake assays were performed as described in Section 2.6.1. Cells were seeded at 5.0×10^4 cells per well in 24-well plates. Cells were serum starved for 2 days, then treated with varying concentrations of either noradrenaline, A61603 or dabuzalgron for 2 h. Insulin was used a positive control in each experiment performed. Where indicated, antagonists of the α_1-AR (prazosin; 1 μM) or $\alpha_{1A/1D}$-AR (tamsulosin; 100 nM), or inhibitors for Gαq/11 (UBO-QIC; 100 nM), PKCζ (PKCζ pseudosubstrate ;1 μM), mTORC1/2 (KU0063794; 1 μM, rapamycin; 100 nM, 24 h), mTORC1 (rapamycin; 1 μM), PKA (PKI; 1 μM), or MEK (U0126; 10 μM), or the Ca^{2+} chelator (BAPTA AM; 10 μM) were added 30 min prior to addition of insulin (100 nM), noradrenaline (100 nM), A61603 (10 nM) or dabuzalgron (100 nM) with an excecption of rapamycin 100 nM pre-treatment. These concentrations of agonists were chosen to give a response equivalent to a pEC_{80} value based on the glucose uptake concentration response curves. Results are expressed as a percentage of glucose uptake in vehicle treated cells in each independent experiment. Analysis of data is detailed in Section 2.11.1.

5.2.9 Data analysis

All results are expressed as mean ± s.e.mean of n independent experiments. Since clonal cells are used, each n number is defined as an experiment performed on different days from cells from different passages. Data was analysed with GraphPad PRISM v7.02. The statistical significant difference was analysed by using (1) Student's paired t tests to make comparison of inhibitory effects where inhibitors were used, (2) Student's unpaired t tests to make pairwise comparisons between two ligands or two pathways (3) One-way ANOVA Dunnett's or Tukey's multiple comparisons test to make comparison among multiple ligands, or (4) Two-way ANOVA to make comparison of curves. P values less than 0.05 were considered significant.

The operational model, an analytical approach to quantify agonist bias, (Black & Leff, 1983; Riddy et al., 2017) (Section 2.11.7) was used to determine the transduction ratio R (=τ /K_A), and to compare the effects of noradrenaline vs A61603 vs dabuzalgron as below;

Transduction coefficient (R) is defined by the ration of τ /K_A as follows;

$$\text{Equation 1,} \qquad R = \frac{\tau}{k_A}$$

Where τ is an index of the coupling efficacy of the agonist, K_A is the functional equilibrium dissociation constant of the agonist.

The logarithm of the "transduction coefficient" (LogR) was obtained by fitting concentration response curves using equation 2, respectively on GraphPad Prism (v7.0; GraphPad Software, La Jolla, CA).

$$\text{Equation 2,} \qquad \text{Effect of the ligand} = \text{Basal} + \frac{(E_m - \text{Basal})}{1 + \left(\dfrac{\dfrac{[A]}{10^{LogK_A}} + 1}{10^{LogR} \text{ x } [A]} \right)^n}$$

Where [A] is the concentration of agonist, Em is the maximal possible response of the system, Basal is the response in unstimulated system, $logK_A$ is the logarithm of the functional equilibrium dissociation constant of the agonist, n is the slope of the transducer function that links occupancy to response. To note, full agonists were placed into column A – O on the Prism sheet, and $LogK_A$ was

constrained to 0. In contrast, partial agonists were placed into column P onwards, and $LogK_A$ was fitted (van der Westhuizen et al., 2014).

To determine the relative effectiveness of ligand; (1) the difference between LogR (ΔLogR) value was calculated using equation 3, (2) the estimated standard error of mean of equation 3 was calculated using equation 4, respectively, (3) the relative effectiveness toward each pathway, relative to noradrenaline, were calculated using equation 5.

Equation 3, $\Delta LogR = LogR_{Ligand} - LogR_{Noradrenaline}$

Where ligand is either A61603 or dabuzalgron.

Equation 4, $\text{s.e.m}_{\Delta LogR} = \sqrt{\left(\text{s.e. } m_{Ligand}\right)^2 + (\text{s.e. } m_{Noradrenaline})^2}$

Equation 5, $\text{Relative effectivness} = 10^{\Delta LogR}$

To determine bias factor, (1) the difference between the ΔlogR values ($\Delta\Delta$logR) was calculated using equation 6, (2) the estimated standard error of mean of equation 6 was calculated using equation 7, (3) bias factor was calculated using equation 8.

Equation 6, $\Delta\Delta LogR_{Path} = \Delta LogR_{Path1} - \Delta LogR_{Path2}$

Equation 7, $\text{s.e.m}_{\Delta\Delta LogR_{Path}} = \sqrt{\left(\text{s.e.m}_{\Delta LogR_{Path1-Path2}}\right)^2 + \left(\text{s.e.m}_{\Delta LogR_{Path1-Path2}}\right)^2}$

Equation 8, $\text{Bias factor} = 10^{\Delta\Delta LogR_{Path}}$

5.3 Results

5.3.1 Saturation binding characterization of [³H]-prazosin in CHOGLUT4myc cells expressing the wild type human α_{1A}-AR

[³H]-prazosin binding occurred in a saturable manner to a single binding site in CHOGLUT4myc cells stably expressing the wild type α_{1A}-AR (B_{max} 189. 4± 19.4 fmol/mg of protein; pK_D 7.8 ± 0.09; n=8; Figure 5.1). This receptor expression level is approximately 3-fold higher compared to those measured in neonatal rat ventricular myocytes (NRVM) (Sato et al., 2018).

5.3.2 α_{1A}-AR mediated increases in glucose uptake in CHOGLUT4myc cells expressing the human α_{1A}-AR

In CHOGLUT4myc cells, noradrenaline, A61603, and dabuzalgron did not increase glucose uptake (Figure 5.2A). In CHOGLUT4myc cells expressing the human α_{1A}-AR, noradrenaline, A61603, or dabuzalgron increased glucose uptake in a time (Figure 5.2B) and concentration dependent manner (Figure 5.2C, Table 5.1), as did the positive control insulin. All four ligands produced similar maximal effects on glucose uptake, but the rank order of potency was A61603 > dabuzalgron > noradrenaline=insulin. To confirm whether this effect resulted from the activation of the α_{1A}-AR, both prazosin (α_1-AR antagonist) and tamsulosin ($\alpha_{1A/1D}$-AR antagonist) were used. Prazosin (1 μM) and tamsulosin (100 nM) blocked noradrenaline (100 nM), A61603(10 nM) or dabuzalgron (100 nM) stimulated glucose uptake, but did not affect insulin-stimulated glucose uptake (**P < 0.01, ***P < 0.001, Student's paired t-test) (Figure 5.2D, 5.2E).

5.3.3 α_{1A}-AR mediated increases in Ca^{2+} mobilization in CHOGLUT4myc cells expressing the human α_{1A}-AR

In CHOGLUT4myc cells, noradrenaline, A61603, and dabuzalgron did not increase Ca^{2+} mobilization (Figure 5.3A). In CHOGLUT4myc cells expressing the human α_{1A}-AR, noradrenaline, A61603, and dabuzalgron all increased Ca^{2+} mobilization in a concentration dependent manner (Figure 5.3B; Table 5.1). Ca^{2+} mobilization in response to A61603 or noradrenaline showed similar efficacies, whereas dabuzalgron exhibited a partial response compared to these agonists. The rank order of potency was A61603 >> noradrenaline >> dabuzalgron.
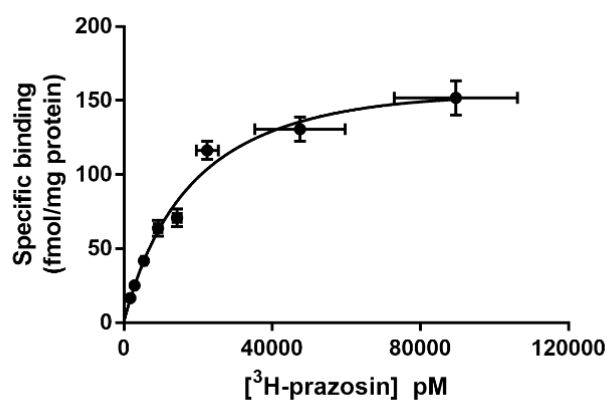
Figure 5.1: Saturation binding of [³H]-prazosin in CHOGLUT4myc cells stably expressing the human α$_{1A}$-AR

Specific binding (expressed as fmol/mg protein) was determined in CHOGLUT4myc cells stably expressing the human α$_{1A}$-AR. Cells were incubated with increasing concentrations of [³H]-prazosin for 1 h. Non-specific binding was determined in the presence of 40 µM phentolamine. Points show mean ± s.e.mean of 5 independent experiments performed in duplicate.
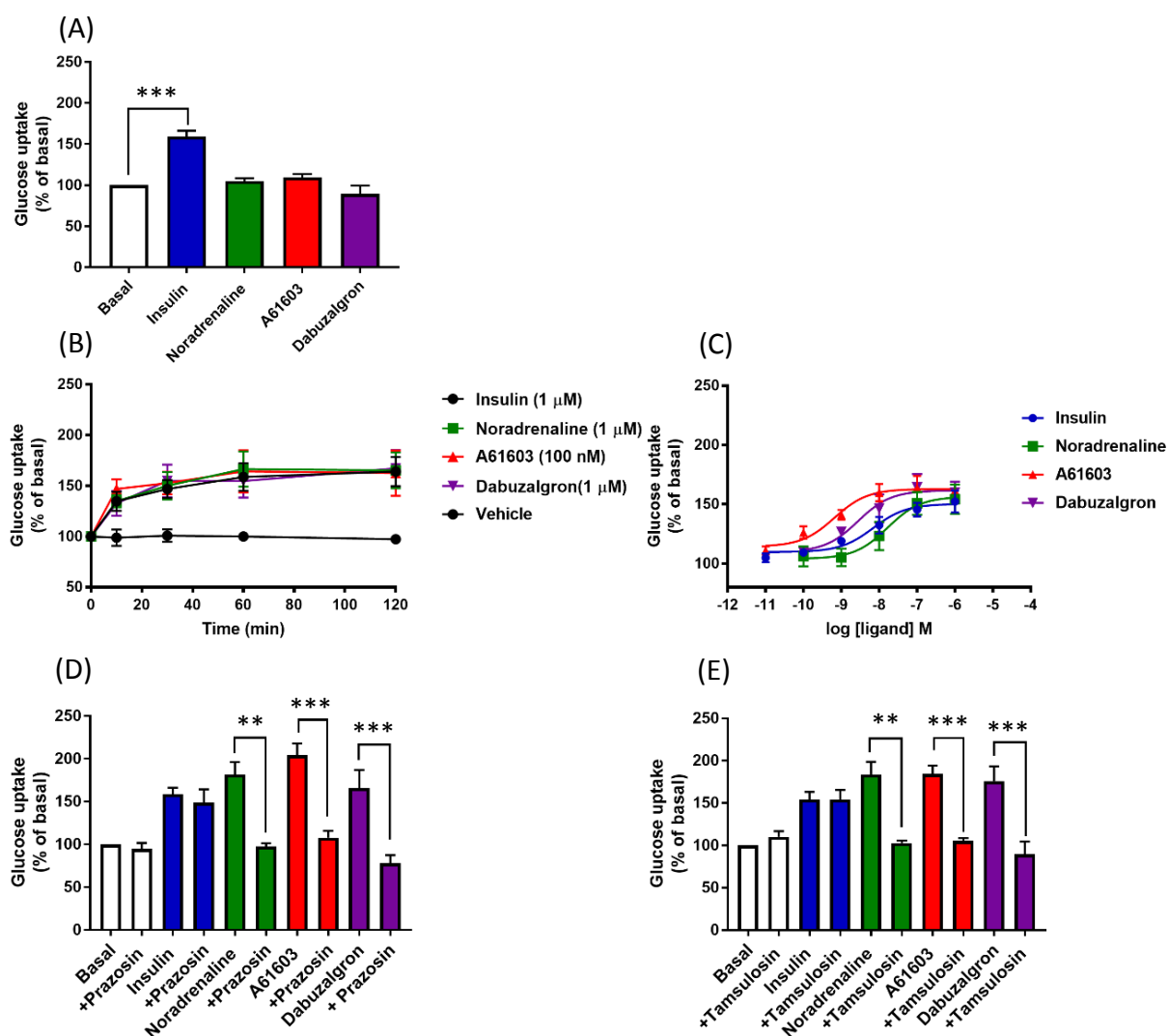
Figure 5.2: Effect of insulin, noradrenaline, A61603 or dabuzalgron on glucose uptake in CHOGLUT4myc cells stably expressing the human α_{1A}-AR

(A) Effect of insulin (10 µM), noradrenaline (100 nM), A61603 (10 nM) or dabuzalgron (100 nM) on glucose uptake in CHOGLUT4myc cells (120 min). Effect of (B) time or (C) concentration on insulin, noradrenaline, A61603 or dabuzalgron mediated increases in glucose uptake in CHOGLUT4myc cells expressing the human α_{1A}-AR (120 min). Effect of (D) prazosin (1 µM) or (E) tamsulosin (100 nM) on insulin (100 nM), noradrenaline (100 nM), A61603 (10 nM) or dabuzalgron (100 nM) stimulated glucose uptake in CHOGLUT4myc cells expressing the human α_{1A}-AR. Values are mean ± s.e.mean of 5-6 independent experiments performed in duplicate. Data are normalized to values in vehicle treated cells. Asterisks represent statistical differences as analysed by Student's paired t-test to make pairwise comparisons of inhibitory effects between two groups (**$P < 0.01$, ***$P < 0.001$).
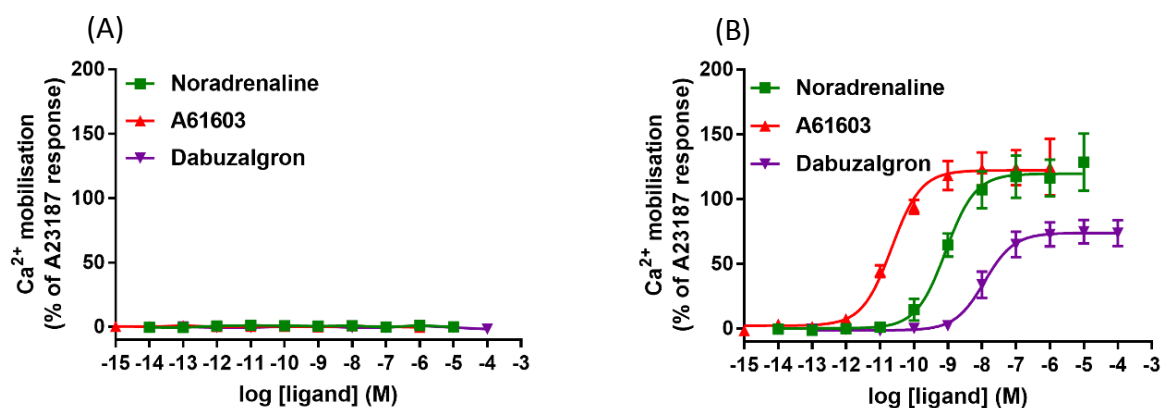
Figure 5.3: Effect of noradrenaline, A61603 or dabuzalgron on Ca^{2+} mobilisation in CHOGLUT4myc cells stably expressing the human α_{1A}-AR

Concentration effect of noradrenaline, A61603 or dabuzalgron on Ca^{2+} release in (A) CHOGLUT4myc cells, or (B) CHOGLUT4myc cells stably expressing the human α_{1A}-AR (1 min). Values are mean ± s.e.mean of 5-6 independent experiments performed in duplicate. Data are normalized to the maximum response generated by 1 µM A23187 in each experiment.

Table 5.1: Potency and maximal response of ligands for glucose uptake, Ca^{2+} mobilization, cAMP accumulation, S6RP phosphorylation, ERK1/2 phosphorylation, and NDRG1 phosphorylation

Values represent mean ± SEM from 4-7 individual experiments performed in duplicate. $Rmax^{NA}$ is expressed as percentage of maximal noradrenaline response. Data of $Rmax^{NA}$ were analysed in using one-way ANOVA and Dunnett's multiple comparisons test between noradrenaline and test ligand either A61603 or dabuzalgron, *$P < 0.05$, **$P < 0.01$, ***$P < 0.001$. NA = Not applicable. ND = Not determined. Statistical significance of differences of pEC_{50} and Rmax values is listed in Table 5.2.

		Insulin	Noradrenaline	A61603	Dabuzalgron
Glucose uptake (% of basal)	pEC_{50}	8.16 ± 0.30	7.78 ± 0.43	9.18 ± 0.29	8.56 ± 0.29
	Rmax	150.3 ± 4.54	156.4 ± 8.79	162.9 ± 4.64	161.6 ± 6.26
	$Rmax^{NA}$	NA	100	113.4 ± 7.83	113.7 ± 11.5
Ca^{2+} mobilization (% of A23187)	pEC_{50}	NA	9.06 ± 0.16	10.66 ± 0.15	7.92 ± 0.15
	Rmax	NA	119.6 ± 5.76	122.2 ± 4.57	73.83 ± 3.60
	$Rmax^{NA}$	NA	100	95.25 ± 3.96	58.0 ± 2.76***
cAMP production (pmole/well)	pEC_{50}	NA	5.12 ± 0.15	6.55 ± 0.14	ND
	Rmax	NA	1.29 ± 0.07	1.91 ± 0.09	ND
	$Rmax^{NA}$	NA	100	133.6 ± 6.46***	0.31 ± 0.64***
p-S6RP (% of vehicle)	pEC_{50}	8.71 ± 0.17	6.79 ± 0.15	8.65 ± 0.13	7.08 ± 0.15
	Rmax	250.8 ± 9.24	253.1 ± 9.83	246.4 ± 7.60	211.6 ± 6.90
	$Rmax^{NA}$	NA	100	89.97 ± 3.43*	60.6 ± 3.48***
p-Erk1/2 (% of vehicle)	pEC_{50}	7.07 ± 0.18	6.62 ± 0.19	8.50 ± 0.14	6.26 ± 0.11
	Rmax	374.6 ± 25.2	294.7 ± 18.2	292.2 ± 13.7	303.6 ± 11.6
	$Rmax^{NA}$	NA	100	106.2 ± 5.52	104.3 ± 5.12
p-NDRG1 (% of vehicle)	pEC_{50}	7.34 ± 0.59	6.64 ± 0.27	8.27 ± 0.20	7.72 ± 0.37
	Rmax	201.1 ± 21.7	281.1 ± 20.6	253.3 ± 10.7	188.2 ± 9.33
	$Rmax^{NA}$	NA	100	86.71 ± 6.09	49.4 ± 5.34***

Table 5.2 Statistical significance of differences of pEC$_{50}$ and Rmax values among ligands in glucose uptake, Ca^{2+} mobilization, cAMP accumulation, p-S6RP, p-Erk1/2, p-NDRG1

pEC$_{50}$ and Rmax values used for this statistical analysis were obtained from Table 5.1. Data of glucose uptake, Ca^{2+} mobilization, p-S6RP, p-Erk1/2 and p-NDRG1 were analysed in using one-way ANOVA and Tukey's multiple comparisons test, and data of cAMP accumulation were analysed in using a two-tailed unpaired student's t-test, $*P < 0.05$, $**P < 0.01$, $***P < 0.001$. ns = Not significant. NA = Not applicable.

	Glucose uptake	Ca^{2+} mobilization	cAMP accumulation	p-S6RP	p-Erk1/2	p-NDRG1	
Insulin Vs. Noradrenaline	ns	NA	NA	***	ns	ns	pEC$_{50}$
	ns	NA	NA	ns	*	*	Rmax
Insulin Vs. A61603	ns	NA	NA	ns	***	ns	pEC$_{50}$
	ns	NA	NA	ns	*	ns	Rmax
Insulin vs. Dabuzalgron	ns	NA	NA	***	**	ns	pEC$_{50}$
	ns	NA	NA	ns	*	ns	Rmax
Noradrenaline vs. A61603	*	***	***	***	***	*	pEC$_{50}$
	ns	ns	**	ns	ns	ns	Rmax
Noradrenaline vs. Dabuzalgron	ns	**	NA	ns	ns	ns	pEC$_{50}$
	ns	***	NA	*	ns	**	Rmax
A61603 vs. Dabuzalgron	ns	***	NA	***	***	ns	pEC$_{50}$
	ns	***	NA	ns	ns	ns	Rmax

5.3.4 α_{1A}-AR mediated glucose uptake is dependent on Gαq/11, Ca^{2+} and PKCζ

α_{1A}-ARs primarily couple to Gαq/11 proteins to increase Ca^{2+} mobilization, and lead to activation of PKC. To investigate whether these proteins are involved in noradrenaline or A61603 stimulated glucose uptake, experiments were performed in the absence/presence of UBO-QIC (Gαq/11 inhibitor), BAPTA AM (intracellular and extracellular Ca^{2+} chelator), or PKCζ pseudosubstrate (PKCζ inhibitor). Glucose uptake in response to noradrenaline (100 nM) or A61603 (10 nM) was significantly decreased by UBO-QIC, BAPTA AM and PKCζ pseudosubstrate (*$P < 0.01$, **$P < 0.01$, ***$P < 0.001$, Student's paired t-test) (Figure 5.4A-C).

5.3.5 α_{1A}-AR mediated increases in glucose uptake may involve cAMP

In CHOGLUT4myc cells expressing the human α_{1A}-AR, noradrenaline and A61603 increased cAMP levels in a time and concentration dependent manner (Figure 5.5A-B; Table 5.1), with A61603 being more potent and displaying higher efficacy compared to noradrenaline. Dabuzalgron failed to increase cAMP levels (Figure 5.5A-B). Using FRET, production of cAMP at the plasma membrane or cytosol was determined following transient transfection of the α_{1A}-AR and FRET sensors (pmEpac2/cytoEpac2) into CHOGLUT4myc cells. In the cytosol, it appeared that noradrenaline (10 nM) and A61603 (1 nM) produced the same degree of cAMP (Figure 5.5C) (***$P < 0.001$, Two-way ANOVA). However, noradrenaline (10 nM) showed relatively lower cAMP response than A61603 (1 nM) when measured at the plasma membrane (***$P < 0.001$, Two-way ANOVA) (Figure 5.5D). Since cAMP is involved in β_2-AR mediated increases in mTOR phosphorylation and subsequent glucose uptake, we investigated whether cAMP is involved in α_{1A}-AR mediated glucose uptake. The cell permeable cAMP-dependent protein kinase (PKA) inhibitor PKI significantly inhibited noradrenaline and A61603 mediated glucose uptake, but had no effect on dabuzalgron mediated glucose uptake (*$P < 0.01$, ***$P < 0.001$, Student's paired t-test) (Figure 5.5E), consistent with the lack of cAMP produced following dabuzalgron treatment (Figure 5.5A-B). In addition, stimulation with the cell-permeable cAMP analogues 8-Bromoadenosine 3',5'-cyclic adenosine monophosphate (8-Br-cAMP) or N^6-Benzoyladenosine-3',5'-cyclic monophosphate (6-Benz-cAMP), significantly increased glucose uptake (*$P < 0.01$, Student's paired t-test) (Figure 5.5F), indicating that elevations in cAMP can increase glucose uptake themselves in these cells. Elevations in cAMP levels can occur through Gαs mediated pathways, and in some cases due to activation of adenylate cyclase isoforms that are sensitive to Ca^{2+} elevation (Halls & Cooper, 2011). To investigate this, CHOGLUT4myc cells expressing the human α_{1A}-AR were pretreated with the Gαq/11 inhibitor UBO-QIC, the PLC inhibitor

U73122, the Ca^{2+} chelator BAPTA AM, or the PKCζ inhibitor PKCζ pseudosubstrate, and noradrenaline or A61603-stimulated increases in cAMP levels were measured. Noradrenaline- or A61603-stimulated cAMP production was partially blocked by UBO-QIC (***$P < 0.001$, Student's paired t-test) or U73122 (**$P < 0.01$, ***$P < 0.001$, Student's paired t-test) (Figure 5.6A-B). However, BAPTA AM or PKCζ pseudosubstrate had no significant effect on cAMP production in response to noradrenaline (Figure 5.6C-D). This same concentration of UBO-QIC totally abolishes α_{1A}-AR mediated increases in Ca^{2+} mobilization (Sato et al., 2018), suggesting that perhaps noradrenaline and A61603 increase cAMP levels through a Ca^{2+} sensitive adenylate cyclase isoform, as well as perhaps a direct interaction with Gαs since UBO-QIC failed to totally inhibit cAMP levels.

5.3.6 α_A-AR mediated glucose uptake involve mTORC2, but not mTORC1

The involvement of mTOR in α_{1A}-AR mediated glucose uptake was examined by using two mTOR inhibitors, KU0063794 or rapamycin. KU0063794 does not discriminate between mTORC1 or mTORC2 (Garcia-Martinez et al., 2009). Rapamycin inhibits both mTORC1 and mTORC2, but this is dependent upon the length of treatment: short-term incubation with rapamycin inhibits mTORC1 activity by binding to FK506-binding protein 12 (FKBP12), which directly associates with mTORC1 (Weichhart et al., 2015), while long-term treatment with rapamycin can prevent not only mTORC1 but also mTORC2 assembly (although the FKBP12-rapamycin complex does not appear to bind to mTORC2) (Ballou & Lin, 2008; Sarbassov et al., 2006). In CHOGLUT4myc cells expressing the human α_{1A}-AR, short term (30 min) rapamycin treatment (1 μM) did not inhibit glucose uptake in response to noradrenaline (100 nM), A61603 (10 nM), or dabuzalgron (100 nM) (Figure 5.7A), whereas long term (24 h) rapamycin treatment (100 nM) or KU0063794 significantly inhibited α_{1A}-AR mediated glucose uptake (Rapamycin treatment;**$P < 0.01$, ***$P < 0.001$, Student's paired t-test, KU0063794 treatment;*$P < 0.01$, **$P < 0.01$, ***$P < 0.001$, Student's paired t-test) (Figure 5.7B-C). This suggests that mTORC2 and not mTORC1 is involved in α_{1A}-AR mediated glucose uptake.
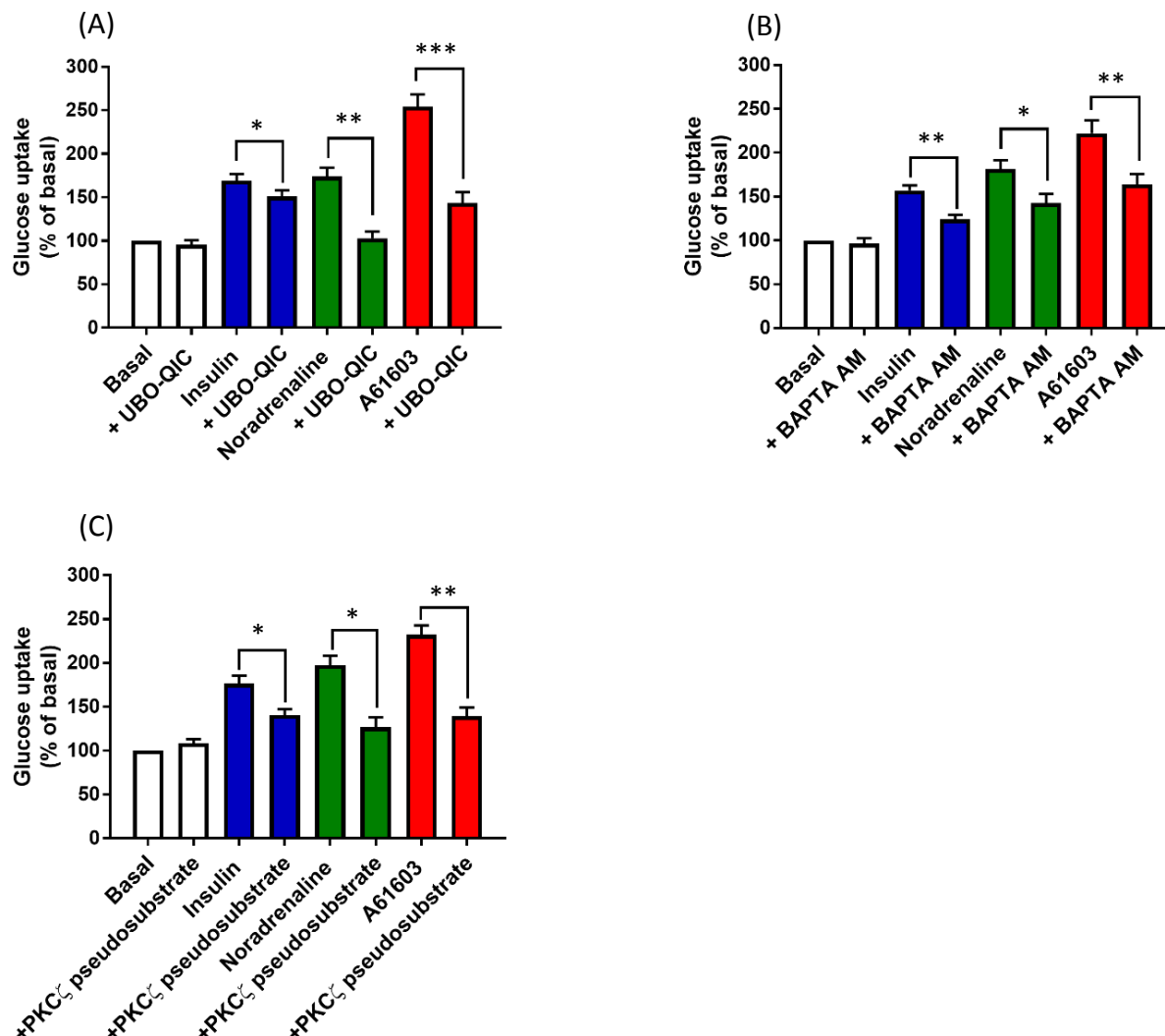
Figure 5.4: Noradrenaline, A61603 or dabuzalgron mediated increases in glucose uptake are dependent upon Gαq/11, calcium and PKCζ in CHOGLUT4myc cells stably expressing the α$_{1A}$-AR

Effect of (A) UBO-QIC (100 nM), (B) BAPTA AM (100 nM) or (C) a PKCζ pseudosubstrate inhibitor (1 µM) on insulin (100 nM), noradrenaline (100 nM), A61603 (10 nM) or dabuzalgron (100 nM) stimulated glucose uptake. Values are mean ± s.e.mean of 5-6 independent experiments performed in duplicate. Data are normalized to values in vehicle treated cells. Asterisks represent statistical differences as analysed by Student's paired t-test to make pairwise comparisons of inhibitory effects between two groups (*P < 0.01, **P < 0.01, ***P < 0.001).
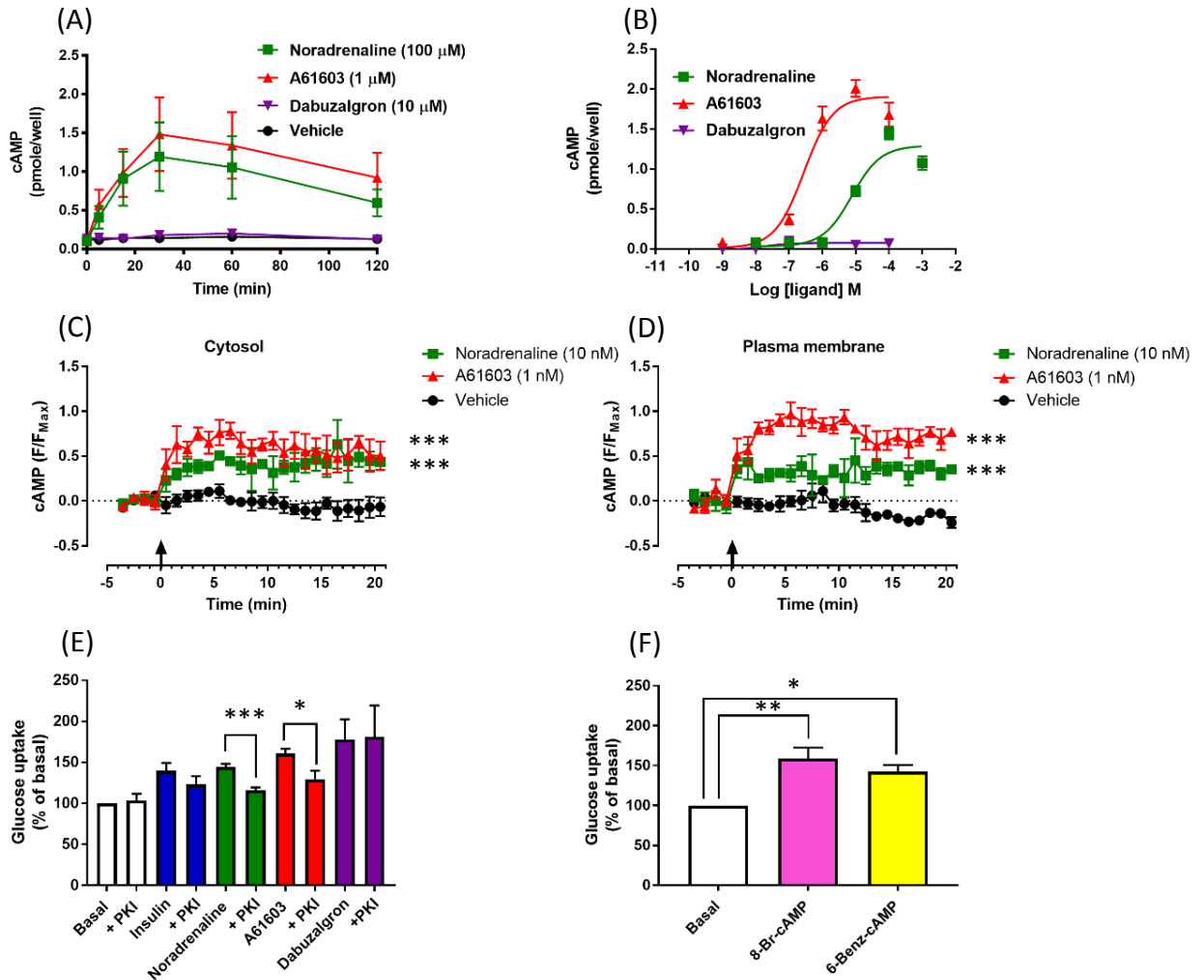
Figure 5.5: Role of cAMP in α_{1A}-AR mediated glucose uptake

Effect of (A) time on cAMP production or (B) concentration on cAMP accumulation in response to noradrenaline, A61603 or dabuzalgron in CHOGLUT4myc cells expressing the human α_{1A}-AR (30 min). Localisation of cAMP production in the cytosol (C) or at the plasma membrane (D) in CHO-K1 cells expressing the human α_{1A}-AR. (E) Effect of PKI (1 μM) on insulin (100 nM), noradrenaline (100 nM), A61603 (10 nM) or dabuzalgron (100 nM) stimulated glucose uptake in CHOGLUT4myc cells expressing the human α_{1A}-AR. (F) Effect of 8-Br-cAMP (1 mM) or 6-Benz-cAMP (1 mM) on glucose uptake in CHOGLUT4myc cells expressing the human α_{1A}-AR. Values are mean ± s.e.mean of 3-6 independent experiments performed in duplicate. Data are normalized to values in vehicle treated cells. Asterisks represent statistical differences as analysed by Two way ANOVA between vehicle and treated samples (***$P < 0.001$) in (C) and (D), Student's paired t-test to make pairwise comparisons of inhibitory effects between two groups (*$P < 0.05$, ***$P < 0.001$) in (E) or One-way ANOVA between samples(*$P < 0.05$, **$P < 0.01$) in (F).
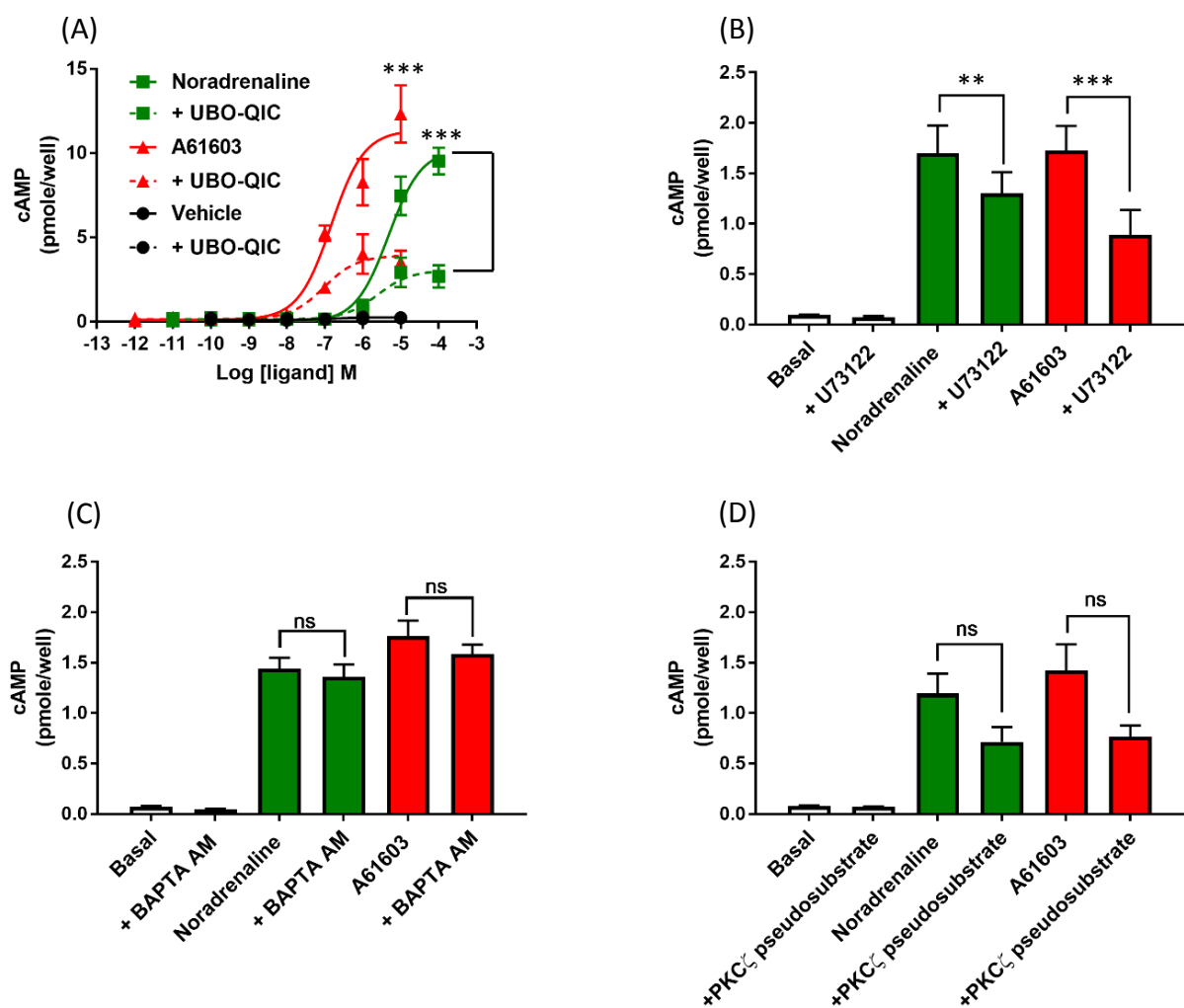
Figure 5.6: Noradrenaline or A61603 mediated increases in cAMP levels are through a Gαq/11 and PLC mediated mechanism in CHOGLUT4myc cells stably expressing the α$_{1A}$-AR

Effect of (A) UBO-QIC (100 nM), (B) U73122 (10 µM), (C) BAPTA AM (10 µM) or (D) PKCζ inhibitor (1 µM) on noradrenaline (1 µM) or A61603 (100 nM) stimulated cAMP accumulation. Values are mean ± s.e.mean of 4-5 independent experiments performed in duplicate. Data are normalized to values in vehicle treated cells. Asterisks represent statistical differences as analysed by Student's paired t-test to make pairwise comparisons of inhibitory effects between two groups (**P < 0.01, ***P < 0.001).
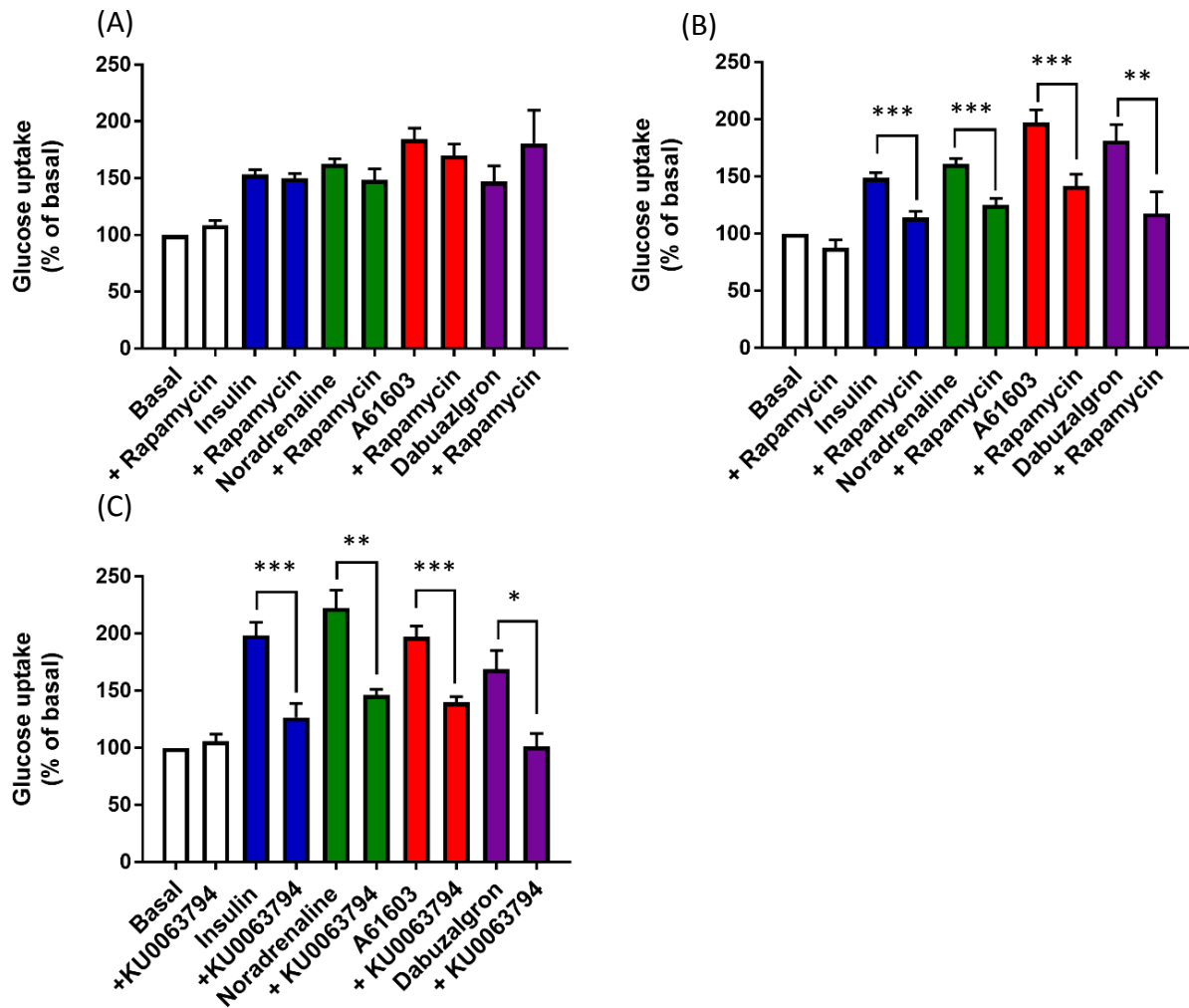
Figure 5.7: Insulin, noradrenaline, A61603 and dabuzalgron increase glucose uptake through mTORC2 in CHOGLUT4myc cells stably expressing the human α_{1A}-AR

Effect of (A) short term rapamycin treatment (1 µM, 30 min), (B) long term rapamycin treatment (100 nM, 24 h) or (C) KU0063794 (1 µM, 30 min) on insulin (100 nM), noradrenaline (100 nM), A61603 (10 nM) or dabuzalgron (100 nM) stimulated glucose uptake. Values are mean ± s.e.mean of 4-6 independent experiments performed in duplicate. Data are normalized to values in vehicle treated cells. Asterisks represent statistical differences as analysed by Student's paired t-test to make pairwise comparisons of inhibitory effects between two groups (*P < 0.05, **P < 0.01, ***P < 0.001).

5.3.7 α_{1A}-AR activation phosphorylates S6RP, a downstream target of mTORC1

In CHOGLUT4myc cells, noradrenaline, A61603, and dabuzalgron did not phosphorylate S6RP, a downstream target of mTORC1, whereas the positive control insulin did (Figure 5.8A). In CHOGLUT4myc cells expressing the human α_{1A}-AR, noradrenaline, A61603, dabuzalgron, and the positive control insulin all increased S6RP phosphorylation in a time and concentration dependent manner (Figure 5.8B-C; Table 5.1), with similar efficacies. The rank order of potency was A61603=insulin >> noradrenaline=dabuzalgron.

5.3.8 α_{1A}-AR activation phosphorylates NDRG1, a downstream target of mTORC2

In CHOGLUT4myc cells, noradrenaline, A61603, and dabuzalgron did not phosphorylate NDRG1, whereas the positive control insulin did (Figure 5.9A). In CHOGLUT4myc cells expressing the human α_{1A}-AR, noradrenaline, A61603, dabuzalgron, and the positive control insulin all increased NDRG1 phosphorylation in a time and concentration dependent manner (Figure 5.9B-C, Table 5.1). Noradrenaline and insulin were more efficacious compared to insulin and dabuzalgron, and the rank order of potency was A61603 >> insulin=dabuzalgron > noradrenaline.

5.3.9 α_{1A}-AR mediated increases in Erk1/2 phosphorylation in CHOGLUT4myc cells expressing the human α_{1A}-AR

In CHOGLUT4myc cells, noradrenaline, A61603, and dabuzalgron did not phosphorylate Erk1/2, whereas the positive control insulin did (Figure 5.10A). In CHOGLUT4myc cells expressing the human α_{1A}-AR, noradrenaline, A61603, dabuzalgron, and the positive control insulin all rapidly increased Erk1/2 phosphorylation in a time and concentration dependent manner (Figure 5.10B-C; Table 5.1), with similar efficacies. The rank order of potency was A61603 > insulin > noradrenaline = dabuzalgron. To assess whether Erk1/2 is involved in α_{1A}-AR mediated glucose uptake, experiments were performed in the absence/presence of the MEK inhibitor U0126. U0126 did not affect insulin or α_{1A}-AR mediated glucose uptake (Figure 5.10D).
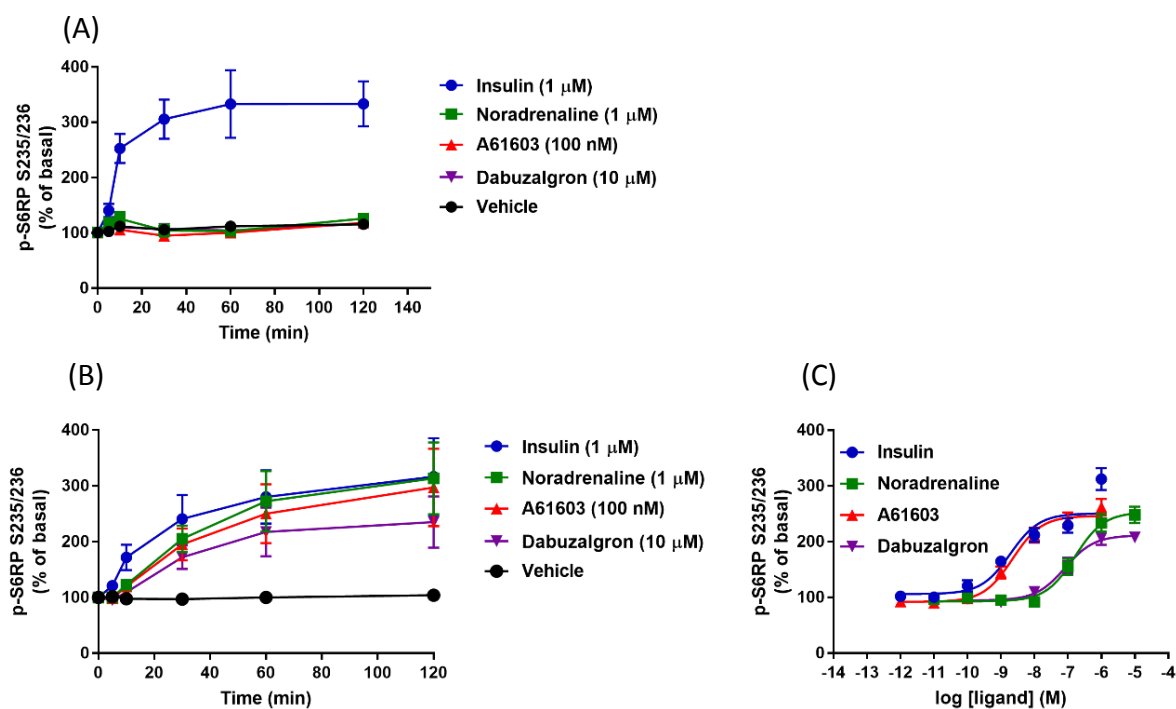
Figure 5.8: Effect of insulin, noradrenaline, A61603 and dabuzalgron on S6RP phosphorylation in CHOGLUT4myc cells stably expressing the human α_{1A}-AR

Time course effect of insulin (1 µM), noradrenaline (1 µM), A61603 (100 nM) or dabuzalgron (10 µM) on S6RP phosphorylation in (A) CHOGLUT4myc cells (n=5) or in (B) CHOGLUT4myc cells stably expressing the human α_{1A}-AR (n=6). (C) Concentration dependent effect of insulin, noradrenaline, A61603 or dabuzalgron on S6RP phosphorylation in CHOGLUT4myc cells stably expressing the α_{1A}-AR (120 min) (n=10). Values are mean ± s.e.mean of 5-10 independent experiments performed in duplicate. Data are normalized to values in vehicle treated cells.
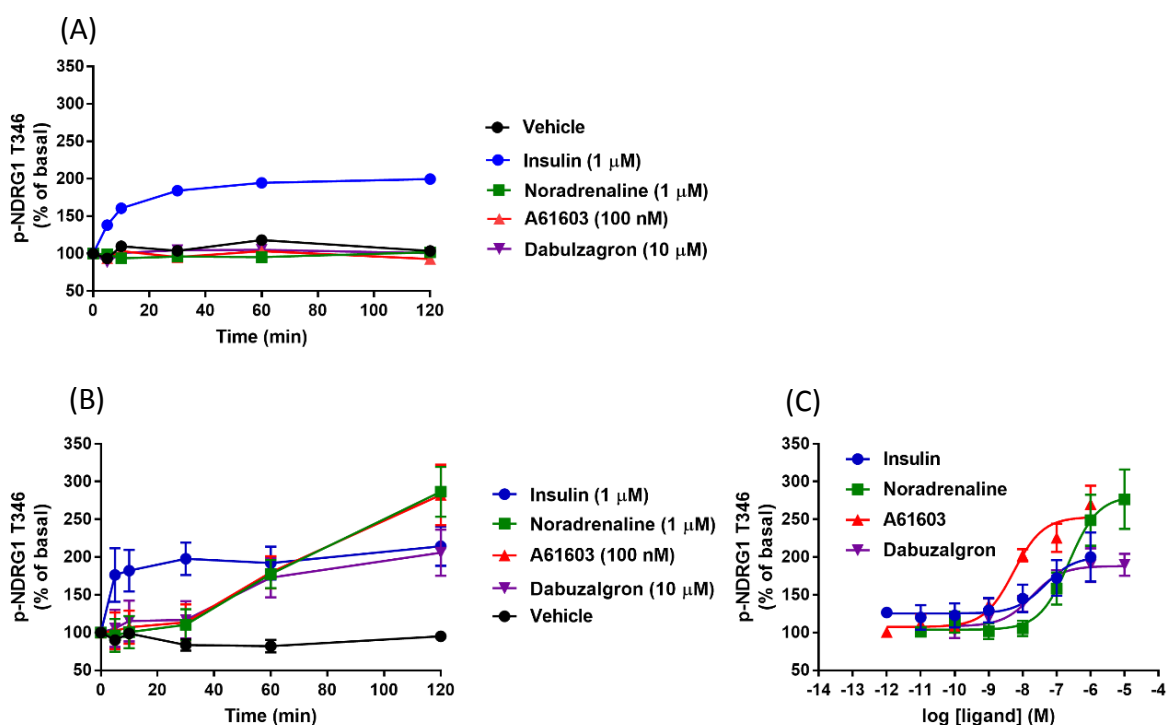
Figure 5.9: Effect of insulin, noradrenaline, A61603 and dabuzalgron on NDRG1 phosphorylation in CHOGLUT4myc cells stably expressing the human α_{1A}-AR

Time course effect of insulin (1 µM), noradrenaline (1 µM), A61603 (100 nM) or dabuzalgron (10 µM) on NDRG1 phosphorylation in (A) CHOGLUT4myc cells (n=1) or in (B) CHOGLUT4myc cells stably expressing the human α_{1A}-AR (n=6). (C) Concentration dependent effect of insulin, noradrenaline, A61603 or dabuzalgron on NDRG1 phosphorylation in CHOGLUT4myc cells stably expressing the α_{1A}-AR (120 min) (n=5). Values are mean ± s.e.mean of 1-6 independent experiments performed in duplicate. Data are normalized to values in vehicle treated cells.
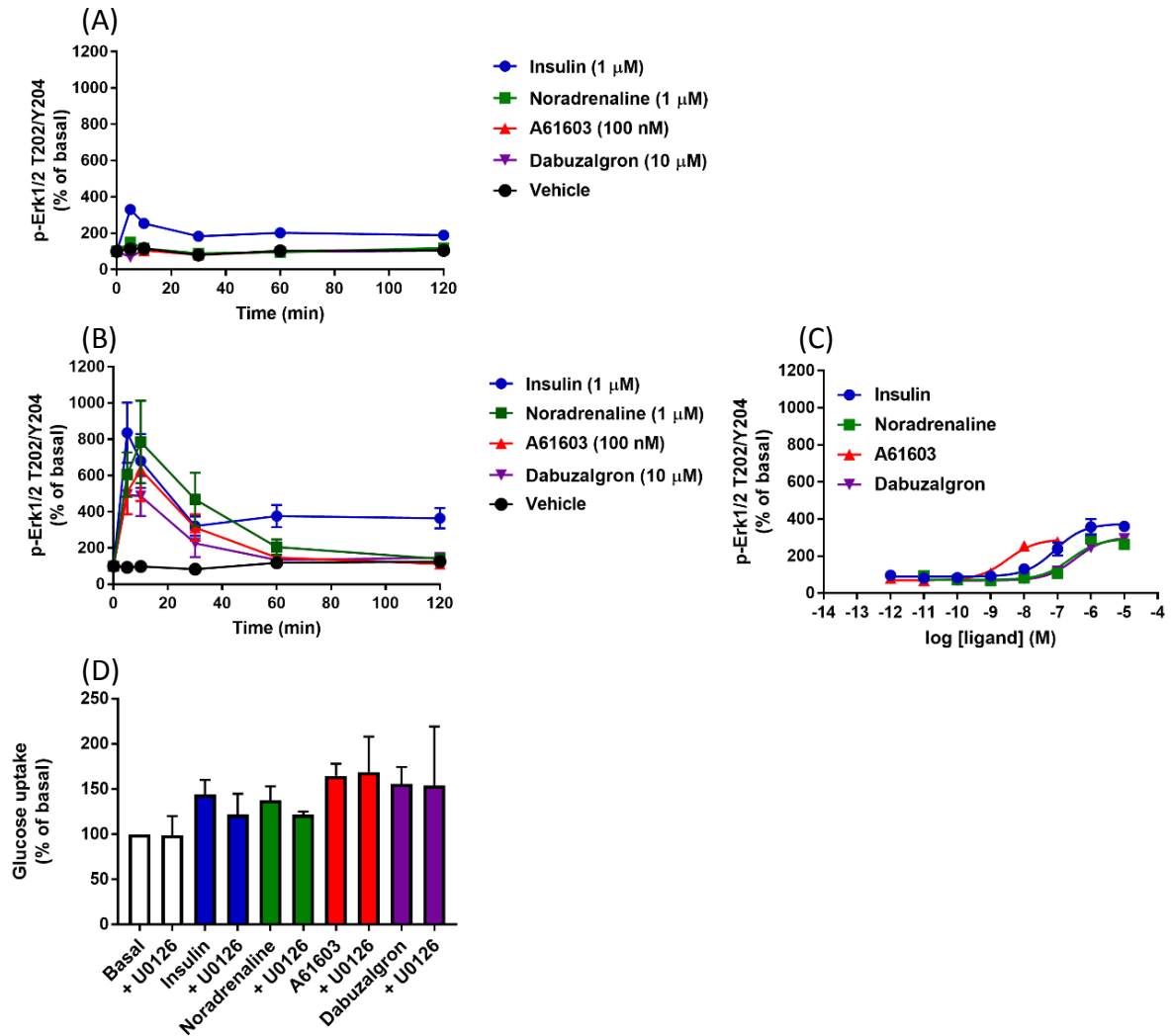
Figure 5.10: Effect of insulin, noradrenaline, A61603 or dabuzalgron on ERk1/2 phosphorylation in CHOGLUT4myc cells stably expressing the human α_{1A}-AR

Time course of insulin (1 µM), noradrenaline (1 µM), A61603 (100 nM) or dabuzalgron (10 µM) stimulated Erk1/2 phosphorylation in (A) CHOGLUT4myc cells (n=1) or in (B) CHOGLUT4myc cells stably expressing the human α_{1A}-AR (n=7). (C) Concentration dependent effect of insulin, noradrenaline, A61603 or dabuzalgron on Erk1/2 phosphorylation in CHOGLUT4myc cells stably expressing the α_{1A}-AR (10 min) (n=7). (D) Effect of U0126 (10 µM) on insulin (100 nM), noradrenaline (100 nM), A61603 (10 nM) or dabuzalgron (100 nM) stimulated glucose uptake (n=2-3). Values are mean ± s.e.mean of 1-7 independent experiments performed in duplicate. Data are normalized to values in vehicle treated cells.

5.3.10 Agonist bias at α₁ₐ-AR stably expressed in CHOGLUT4myc cells

The efficacies and potencies of A61603 and dabuzalgron, relative to the reference agonist noradrenaline, in glucose uptake, Ca^{2+} mobilization, cAMP production, p-S6RP, p-Erk1/2, and p-NDRG1, were determined (Figure 5.11, Table 5.1). S6RP and NDRG1 are downstream targets of mTORC1, and mTORC2, respectively, and are therefore shown as the markers of their activation. Noradrenaline and A61603 were full agonists toward glucose uptake, Ca^{2+} mobilization, p-S6RP, p-Erk 1/2 and p-NDRG1, and the maximal response of A61603 toward cAMP production was higher than noradrenaline. The rank order of potency for noradrenaline and A61603 was the same: Ca^{2+} > glucose uptake > S6RP = Erk 1/2 = NDRG1 > cAMP. In contrast, dabuzalgron was a full agonist toward glucose uptake and Erk1/2, a partial agonist toward Ca^{2+} mobilization, p-S6RP, p-NDRG1, and did not cause any production of cAMP. The rank order of potency for dabuzalgron was glucose uptake > Ca^{2+} = NDRG1 > S6RP > Erk 1/2.

Signalling bias at the α₁ₐ-AR in response to noradrenaline, A61603 and dabuzalgron in CHOGLUT4myc cells expressing the human α₁ₐ-AR was quantified. The transduction ratio R (τ/K_A) was derived from the operational model (van der Westhuizen et al., 2014) for each agonist at each pathway (Table 5.3). Effect of A61603 or dabuzalgron relative to noradrenaline within each pathway (ΔLogR) and across different signalling pathways (ΔΔLogR) was determined using noradrenaline as a reference ligand (Figure 5.12, Table 5.3, 5.4). ΔΔLogR values significantly different from 0 indicate the occurrence of biased signalling between pathways (two-tailed unpaired Student's t-test on the ΔlogR ratios). Dabuzalgron showed bias towards glucose uptake, Erk1/2 phosphorylation, S6RP phosphorylation, and NDRG1 phosphorylation as compared to Ca^{2+} mobilization (Figure 5.12), whereas A61603 showed no bias between any pathways (Figure 5.12).
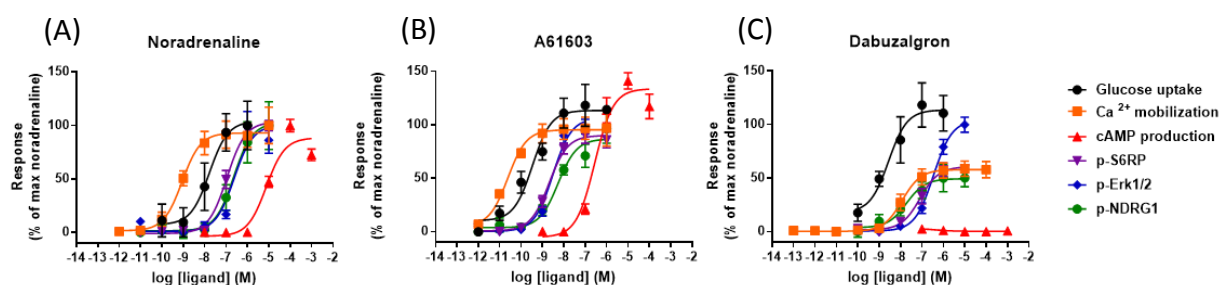
Figure 5.11: The profile of noradrenaline, A61603, and dabuzalgron toward the 6 different pathways in CHOGLUT4myc cells stably expressing the human α_{1A}-AR

Efficacies and potencies for 6 different pathways towards glucose uptake (2 h), cAMP production (30 min), Ca^{2+} mobilization (1 min), Erk1/2 phosphorylation (10 min), S6RP phosphorylation (2 h) or NDRG1 phosphorylation (2 h) in response to either (A) noradrenaline, (B) A61603, or (C) dabuzalgron in CHOGLUT4myc cells stably expressing the human α_{1A}-AR were summarized. Values are mean ± s.e.mean of 4-7 independent experiments performed in duplicate. Data are normalized to values in cells with maximal noradrenaline response.
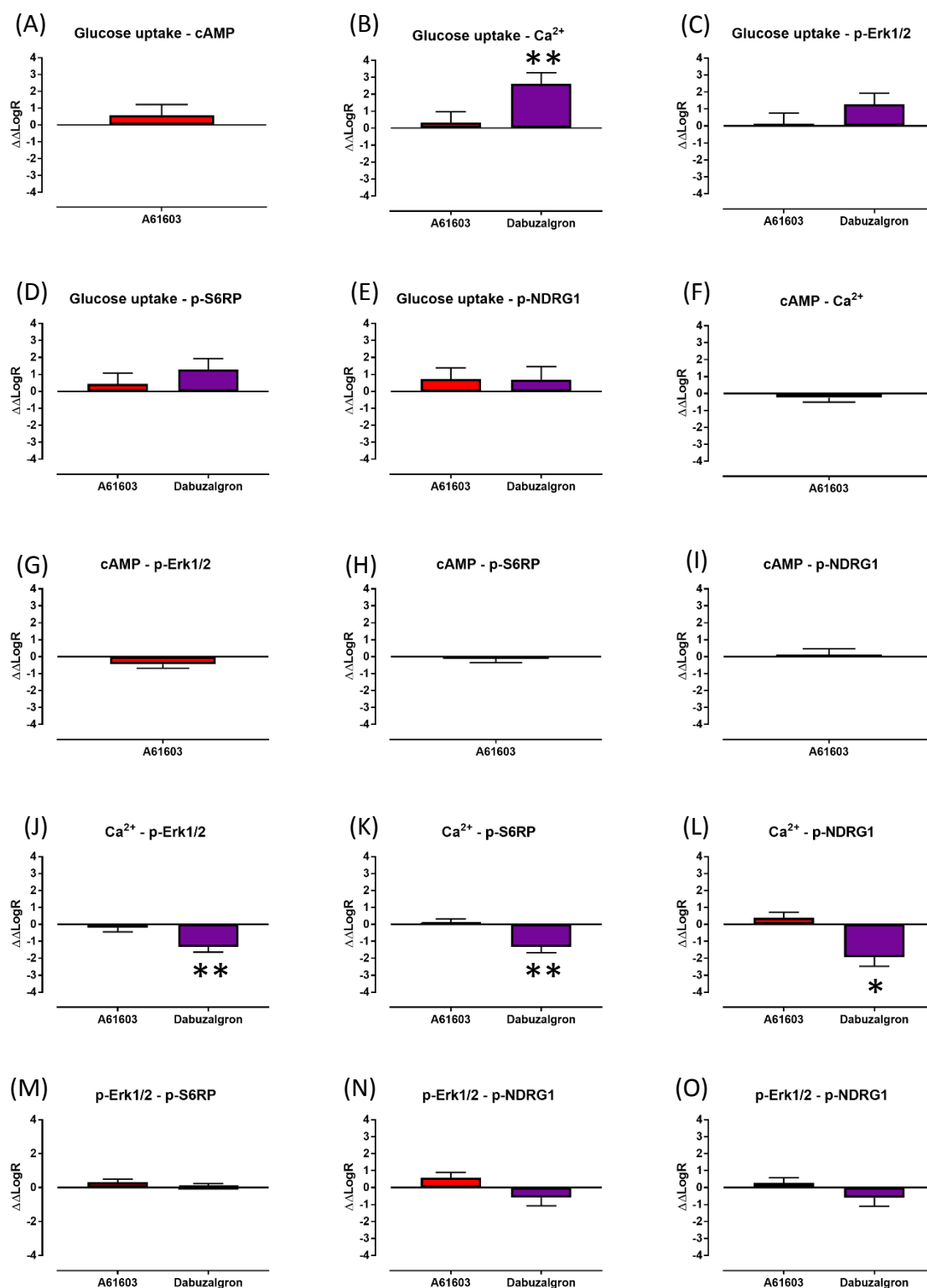
Figure 5.12: Ligand bias between different signalling pathways

Ligand bias (ΔΔLogR) of A61603 or dabuzalgron between pathways, relative to the reference ligand, noradrenaline. Values are mean ± s.e.mean of 4-7 independent experiments performed in duplicate. Asterisks represent statistical differences as analysed on ΔLogR by Student's unpaired t-test to make pairwise comparisons of two pathways (*P < 0.05, **P < 0.01).

Table 5.3: Transduction ratios for noradrenaline, A61603 and dabuzalgron towards glucose uptake, cAMP production, Ca^{2+} mobilization, Erk1/2 phosphorylation, S6RP phosphorylation and NDRG1 phosphorylation in CHOGLUT4myc cells expressing the human α_{1A}-AR

LogR values were obtained from non-linear regression curves using the operational model equation 2. ΔlogR ratios were calculated from the logR ratios, considering noradrenaline as the reference ligand using equation 3. The standard error of the mean was estimated using equation 4. The relative effectiveness (RE) of the ligands toward glucose uptake, cAMP production, Ca^{2+} mobilization, Erk1/2 phosphorylation, S6RP phosphorylation and NDRG1 phosphorylation pathway, relative to noradrenaline, was determined by equation 5. Values represent mean ± s.e.mean of 4-7 independent experiments in duplicate. Data were analysed in using a two-tailed unpaired student's t-test on the ΔlogR ratios to make pairwise comparisons between noradrenaline and test ligand either A61603 or dabuzalgron, $*P < 0.05$, $**P < 0.01$, $***P < 0.001$. ND = Not determined.

		Noradrenaline	A61603	Dabuzalgron
Glucose uptake	**LogR**	6.54 ± 0.45	8.51 ± 0.41	7.65 ± 0.41
	ΔLogR	0.0 ± 0.64	1.97 ± 0.61**	1.11 ± 0.61
	RE	1.00	93.97	12.88
cAMP accumulation	**LogR**	5.05 ± 0.15	6.44 ± 0.08	ND
	ΔLogR	0.0 ± 0.22	1.39 ± 0.18**	ND
	RE	1.00	24.32	ND
Ca^{2+} mobilization	**LogR**	8.99 ± 0.13	10.63 ± 0.13	7.48 ± 0.23
	ΔLogR	0.0 ± 0.19	1.64 ± 0.19**	-1.51 ± 0.27**
	RE	1.00	43.55	0.33
p-Erk1/2	**LogR**	6.53 ± 0.1	8.36 ± 0.1	6.36 ± 0.1
	ΔLogR	0.0 ± 0.14	1.84 ± 0.14**	-0.17 ± 0.14
	RE	1.00	68.39	0.67
p-S6RP	**LogR**	6.91 ± 0.09	8.44 ± 0.09	6.73 ± 0.17
	ΔLogR	0.0 ± 0.12	1.53 ± 0.12***	-0.18 ± 0.19
	RE	1.00	33.65	0.66
p-NDRG1	**LogR**	6.46 ± 0.20	7.72 ± 0.20	6.88 ± 0.42
	ΔLogR	0.0 ± 0.28	1.26 ± 0.28*	0.42 ± 0.47
	RE	1.00	18.07	2.61

Table 5.4: ΔΔlogR ratios and bias factors for noradrenaline, A61603 and dabuzalgron in CHOGLUT4myc cells expressing the human α$_{1A}$-AR

ΔΔlogR ratios were calculated from the ΔlogR ratios (Table 5.3) using equation 6. The standard error of mean was estimated using equation 7. The ligand bias factors (BF), relative to noradrenaline were determined using equation 8. Values represent the mean ± standard error of 4-7 independent experiments with repeats in duplicate. Data were analysed in using a two-tailed unpaired Student's t-test on the ΔlogR ratios to make pairwise comparison between two pathways, *P<0.05. ND = Not determined.

		Noradrenaline	A61603	Dabuzalgron
Glucose uptake - cAMP	ΔΔLogR	0.0 ± 0.67	0.59 ± 0.63	ND
	BF	1.00	3.86	ND
Glucose uptake – Ca^{2+}	ΔΔLogR	0.0 ± 0.66	0.33 ± 0.64	2.62 ± 0.66**
	BF	1.00	2.16	417.83
Glucose uptake – p-Erk1/2	ΔΔLogR	0.0 ± 0.14	0.14 ± 0.62	1.28 ± 0.66
	BF	1.00	1.37	19.14
Glucose uptake – p-S6RP	ΔΔLogR	0.0 ± 0.65	0.45 ± 0.62	1.29 ± 0.64
	BF	1.00	2.79	19.54
Glucose uptake – p-NDRG1	ΔΔLogR	0.0 ± 0.70	0.72 ± 0.67	0.69± 0.77
	BF	1.00	5.20	4.94
cAMP- Ca^{2+}	ΔΔLogR	0.0 ± 0.29	-0.25 ± 0.26	ND
	BF	1.00	0.56	ND
cAMP - p-Erk1/2	ΔΔLogR	0.0 ± 0.26	-0.45 ± 0.23	ND
	BF	1.00	0.36	ND
cAMP - p-S6RP	ΔΔLogR	0.0 ± 0.25	-0.14 ± 0.21	ND
	BF	1.00	0.001	ND
cAMP – p-NDRG1	ΔΔLogR	0.0 ± 0.36	0.13 ± 0.33	ND
	BF	1.00	1.35	ND
Ca^{2+}– p-Erk1/2	ΔΔLogR	0.0 ± 0.24	-0.20 ± 0.24	-1.34 ± 0.30**
	BF	1.00	0.65	0.05
Ca^{2+}– p-S6RP	ΔΔLogR	0.0 ± 0.22	0.11 ± 0.22	-1.33 ± 0.33**
	BF	1.00	1.29	0.05
Ca^{2+}– p-NDRG1	ΔΔLogR	0.0 ± 0.34	0.38 ± 0.34	-1.93 ± 0.54*
	BF	1.00	2.41	0.01
p-Erk1/2- p-S6RP	ΔΔLogR	0.0 ± 0.19	0.31 ± 0.19	0.01 ± 0.23
	BF	1.00	2.13	1.02
p-Erk1/2- p-NDRG1	ΔΔLogR	0.0 ± 0.32	0.58 ± 0.32	-0.59 ± 0.49
	BF	1.00	3.78	0.26
p-S6RP - p-NDRG1	ΔΔLogR	0.0 ± 0.31	0.27 ± 0.31	-0.60 ± 0.50
	BF	1.00	1.86	0.25

5.4 Discussion

Dabuzalgron (Ro 115-1240) is a highly selective, orally active α_{1A}-AR agonist, originally developed for the treatment of urinary incontinence. In animal studies, intravenous administration of dabuzalgron (300 µg/kg) showed a maximal increase in urethral tension without affecting blood pressure or heart rate (Blue et al., 2004). However in human clinical trials, dabuzalgron failed to show a significant difference in urethral incontinence compared to placebo, thus this study was discontinued in phase II clinical trials (Musselman et al., 2004).

Although dabuzalgron failed to show clinical efficacy in improving urethral incontinence, it was quickly identified as a possible drug in the use of heart failure (Beak et al., 2017). Human cardiomyocytes express both α_{1A}-ARs and α_{1B}-ARs, where activation of α_{1A}-ARs is likely involved in producing adaptive and protective effects in the heart (Huang et al., 2007; O'Connell et al., 2003; Rorabaugh et al., 2005). One study showed that dabuzalgron treatment protects against doxorubicin induced cardiotoxicity in wild type mice, but not in mice lacking the α_{1A}-AR (Beak et al., 2017). In addition, dabuzalgron treatment improved contractile function without causing fibrosis in wild type mice treated with doxorubicin. This mechanism of dabuzalgron induced cardiac protection was postulated to involve the activation of ERK1/2 (Beak et al., 2017). It should be noted that dabuzalgron was well tolerated in human studies, and did not cause any significant changes in blood pressure (Musselman et al., 2004). This is of importance as activation of α_1-ARs (mainly via activation of α_{1D}-ARs) is associated with vasoconstriction, leading to increased blood pressure (Jensen et al., 2009b; Jensen et al., 2010). Another α_{1A}-AR agonist, A61603, has also been examined for cardioprotection, with A61603 preventing cardiac apoptosis in doxorubicin treated mice (Dash et al., 2011). Additionally, infusion of A61603 in doxorubicin-treated mice preserved fractional shortening, and increased heart rate, stroke volume, cardiac output and survival, and all these effects were not observed in α_{1A}-AR knockout mice (Montgomery et al., 2017). While A61603 can increase blood pressure at higher doses, a very low dose of A61603 (10 ng/kg) is sufficient to produce these cardioprotective effects without affecting blood pressure (Montgomery et al., 2017). In mice, A61603 only significantly increased blood pressure at ED_{50} of 300 ng/kg (Rokosh & Simpson, 2002α).

In this study, we have aimed to assess any potential signalling bias of dabuzalgron and A61603 across canonical pathways important for cell survival, as well as metabolic pathways, including

Ca^{2+}mobilization, cAMP production, NDRG1 phosphorylation, S6RP phosphorylation, ERK1/2 phosphorylation and glucose uptake. Furthermore, we have examined the mechanism of A61603- or dabuzalgron-stimulated glucose uptake, especially with respect to the role of cAMP in glucose uptake. We have performed these experiments using a simplified model system: CHOGLUT4myc cells stably expressing the human α_{1A}-AR, which has been used to demonstrate mechanisms of α_{1A}-AR mediated glucose uptake (Sato et al., 2018), and CHO-K1 cells have been used previously to demonstrate ligand bias at the α_{1A}-AR (da Silva Junior et al., 2017; Evans et al., 2013).

Ligand bias refers to the ability of ligands to stabilize different unique receptor conformations, but also kinetic influences and cell context resulting in selective activation of different signalling pathway(s) (Kenakin & Christopoulos, 2013). Identification of biased agonists, which can activate physiologically beneficial signalling pathways while inhibiting others that could cause unwanted effects, is considered important for the development of therapeutic agents (Gundry et al., 2017). The results here clearly indicate that dabuzalgron is a full agonist for glucose uptake and Erk1/2 phosphorylation, and a partial agonist for Ca^{2+} mobilization, S6RP phosphorylation, and NDRG1 phosphorylation, whereas noradrenaline and A61603 were full agonists for all of these signalling pathways. Importantly, dabuzalgron failed to have any effect on cAMP production. The observed effects were all due to actions at the α_{1A}-AR since stimulation with noradrenaline, A61603, or dabuzalgron did not produce any effects in CHOGLUT4myc cells, thereby eliminating the possible 'off-target' effects due to the activation of other endogenous receptors expressed in CHOGLUT4myc cells expressing the human α_{1A}-AR (da Silva Junior et al., 2017). Demonstrating a lack of responses in untransfected cells is important as it demonstrates that all the response measured originate from activation of the transfected receptor. For example, the α_{1A}-AR agonist oxymetazoline showed great efficacy for ERK1/2 phosphorylation at the human α_{1A}-AR expressed in CHO-K1 cells and was considered a "supra" agonist for Erk1/2, but this was due to 'off-target effects' at 5-HT$_{1B}$ receptors endogenously expressed in CHO-K1 cells (da Silva Junior et al., 2017). Finally, use of the operational model, which is an approach to quantify concentration-dependent biased agonism and elucidate consequences of selective signal pathways, revealed that dabuzalgron showed significant bias towards glucose uptake and phosphorylation of S6RP, ERK1/2 and NDRG1, over stimulation of the Ca^{2+} pathway.

However, the primary factor responsible for biased signalling in this study could be the kinetic properties of each agonist (Klein Herenbrink et al., 2016). Dabuzalgron displays significant bias towards glucose uptake and phosphorylation of ERK1/2, S6RP and NDRG1 only when compared to Ca^{2+} mobilization (Table 5.4), which unlike the other responses is measured after 1 min incubation (peak response) following agonist addition. This makes this assay very prone to non-equilibrium kinetic influences. Differences in these kinetics can give rise to apparent "bias" in signalling assays measured at different time-points. For example, Klein-Herenbrink and co-workers measured association and dissociation rates of agonists at the dopamine D2 receptor, and modelled the time required to achieve full receptor occupancy (Klein Herenbrink et al., 2016). This varied from less than 1 min up to 10 mins or longer, emphasizing that Ca^{2+} release measurements performed after 1 min incubation are particularly sensitive to the kinetic parameters of the agonist. This should be investigated for α_{1A}-AR agonists, particularly for dabuzalgron that displayed bias relative to Ca^{2+} release. It would require expression of α_{1A}-ARs carrying an N-terminal SNAP-tag in the CHOGLUT4myc cells, as outlined in Chapter 4 for the β_2-AR. This would allow us to measure association and dissociation rates for noradrenaline, A61603 and dabuzalgron using Tag-Lite technology available for the α_{1A}-AR (CisBio). Or alternatively, [^{3}H]-prazosin binding using competitive association assays can be performed. Additionally, it is worthwhile to measure inositol phosphates (IPone), that are downstream of $G\alpha q/11$ and phospholipase C, at longer time points after agonist binding has reached equilibrium.

In addition, a further examination is required to assess whether dabuzalgron can be biased in a native system since different levels of receptor expression influence the observation of signalling bias (van der Westhuizen et al., 2014). In this study, it showed that dabuzalgron is a biased agonist in CHOGLUT4myc cells expressing the α_{1A}-AR, which is 3 times higher than that in neonatal rat ventricular cardiomyocytes (Sato et al., 2018). For example, a study in CHO-K1 cells expressing high levels of the β_3-AR showed more substantial effects on cAMP accumulation, leading to less phosphorylation of p38 MAPK in relation to cells expressing low levels of the β_3-AR (Sato et al., 2007). Also, performing assays in different systems is known to affect signalling bias. In HEK293 cells expressing human or mouse κ opioid receptors, stimulation with either ICI204448 or asimadoline showed no bias following activation of two different signalling pathways. In native tissues naturally expressing κ opioid receptors, however, ICI204448 and asimadoline showed different inhibitory responses of nerve-mediated muscle contraction in human intestine, although they acted equally in

mouse intestine (Broad et al., 2016). As such, receptor density and the system used for the assays are important factors to be considered when determining potential ligand bias.

Overall, the activation of the signalling pathways we measured are associated with different cardioprotective effects: Ca^{2+} mobilization is important for contractility, mTORC1 activation observed by S6RP phosphorylation is associated with hypertrophy, mTORC2 activation observed by NDRG1 phosphorylation affects cell survival and glucose uptake, and Erk1/2 phosphorylation has also been linked to cell survival. Therefore, stimulation with dabuzalgron might be predicted to produce greater effects towards hypertrophy, cell survival and glucose uptake than contractility, unlike A61603, which shows full responses toward all these pathways. However, dabuzalgron is a relatively new drug and the mechanisms of dabuzalgron in cardioprotection should be further investigated in cardiomyocytes and also *in vivo*.

mTORC1 (including raptor) and mTORC2 (including rictor) have a variety of roles in the heart including cell growth, proliferation, autophagy and metabolism (Sciarretta et al., 2014). Cardiomyocyte specific mTOR deletion causes a significant detrimental effect on the survival and proliferation of the embryonic heart in mice (Zhu et al., 2013), and cardiac-specific inducible mTOR knockout mice, but not wild type mice, showed a lethal enlarged heart along with enhanced cell death and fibrosis following tamoxifen administration (Zhang et al., 2010). Furthermore, cardiac raptor knockout mice failed to show adaptive cardiomyocyte growth and developed fatal dilated cardiomyopathy (Shende et al., 2011), thought to be due to a lack of mTORC1/S6RP activity. In contrast, mTORC2 is more likely involved in glucose metabolism in heart. In NRVMs, both mTORC1 and mTORC2 inhibition by KU0063794 reduced α_{1A}-AR mediated glucose uptake whereas mTORC1 inhibition by acute rapamycin had no effect (Sato et al., 2018), and in CHOGLUT4myc cells stably expressing human α_{1A}-AR, siRNA against rictor but not raptor blocks α_{1A}-AR mediated glucose uptake (Sato et al., 2018). In the current study in CHOGLUT4myc cells expressing the human α_{1A}-AR, we also demonstrate that mTORC2 is involved in noradrenaline-, A61603-, and dabuzalgron-stimulated glucose uptake since (1) both mTORC1 and mTORC2 inhibition with either KU0063794 or long-term rapamycin treatment inhibited glucose uptake mediated by α_{1A}-AR stimulation and (2) mTORC1 inhibition with short-term rapamycin treatment failed to affect α_{1A}-AR mediated glucose uptake. This confirms that mTORC2 but not mTORC1 has a crucial role in glucose uptake. However, the mechanism(s) resulting in increased glucose uptake via mTORC2 are still not known. PI3K is a

potential upstream target that activates mTORC2 in response to insulin (Gan et al., 2011; Zinzalla et al., 2011), however, it is not activated following the activation of α_{1A}-AR in this system because Akt (a downstream target of PI3K) phosphorylation at Ser473/Thr308 was not observed following stimulation by α_{1A}-AR agonists in either CHOGLUT4myc cells expressing the α_{1A}-AR or in NRVMs endogenously expressing the α_{1A}-AR (Sato et al., 2018). Furthermore, the Akt inhibitor X did not affect α_{1A}-AR mediated glucose uptake (Sato et al., 2018). Although AMPK is also involved in α_{1A}-AR mediated glucose uptake in CHOGLUT4myc cells stably expressing the human α_{1A}-AR and in NRVM (Sato et al., 2018), AMPK is completely independent of mTORC2, since pretreatment with KU0063794 or the AMPK inhibitor compound C did not affect the phosphorylation of AMPK or mTORC2 respectively, following activation of the α_{1A}-AR (Sato et al., 2018). One of the upstream kinases of AMPK is CaMKK (Abbott et al., 2009; Hurley et al., 2005), which is activated by Ca^{2+} release from endoplasmic reticulum (ER). However, Ca^{2+} is not a signalling molecule responsible for mTOR phosphorylation following α_{1A}-AR activation since A23187 (Ca^{2+} ionophore) failed to phosphorylate mTORC2 (Sato et al., 2018).

Another potential contributor to mTORC2 activation may be cAMP. In L6 skeletal muscle cells, β_2-ARs phosphorylate mTORC2 through a cAMP and PKA mediated mechanism that results in increased glucose uptake (Sato et al., 2014a). In the current study, stimulation with noradrenaline or A61603 increased global cAMP production, while stimulation with dabuzalgron showed no effect on cAMP production. Additionally, 8-Br-cAMP and 6-Bz-cAMP increased glucose uptake, and inhibition of PKA using PKI partially inhibited A61603 and noradrenaline mediated glucose uptake without affecting dabuzalgron mediated glucose uptake. It seemed to be conflicting that concentrations of noradrenaline (100 nM) or A61603 (10 nM) produced a small amount of global cAMP (Figure 5.5B) while producing a maximal response in glucose uptake (Figure 5.2C). However, a study with FRET biosensors that assessed the magnitude of cAMP response in two different compartments demonstrated an increased cAMP response both at plasma membrane and cytosol in response to noradrenaline (10 nM) or A61603 (1 nM). This indicates a small possible role for cAMP in α_{1A}-AR mediated glucose uptake, but whether cAMP is involved in mTORC2 activation is still unclear. Certainly, the results with dabuzalgron indicate that α_{1A}-ARs can activate mTORC2 resulting in increased glucose uptake without any cAMP production. This indicates that a non-cAMP-dependent mechanism of mTORC2 activation must exist.

The production of cAMP by noradrenaline or A61603 was elicited via $G\alpha q/11$ and PLC based on studies using the $G\alpha q/11$ and PLC inhibitors. It has been suggested that AC can be directly activated

by Ca^{2+} or by PKC (Chakrabarti et al., 1998; Halls & Cooper, 2011; Jacobowitz & Iyengar, 1994; Zimmermann & Taussig, 1996). In this system, Ca^{2+} or atypical PKCζ was not upstream of increases in cAMP levels since BAPTA AM or PKCζ pseudosubstrate did not significantly decease cAMP production. However, some other PKC isoforms can increase cAMP production including conventional PKCα (Kawabe et al., 1994; Zimmermann & Taussig, 1996), and novel PKCδ and PKCε (Lai et al., 1997). Hence PKC – AC – cAMP -PKA could be one consequence of $α_{1A}$-AR activation, at least with noradrenaline and A61603. Besides, both Ca^{2+} and PKCζ are still important for glucose uptake considering the fact that BAPTA AM and PKCζ pseudosubstrate reduced noradrenaline- or A61603-stimulated glucose uptake.

Overall, this study using pharmacological inhibitors and our previous study (Sato et al., 2018) both suggest that the potential $α_{1A}$-AR mediated glucose uptake pathway stimulated by dabuzalgron is distinct from A61603 (Figure 5.13). A61603 stimulation causes translocation of GLUT4/glucose uptake via 2 pathways including (1) activation of PLC - IP3 - Ca^{2+} - CAMKK - AMPK (Sato et al., 2018), or (2) activation of PLC – DAG – PKC – AC – cAMP – PKA - mTOR. However, the direct link of PKA and mTOR needs to be examined by using PKI in a mTOR phosphorylation assay. In contrast, dabuzalgron- stimulated glucose uptake pathway is less clear. There must be a pathway via mTORC2 that is nonetheless independent of cAMP. While the role of Ca^{2+}, CAMKK and AMPK in glucose uptake is still uncertain, dabuzalgron increases Ca^{2+} mobilization, leading to mTORC1 phosphorylation, necessary for protein translation.

Activation of mTORC1 and its downstream target S6RP has been suggested to increase protein translation and cell growth (Boluyt et al., 1997; Huang et al., 2009; Shioi et al., 2003). Our previous study in both CHOGLUT4myc cells stably expressing human $α_{1A}$-AR and NRVMs showed that $α_{1A}$-AR stimulation of S6RP phosphorylation and cell growth was abolished by acute rapamycin incubation or KU0063794 pretreatment, respectively (Sato et al., 2018), suggesting that $α_{1A}$-ARs increase cellular growth via mTORC1. Here, we show that dabuzalgron was less potent than A61603 in phosphorylating S6RP, and therefore the effect of dabuzalgron on cell growth should be determined. In addition, some studies have suggested a role of Erk1/2 in glucose uptake (Chen et al., 2002; Sajan et al., 2002), however, we found that the MEK1/2 inhibitor U0126 had no effect on insulin or $α_{1A}$-AR mediated glucose uptake. Erk1/2 might be associated with ATP generation and positive inotropy in heart since a study in cardiomyocytes showed that inhibition of Erk1/2 by another MEK inhibitor,

trametinib, caused reduction of ATP synthesis in mitochondria as well as contractile function (Beak et al., 2017).

In this study, we demonstrated that the α_{1A}-AR is involved in the activation of 6 pathways including Ca^{2+}, cAMP, glucose uptake, p-NDRG1, p-S6RP and p-Erk1/2 using CHOGLUT4myc cells stably expressing human α_{1A}-AR. However, further investigation is required to elucidate which G protein is associated with activation of these pathways. In fact, pretreatment with UBO-QIC did not completely abolish production of cAMP in response to noradrenaline or A61603, suggested the involvement of additional G protein(s). This can be assessed by clustered regularly interspaced short palindromic repeats (CRISPR/Cas9 system) technology, which enables the generation of cells with deletion of the gene of interest (Mandal et al., 2014). For example, this technology has been used to generate HEK293 cells with deletion of either Gαq and Gα11, or arrestin2 and arrestin3 (Alvarez-Curto et al., 2016). As such, this will also allow us to generate Gαs, Gαq/11 or Gαi/o knockout cells to determine the relative contribution of G protein(s) responsible for activation of each pathway without depending on the selectivity of G protein inhibitors. In addition, it would be worthwhile to examine the mechanism of A61603 or dabuzalgron mediated glucose uptake and adaptive hypertrophy in other systems such as rat cardiomyocytes.

Conclusion

This study utilizing CHOGLUT4myc cells stably expressing human α_{1A}-AR showed that dabuzalgron is a biased agonist towards glucose uptake, Erk1/2 phosphorylation, S6RP phosphorylation, and NDRG1 phosphorylation relative to Ca^{2+} mobilization. However, future work to investigate kinetic or conformational influence on the perceived signalling bias, and to elucidate the mechanism of mTOR activation in metabolic pathways as well as canonical pathways is required.
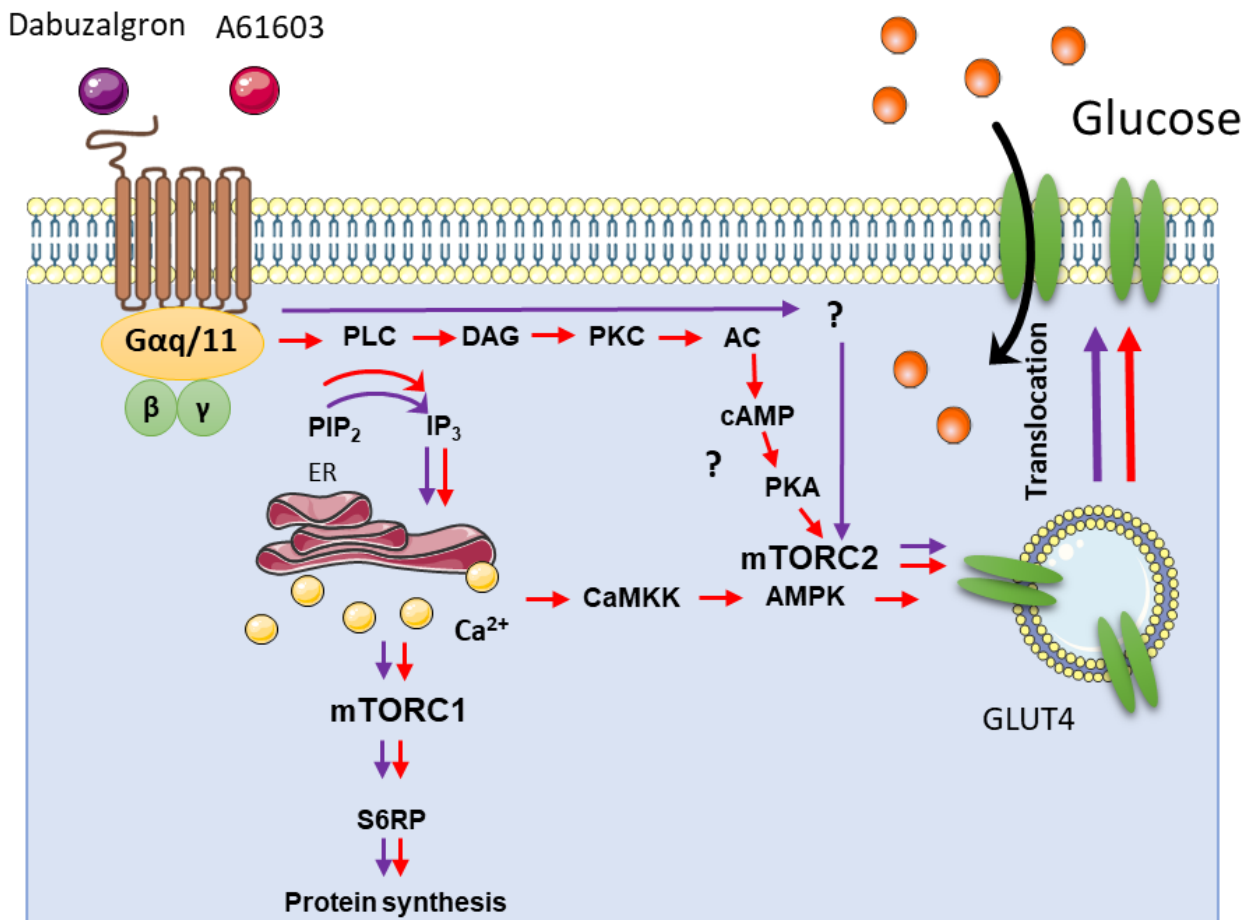
Figure 5.13: Potential pathways for glucose uptake and protein synthesis in response to A61603 or dabuzalgron

Glucose uptake: A61603 stimulation of the α_{1A}-AR causes PIP2 hydrolysis by PLC at the plasma membrane releases IP3 and DAG. IP3 binding to the IP3 receptor on the endoplasmic reticulum stimulates Ca^{2+} release, in turn, activates CaMKK and AMPK. DAG at plasma membrane activates PKC, also AC, resulting in cAMP/PKA mediated mTORC2 activation. Their activation (AMPK, mTORC2) stimulates GLUT4 translocation to the plasma membrane and increases glucose uptake. Like A61603, dabuzalgron stimulation to α_{1A}-AR activates mTORC2, leading to increase GLUT4 translocation. Activation of AMPK in response to dabuzalgron is still not known.

Protein synthesis; mTORC1 is activated following Ca^{2+} release from ER, leading to stimulate protein synthesis.
Red arrows = A61603, Purple arrows = dabuzalgron

CHAPTER 6

General discussion

6.1 Introduction

The increased prevalence of Type 2 diabetes (T2D) worldwide is a significant health concern, causing long term complications such as cardiovascular disease and renal failure (Melville et al., 2000). The progression of T2D is associated with decreased glucose utilization in response to insulin. In healthy people, insulin increases glucose uptake in key tissues such as skeletal muscle and adipose tissue by the activation of signalling molecules that include phosphoinositide 3-kinase (PI3K), Akt, and the mechanistic/mammalian target of rapamycin complex 2 (mTORC2), which leads to the translocation of glucose transporter 4 (GLUT4) to the cell surface, allowing for increased glucose uptake (Bjornholm & Zierath, 2005; Satoh, 2014; Yoon, 2017b). However, insulin-stimulated PI3K/Akt signalling is impaired in T2D (Cozzone et al., 2008; Meyer et al., 2002; Sasaoka et al., 2006). Therefore, identifying targets that can increase glucose uptake independently of the insulin signalling pathway would be advantageous. This is also the case in diabetic cardiomyocytes. In order to generate ATP, the healthy heart predominantly utilizes free fatty acids as its main energy substrate via the oxygen-consuming β-oxidation pathway (Nagoshi et al., 2011). In heart failure, however, cardiomyocytes are exposed to hypoxic conditions, under which ATP generation relies more on glucose utilization via glycolysis, thereby providing the energy required to maintain cardiac function (Doenst et al., 2013; Kolwicz & Tian, 2011; Lionetti et al., 2011; Lopaschuk et al., 2010; Nagoshi et al., 2011). Nevertheless, this energy switch is less efficient in diabetic heart failure as loss of insulin sensitivity causes reductions in cardiomyocyte glucose uptake. Thus α_{1A}-AR mediated glucose uptake, occurring independently of insulin, becomes more important in this situation.

G protein-coupled receptors (GPCRs) are a large group of cell surface receptors that can be targeted for the treatment of diabetes and other metabolic disorders (Reimann & Gribble, 2016). Agonists acting at the glucagon-like peptide 1 (GLP-1) receptor target the release of insulin by pancreatic β-cells, and have been studied and approved clinically for treatment of human patients (Frias et al., 2017; Frias et al., 2018; Katz et al., 2012). Another important group of GPCRs are the adrenoceptors (ARs), of which several subtypes (α_{1A}-AR in cardiac muscle, β_2-AR in skeletal muscle, and the β_3-AR in adipose tissue) (Liu & Stock, 1995; Merlin et al., 2018; Nevzorova et al., 2002; Nevzorova et al., 2006; Ngala et al., 2008; Ngala et al., 2009; Olsen et al., 2014; Sato et al., 2014a; Sato et al., 2018) can increase glucose uptake in the insulin-resistant target tissues of diabetic patients. In this thesis, we have examined α_{1A}-AR and β_2-AR mediated glucose uptake, including mechanisms whereby this occurs.

The mechanism of glucose uptake utilized by ARs is distinct from insulin since key signalling molecules such as PI3K/Akt activated by insulin are not involved in α_{1A}-AR or β_2-AR mediated responses (Sato et al., 2014a; Sato et al., 2018). Supporting evidence for this was obtained by several approaches as follows, (1) pharmacological inhibition of PI3K with LY294002 and wortmannin reduced β_2-AR mediated glucose uptake in L6 cells (Nevzorova et al., 2002; Nevzorova et al., 2006), but these inhibitors were found to inhibit other kinases such as mTOR, which is involved in β_2-AR mediated glucose uptake (Gharbi et al., 2007), (2) β_2-AR agonists failed to enhance phosphatidylinositol (3,4,5)-trisphosphate (PIP3) levels in L6 cells (Sato et al., 2014a), and (3) stimulation with either β_2-AR or α_{1A}-AR agonists did not cause phosphorylation of Akt (the downstream target of PI3K) in L6 cells or neonatal rat ventricular myocytes (NRVM), and inhibition of Akt with the selective Akt inhibitor X did not reduce agonist-stimulated glucose uptake (Nevzorova et al., 2006; Sato et al., 2014a; Sato et al., 2018).

mTOR is a serine-threonine kinase in the family of PI3K related kinases, that exists as 2 different complexes with different functions: mTORC1 that includes raptor, and mTORC2 that includes rictor (Laplante & Sabatini, 2009). mTORC1 has a major role in the growth of muscle mass (Castets et al., 2013; Tang et al., 2014; Yoon, 2017a). Muscle specific mTOR knockout mice but not wild type mice had significantly reduced mass of fast-twitch glycolytic muscles and developed severe myopathy (Risson et al., 2009). Similarly, muscle specific raptor knockout mice showed progressive muscle dystrophy while muscle specific rictor knockout mice were not distinguishable from wild type mice with respect to muscle mass (Bentzinger et al., 2008). Also, adaptive cardiomyocyte growth was impaired in cardiac raptor knockout mice, potentially due to a deficiency of mTORC1/S6RP activity (Shende et al., 2011). In contrast, mTORC2 is more important for the regulation of glucose metabolism (Lamming et al., 2012; Yuan et al., 2018). Studies using transgenic mice demonstrated that insulin-stimulated glucose uptake is significantly reduced both in the muscle specific rictor KO mice and in fat cell specific rictor KO mice, compared to wild type mice (Kumar et al., 2008; Kumar et al., 2010). An *in vitro* study using siRNA showed that rictor inhibition but not raptor inhibition markedly decreases both insulin and β_2-AR mediated glucose uptake in rat L6 cells (Sato et al., 2014a). Another study using pharmacological inhibitors demonstrated that KU0063794 (which inhibits both mTORC1 and mTORC2) reduces both insulin and α_{1A}-AR mediated glucose uptake whereas acute rapamycin (inhibition of mTORC1) has no such effect in NRVM (Sato et al., 2018). Collectively, these results indicate that the pathways that link both insulin and AR signalling to

increased GLUT4 translocation and glucose uptake intersect at the level of mTORC2. Therefore, ARs could provide an alternative pathway to regulate GLUT4 translocation and glucose uptake via mTORC2, which does not involve activation of signalling intermediates such as PI3K/Akt that are down-regulated in T2D (Sato et al., 2014a). However, it is unclear how ARs increase GLUT4 translocation/glucose uptake upstream of mTORC2, and whether other signalling pathways are involved.

6.2 Stimulation of skeletal muscle glucose uptake by isoprenaline and BRL37344

In chapter 3, we examined signalling responses including glucose uptake, GLUT4 translocation, cyclic AMP (cAMP) accumulation, β-arrestin recruitment and phosphorylation of Akt and mTOR, following activation of β_2-ARs in rat L6 skeletal muscle cells (Table 6.1). Skeletal muscle has been considered as a potential target for antidiabetic therapies as it constitutes approximately 40% of body mass, and it is the major site of insulin- or exercise-stimulated glucose uptake in the body (Jensen et al., 2011b; Park et al., 2009; Richter & Hargreaves, 2013). However, there are few available therapies targeting enhanced peripheral glucose utilization in skeletal muscle. In addition, it is noteworthy that skeletal muscle is a primary site for potential therapies for muscle wasting disorders (Bonaldo & Sandri, 2013; Lynch et al., 2007), and mTORC1 is largely associated with activity of myostatin, involved in inhibition of muscle growth and differentiation (Amirouche et al., 2009; Yoon, 2017a). β_2-ARs are the predominant AR expressed in skeletal muscle (Evans et al., 1996; Rosenbaum et al., 2009), and have a variety of roles including muscle growth, contraction and glucose uptake (Figure 6.1). Their activation increases glucose uptake (Evans et al., 2013; Nevzorova et al., 2006; Ngala et al., 2009; Ngala et al., 2013) via a mechanism involving cAMP, mTORC2 and GLUT4 translocation (Sato et al., 2014a). However, β_2-ARs are distributed throughout the body, and cAMP produced following their activation is involved in other important physiological processes including altered vasoreactivity (leading to changes in heart rate and blood pressure), cardiac hypertrophy and hepatic gluconeogenesis (Berdeaux & Stewart, 2012; El-Armouche & Eschenhagen, 2009; Sutherland & Robison, 1969), which would be detrimental in a therapeutic setting. Therefore, β_2-AR agonists that can increase skeletal muscle glucose uptake without causing major effects on cAMP accumulation may be advantageous in the context of metabolic disorders. Conventional β-AR agonists (isoprenaline) and selective β_2-AR agonists (clenbuterol, zinterol) increase skeletal muscle glucose uptake, but their stimulation is also associated with the production of high levels of cAMP (Berdeaux & Stewart, 2012; Dehvari et al., 2012; Nevzorova et al., 2006; Sato et al., 2014a).
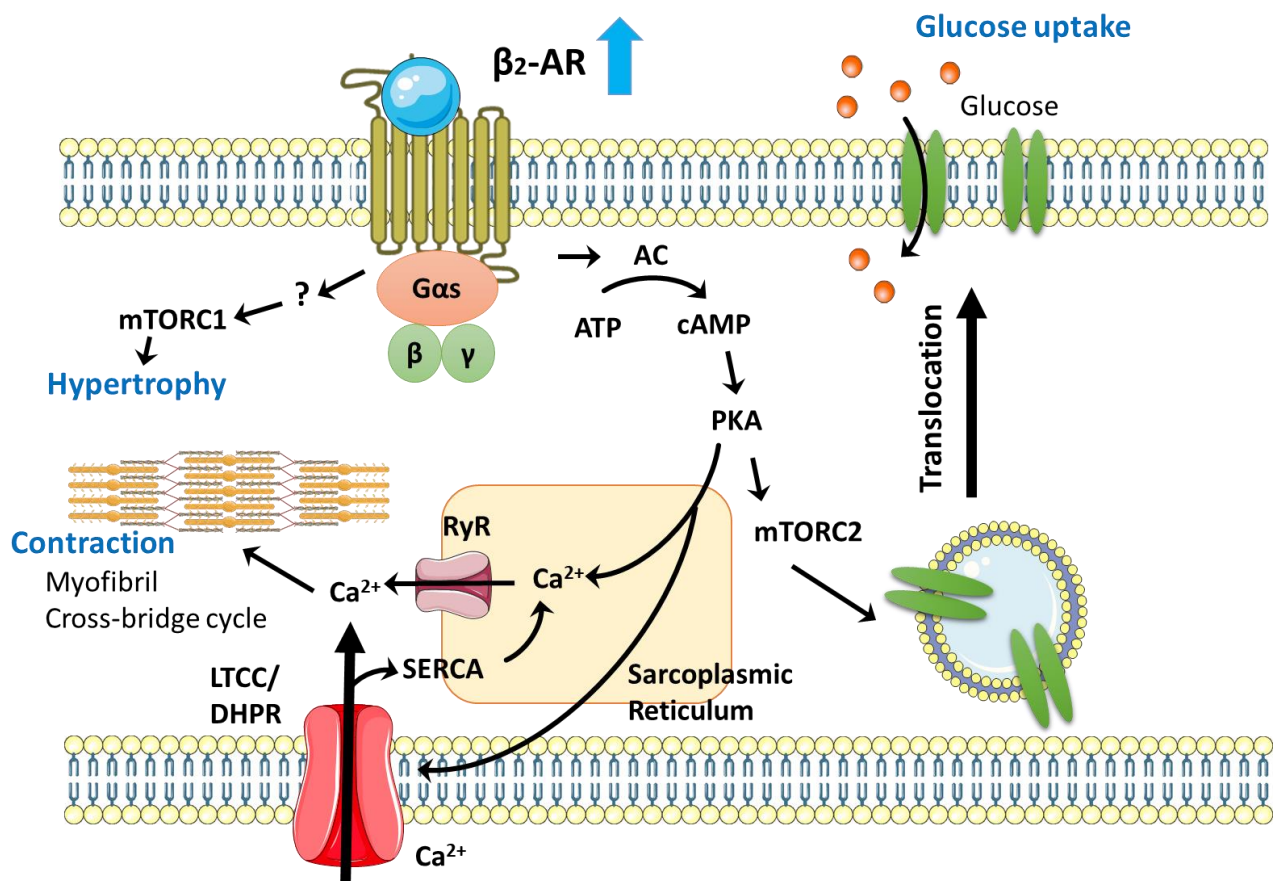
Figure 6.1: Overview of signal transduction and potential effects following activation of β-adrenoceptors in skeletal muscle (Cairns & Borrani, 2015; Kuo & Ehrlich, 2015; Sato et al., 2014a)

Skeletal muscle predominantly expresses β_2-AR > β_1-AR. In diabetes, β-AR expression level in skeletal muscle remains unchanged or increases (Xavier et al., 2012; Yang et al., 2002). Activation of β_2-AR increases glucose uptake, contraction, and hypertrophy through different Gαs-mediated pathways (Sato et al., 2014a).

Abbreviations: AC – adenylyl cyclase, cAMP – cyclic AMP, DHPR - dihydropyridine receptor, LTCC - L-type calcium channel, mTORC1 – mammalian target of rapamycin complex 1, mTORC2 – mammalian target of rapamycin complex 2, PKA – protein kinase A, PKC - protein kinase C, PLB - phospholamban, RyR - ryanodine receptor, SERCA - sarcoplasmic/endoplasmic reticulum Ca^{2+}-ATPase.

In contrast, BRL37344, a dual β₂/β₃-AR agonist originally developed for the treatment of obesity (Arch et al., 1984), increases skeletal muscle glucose uptake via β₂-ARs independently of cAMP in L6 cells (Nevzorova et al., 2002). In our study, BRL37344 acted as a full agonist at β₂-ARs for GLUT4 translocation and glucose uptake with an efficacy similar to that of isoprenaline, but was a weak partial agonist with respect to increasing cAMP levels (global, plasma membrane and cytosol). Furthermore, BRL37344-stimulated glucose uptake occurred via a mechanism involving mTORC2 but not Akt, which may be beneficial in a T2D setting. Indeed, BRL37344 was effective for improving glucose tolerance in a diabetic mouse model with global deletion of the β₃-AR gene. In addition, BRL37344 does not induce receptor desensitisation or internalisation to the same degree as isoprenaline, indicating that prolonged treatment of T2D patients with BRL37344 or a related drug would not result in desensitisation and therefore continue to be effective for glucose disposal. Overall, BRL37344 increased glucose uptake without causing a major impact on cAMP production and without causing cause receptor desensitisation/internalisation, and this combination of properties of BRL37344-stimulated signalling potentially provides new opportunities for the treatment of T2D (Chapter 3). In chapter 4, we examined the more detailed mechanism of glucose uptake in response to stimulation with isoprenaline or BRL37344.

6.3 Role of GRKs in β₂-AR mediated glucose uptake

The links between β₂-AR activation and glucose uptake are still unclear because of the difference in kinetics between glucose uptake and cAMP accumulation. Activation of β₂-AR causes a sustained increase in skeletal muscle glucose uptake (at least 24 h *in vitro*), in comparison to a transient increase in cAMP levels (Nevzorova et al., 2006). This may imply the existence of an alternative signalling pathway involving receptor internalisation. It has been discussed that desensitisation of the β₂-AR occurs following receptor phosphorylation by cAMP dependent protein kinase A (PKA) and G protein-coupled receptor kinase (GRK), leading to β-arrestin binding, resulting in receptor internalisation and desensitisation. However, PKA-mediated receptor phosphorylation has been considered less important for receptor desensitisation (Clark et al., 1988; Hausdorff et al., 1989; Yuan et al., 1994). A study in H9c2 cardiac myoblasts showed that isoprenaline stimulation of the β₂-AR causes receptor internalisation through phosphorylation at GRK sites and not PKA sites (Fu et al., 2015). As such, receptor phosphorylation by GRKs is a crucial step to promote receptor desensitisation (Ferguson et al., 1996; Ferguson et al., 1995; Goodman et al., 1996; Tsuga et al., 1994). In addition to the role of GRKs in receptor desensitisation, there is accumulating evidence

that GRKs, particularly GRK2 and GRK5, are involved in the regulation of glucose metabolism (Mayor et al., 2018). Whole body GRK5 knockout mice showed higher plasma glucose levels and lower insulin sensitivity compared to wild type mice (Wang et al., 2012). In general, however, GRKs are found to have an inhibitory effect on insulin-stimulated glucose uptake (Ciccarelli et al., 2012; Usui et al., 2004); (i) up-regulation of GRK2 inhibited GLUT4 translocation in response to insulin in adult rat ventricular cardiomyocytes, while a reduction of GRK2 levels during heart failure improved glucose uptake (Ciccarelli et al., 2011), and (ii) overexpression of GRK2 reduced insulin-stimulated glucose uptake in skeletal muscle C2C12 cells compared to wild type cells (Garcia-Guerra et al., 2010). In cardiomyocytes, attenuation of insulin signalling is thought to be due to the kinase activity of GRK2, which increases phosphorylation of insulin receptor substrate (IRS)-1 at Ser307 (Ciccarelli et al., 2011). Enhanced phosphorylation at Ser307 rapidly reduces IRS-1 binding affinity to the insulin receptor, causing inhibitory effects on insulin-stimulated glucose uptake (Aguirre et al., 2002). This negative effect of GRK2 on insulin signalling accompanies the increased β-AR desensitisation observed in heart failure (Ciccarelli et al., 2011). While GRK2 may negatively affect insulin-stimulated glucose uptake, it has a positive role in β_2-AR mediated glucose uptake in skeletal muscle, since truncation of the β_2-AR C-terminal tail, mutation of GRK phosphorylation sites or a β_2-AR(-)GRK mutant were all associated with reduced glucose uptake in response to isoprenaline in CHOGLUT4myc cells expressing human β_2-AR (Dehvari et al., 2012). This led to the hypothesis that β_2-AR mediated GLUT4 translocation/glucose uptake occurs through a GRK meditated mechanism due to phosphorylation of the β_2-AR at specific sites in the C-terminus.

In chapter 4, we examined the role of these GRK phosphorylation sites in the β_2-AR C-terminal tail in glucose uptake (Table 6.1). These experiments were performed in a simple recombinant system (CHOGLUT4myc cells), as it enabled us to generate mutant β_2-AR cell lines, and easy visualization of GLUT4 plasma membrane trafficking since GLUT4 is tagged with an exofacial myc tag. This study highlighted a significant role of GRK phosphorylation sites in isoprenaline-stimulated receptor internalisation as this was lost in cells expressing β_2-ARs with mutated GRK phosphorylation sites. However, the GRK phosphorylation sites were not critical in β_2-AR mediated GLUT4 translocation since stimulation with either isoprenaline or BRL37344 still promoted GLUT4 translocation in cells expressing receptors that completely lacked the GRK phosphorylation sites, as compared to wild type cells. This result was unexpected because in a previous study there was a significant reduction in isoprenaline-stimulated GLUT4 translocation in cells overexpressing GRK2 DN (K220R) (Dehvari

et al., 2012). These conflicting findings on GLUT4 translocation were potentially due to differences in the receptor expression level (transient expression vs stable expression), assay protocol (length of primary antibody incubation following a post fixation) and analysis (ImageJ program vs multi-wave scoring, MetaXpress 5.01). However, stimulation with either isoprenaline or BRL37344 certainly increased [^{3}H]-2-deoxyglucose uptake via activation of mutant β_2-AR lacking GRK phosphorylation sites. This indicated that GRK phosphorylation sites were not important for GLUT4 translocation/glucose uptake in this system. We, however, still cannot rule out the involvement of GRK2 at least in β_2-AR mediated glucose uptake as siRNA knock down of GRK2 dramatically decreased isoprenaline or BRL37344-stimulated glucose uptake in L6 myoblasts (Chapter 4). One explanation could be that GRKs act as scaffolding proteins (Gurevich et al., 2012). Among all the binding partners discovered (Penela et al., 2010), two potential partners in this system are clathrin (Shiina et al., 2001) and caveolin (Schutzer et al., 2005), which mediate internalisation of β-AR. We will be able to confirm whether the importance of GRK in glucose uptake is due to its binding activity by performing glucose uptake assays using specific GRK inhibitors or siRNA that selectively knock down GRK2, GRK5 or GRK6, or the combination of GRKs.

Furthermore, β-arrestins can adopt multiple conformations that are dependent both on the pattern or barcode of receptor phosphorylation by GRKs, and on the core receptor conformation induced or stabilised by different agonists (Cahill et al., 2017; Lee et al., 2016; Nuber et al., 2016). This affects β-arrestin mediated downstream signalling events, hence it would be worthwhile to investigate the effect of β-arrestin on glucose uptake by utilizing clustered regularly interspaced short palindromic repeats (CRISPR/Cas9 system) technology (Mandal et al., 2014), which enables generation of HEK293 cells with deletion of either β-arrestin1 or β-arrestin2 (Alvarez-Curto et al., 2016). Using CRISPR in conjunction with expression of GLUT4myc would allow us to examine the relative importance of β-arrestin in β_2-AR mediated glucose uptake in a model system. We would also investigate the effect of β-arrestin 1/2 siRNA in L6 skeletal muscle cells, as we did successfully with rictor and raptor siRNA (Sato et al., 2014). Finally, it would be interesting to investigate the effect of GRKs on mTOR phosphorylation using our current systems. As such, this study shows that GRK phosphorylation sites in β_2-AR have no crucial role in glucose uptake, which leads us to further investigation of the role of GRK binding/kinase activity in glucose uptake (Chapter 4). Overall, further studies should be conducted to examine the effect of BRL37344 in T2D or other metabolic disorders considering the fact that BRL37344 effectively increases glucose uptake both in recombinant

systems and L6 cell lines. Additionally, the effect of BRL37344 on muscle hypertrophy should be investigated (Chapter 3 and 4).

6.4 Role of α_{1A}-ARs in cardiomyocyte glucose uptake

α_1-ARs are expressed in cardiac muscle and have important roles in the regulation of glucose uptake. In human cardiac failure, α_{1A}-AR expression increases and is thought to have a cardioprotective role, via adaptive processes that include hypertrophy, increased cell survival and improved contractility (Jensen et al., 2011a; O'Connell et al., 2014), as well as enhanced glucose uptake (Sato et al., 2018), unlike β-ARs, which are down-regulated (Figure 6.2). Increased cardiomyocyte glucose uptake has been considered as one potential mechanism for cardioprotection (Domenighetti et al., 2010; Liao et al., 2002). α_{1A}-ARs can increase glucose uptake in skeletal muscle cells through a phospholipase C (PLC)-Ca^{2+}- $Ca^{(2+)}$/calmodulin-dependent protein kinase kinase β (CAMKK β)- AMP-activated protein kinase (AMPK) dependent mechanism (Hutchinson & Bengtsson, 2005) that also exists in cardiomyocytes (Sato et al., 2018). Another signalling pathway involving mTORC2 that also increases cardiomyocyte glucose uptake exists in parallel (Sato et al., 2018). The mechanism of mTORC2 activation by α_{1A}-ARs is not defined, but it is independent of Ca^{2+} and AMPK (Kamimura et al., 2008). One potential upstream regulator of mTORC2 activation is cAMP/PKA (Sato et al., 2014a). Hence, in chapter 5, we examined the role of cAMP in glucose uptake using a recombinant system (CHOGLUT4myc cells expressing the human α_{1A}-AR) (Table 6.1), which has been extensively used to demonstrate mechanisms of α_{1A} -AR mediated glucose uptake (Sato et al., 2018). Our studies employed two highly selective α_{1A}-AR agonists, A61603 and dabuzalgron. These 2 drugs were chosen because at doses effective in promoting cardioprotective effects against doxorubicin-induced cardiotoxicity, they have minimal effects on blood pressure in animal studies (Beak et al., 2017; Cowley et al., 2015; Jensen et al., 2011a; Vakhrusheva et al., 2008). In our study, the mechanism of glucose uptake in response to A61603 or dabuzalgron differed, but they exhibited very similar potency and efficacy in increasing glucose uptake. mTORC2 was involved in both A61603- or dabuzalgron- stimulated glucose uptake pathways whereas cAMP and PKA were involved only in the A61603-stimulated pathway. Although β_2-AR mediated production of cAMP might cause adverse side effects in heart, α_{1A}-ARs are only expressed in cardiac ventricles, and would not affect heart rate (Lindskog et al., 2015). More importantly, the potency of A61603 for cAMP generation is 2-4 orders of magnitude lower than that for intracellular Ca^{2+} release and the other measured responses (Chapter 5), thus the amount of cAMP produced by therapeutic

concentrations of α_{1A}-AR agonists would be far less than that observed in response to β-AR agonists or endogenous noradrenaline and adrenaline. One hypothesis concerning the role of cAMP in α_{1A}-AR mediated mTORC2 activation and glucose uptake is that low levels of highly compartmentalised cAMP may be sufficient to interact with key effectors that are brought together in localised signalling complexes (as outlined in Chapter 3 for BRL37344 acting at the β_2-AR).

We have compared the signalling responses that are important in cardiomyocyte function and survival including Ca^{2+} mobilization (contractility) (Capogrossi et al., 1991), p-S6RP (a marker of mTORC1 activation-hypertrophy) (Sato et al., 2018), p-NDRG1 (a marker of mTORC2 activation - cell survival and glucose uptake) (Hung et al., 2012; Sato et al., 2018) and p-Erk1/2 (cell survival) (Huang et al., 2007; Lu & Xu, 2006) in response to these drugs. This study clearly demonstrated that both A61603 and dabuzalgron act as full agonists for glucose uptake and Erk1/2 phosphorylation, but dabuzalgron only caused a partial response in Ca^{2+} mobilization, S6RP phosphorylation, and NDRG1 phosphorylation assays, unlike A61603. Furthermore, dabuzalgron was a biased agonist for glucose uptake, Erk1/2 phosphorylation, S6RP phosphorylation, and NDRG1 phosphorylation compared to Ca^{2+} mobilization, suggesting that dabuzalgron may produce a receptor conformation different from A61603 following agonist exposure. Alternatively, dabuzalgron may require longer to achieve full receptor occupancy than A61603 or noradrenaline, and this would have an impact primarily in Ca^{2+} release assays that are conducted at 1 min, in comparison to other assays done at 10, 30 or 120 min. Nonetheless, our findings indicate that dabuzalgron produces favourable effects on cell survival and glucose uptake. Additionally, dabuzalgron is an orally active drug unlike A61603, which provides advantages for patients including easy drug administration and flexible dosage. It is however a relatively new drug, and we will need further examination of its cardioprotective effects both *ex vivo* and *in vivo.* It is essential that we determine the kinetic properties of dabuzalgron at the α_{1A}-AR, compared to A61603 or endogenous noradrenaline (Klein Herenbrink et al., 2016), and thus the mechanism whereby dabuzalgron causes biased signalling following interaction with receptors (chapter 5).
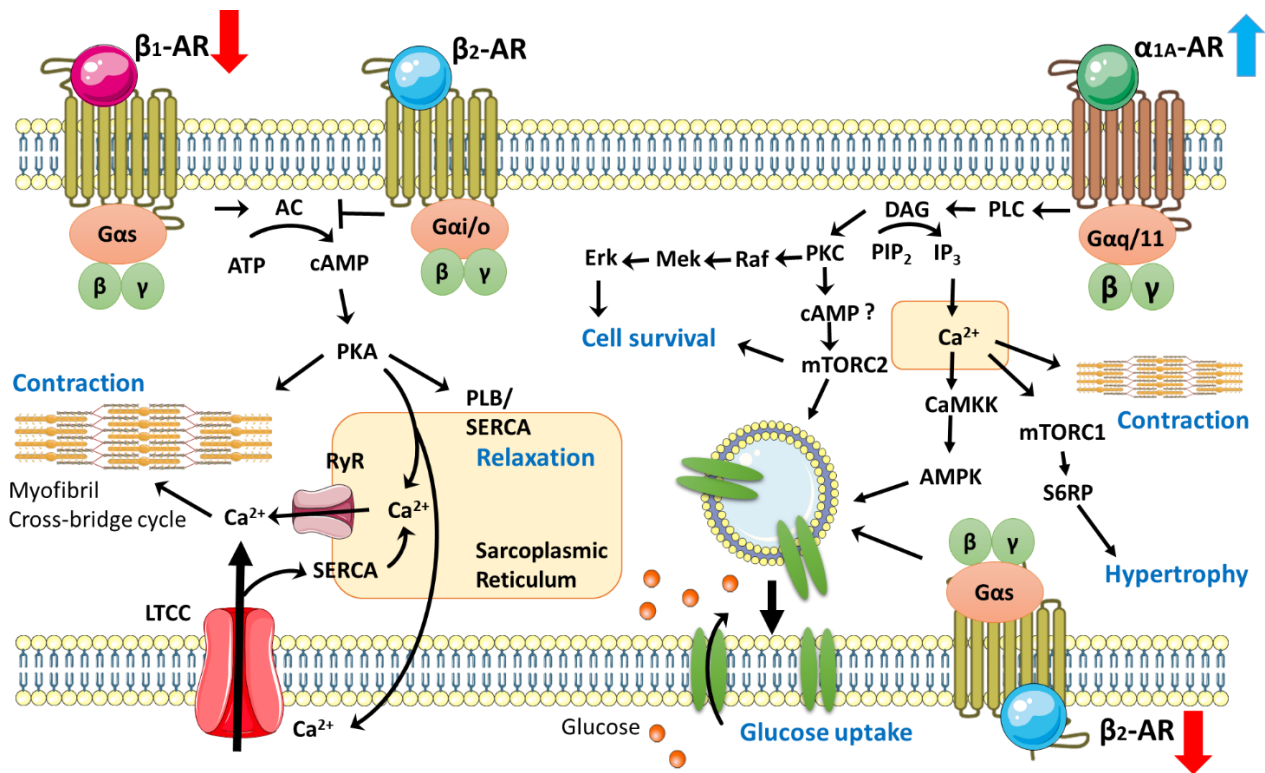
Figure 6.2: Overview of signal transduction and potential effects following activation of cardiac adrenoceptors (Jensen et al., 2014; Kuo & Ehrlich, 2015; Lymperopoulos et al., 2013; Mangmool et al., 2017; O'Connell et al., 2014; Sato et al., 2018)

Cardiac muscle expresses β_1-AR > β_2-AR > α_{1A}-AR in normal heart. Activation of β_1-ARs increases contractility via Gαs (Lohse et al., 2003). β_2-ARs also increase glucose uptake via Gαs (Mangmool et al., 2017), but may reduce cardiac contractility through additional coupling via Gαi/o (Madamanchi, 2007). In heart failure, β-ARs (especially β_1-AR) are desensitised and down-regulated, leading to reduced contractility. In contrast, α_{1A}-AR expression is increased, producing cardioprotective effects including improved contractility, adaptive hypertrophy, cell survival and glucose uptake via Gαq/11 (Jensen et al., 2014; Sato et al., 2018) (Chapter 5).

Abbreviations: AC – adenylyl cyclase, AMPK – AMP-activated protein kinase, CaMKK – Calcium/Calmodulin-dependent protein kinase kinase, cAMP – cyclic AMP, DAG – diacylglycerol, Erk - extracellular signal regulated kinases, IP3 – inositol 1,4,5-trisphosphate, LTCC - L-type calcium channel, MEK - mitogen-activated protein kinase kinase, mTORC1 – mammalian target of rapamycin complex 1, mTORC2 – mammalian target of rapamycin complex 2, PIP2 - phosphatidylinositol 4,5-bisphosphate, PLC – phospholipase C, PKA – protein kinase A PKC - protein kinase C, PLB – phospholamban, RyR - ryanodine receptor, S6RP - S6 ribosomal protein, SERCA - sarcoplasmic/endoplasmic reticulum Ca^{2+}-ATPase.

Table 6.1 Summary of results from Chapter 3-5

Chapter 3	
Background	- BRL37344, a dual $\beta_{2/3}$-AR agonist, increases glucose uptake in skeletal muscle - The mechanism of BRL37344 stimulated glucose uptake has not been rigorously investigated
Major findings	- BRL37344 promoted glucose uptake in skeletal muscle *in* vitro, *in* vivo and *ex* vivo - BRL37344 increased skeletal muscle glucose uptake with minimal increases in cAMP production as opposed to isoprenaline - Unlike isoprenaline, BRL37344 does not induce receptor desensitisation - Unlike the insulin signalling pathway, Akt is not involved in BRL37344 stimulated glucose uptake
Limitation	- The mechanism whereby BRL37344 increases glucose uptake is still not defined
Future direction	- The effects of BRL37344 on whole body glucose utilisation in animal models of type 2 diabetes would be important to pursue - To verify that BRL37344 increases glucose uptake independently of cAMP, and fully investigate the mechanism whereby BRL37344 increases glucose uptake
Chapter 4	
Background	- Based on Chapter 3, a cAMP independent pathway following β_2-AR stimulation to increase glucose uptake was proposed - GRKs are involved in the regulation of glucose metabolism - The role of GRK phosphorylation sites in the β_2-AR C-terminal tail on glucose uptake is not known
Major findings	- GRK phosphorylation sites in β_2-AR are important for agonist dependent receptor internalisation - These phosphorylation sites are not involved in β_2-AR mediated glucose uptake, yet siRNA directed against GRK2 abolishes β_2-AR mediated glucose uptake
Limitation	- The role of GRK itself in β_2-AR mediated glucose uptake is still not determined
Future direction	- GRK isoform recruited to the β_2-AR following agonist treatment needs to be identified - Effects of β-arrestin on β_2-AR mediated glucose uptake needs to be determined - Investigation on the role of GRK in β_2-AR mediated glucose uptake is required ie. does GRK act as a scaffolding protein, or is the kinase domain of GRK important for increasing glucose uptake instead
Chapter 5	
Background	- The α_{1A}-AR agonists A61603 and dabuzalgron produce cardioprotective effects, which may be due to effects on cardiac glucose uptake - The role of cAMP on α_{1A}-AR mediated glucose uptake is unknown
Major findings	- Dabuzalgron is full agonist for glucose uptake and p-Erk1/2, and a partial agonist for Ca^{2+} mobilization, p-S6RP, and p-NDRG1, as compared to A61603 which is a full agonist for all these pathways - cAMP might be involved in A61603 (but not dabuzalgron) mediated glucose uptake
Limitation	- It is still not clear whether dabuzalgron is a biased agonist in other cell/tissue types
Future direction	- Performing IP1 assays is required to confirm that kinetic calcium effects are not reason why dabuzalgron shows a biased effect - Cardiomyocyte should be used to examine whether bias profile is retained - Both *ex* vivo and *in* vivo studies are required to test their cardioprotective effects

6.5 A future for GPCRs/adrenoceptors in the treatment of metabolic disorders

To date, more than 30 GPCRs have been targeted for the treatment of β-cell dysfunction, insulin resistance, T2D and obesity (Riddy et al., 2018). This includes the GLP-1 receptor, where at least 6 agonists are used clinically to increase insulin secretion from the pancreas in type 2 diabetic patients. ARs ligands may also be viable options in the treatment of T2D and related co-morbidities. The results in Chapter 3 and 4 show that the β_2-AR agonist BRL37344 may be useful in promoting skeletal muscle glucose uptake in animal models, with older studies suggesting it can improve glucose homeostasis in humans (Mitchell et al., 1989). One limitation of using β_2-AR agonists therapeutically are potential on-target and off-target adverse effects in other cells/tissues, such as effects on the cardiovascular system. This could be overcome with the design of BRL37344 derivatives that are able to increase skeletal muscle glucose uptake and GLUT4 translocation with minimal effects on cAMP levels, which may minimise adverse effects in the heart. The results in Chapter 5 show that the α_{1A}-AR agonists A61603 and dabuzalgron increase glucose uptake, which may have implications in heart failure. A61603 has reported cardioprotective effects (Sato et al., 2018) and in heart failure, there is a switch in the failing heart from fatty acid as a primary source of fuel to glucose (Buchanan et al., 2005; Liu et al., 2002). Therefore, these α_{1A} -AR agonists may have their cardioprotective effects via increasing glucose uptake and utilisation in the heart, which warrants future investigation.

In addition to the α_{1A}-AR or β_2-AR, β_3-AR agonists have been proposed for the treatment of T2D. β_3-ARs are primarily expressed in brown adipose tissue to increase glucose uptake (Cannon & Nedergaard, 2004). While originally thought to be present only in small hibernating mammals, brown adipose tissue has been demonstrated in humans (Nedergaard et al., 2007), with the β_3-AR agonist mirabegron increasing brown adipose tissue glucose uptake in humans (Cypess et al., 2015). Hence, the β_3-AR is an attractive therapeutic target for T2D. Overall, the increased knowledge of AR-stimulated glucose uptake afforded by the current studies facilitates further studies in this area and contributes to the future development of effective drugs.

6.6 Concluding remarks

The work outlined in this thesis aimed to elucidate the mechanisms mediating increased glucose uptake following activation of the β_2-AR and the α_{1A}-AR. Collectively, these studies extended our knowledge of AR mediated glucose uptake and indicated the potential for developing BRL37344 or

related compounds and α_{1A}-AR selective agonists as treatments for T2D or cardiac failure complicated by insulin resistance, respectively. In the future, it will be essential to characterize the more detailed mechanisms of these drugs in glucose homeostasis, and their *in vivo* effects in mouse models of human diseases.

CHAPTER 7

References

Abbott MJ, Edelman AM, & Turcotte LP (2009). CaMKK is an upstream signal of AMP-activated protein kinase in regulation of substrate metabolism in contracting skeletal muscle. Am J Physiol Regul Integr Comp Physiol 297: R1724-1732.

Abdul-Ghani MA (2013). Type 2 diabetes and the evolving paradigm in glucose regulation. Am J Manag Care 19: S43-50.

Abdul-Ghani MA, & DeFronzo RA (2010). Pathogenesis of insulin resistance in skeletal muscle. J Biomed Biotechnol 2010: 476279.

Abe H, Minokoshi Y, & Shimazu T (1993). Effect of a β_3-adrenergic agonist, BRL35135A, on glucose uptake in rat skeletal muscle in vivo and in vitro. J Endocrinol 139: 479-486.

Aerni-Flessner L, Abi-Jaoude M, Koenig A, Payne M, & Hruz PW (2012). GLUT4, GLUT1, and GLUT8 are the dominant GLUT transcripts expressed in the murine left ventricle. Cardiovasc Diabetol 11: 63.

Aguero J, Almenar L, Monto F, Oliver E, Sanchez-Lazaro I, Vicente D, et al. (2012). Myocardial G protein receptor-coupled kinase expression correlates with functional parameters and clinical severity in advanced heart failure. J Card Fail 18: 53-61.

Aguirre V, Werner ED, Giraud J, Lee YH, Shoelson SE, & White MF (2002). Phosphorylation of Ser307 in insulin receptor substrate-1 blocks interactions with the insulin receptor and inhibits insulin action. J Biol Chem 277: 1531-1537.

Ahren B, & Lundquist I (1981). Effects of selective and non-selective β-adrenergic agents on insulin secretion in vivo. Eur J Pharmacol 71: 93-104.

Al-Hasani H, Kunamneni RK, Dawson K, Hinck CS, Muller-Wieland D, & Cushman SW (2002). Roles of the N- and C-termini of GLUT4 in endocytosis. J Cell Sci 115: 131-140.

Alvarez-Curto E, Inoue A, Jenkins L, Raihan SZ, Prihandoko R, Tobin AB, et al. (2016). Targeted Elimination of G Proteins and Arrestins Defines Their Specific Contributions to Both Intensity and Duration of G Protein-coupled Receptor Signaling. J Biol Chem 291: 27147-27159.

Amirouche A, Durieux AC, Banzet S, Koulmann N, Bonnefoy R, Mouret C, et al. (2009). Down-regulation of Akt/mammalian target of rapamycin signaling pathway in response to myostatin overexpression in skeletal muscle. Endocrinology 150: 286-294.

Antonescu CN, Huang C, Niu W, Liu Z, Eyers PA, Heidenreich KA, et al. (2005). Reduction of insulin-stimulated glucose uptake in L6 myotubes by the protein kinase inhibitor SB203580 is independent of p38MAPK activity. Endocrinology 146: 3773-3781.

Aoyama T, Matsui T, Novikov M, Park J, Hemmings B, & Rosenzweig A (2005). Serum and glucocorticoid-responsive kinase-1 regulates cardiomyocyte survival and hypertrophic response. Circulation 111: 1652-1659.

Arch JR, Ainsworth AT, Cawthorne MA, Piercy V, Sennitt MV, Thody VE, et al. (1984). Atypical β-adrenoceptor on brown adipocytes as target for anti-obesity drugs. Nature 309: 163-165.

Armstrong PW, Chiong MA, & Parker JO (1977). Effects of propranolol on the hemodynamic, coronary sinus blood flow and myocardial metabolic response to atrial pacing. Am J Cardiol 40: 83-89.

Arsham AM, Howell JJ, & Simon MC (2003). A novel hypoxia-inducible factor-independent hypoxic response regulating mammalian target of rapamycin and its targets. J Biol Chem 278**:** 29655-29660.

Asensio C, Jimenez M, Kuhne F, Rohner-Jeanrenaud F, & Muzzin P (2005). The lack of β-adrenoceptors results in enhanced insulin sensitivity in mice exhibiting increased adiposity and glucose intolerance. Diabetes 54**:** 3490-3495.

Autelitano DJ, & Woodcock EA (1998). Selective activation of α_{1A}-adrenergic receptors in neonatal cardiac myocytes is sufficient to cause hypertrophy and differential regulation of α_1-adrenergic receptor subtype mRNAs. J Mol Cell Cardiol 30**:** 1515-1523.

Avogaro A, de Kreutzenberg SV, & Fadini GP (2010). Insulin signaling and life span. Pflugers Arch 459**:** 301-314.

Babbey CM, Bacallao RL, & Dunn KW (2010). Rab10 associates with primary cilia and the exocyst complex in renal epithelial cells. Am J Physiol Renal Physiol 299**:** F495-506.

Badawi JK, Seja T, Uecelehan H, Honeck P, Kwon ST, Bross S*, et al.* (2007). Relaxation of human detrusor muscle by selective β_2 and β_3 agonists and endogenous catecholamines. Urology 69**:** 785-790.

Bakay M, Pandey R, & Hakonarson H (2013). Genes involved in type 1 diabetes: an update. Genes (Basel) 4**:** 499-521.

Baker JG (2010a). A full pharmacological analysis of the three turkey β-adrenoceptors and comparison with the human β-adrenoceptors. PLoS One 5**:** e15487.

Baker JG (2010b). The selectivity of β-adrenoceptor agonists at human β_1-, β_2- and β_3-adrenoceptors. Br J Pharmacol 160**:** 1048-1061.

Ballou LM, & Lin RZ (2008). Rapamycin and mTOR kinase inhibitors. J Chem Biol 1**:** 27-36.

Bano G (2013). Glucose homeostasis, obesity and diabetes. Best Pract Res Clin Obstet Gynaecol 27**:** 715-726.

Bartelt A, Bruns OT, Reimer R, Hohenberg H, Ittrich H, Peldschus K*, et al.* (2011). Brown adipose tissue activity controls triglyceride clearance. Nat Med 17**:** 200-205.

Basith S, Cui M, Macalino SJY, Park J, Clavio NAB, Kang S*, et al.* (2018). Exploring G Protein-Coupled Receptors (GPCRs) Ligand Space via Cheminformatics Approaches: Impact on Rational Drug Design. Front Pharmacol 9**:** 128.

Battiprolu PK, Hojayev B, Jiang N, Wang ZV, Luo X, Iglewski M*, et al.* (2012). Metabolic stress-induced activation of FoxO1 triggers diabetic cardiomyopathy in mice. J Clin Invest 122**:** 1109-1118.

Beak J, Huang W, Parker JS, Hicks ST, Patterson C, Simpson PC*, et al.* (2017). An Oral Selective α_{-1A} Adrenergic Receptor Agonist Prevents Doxorubicin Cardiotoxicity. JACC Basic Transl Sci 2**:** 39-53.

Bellacosa A, Franke TF, Gonzalez-Portal ME, Datta K, Taguchi T, Gardner J*, et al.* (1993). Structure, expression and chromosomal mapping of c-akt: relationship to v-akt and its implications. Oncogene 8**:** 745-754.

Bentzinger CF, Romanino K, Cloetta D, Lin S, Mascarenhas JB, Oliveri F, *et al.* (2008). Skeletal muscle-specific ablation of raptor, but not of rictor, causes metabolic changes and results in muscle dystrophy. Cell Metab 8**:** 411-424.

Berdeaux R, & Stewart R (2012). cAMP signaling in skeletal muscle adaptation: hypertrophy, metabolism, and regeneration. Am J Physiol Endocrinol Metab 303**:** E1-17.

Berkowitz DE, Price DT, Bello EA, Page SO, & Schwinn DA (1994). Localization of messenger RNA for three distinct α_2-adrenergic receptor subtypes in human tissues. Evidence for species heterogeneity and implications for human pharmacology. Anesthesiology 81**:** 1235-1244.

Bevan P (2001). Insulin signalling. J Cell Sci 114**:** 1429-1430.

Bjornholm M, & Zierath JR (2005). Insulin signal transduction in human skeletal muscle: identifying the defects in Type II diabetes. Biochem Soc Trans 33**:** 354-357.

Black JW, & Leff P (1983). Operational models of pharmacological agonism. Proc R Soc Lond B Biol Sci 220**:** 141-162.

Black JW, Leff P, Shankley NP, & Wood J (1985). An operational model of pharmacological agonism: the effect of E/[A] curve shape on agonist dissociation constant estimation. Br J Pharmacol 84**:** 561-571.

Blot V, & McGraw TE (2006). GLUT4 is internalized by a cholesterol-dependent nystatin-sensitive mechanism inhibited by insulin. EMBO J 25**:** 5648-5658.

Blue DR, Daniels DV, Gever JR, Jett MF, O'Yang C, Tang HM, *et al.* (2004). Pharmacological characteristics of Ro 115-1240, a selective $\alpha_{1A/1L}$-adrenoceptor partial agonist: a potential therapy for stress urinary incontinence. BJU Int 93**:** 162-170.

Board M, Doyle P, & Cawthorne MA (2000). BRL37344, but not CGP12177, stimulates fuel oxidation by soleus muscle in vitro. Eur J Pharmacol 406**:** 33-40.

Bogan JS, & Kandror KV (2010). Biogenesis and regulation of insulin-responsive vesicles containing GLUT4. Curr Opin Cell Biol 22**:** 506-512.

Bologna Z, Teoh JP, Bayoumi AS, Tang Y, & Kim IM (2017). Biased G Protein-Coupled Receptor Signaling: New Player in Modulating Physiology and Pathology. Biomol Ther (Seoul) 25**:** 12-25.

Boluyt MO, Zheng JS, Younes A, Long X, O'Neill L, Silverman H, *et al.* (1997). Rapamycin inhibits α_1-adrenergic receptor-stimulated cardiac myocyte hypertrophy but not activation of hypertrophy-associated genes. Evidence for involvement of p70 S6 kinase. Circ Res 81**:** 176-186.

Bonaldo P, & Sandri M (2013). Cellular and molecular mechanisms of muscle atrophy. Dis Model Mech 6**:** 25-39.

Boucher J, Kleinridders A, & Kahn CR (2014). Insulin receptor signaling in normal and insulin-resistant states. Cold Spring Harb Perspect Biol 6.

Bouvier M, Collins S, O'Dowd BF, Campbell PT, de Blasi A, Kobilka BK, *et al.* (1989). Two distinct pathways for cAMP-mediated down-regulation of the β_2-adrenergic receptor. Phosphorylation of the receptor and regulation of its mRNA level. J Biol Chem 264**:** 16786-16792.

Bouvier M, Hausdorff WP, De Blasi A, O'Dowd BF, Kobilka BK, Caron MG, *et al.* (1988). Removal of phosphorylation sites from the β_2-adrenergic receptor delays onset of agonist-promoted desensitization. Nature 333**:** 370-373.

Brede M, Philipp M, Knaus A, Muthig V, & Hein L (2004). α_2-adrenergic receptor subtypes - novel functions uncovered in gene-targeted mouse models. Biol Cell 96**:** 343-348.

Bristow MR (1993). Changes in myocardial and vascular receptors in heart failure. J Am Coll Cardiol 22**:** 61A-71A.

Bristow MR, Ginsburg R, Minobe W, Cubicciotti RS, Sageman WS, Lurie K*, et al.* (1982). Decreased catecholamine sensitivity and β-adrenergic-receptor density in failing human hearts. N Engl J Med 307**:** 205-211.

Bristow MR, Ginsburg R, Umans V, Fowler M, Minobe W, Rasmussen R*, et al.* (1986). β_1- and β_2-adrenergic-receptor subpopulations in nonfailing and failing human ventricular myocardium: coupling of both receptor subtypes to muscle contraction and selective β_1-receptor down-regulation in heart failure. Circ Res 59**:** 297-309.

Broad J, Maurel D, Kung VW, Hicks GA, Schemann M, Barnes MR*, et al.* (2016). Human native kappa opioid receptor functions not predicted by recombinant receptors: Implications for drug design. Sci Rep 6**:** 30797.

Buchanan J, Mazumder PK, Hu P, Chakrabarti G, Roberts MW, Yun UJ*, et al.* (2005). Reduced cardiac efficiency and altered substrate metabolism precedes the onset of hyperglycemia and contractile dysfunction in two mouse models of insulin resistance and obesity. Endocrinology 146**:** 5341-5349.

Buse MG, Robinson KA, Marshall BA, & Mueckler M (1996). Differential effects of GLUT1 or GLUT4 overexpression on hexosamine biosynthesis by muscles of transgenic mice. J Biol Chem 271**:** 23197-23202.

Bychkov E, Zurkovsky L, Garret MB, Ahmed MR, & Gurevich EV (2012). Distinct cellular and subcellular distributions of G protein-coupled receptor kinase and arrestin isoforms in the striatum. PLoS One 7**:** e48912.

Cahill TJ, 3rd, Thomsen AR, Tarrasch JT, Plouffe B, Nguyen AH, Yang F*, et al.* (2017). Distinct conformations of GPCR- β-arrestin complexes mediate desensitization, signaling, and endocytosis. Proc Natl Acad Sci U S A 114**:** 2562-2567.

Cairns SP, & Borrani F (2015). β-Adrenergic modulation of skeletal muscle contraction: key role of excitation-contraction coupling. J Physiol 593**:** 4713-4727.

Cairns SP, & Dulhunty AF (1993). The effects of β-adrenoceptor activation on contraction in isolated fast- and slow-twitch skeletal muscle fibres of the rat. Br J Pharmacol 110**:** 1133-1141.

Cannon B, & Nedergaard J (2004). Brown adipose tissue: function and physiological significance. Physiol Rev 84**:** 277-359.

Capogrossi MC, Kachadorian WA, Gambassi G, Spurgeon HA, & Lakatta EG (1991). Ca2+ dependence of α-adrenergic effects on the contractile properties and Ca2+ homeostasis of cardiac myocytes. Circ Res 69**:** 540-550.

Carriere A, Romeo Y, Acosta-Jaquez HA, Moreau J, Bonneil E, Thibault P*, et al.* (2011). ERK1/2 phosphorylate Raptor to promote Ras-dependent activation of mTOR complex 1 (mTORC1). J Biol Chem 286**:** 567-577.

Cartee GD (2015). Roles of TBC1D1 and TBC1D4 in insulin- and exercise-stimulated glucose transport of skeletal muscle. Diabetologia 58**:** 19-30.

Castets P, Lin S, Rion N, Di Fulvio S, Romanino K, Guridi M, *et al.* (2013). Sustained activation of mTORC1 in skeletal muscle inhibits constitutive and starvation-induced autophagy and causes a severe, late-onset myopathy. Cell Metab 17**:** 731-744.

Cawthorne MA, Sennitt MV, Arch JR, & Smith SA (1992). BRL 35135, a potent and selective atypical β-adrenoceptor agonist. Am J Clin Nutr 55**:** 252s-257s.

Chakrabarti S, Wang L, Tang WJ, & Gintzler AR (1998). Chronic morphine augments adenylyl cyclase phosphorylation: relevance to altered signaling during tolerance/dependence. Mol Pharmacol 54**:** 949-953.

Charron MJ, Katz EB, & Olson AL (1999). GLUT4 gene regulation and manipulation. J Biol Chem 274**:** 3253-3256.

Chaudhury A, Duvoor C, Reddy Dendi VS, Kraleti S, Chada A, Ravilla R, *et al.* (2017). Clinical Review of Antidiabetic Drugs: Implications for Type 2 Diabetes Mellitus Management. Front Endocrinol (Lausanne) 8**:** 6.

Cheatham B, Volchuk A, Kahn CR, Wang L, Rhodes CJ, & Klip A (1996). Insulin-stimulated translocation of GLUT4 glucose transporters requires SNARE-complex proteins. Proc Natl Acad Sci U S A 93**:** 15169-15173.

Cheeseman C (2008). GLUT7: a new intestinal facilitated hexose transporter. Am J Physiol Endocrinol Metab 295**:** E238-241.

Chen C, Cohrs CM, Stertmann J, Bozsak R, & Speier S (2017). Human β cell mass and function in diabetes: Recent advances in knowledge and technologies to understand disease pathogenesis. Mol Metab 6**:** 943-957.

Chen HC, Bandyopadhyay G, Sajan MP, Kanoh Y, Standaert M, Farese RV, Jr.*, et al.* (2002). Activation of the ERK pathway and atypical protein kinase C isoforms in exercise- and aminoimidazole-4-carboxamide-1-β-D-riboside (AICAR)-stimulated glucose transport. J Biol Chem 277**:** 23554-23562.

Cheng Y, & Prusoff WH (1973). Relationship between the inhibition constant (K1) and the concentration of inhibitor which causes 50 per cent inhibition (I50) of an enzymatic reaction. Biochem Pharmacol 22**:** 3099-3108.

Chernogubova E, Hutchinson DS, Nedergaard J, & Bengtsson T (2005). α_1- and β_1-Adrenoceptor signaling fully compensate for β_3-adrenoceptor deficiency in brown adipocyte norepinephrine-stimulated glucose uptake. Endocrinology 146**:** 2271-2284.

Cho H, Mu J, Kim JK, Thorvaldsen JL, Chu Q, Crenshaw EB, 3rd*, et al.* (2001). Insulin resistance and a diabetes mellitus-like syndrome in mice lacking the protein kinase Akt2 (PKB β). Science 292**:** 1728-1731.

Choi J, Chen J, Schreiber SL, & Clardy J (1996). Structure of the FKBP12-rapamycin complex interacting with the binding domain of human FRAP. Science 273**:** 239-242.

Chokshi A, Drosatos K, Cheema FH, Ji R, Khawaja T, Yu S, *et al.* (2012). Ventricular assist device implantation corrects myocardial lipotoxicity, reverses insulin resistance, and normalizes cardiac metabolism in patients with advanced heart failure. Circulation 125**:** 2844-2853.

Ciccarelli M, Chuprun JK, Rengo G, Gao E, Wei Z, Peroutka RJ*, et al.* (2011). G protein-coupled receptor kinase 2 activity impairs cardiac glucose uptake and promotes insulin resistance after myocardial ischemia. Circulation 123**:** 1953-1962.

Ciccarelli M, Cipolletta E, & Iaccarino G (2012). GRK2 at the control shaft of cellular metabolism. Curr Pharm Des 18**:** 121-127.

Clairfeuille T, Mas C, Chan AS, Yang Z, Tello-Lafoz M, Chandra M*, et al.* (2016). A molecular code for endosomal recycling of phosphorylated cargos by the SNX27-retromer complex. Nat Struct Mol Biol 23**:** 921-932.

Clark RB, Kunkel MW, Friedman J, Goka TJ, & Johnson JA (1988). Activation of cAMP-dependent protein kinase is required for heterologous desensitization of adenylyl cyclase in S49 wild-type lymphoma cells. Proc Natl Acad Sci U S A 85**:** 1442-1446.

Clegg RM (1995). Fluorescence resonance energy transfer. Curr Opin Biotechnol 6**:** 103-110.

Colciago A, Mornati O, Ferri N, Castelnovo LF, Fumagalli L, Bolchi C*, et al.* (2016). A selective α_{1D}-adrenoreceptor antagonist inhibits human prostate cancer cell proliferation and motility "in vitro". Pharmacol Res 103**:** 215-226.

Consoli A, Kennedy F, Miles J, & Gerich J (1987). Determination of Krebs cycle metabolic carbon exchange in vivo and its use to estimate the individual contributions of gluconeogenesis and glycogenolysis to overall glucose output in man. J Clin Invest 80**:** 1303-1310.

Couvineau A, Fabre C, Gaudin P, Maoret JJ, & Laburthe M (1996). Mutagenesis of N-glycosylation sites in the human vasoactive intestinal peptide 1 receptor. Evidence that asparagine 58 or 69 is crucial for correct delivery of the receptor to plasma membrane. Biochemistry 35**:** 1745-1752.

Cowley PM, Wang G, Chang AN, Makwana O, Swigart PM, Lovett DH*, et al.* (2015). The α_{1A}-adrenergic receptor subtype mediates increased contraction of failing right ventricular myocardium. Am J Physiol Heart Circ Physiol 309**:** H888-896.

Cozzone D, Frojdo S, Disse E, Debard C, Laville M, Pirola L*, et al.* (2008). Isoform-specific defects of insulin stimulation of Akt/protein kinase B (PKB) in skeletal muscle cells from type 2 diabetic patients. Diabetologia 51**:** 512-521.

Cypess AM, Weiner LS, Roberts-Toler C, Franquet Elia E, Kessler SH, Kahn PA*, et al.* (2015). Activation of human brown adipose tissue by a β_3-adrenergic receptor agonist. Cell Metab 21**:** 33-38.

D'Andrea-Merrins M, Chang L, Lam AD, Ernst SA, & Stuenkel EL (2007). Munc18c interaction with syntaxin 4 monomers and SNARE complex intermediates in GLUT4 vesicle trafficking. J Biol Chem 282**:** 16553-16566.

da Silva Junior ED, Sato M, Merlin J, Broxton N, Hutchinson DS, Ventura S*, et al.* (2017). Factors influencing biased agonism in recombinant cells expressing the human α_{1A} -adrenoceptor. Br J Pharmacol 174**:** 2318-2333.

Daaka Y, Luttrell LM, & Lefkowitz RJ (1997). Switching of the coupling of the β_2-adrenergic receptor to different G proteins by protein kinase A. Nature 390**:** 88-91.

Dan HC, Ebbs A, Pasparakis M, Van Dyke T, Basseres DS, & Baldwin AS (2014). Akt-dependent activation of mTORC1 complex involves phosphorylation of mTOR (mammalian target of rapamycin) by IkappaB kinase α (IKK α). J Biol Chem 289**:** 25227-25240.

Daneshgari F, & Moore C (2006). Diabetic uropathy. Semin Nephrol 26**:** 182-185.

Dash R, Chung J, Chan T, Yamada M, Barral J, Nishimura D*, et al.* (2011). A molecular MRI probe to detect treatment of cardiac apoptosis in vivo. Magn Reson Med 66**:** 1152-1162.

Davis E, Loiacono R, & Summers RJ (2008). The rush to adrenaline: drugs in sport acting on the β-adrenergic system. Br J Pharmacol 154**:** 584-597.

DeFronzo RA, & Tripathy D (2009). Skeletal muscle insulin resistance is the primary defect in type 2 diabetes. Diabetes Care 32 Suppl 2**:** S157-163.

Dehvari N, da silva Junior ED, Bengtsson T, & Hutchinson DS (2018). Mirabegron: potential off target effects and uses beyond the bladder. Br J Pharmacol accepted 16 Nov 2017 2017-BJP-1101-RCT-G.R1.

Dehvari N, Hutchinson DS, Nevzorova J, Dallner OS, Sato M, Kocan M*, et al.* (2012). β_2-Adrenoceptors increase translocation of GLUT4 via GPCR kinase sites in the receptor C-terminal tail. Br J Pharmacol 165**:** 1442-1456.

Depre C, Vanoverschelde JL, & Taegtmeyer H (1999). Glucose for the heart. Circulation 99**:** 578-588.

Desbuquois B, Tozzo E, Collinet M, Lopez S, Bortoli S, & Amessou M (1993). [Regulation of insulin receptor expression and its gene]. Ann Endocrinol (Paris) 54**:** 373-384.

Dimitriadis G, Mitrou P, Lambadiari V, Maratou E, & Raptis SA (2011). Insulin effects in muscle and adipose tissue. Diabetes Res Clin Pract 93 Suppl 1**:** S52-59.

Doege H, Bocianski A, Joost HG, & Schurmann A (2000). Activity and genomic organization of human glucose transporter 9 (GLUT9), a novel member of the family of sugar-transport facilitators predominantly expressed in brain and leucocytes. Biochem J 350 Pt 3**:** 771-776.

Doege H, Bocianski A, Scheepers A, Axer H, Eckel J, Joost HG*, et al.* (2001). Characterization of human glucose transporter (GLUT) 11 (encoded by SLC2A11), a novel sugar-transport facilitator specifically expressed in heart and skeletal muscle. Biochem J 359**:** 443-449.

Doenst T, Nguyen TD, & Abel ED (2013). Cardiac metabolism in heart failure: implications beyond ATP production. Circ Res 113**:** 709-724.

Domenighetti AA, Danes VR, Curl CL, Favaloro JM, Proietto J, & Delbridge LM (2010). Targeted GLUT-4 deficiency in the heart induces cardiomyocyte hypertrophy and impaired contractility linked with Ca(2+) and proton flux dysregulation. J Mol Cell Cardiol 48**:** 663-672.

Douard V, & Ferraris RP (2008). Regulation of the fructose transporter GLUT5 in health and disease. Am J Physiol Endocrinol Metab 295**:** E227-237.

Douris N, Desai BN, Fisher FM, Cisu T, Fowler AJ, Zarebidaki E*, et al.* (2017). β-adrenergic receptors are critical for weight loss but not for other metabolic adaptations to the consumption of a ketogenic diet in male mice. Mol Metab 6**:** 854-862.

Drucker DJ, Philippe J, Mojsov S, Chick WL, & Habener JF (1987). Glucagon-like peptide I stimulates insulin gene expression and increases cyclic AMP levels in a rat islet cell line. Proc Natl Acad Sci U S A 84**:** 3434-3438.

Du XJ, Gao XM, Kiriazis H, Moore XL, Ming Z, Su Y*, et al.* (2006). Transgenic α_{1A}-adrenergic activation limits post-infarct ventricular remodeling and dysfunction and improves survival. Cardiovasc Res 71**:** 735-743.

Egawa T, Hamada T, Ma X, Karaike K, Kameda N, Masuda S*, et al.* (2011). Caffeine activates preferentially α1-isoform of 5'AMP-activated protein kinase in rat skeletal muscle. Acta Physiol (Oxf) 201**:** 227-238.

El-Armouche A, & Eschenhagen T (2009). β-adrenergic stimulation and myocardial function in the failing heart. Heart Fail Rev 14**:** 225-241.

Elfellah MS, Dalling R, Kantola IM, & Reid JL (1989). β-adrenoceptors and human skeletal muscle characterisation of receptor subtype and effect of age. Br J Clin Pharmacol 27**:** 31-38.

Emorine LJ, Marullo S, Briend-Sutren MM, Patey G, Tate K, Delavier-Klutchko C*, et al.* (1989). Molecular characterization of the human β_3-adrenergic receptor. Science 245**:** 1118-1121.

Erdtmann-Vourliotis M, Mayer P, Ammon S, Riechert U, & Hollt V (2001). Distribution of G-protein-coupled receptor kinase (GRK) isoforms 2, 3, 5 and 6 mRNA in the rat brain. Brain Res Mol Brain Res 95**:** 129-137.

Essop MF (2007). Cardiac metabolic adaptations in response to chronic hypoxia. J Physiol 584**:** 715-726.

Evans BA, Broxton N, Merlin J, Sato M, Hutchinson DS, Christopoulos A*, et al.* (2011). Quantification of functional selectivity at the human α_{1A}-adrenoceptor. Mol Pharmacol 79**:** 298-307.

Evans BA, Hutchinson DS, & Summers RJ (2013). β_2-Adrenoceptor-mediated regulation of glucose uptake in skeletal muscle--ligand-directed signalling or a reflection of system complexity? Naunyn Schmiedebergs Arch Pharmacol 386**:** 757-760.

Evans BA, Papaioannou M, Bonazzi VR, & Summers RJ (1996). Expression of β_3-adrenoceptor mRNA in rat tissues. Br J Pharmacol 117**:** 210-216.

Evans BA, Sato M, Sarwar M, Hutchinson DS, & Summers RJ (2010). Ligand-directed signalling at β-adrenoceptors. Br J Pharmacol 159**:** 1022-1038.

Exton JH (1987). Mechanisms of hormonal regulation of hepatic glucose metabolism. Diabetes Metab Rev 3**:** 163-183.

Fantin VR, Wang Q, Lienhard GE, & Keller SR (2000). Mice lacking insulin receptor substrate 4 exhibit mild defects in growth, reproduction, and glucose homeostasis. Am J Physiol Endocrinol Metab 278**:** E127-133.

Ferguson SS, Downey WE, 3rd, Colapietro AM, Barak LS, Menard L, & Caron MG (1996). Role of β-arrestin in mediating agonist-promoted G protein-coupled receptor internalization. Science 271**:** 363-366.

Ferguson SS, Menard L, Barak LS, Koch WJ, Colapietro AM, & Caron MG (1995). Role of phosphorylation in agonist-promoted β_2-adrenergic receptor sequestration. Rescue of a sequestration-defective mutant receptor by β ARK1. J Biol Chem 270**:** 24782-24789.

Fingar DC, Salama S, Tsou C, Harlow E, & Blenis J (2002). Mammalian cell size is controlled by mTOR and its downstream targets S6K1 and 4EBP1/eIF4E. Genes Dev 16**:** 1472-1487.

Fischer Y, Thomas J, Sevilla L, Munoz P, Becker C, Holman G, *et al.* (1997). Insulin-induced recruitment of glucose transporter 4 (GLUT4) and GLUT1 in isolated rat cardiac myocytes. Evidence of the existence of different intracellular GLUT4 vesicle populations. J Biol Chem 272**:** 7085-7092.

Flatman JA, & Clausen T (1979). Combined effects of adrenaline and insulin on active electrogenic Na+-K+ transport in rat soleus muscle. Nature 281**:** 580-581.

Fletcher LM, Welsh GI, Oatey PB, & Tavare JM (2000). Role for the microtubule cytoskeleton in GLUT4 vesicle trafficking and in the regulation of insulin-stimulated glucose uptake. Biochem J 352 Pt 2**:** 267-276.

Foley K, Boguslavsky S, & Klip A (2011). Endocytosis, recycling, and regulated exocytosis of glucose transporter 4. Biochemistry 50**:** 3048-3061.

Fredericks ZL, Pitcher JA, & Lefkowitz RJ (1996). Identification of the G protein-coupled receptor kinase phosphorylation sites in the human β_2-adrenergic receptor. J Biol Chem 271**:** 13796-13803.

Fredriksson R, Lagerstrom MC, Lundin LG, & Schioth HB (2003). The G-protein-coupled receptors in the human genome form five main families. Phylogenetic analysis, paralogon groups, and fingerprints. Mol Pharmacol 63**:** 1256-1272.

Freedman NJ, & Lefkowitz RJ (2004). Anti- β_1-adrenergic receptor antibodies and heart failure: causation, not just correlation. J Clin Invest 113**:** 1379-1382.

Frias JP, Bastyr EJ, 3rd, Vignati L, Tschop MH, Schmitt C, Owen K, *et al.* (2017). The Sustained Effects of a Dual GIP/GLP-1 Receptor Agonist, NNC0090-2746, in Patients with Type 2 Diabetes. Cell Metab 26**:** 343-352 e342.

Frias JP, Nauck MA, Van J, Kutner ME, Cui X, Benson C, *et al.* (2018). Efficacy and safety of LY3298176, a novel dual GIP and GLP-1 receptor agonist, in patients with type 2 diabetes: a randomised, placebo-controlled and active comparator-controlled phase 2 trial. Lancet.

Frojdo S, Vidal H, & Pirola L (2009). Alterations of insulin signaling in type 2 diabetes: a review of the current evidence from humans. Biochim Biophys Acta 1792**:** 83-92.

Fu Q, Xu B, Parikh D, Cervantes D, & Xiang YK (2015). Insulin induces IRS2-dependent and GRK2-mediated β_2AR internalization to attenuate βAR signaling in cardiomyocytes. Cell Signal 27**:** 707-715.

Fujita H, Hatakeyama H, Watanabe TM, Sato M, Higuchi H, & Kanzaki M (2010). Identification of three distinct functional sites of insulin-mediated GLUT4 trafficking in adipocytes using quantitative single molecule imaging. Mol Biol Cell 21**:** 2721-2731.

Furukawa K, Rosario DJ, Smith DJ, Chapple CR, Uchiyama T, & Chess-Williams R (1995). α_{1A}-adrenoceptor-mediated contractile responses of the human vas deferens. Br J Pharmacol 116**:** 1605-1610.

Gage RM, Kim KA, Cao TT, & von Zastrow M (2001). A transplantable sorting signal that is sufficient to mediate rapid recycling of G protein-coupled receptors. J Biol Chem 276**:** 44712-44720.

Gan X, Wang J, Su B, & Wu D (2011). Evidence for direct activation of mTORC2 kinase activity by phosphatidylinositol 3,4,5-trisphosphate. J Biol Chem 286**:** 10998-11002.

Garcia-Guerra L, Nieto-Vazquez I, Vila-Bedmar R, Jurado-Pueyo M, Zalba G, Diez J, *et al.* (2010). G protein-coupled receptor kinase 2 plays a relevant role in insulin resistance and obesity. Diabetes 59**:** 2407-2417.

Garcia-Guerra L, Vila-Bedmar R, Carrasco-Rando M, Cruces-Sande M, Martin M, Ruiz-Gomez A, *et al.* (2014). Skeletal muscle myogenesis is regulated by G protein-coupled receptor kinase 2. J Mol Cell Biol 6**:** 299-311.

Garcia-Martinez JM, Moran J, Clarke RG, Gray A, Cosulich SC, Chresta CM, *et al.* (2009). Ku-0063794 is a specific inhibitor of the mammalian target of rapamycin (mTOR). Biochem J 421**:** 29-42.

Garofalo RS, Orena SJ, Rafidi K, Torchia AJ, Stock JL, Hildebrandt AL, *et al.* (2003). Severe diabetes, age-dependent loss of adipose tissue, and mild growth deficiency in mice lacking Akt2/PKB β. J Clin Invest 112**:** 197-208.

George S, Rochford JJ, Wolfrum C, Gray SL, Schinner S, Wilson JC, *et al.* (2004). A family with severe insulin resistance and diabetes due to a mutation in AKT2. Science 304**:** 1325-1328.

Ghanouni P, Gryczynski Z, Steenhuis JJ, Lee TW, Farrens DL, Lakowicz JR, *et al.* (2001a). Functionally different agonists induce distinct conformations in the G protein coupling domain of the β_2 adrenergic receptor. J Biol Chem 276**:** 24433-24436.

Ghanouni P, Steenhuis JJ, Farrens DL, & Kobilka BK (2001b). Agonist-induced conformational changes in the G-protein-coupling domain of the β_2 adrenergic receptor. Proc Natl Acad Sci U S A 98**:** 5997-6002.

Gharbi SI, Zvelebil MJ, Shuttleworth SJ, Hancox T, Saghir N, Timms JF, *et al.* (2007). Exploring the specificity of the PI3K family inhibitor LY294002. Biochem J 404**:** 15-21.

Gibbs EM, Stock JL, McCoid SC, Stukenbrok HA, Pessin JE, Stevenson RW, *et al.* (1995). Glycemic improvement in diabetic db/db mice by overexpression of the human insulin-regulatable glucose transporter (GLUT4). J Clin Invest 95**:** 1512-1518.

Giovannitti JA, Jr., Thoms SM, & Crawford JJ (2015). α_2 adrenergic receptor agonists: a review of current clinical applications. Anesth Prog 62**:** 31-39.

Glidden EJ, Gray LG, Vemuru S, Li D, Harris TE, & Mayo MW (2012). Multiple site acetylation of Rictor stimulates mammalian target of rapamycin complex 2 (mTORC2)-dependent phosphorylation of Akt protein. J Biol Chem 287**:** 581-588.

Goodman OB, Jr., Krupnick JG, Santini F, Gurevich VV, Penn RB, Gagnon AW, *et al.* (1996). β-arrestin acts as a clathrin adaptor in endocytosis of the β_2-adrenergic receptor. Nature 383**:** 447-450.

Gordan R, Gwathmey JK, & Xie LH (2015). Autonomic and endocrine control of cardiovascular function. World J Cardiol 7**:** 204-214.

Gormand A, Henriksson E, Strom K, Jensen TE, Sakamoto K, & Goransson O (2011). Regulation of AMP-activated protein kinase by LKB1 and CaMKK in adipocytes. J Cell Biochem 112**:** 1364-1375.

Granneman JG, Lahners KN, & Chaudhry A (1991). Molecular cloning and expression of the rat β_3-adrenergic receptor. Mol Pharmacol 40**:** 895-899.

Gros J, Gerhardt CC, & Strosberg AD (1999). Expression of human β_3-adrenergic receptor induces adipocyte-like features in CHO/K1 fibroblasts. J Cell Sci 112 (Pt 21)**:** 3791-3797.

Guilherme A, Emoto M, Buxton JM, Bose S, Sabini R, Theurkauf WE*, et al.* (2000). Perinuclear localization and insulin responsiveness of GLUT4 requires cytoskeletal integrity in 3T3-L1 adipocytes. J Biol Chem 275**:** 38151-38159.

Guillet-Deniau I, Leturque A, & Girard J (1994). Expression and cellular localization of glucose transporters (GLUT1, GLUT3, GLUT4) during differentiation of myogenic cells isolated from rat foetuses. J Cell Sci 107 (Pt 3)**:** 487-496.

Gundry J, Glenn R, Alagesan P, & Rajagopal S (2017). A Practical Guide to Approaching Biased Agonism at G Protein Coupled Receptors. Front Neurosci 11**:** 17.

Gunton JE, Cheung NW, Davis TM, Zoungas S, Colagiuri S, & Australian Diabetes S (2014). A new blood glucose management algorithm for type 2 diabetes: a position statement of the Australian Diabetes Society. Med J Aust 201**:** 650-653.

Gurevich EV, Tesmer JJ, Mushegian A, & Gurevich VV (2012). G protein-coupled receptor kinases: more than just kinases and not only for GPCRs. Pharmacol Ther 133**:** 40-69.

Hahn-Windgassen A, Nogueira V, Chen CC, Skeen JE, Sonenberg N, & Hay N (2005). Akt activates the mammalian target of rapamycin by regulating cellular ATP level and AMPK activity. J Biol Chem 280**:** 32081-32089.

Halls ML, & Canals M (2018). Genetically Encoded FRET Biosensors to Illuminate Compartmentalised GPCR Signalling. Trends Pharmacol Sci 39**:** 148-157.

Halls ML, & Cooper DM (2011). Regulation by Ca2+-signaling pathways of adenylyl cyclases. Cold Spring Harb Perspect Biol 3**:** a004143.

Halls ML, Poole DP, Ellisdon AM, Nowell CJ, & Canals M (2015). Detection and quantification of intracellular signaling using FRET-based biosensors and high content imaging. Methods Mol Biol 1335**:** 131-161.

Haney PM, Levy MA, Strube MS, & Mueckler M (1995). Insulin-sensitive targeting of the GLUT4 glucose transporter in L6 myoblasts is conferred by its COOH-terminal cytoplasmic tail. J Cell Biol 129**:** 641-658.

Hausdorff WP, Bouvier M, O'Dowd BF, Irons GP, Caron MG, & Lefkowitz RJ (1989). Phosphorylation sites on two domains of the β_2-adrenergic receptor are involved in distinct pathways of receptor desensitization. J Biol Chem 264**:** 12657-12665.

Hausdorff WP, Campbell PT, Ostrowski J, Yu SS, Caron MG, & Lefkowitz RJ (1991). A small region of the β-adrenergic receptor is selectively involved in its rapid regulation. Proc Natl Acad Sci U S A 88**:** 2979-2983.

Hiles ID, Otsu M, Volinia S, Fry MJ, Gout I, Dhand R*, et al.* (1992). Phosphatidylinositol 3-kinase: structure and expression of the 110 kd catalytic subunit. Cell 70**:** 419-429.

Hollenga C, & Zaagsma J (1989). Direct evidence for the atypical nature of functional β-adrenoceptors in rat adipocytes. Br J Pharmacol 98**:** 1420-1424.

Holloszy JO, & Narahara HT (1967). Enhanced permeability to sugar associated with muscle contraction. Studies of the role of Ca++. J Gen Physiol 50**:** 551-562.

Homan KT, & Tesmer JJ (2014). Structural insights into G protein-coupled receptor kinase function. Curr Opin Cell Biol 27**:** 25-31.

Howell JJ, Ricoult SJ, Ben-Sahra I, & Manning BD (2013). A growing role for mTOR in promoting anabolic metabolism. Biochem Soc Trans 41**:** 906-912.

Hribal ML, Tornei F, Pujol A, Menghini R, Barcaroli D, Lauro D*, et al.* (2008). Transgenic mice overexpressing human G972R IRS-1 show impaired insulin action and insulin secretion. J Cell Mol Med 12**:** 2096-2106.

Huang BP, Wang Y, Wang X, Wang Z, & Proud CG (2009). Blocking eukaryotic initiation factor 4F complex formation does not inhibit the mTORC1-dependent activation of protein synthesis in cardiomyocytes. Am J Physiol Heart Circ Physiol 296**:** H505-514.

Huang C, Thirone AC, Huang X, & Klip A (2005a). Differential contribution of insulin receptor substrates 1 versus 2 to insulin signaling and glucose uptake in l6 myotubes. J Biol Chem 280**:** 19426-19435.

Huang J, Imamura T, Babendure JL, Lu JC, & Olefsky JM (2005b). Disruption of microtubules ablates the specificity of insulin signaling to GLUT4 translocation in 3T3-L1 adipocytes. J Biol Chem 280**:** 42300-42306.

Huang K, & Fingar DC (2014). Growing knowledge of the mTOR signaling network. Semin Cell Dev Biol 36**:** 79-90.

Huang Y, Wright CD, Merkwan CL, Baye NL, Liang Q, Simpson PC*, et al.* (2007). An α_{1A}-adrenergic-extracellular signal-regulated kinase survival signaling pathway in cardiac myocytes. Circulation 115**:** 763-772.

Hullmann JE, Grisanti LA, Makarewich CA, Gao E, Gold JI, Chuprun JK*, et al.* (2014). GRK5-mediated exacerbation of pathological cardiac hypertrophy involves facilitation of nuclear NFAT activity. Circ Res 115**:** 976-985.

Hung CM, Garcia-Haro L, Sparks CA, & Guertin DA (2012). mTOR-dependent cell survival mechanisms. Cold Spring Harb Perspect Biol 4.

Hurley RL, Anderson KA, Franzone JM, Kemp BE, Means AR, & Witters LA (2005). The Ca2+/calmodulin-dependent protein kinase kinases are AMP-activated protein kinase kinases. J Biol Chem 280**:** 29060-29066.

Hutchinson DS, & Bengtsson T (2005). α_{1A}-adrenoceptors activate glucose uptake in L6 muscle cells through a phospholipase C-, phosphatidylinositol-3 kinase-, and atypical protein kinase C-dependent pathway. Endocrinology 146**:** 901-912.

Hutchinson DS, & Bengtsson T (2006). AMP-activated protein kinase activation by adrenoceptors in L6 skeletal muscle cells: mediation by α_1-adrenoceptors causing glucose uptake. Diabetes 55**:** 682-690.

Hutchinson DS, Summers RJ, & Bengtsson T (2008). Regulation of AMP-activated protein kinase activity by G-protein coupled receptors: potential utility in treatment of diabetes and heart disease. Pharmacol Ther 119**:** 291-310.

Iseli TJ, Walter M, van Denderen BJ, Katsis F, Witters LA, Kemp BE*, et al.* (2005). AMP-activated protein kinase β subunit tethers α and γ subunits via its C-terminal sequence (186-270). J Biol Chem 280**:** 13395-13400.

Ishiki M, Randhawa VK, Poon V, Jebailey L, & Klip A (2005). Insulin regulates the membrane arrival, fusion, and C-terminal unmasking of glucose transporter-4 via distinct phosphoinositides. J Biol Chem 280**:** 28792-28802.

Iwai-Kanai E, Hasegawa K, Araki M, Kakita T, Morimoto T, & Sasayama S (1999). α- and β-adrenergic pathways differentially regulate cell type-specific apoptosis in rat cardiac myocytes. Circulation 100**:** 305-311.

Jacinto E, Loewith R, Schmidt A, Lin S, Ruegg MA, Hall A, *et al.* (2004). Mammalian TOR complex 2 controls the actin cytoskeleton and is rapamycin insensitive. Nat Cell Biol 6**:** 1122-1128.

Jacobowitz O, & Iyengar R (1994). Phorbol ester-induced stimulation and phosphorylation of adenylyl cyclase 2. Proc Natl Acad Sci U S A 91**:** 10630-10634.

James DE, Brown R, Navarro J, & Pilch PF (1988). Insulin-regulatable tissues express a unique insulin-sensitive glucose transport protein. Nature 333**:** 183-185.

Jensen BC, O'Connell TD, & Simpson PC (2011a). α_1-adrenergic receptors: targets for agonist drugs to treat heart failure. J Mol Cell Cardiol 51**:** 518-528.

Jensen BC, O'Connell TD, & Simpson PC (2014). α_1-adrenergic receptors in heart failure: the adaptive arm of the cardiac response to chronic catecholamine stimulation. J Cardiovasc Pharmacol 63**:** 291-301.

Jensen BC, Swigart PM, De Marco T, Hoopes C, & Simpson PC (2009a). α_1-Adrenergic receptor subtypes in nonfailing and failing human myocardium. Circ Heart Fail 2**:** 654-663.

Jensen BC, Swigart PM, Laden ME, DeMarco T, Hoopes C, & Simpson PC (2009b). The α_{1D} Is the predominant α_1-adrenergic receptor subtype in human epicardial coronary arteries. J Am Coll Cardiol 54**:** 1137-1145.

Jensen BC, Swigart PM, Montgomery MD, & Simpson PC (2010). Functional α_{-1B} adrenergic receptors on human epicardial coronary artery endothelial cells. Naunyn Schmiedebergs Arch Pharmacol 382**:** 475-482.

Jensen J, Brors O, & Dahl HA (1995). Different β-adrenergic receptor density in different rat skeletal muscle fibre types. Pharmacol Toxicol 76**:** 380-385.

Jensen J, Rustad PI, Kolnes AJ, & Lai YC (2011b). The role of skeletal muscle glycogen breakdown for regulation of insulin sensitivity by exercise. Front Physiol 2**:** 112.

Jensen TE, Rose AJ, Hellsten Y, Wojtaszewski JF, & Richter EA (2007). Caffeine-induced Ca(2+) release increases AMPK-dependent glucose uptake in rodent soleus muscle. Am J Physiol Endocrinol Metab 293**:** E286-292.

Jiang ZY, Zhou QL, Coleman KA, Chouinard M, Boese Q, & Czech MP (2003). Insulin signaling through Akt/protein kinase B analyzed by small interfering RNA-mediated gene silencing. Proc Natl Acad Sci U S A 100**:** 7569-7574.

Jimenez-Sainz MC, Murga C, Kavelaars A, Jurado-Pueyo M, Krakstad BF, Heijnen CJ, *et al.* (2006). G protein-coupled receptor kinase 2 negatively regulates chemokine signaling at a level downstream from G protein subunits. Mol Biol Cell 17**:** 25-31.

Jones PF, Jakubowicz T, Pitossi FJ, Maurer F, & Hemmings BA (1991). Molecular cloning and identification of a serine/threonine protein kinase of the second-messenger subfamily. Proc Natl Acad Sci U S A 88**:** 4171-4175.

Jones SW, Baker DJ, & Greenhaff PL (2003). G protein-coupled receptor kinases 2 and 5 are differentially expressed in rat skeletal muscle and remain unchanged following β2-agonist administration. Exp Physiol 88: 277-284.

Kahn CR (1994). Banting Lecture. Insulin action, diabetogenes, and the cause of type II diabetes. Diabetes 43: 1066-1084.

Kamimura Y, Xiong Y, Iglesias PA, Hoeller O, Bolourani P, & Devreotes PN (2008). PIP3-independent activation of TorC2 and PKB at the cell's leading edge mediates chemotaxis. Curr Biol 18: 1034-1043.

Kanai F, Nishioka Y, Hayashi H, Kamohara S, Todaka M, & Ebina Y (1993). Direct demonstration of insulin-induced GLUT4 translocation to the surface of intact cells by insertion of a c-myc epitope into an exofacial GLUT4 domain. J Biol Chem 268: 14523-14526.

Kao AW, Ceresa BP, Santeler SR, & Pessin JE (1998). Expression of a dominant interfering dynamin mutant in 3T3L1 adipocytes inhibits GLUT4 endocytosis without affecting insulin signaling. J Biol Chem 273: 25450-25457.

Kasuga M, Karlsson FA, & Kahn CR (1982). Insulin stimulates the phosphorylation of the 95,000-dalton subunit of its own receptor. Science 215: 185-187.

Katz A, Broberg S, Sahlin K, & Wahren J (1986). Leg glucose uptake during maximal dynamic exercise in humans. Am J Physiol 251: E65-70.

Katz AM (1998). Evolving concepts of heart failure: cooling furnace, malfunctioning pump, enlarging muscle. Part II: Hypertrophy and dilatation of the failing heart. J Card Fail 4: 67-81.

Katz LB, Gambale JJ, Rothenberg PL, Vanapalli SR, Vaccaro N, Xi L, *et al.* (2012). Effects of JNJ-38431055, a novel GPR119 receptor agonist, in randomized, double-blind, placebo-controlled studies in subjects with type 2 diabetes. Diabetes Obes Metab 14: 709-716.

Kawabe J, Iwami G, Ebina T, Ohno S, Katada T, Ueda Y, *et al.* (1994). Differential activation of adenylyl cyclase by protein kinase C isoenzymes. J Biol Chem 269: 16554-16558.

Kebede M, Alquier T, Latour MG, Semache M, Tremblay C, & Poitout V (2008). The fatty acid receptor GPR40 plays a role in insulin secretion in vivo after high-fat feeding. Diabetes 57: 2432-2437.

Kelly P, Casey PJ, & Meigs TE (2007). Biologic functions of the G12 subfamily of heterotrimeric g proteins: growth, migration, and metastasis. Biochemistry 46: 6677-6687.

Kenakin T, & Christopoulos A (2013). Signalling bias in new drug discovery: detection, quantification and therapeutic impact. Nat Rev Drug Discov 12: 205-216.

Kenny BA, Miller AM, Williamson IJ, O'Connell J, Chalmers DH, & Naylor AM (1996). Evaluation of the pharmacological selectivity profile of α_1 adrenoceptor antagonists at prostatic α_1 adrenoceptors: binding, functional and in vivo studies. Br J Pharmacol 118: 871-878.

Keppler A, Gendreizig S, Gronemeyer T, Pick H, Vogel H, & Johnsson K (2003). A general method for the covalent labeling of fusion proteins with small molecules in vivo. Nat Biotechnol 21: 86-89.

Keppler A, Pick H, Arrivoli C, Vogel H, & Johnsson K (2004). Labeling of fusion proteins with synthetic fluorophores in live cells. Proc Natl Acad Sci U S A 101: 9955-9959.

Khamzina L, Veilleux A, Bergeron S, & Marette A (2005). Increased activation of the mammalian target of rapamycin pathway in liver and skeletal muscle of obese rats: possible involvement in obesity-linked insulin resistance. Endocrinology 146**:** 1473-1481.

Kilpatrick LE, Humphrys LJ, & Holliday ND (2015). A G protein-coupled receptor dimer imaging assay reveals selectively modified pharmacology of neuropeptide Y Y1/Y5 receptor heterodimers. Mol Pharmacol 87**:** 718-732.

Klein Herenbrink C, Sykes DA, Donthamsetti P, Canals M, Coudrat T, Shonberg J*, et al.* (2016). The role of kinetic context in apparent biased agonism at GPCRs. Nat Commun 7**:** 10842.

Knepper SM, Buckner SA, Brune ME, DeBernardis JF, Meyer MD, & Hancock AA (1995). A-61603, a potent α_1-adrenergic receptor agonist, selective for the α1A receptor subtype. J Pharmacol Exp Ther 274**:** 97-103.

Kocan M, Dalrymple MB, Seeber RM, Feldman BJ, & Pfleger KD (2010). Enhanced BRET Technology for the Monitoring of Agonist-Induced and Agonist-Independent Interactions between GPCRs and β-Arrestins. Front Endocrinol (Lausanne) 1**:** 12.

Kocan M, & Pfleger KD (2011). Study of GPCR-protein interactions by BRET. Methods Mol Biol 746**:** 357-371.

Kocan M, See HB, Seeber RM, Eidne KA, & Pfleger KD (2008). Demonstration of improvements to the bioluminescence resonance energy transfer (BRET) technology for the monitoring of G protein-coupled receptors in live cells. J Biomol Screen 13**:** 888-898.

Koch WJ, Inglese J, Stone WC, & Lefkowitz RJ (1993). The binding site for the βγ subunits of heterotrimeric G proteins on the β-adrenergic receptor kinase. J Biol Chem 268**:** 8256-8260.

Kochl R, Alken M, Rutz C, Krause G, Oksche A, Rosenthal W*, et al.* (2002). The signal peptide of the G protein-coupled human endothelin B receptor is necessary for translocation of the N-terminal tail across the endoplasmic reticulum membrane. J Biol Chem 277**:** 16131-16138.

Kolwicz SC, Jr., & Tian R (2011). Glucose metabolism and cardiac hypertrophy. Cardiovasc Res 90**:** 194-201.

Kotliar N, & Pilch PF (1992). Expression of the glucose transporter isoform GLUT 4 is insufficient to confer insulin-regulatable hexose uptake to cultured muscle cells. Mol Endocrinol 6**:** 337-345.

Krasel C, Bunemann M, Lorenz K, & Lohse MJ (2005). β-arrestin binding to the β_2-adrenergic receptor requires both receptor phosphorylation and receptor activation. J Biol Chem 280**:** 9528-9535.

Kroeze WK, Sheffler DJ, & Roth BL (2003). G-protein-coupled receptors at a glance. J Cell Sci 116**:** 4867-4869.

Kumar A, Harris TE, Keller SR, Choi KM, Magnuson MA, & Lawrence JC, Jr. (2008). Muscle-specific deletion of rictor impairs insulin-stimulated glucose transport and enhances Basal glycogen synthase activity. Mol Cell Biol 28**:** 61-70.

Kumar A, Lawrence JC, Jr., Jung DY, Ko HJ, Keller SR, Kim JK*, et al.* (2010). Fat cell-specific ablation of rictor in mice impairs insulin-regulated fat cell and whole-body glucose and lipid metabolism. Diabetes 59**:** 1397-1406.

Kunapuli P, & Benovic JL (1993). Cloning and expression of GRK5: a member of the G protein-coupled receptor kinase family. Proc Natl Acad Sci U S A 90**:** 5588-5592.

Kuo IY, & Ehrlich BE (2015). Signaling in muscle contraction. Cold Spring Harb Perspect Biol 7**:** a006023.

Lacey RJ, Berrow NS, Scarpello JH, & Morgan NG (1991). Selective stimulation of glucagon secretion by β_2-adrenoceptors in isolated islets of Langerhans of the rat. Br J Pharmacol 103**:** 1824-1828.

Lai HL, Yang TH, Messing RO, Ching YH, Lin SC, & Chern Y (1997). Protein kinase C inhibits adenylyl cyclase type VI activity during desensitization of the A2a-adenosine receptor-mediated cAMP response. J Biol Chem 272**:** 4970-4977.

Lambadiari V, Triantafyllou K, & Dimitriadis GD (2015). Insulin action in muscle and adipose tissue in type 2 diabetes: The significance of blood flow. World J Diabetes 6**:** 626-633.

Lambert DG, & Thomas GD (2005). α-Adrenoceptor constrictor responses and their modulation in slow-twitch and fast-twitch mouse skeletal muscle. J Physiol 563**:** 821-829.

Lamming DW, Ye L, Katajisto P, Goncalves MD, Saitoh M, Stevens DM*, et al.* (2012). Rapamycin-induced insulin resistance is mediated by mTORC2 loss and uncoupled from longevity. Science 335**:** 1638-1643.

Langin D, Portillo MP, Saulnier-Blache JS, & Lafontan M (1991). Coexistence of three β-adrenoceptor subtypes in white fat cells of various mammalian species. Eur J Pharmacol 199**:** 291-301.

Laplante M, & Sabatini DM (2009). mTOR signaling at a glance. J Cell Sci 122**:** 3589-3594.

Laplante M, & Sabatini DM (2012). mTOR signaling in growth control and disease. Cell 149**:** 274-293.

Laporte SA, Oakley RH, Holt JA, Barak LS, & Caron MG (2000). The interaction of β-arrestin with the AP-2 adaptor is required for the clustering of β_2-adrenergic receptor into clathrin-coated pits. J Biol Chem 275**:** 23120-23126.

Laustsen PG, Michael MD, Crute BE, Cohen SE, Ueki K, Kulkarni RN*, et al.* (2002). Lipoatrophic diabetes in Irs1(-/-)/Irs3(-/-) double knockout mice. Genes Dev 16**:** 3213-3222.

Lee MH, Appleton KM, Strungs EG, Kwon JY, Morinelli TA, Peterson YK*, et al.* (2016). The conformational signature of β-arrestin2 predicts its trafficking and signalling functions. Nature 531**:** 665-668.

Lee PG, & Halter JB (2017). The Pathophysiology of Hyperglycemia in Older Adults: Clinical Considerations. Diabetes Care 40**:** 444-452.

Lefort N, St-Amand E, Morasse S, Cote CH, & Marette A (2008). The α-subunit of AMPK is essential for submaximal contraction-mediated glucose transport in skeletal muscle in vitro. Am J Physiol Endocrinol Metab 295**:** E1447-1454.

Lepor H, Tang R, Meretyk S, & Shapiro E (1993). α_1 adrenoceptor subtypes in the human prostate. J Urol 149**:** 640-642.

Liao R, Jain M, Cui L, D'Agostino J, Aiello F, Luptak I*, et al.* (2002). Cardiac-specific overexpression of GLUT1 prevents the development of heart failure attributable to pressure overload in mice. Circulation 106**:** 2125-2131.

Liggett SB, Bouvier M, Hausdorff WP, O'Dowd B, Caron MG, & Lefkowitz RJ (1989). Altered patterns of agonist-stimulated cAMP accumulation in cells expressing mutant β_2-adrenergic receptors lacking phosphorylation sites. Mol Pharmacol 36**:** 641-646.

Lindquist JM, Fredriksson JM, Rehnmark S, Cannon B, & Nedergaard J (2000). β_3- and α_1-adrenergic Erk1/2 activation is Src- but not Gi-mediated in Brown adipocytes. J Biol Chem 275**:** 22670-22677.

Lindskog C, Linne J, Fagerberg L, Hallstrom BM, Sundberg CJ, Lindholm M*, et al.* (2015). The human cardiac and skeletal muscle proteomes defined by transcriptomics and antibody-based profiling. BMC Genomics 16**:** 475.

Lionetti V, Stanley WC, & Recchia FA (2011). Modulating fatty acid oxidation in heart failure. Cardiovasc Res 90**:** 202-209.

Liu JJ, Horst R, Katritch V, Stevens RC, & Wuthrich K (2012). Biased signaling pathways in β_2-adrenergic receptor characterized by ^{19}F-NMR. Science 335**:** 1106-1110.

Liu LB, Omata W, Kojima I, & Shibata H (2007). The SUMO conjugating enzyme Ubc9 is a regulator of GLUT4 turnover and targeting to the insulin-responsive storage compartment in 3T3-L1 adipocytes. Diabetes 56**:** 1977-1985.

Liu ML, Gibbs EM, McCoid SC, Milici AJ, Stukenbrok HA, McPherson RK*, et al.* (1993). Transgenic mice expressing the human GLUT4/muscle-fat facilitative glucose transporter protein exhibit efficient glycemic control. Proc Natl Acad Sci U S A 90**:** 11346-11350.

Liu P, Gan W, Chin YR, Ogura K, Guo J, Zhang J*, et al.* (2015). PtdIns(3,4,5)P3-Dependent Activation of the mTORC2 Kinase Complex. Cancer Discov 5**:** 1194-1209.

Liu Q, Docherty JC, Rendell JC, Clanachan AS, & Lopaschuk GD (2002). High levels of fatty acids delay the recovery of intracellular pH and cardiac efficiency in post-ischemic hearts by inhibiting glucose oxidation. J Am Coll Cardiol 39**:** 718-725.

Liu S, Premont RT, Kontos CD, Zhu S, & Rockey DC (2005). A crucial role for GRK2 in regulation of endothelial cell nitric oxide synthase function in portal hypertension. Nat Med 11**:** 952-958.

Liu YL, Cawthorne MA, & Stock MJ (1996). Biphasic effects of the β-adrenoceptor agonist, BRL 37344, on glucose utilization in rat isolated skeletal muscle. Br J Pharmacol 117**:** 1355-1361.

Liu YL, & Stock MJ (1995). Acute effects of the β_3-adrenoceptor agonist, BRL 35135, on tissue glucose utilisation. Br J Pharmacol 114**:** 888-894.

Livingstone C, James DE, Rice JE, Hanpeter D, & Gould GW (1996). Compartment ablation analysis of the insulin-responsive glucose transporter (GLUT4) in 3T3-L1 adipocytes. Biochem J 315 (Pt 2)**:** 487-495.

Lohse MJ, Engelhardt S, & Eschenhagen T (2003). What is the role of β-adrenergic signaling in heart failure? Circ Res 93**:** 896-906.

Lopaschuk GD, Ussher JR, Folmes CD, Jaswal JS, & Stanley WC (2010). Myocardial fatty acid metabolism in health and disease. Physiol Rev 90**:** 207-258.

Lopez JA, Burchfield JG, Blair DH, Mele K, Ng Y, Vallotton P*, et al.* (2009). Identification of a distal GLUT4 trafficking event controlled by actin polymerization. Mol Biol Cell 20**:** 3918-3929.

Lu Z, & Xu S (2006). ERK1/2 MAP kinases in cell survival and apoptosis. IUBMB Life 58**:** 621-631.

Luo J, Sobkiw CL, Hirshman MF, Logsdon MN, Li TQ, Goodyear LJ*, et al.* (2006). Loss of class IA PI3K signaling in muscle leads to impaired muscle growth, insulin response, and hyperlipidemia. Cell Metab 3**:** 355-366.

Luttrell LM, Ferguson SS, Daaka Y, Miller WE, Maudsley S, Della Rocca GJ*, et al.* (1999). β-arrestin-dependent formation of β_2 adrenergic receptor-Src protein kinase complexes. Science 283**:** 655-661.

Luttrell LM, & Lefkowitz RJ (2002). The role of β-arrestins in the termination and transduction of G-protein-coupled receptor signals. J Cell Sci 115**:** 455-465.

Luttrell LM, Maudsley S, & Bohn LM (2015). Fulfilling the Promise of "Biased" G Protein-Coupled Receptor Agonism. Mol Pharmacol 88**:** 579-588.

Lymperopoulos A, Rengo G, & Koch WJ (2013). Adrenergic nervous system in heart failure: pathophysiology and therapy. Circ Res 113**:** 739-753.

Lynch GS, Schertzer JD, & Ryall JG (2007). Therapeutic approaches for muscle wasting disorders. Pharmacol Ther 113**:** 461-487.

Lyssenko V, & Laakso M (2013). Genetic screening for the risk of type 2 diabetes: worthless or valuable? Diabetes Care 36 Suppl 2**:** S120-126.

Madamanchi A (2007). β-adrenergic receptor signaling in cardiac function and heart failure. Mcgill J Med 10**:** 99-104.

Manara L, Badone D, Baroni M, Boccardi G, Cecchi R, Croci T*, et al.* (1996). Functional identification of rat atypical β-adrenoceptors by the first β_3-selective antagonists, aryloxypropanolaminotetralins. Br J Pharmacol 117**:** 435-442.

Mandal PK, Ferreira LM, Collins R, Meissner TB, Boutwell CL, Friesen M*, et al.* (2014). Efficient ablation of genes in human hematopoietic stem and effector cells using CRISPR/Cas9. Cell Stem Cell 15**:** 643-652.

Mangmool S, Denkaew T, Parichatikanond W, & Kurose H (2017). β-Adrenergic Receptor and Insulin Resistance in the Heart. Biomol Ther (Seoul) 25**:** 44-56.

Marin-Penalver JJ, Martin-Timon I, Sevillano-Collantes C, & Del Canizo-Gomez FJ (2016). Update on the treatment of type 2 diabetes mellitus. World J Diabetes 7**:** 354-395.

Martin OJ, Lee A, & McGraw TE (2006). GLUT4 distribution between the plasma membrane and the intracellular compartments is maintained by an insulin-modulated bipartite dynamic mechanism. J Biol Chem 281**:** 484-490.

Martin WH, 3rd, Murphree SS, & Saffitz JE (1989). β-adrenergic receptor distribution among muscle fiber types and resistance arterioles of white, red, and intermediate skeletal muscle. Circ Res 64**:** 1096-1105.

Mayor F, Jr., Cruces-Sande M, Arcones AC, Vila-Bedmar R, Briones AM, Salaices M*, et al.* (2018). G protein-coupled receptor kinase 2 (GRK2) as an integrative signalling node in the regulation of cardiovascular function and metabolic homeostasis. Cell Signal 41**:** 25-32.

McBride A, Ghilagaber S, Nikolaev A, & Hardie DG (2009). The glycogen-binding domain on the AMPK β subunit allows the kinase to act as a glycogen sensor. Cell Metab 9**:** 23-34.

McCorry LK (2007). Physiology of the autonomic nervous system. Am J Pharm Educ 71**:** 78.

McMullen JR, & Jennings GL (2007). Differences between pathological and physiological cardiac hypertrophy: novel therapeutic strategies to treat heart failure. Clin Exp Pharmacol Physiol 34**:** 255-262.

McVie-Wylie AJ, Lamson DR, & Chen YT (2001). Molecular cloning of a novel member of the GLUT family of transporters, SLC2a10 (GLUT10), localized on chromosome 20q13.1: a candidate gene for NIDDM susceptibility. Genomics 72**:** 113-117.

Melville A, Richardson R, Lister-Sharp D, & McIntosh A (2000). Complications of diabetes: renal disease and promotion of self-management. Qual Health Care 9**:** 257-263.

Merlin J, Sato M, Chia LY, Fahey R, Pakzad M, Nowell CJ*, et al.* (2018). Rosiglitazone and a β_3-Adrenoceptor Agonist Are Both Required for Functional Browning of White Adipocytes in Culture. Front Endocrinol (Lausanne) 9**:** 249.

Merry TL, & McConell GK (2009). Skeletal muscle glucose uptake during exercise: a focus on reactive oxygen species and nitric oxide signaling. IUBMB Life 61**:** 479-484.

Mettlen M, Pucadyil T, Ramachandran R, & Schmid SL (2009). Dissecting dynamin's role in clathrin-mediated endocytosis. Biochem Soc Trans 37**:** 1022-1026.

Meyer MM, Levin K, Grimmsmann T, Beck-Nielsen H, & Klein HH (2002). Insulin signalling in skeletal muscle of subjects with or without Type II-diabetes and first degree relatives of patients with the disease. Diabetologia 45**:** 813-822.

Michel MC, Ochodnicky P, & Summers RJ (2010). Tissue functions mediated by β_3-adrenoceptors-findings and challenges. Naunyn Schmiedebergs Arch Pharmacol 382**:** 103-108.

Mitchell TH, Ellis RD, Smith SA, Robb G, & Cawthorne MA (1989). Effects of BRL 35135, a β-adrenoceptor agonist with novel selectivity, on glucose tolerance and insulin sensitivity in obese subjects. Int J Obes 13**:** 757-766.

Mitsumoto Y, Burdett E, Grant A, & Klip A (1991). Differential expression of the GLUT1 and GLUT4 glucose transporters during differentiation of L6 muscle cells. Biochem Biophys Res Commun 175**:** 652-659.

Montgomery MD, Chan T, Swigart PM, Myagmar BE, Dash R, & Simpson PC (2017). An α_{1A} Adrenergic Receptor Agonist Prevents Acute Doxorubicin Cardiomyopathy in Male Mice. PLoS One 12**:** e0168409.

Mouillac B, Caron M, Bonin H, Dennis M, & Bouvier M (1992). Agonist-modulated palmitoylation of β_2-adrenergic receptor in Sf9 cells. J Biol Chem 267**:** 21733-21737.

Mu J, Brozinick JT, Jr., Valladares O, Bucan M, & Birnbaum MJ (2001). A role for AMP-activated protein kinase in contraction- and hypoxia-regulated glucose transport in skeletal muscle. Mol Cell 7**:** 1085-1094.

Mueckler M, & Thorens B (2013). The SLC2 (GLUT) family of membrane transporters. Mol Aspects Med 34**:** 121-138.

Munro S (2003). Lipid rafts: elusive or illusive? Cell 115**:** 377-388.

Musselman DM, Ford AP, Gennevois DJ, Harbison ML, Laurent AL, Mokatrin AS, *et al.* (2004). A randomized crossover study to evaluate Ro 115-1240, a selective $\alpha_{1A/1L}$-adrenoceptor partial agonist in women with stress urinary incontinence. BJU Int 93**:** 78-83.

Mutlu GM, & Factor P (2008). Alveolar epithelial β_2-adrenergic receptors. Am J Respir Cell Mol Biol 38**:** 127-134.

Muzzin P, Revelli JP, Kuhne F, Gocayne JD, McCombie WR, Venter JC, *et al.* (1991). An adipose tissue-specific β-adrenergic receptor. Molecular cloning and down-regulation in obesity. J Biol Chem 266**:** 24053-24058.

Naga Prasad SV, Laporte SA, Chamberlain D, Caron MG, Barak L, & Rockman HA (2002). Phosphoinositide 3-kinase regulates β_2-adrenergic receptor endocytosis by AP-2 recruitment to the receptor/β-arrestin complex. J Cell Biol 158**:** 563-575.

Nagase I, Yoshida T, Kumamoto K, Umekawa T, Sakane N, Nikami H, *et al.* (1996). Expression of uncoupling protein in skeletal muscle and white fat of obese mice treated with thermogenic β_3-adrenergic agonist. J Clin Invest 97**:** 2898-2904.

Nagoshi T, Yoshimura M, Rosano GM, Lopaschuk GD, & Mochizuki S (2011). Optimization of cardiac metabolism in heart failure. Curr Pharm Des 17**:** 3846-3853.

Nash CA, Nelson CP, Mistry R, Moeller-Olsen C, Christofidou E, Challiss RAJ, *et al.* (2018). Differential regulation of β_2-adrenoceptor and adenosine A2B receptor signalling by GRK and arrestin proteins in arterial smooth muscle. Cell Signal 51**:** 86-98.

Navale AM, & Paranjape AN (2016). Glucose transporters: physiological and pathological roles. Biophys Rev 8**:** 5-9.

Navegantes LC, Resano NM, Migliorini RH, & Kettelhut IC (2001). Catecholamines inhibit Ca^{2+}-dependent proteolysis in rat skeletal muscle through β_2-adrenoceptors and cAMP. Am J Physiol Endocrinol Metab 281**:** E449-454.

Nechamen CA, & Dias JA (2000). Human follicle stimulating hormone receptor trafficking and hormone binding sites in the amino terminus. Mol Cell Endocrinol 166**:** 101-110.

Nedergaard J, Bengtsson T, & Cannon B (2007). Unexpected evidence for active brown adipose tissue in adult humans. Am J Physiol Endocrinol Metab 293**:** E444-452.

Nevzorova J, Bengtsson T, Evans BA, & Summers RJ (2002). Characterization of the β-adrenoceptor subtype involved in mediation of glucose transport in L6 cells. Br J Pharmacol 137**:** 9-18.

Nevzorova J, Evans BA, Bengtsson T, & Summers RJ (2006). Multiple signalling pathways involved in β_2-adrenoceptor-mediated glucose uptake in rat skeletal muscle cells. Br J Pharmacol 147**:** 446-454.

Ngala RA, O'Dowd J, Wang SJ, Agarwal A, Stocker C, Cawthorne MA, *et al.* (2008). Metabolic responses to BRL37344 and clenbuterol in soleus muscle and C2C12 cells via different atypical pharmacologies and β_2-adrenoceptor mechanisms. Br J Pharmacol 155**:** 395-406.

Ngala RA, O'Dowd J, Wang SJ, Stocker C, Cawthorne MA, & Arch JR (2009). β_2-adrenoceptors and non- β-adrenoceptors mediate effects of BRL37344 and clenbuterol on glucose uptake in soleus muscle: studies using knockout mice. Br J Pharmacol 158**:** 1676-1682.

Ngala RA, O'Dowd JF, Stocker CJ, Cawthorne MA, & Arch JR (2013). β_2-adrenoceptor agonists can both stimulate and inhibit glucose uptake in mouse soleus muscle through ligand-directed signalling. Naunyn Schmiedebergs Arch Pharmacol 386: 761-773.

Nikolaev VO, Bunemann M, Hein L, Hannawacker A, & Lohse MJ (2004). Novel single chain cAMP sensors for receptor-induced signal propagation. J Biol Chem 279: 37215-37218.

Nisoli E, Tonello C, Landi M, & Carruba MO (1996). Functional studies of the first selective β_3-adrenergic receptor antagonist SR 59230A in rat brown adipocytes. Mol Pharmacol 49: 7-14.

Nobles KN, Xiao K, Ahn S, Shukla AK, Lam CM, Rajagopal S, et al. (2011). Distinct phosphorylation sites on the β_2-adrenergic receptor establish a barcode that encodes differential functions of β-arrestin. Sci Signal 4: ra51.

Nuber S, Zabel U, Lorenz K, Nuber A, Milligan G, Tobin AB, et al. (2016). β-Arrestin biosensors reveal a rapid, receptor-dependent activation/deactivation cycle. Nature 531: 661-664.

O'Connell TD, Ishizaka S, Nakamura A, Swigart PM, Rodrigo MC, Simpson GL, et al. (2003). The $\alpha_{1A/C}$- and α_{1B}-adrenergic receptors are required for physiological cardiac hypertrophy in the double-knockout mouse. J Clin Invest 111: 1783-1791.

O'Connell TD, Jensen BC, Baker AJ, & Simpson PC (2014). Cardiac α_1-adrenergic receptors: novel aspects of expression, signaling mechanisms, physiologic function, and clinical importance. Pharmacol Rev 66: 308-333.

O'Connell TD, Swigart PM, Rodrigo MC, Ishizaka S, Joho S, Turnbull L, et al. (2006). α_1-adrenergic receptors prevent a maladaptive cardiac response to pressure overload. J Clin Invest 116: 1005-1015.

O'Dowd BF, Hnatowich M, Caron MG, Lefkowitz RJ, & Bouvier M (1989). Palmitoylation of the human β_2-adrenergic receptor. Mutation of Cys341 in the carboxyl tail leads to an uncoupled nonpalmitoylated form of the receptor. J Biol Chem 264: 7564-7569.

Okada T, Kawano Y, Sakakibara T, Hazeki O, & Ui M (1994). Essential role of phosphatidylinositol 3-kinase in insulin-induced glucose transport and antilipolysis in rat adipocytes. Studies with a selective inhibitor wortmannin. J Biol Chem 269: 3568-3573.

Olsen JM, Sato M, Dallner OS, Sandstrom AL, Pisani DF, Chambard JC, et al. (2014). Glucose uptake in brown fat cells is dependent on mTOR complex 2-promoted GLUT1 translocation. J Cell Biol 207: 365-374.

Omata W, Shibata H, Li L, Takata K, & Kojima I (2000). Actin filaments play a critical role in insulin-induced exocytotic recruitment but not in endocytosis of GLUT4 in isolated rat adipocytes. Biochem J 346 Pt 2: 321-328.

Palczewski K, Kumasaka T, Hori T, Behnke CA, Motoshima H, Fox BA, et al. (2000). Crystal structure of rhodopsin: A G protein-coupled receptor. Science 289: 739-745.

Papay RS, Shi T, Piascik MT, Naga Prasad SV, & Perez DM (2013). α_{1A}-adrenergic receptors regulate cardiac hypertrophy in vivo through interleukin-6 secretion. Mol Pharmacol 83: 939-948.

Park SW, Goodpaster BH, Lee JS, Kuller LH, Boudreau R, de Rekeneire N, et al. (2009). Excessive loss of skeletal muscle mass in older adults with type 2 diabetes. Diabetes Care 32: 1993-1997.

Patki V, Buxton J, Chawla A, Lifshitz L, Fogarty K, Carrington W, *et al.* (2001). Insulin action on GLUT4 traffic visualized in single 3T3-l1 adipocytes by using ultra-fast microscopy. Mol Biol Cell 12**:** 129-141.

Pavlos NJ, & Friedman PA (2017). GPCR Signaling and Trafficking: The Long and Short of It. Trends Endocrinol Metab 28**:** 213-226.

Pearce LR, Huang X, Boudeau J, Pawlowski R, Wullschleger S, Deak M, *et al.* (2007). Identification of Protor as a novel Rictor-binding component of mTOR complex-2. Biochem J 405**:** 513-522.

Penela P, Murga C, Ribas C, Lafarga V, & Mayor F, Jr. (2010). The complex G protein-coupled receptor kinase 2 (GRK2) interactome unveils new physiopathological targets. Br J Pharmacol 160**:** 821-832.

Perry SJ, Baillie GS, Kohout TA, McPhee I, Magiera MM, Ang KL, *et al.* (2002). Targeting of cyclic AMP degradation to β_2-adrenergic receptors by β-arrestins. Science 298**:** 834-836.

Peterson TR, Laplante M, Thoreen CC, Sancak Y, Kang SA, Kuehl WM, *et al.* (2009). DEPTOR is an mTOR inhibitor frequently overexpressed in multiple myeloma cells and required for their survival. Cell 137**:** 873-886.

Piascik MT, & Perez DM (2001). α_1-adrenergic receptors: new insights and directions. J Pharmacol Exp Ther 298**:** 403-410.

Pitcher JA, Inglese J, Higgins JB, Arriza JL, Casey PJ, Kim C, *et al.* (1992). Role of $\beta\gamma$ subunits of G proteins in targeting the β-adrenergic receptor kinase to membrane-bound receptors. Science 257**:** 1264-1267.

Pitcher JA, Touhara K, Payne ES, & Lefkowitz RJ (1995). Pleckstrin homology domain-mediated membrane association and activation of the β-adrenergic receptor kinase requires coordinate interaction with G $\beta\gamma$ subunits and lipid. J Biol Chem 270**:** 11707-11710.

Poole-Wilson PA (1999). The Cardiac Insufficiency Bisoprolol Study II. Lancet 353**:** 1360-1361.

Poole-Wilson PA, Swedberg K, Cleland JG, Di Lenarda A, Hanrath P, Komajda M, *et al.* (2003). Comparison of carvedilol and metoprolol on clinical outcomes in patients with chronic heart failure in the Carvedilol Or Metoprolol European Trial (COMET): randomised controlled trial. Lancet 362**:** 7-13.

Porstmann T, Santos CR, Griffiths B, Cully M, Wu M, Leevers S, *et al.* (2008). SREBP activity is regulated by mTORC1 and contributes to Akt-dependent cell growth. Cell Metab 8**:** 224-236.

Pott C, Brixius K, Bundkirchen A, Bolck B, Bloch W, Steinritz D, *et al.* (2003). The preferential β_3-adrenoceptor agonist BRL 37344 increases force via β_1-/β_2-adrenoceptors and induces endothelial nitric oxide synthase via β_3-adrenoceptors in human atrial myocardium. Br J Pharmacol 138**:** 521-529.

Price DT, Lefkowitz RJ, Caron MG, Berkowitz D, & Schwinn DA (1994). Localization of mRNA for three distinct α_1-adrenergic receptor subtypes in human tissues: implications for human α-adrenergic physiology. Mol Pharmacol 45**:** 171-175.

Ramalingam L, Oh E, & Thurmond DC (2013). Novel roles for insulin receptor (IR) in adipocytes and skeletal muscle cells via new and unexpected substrates. Cell Mol Life Sci 70**:** 2815-2834.

Reimann F, & Gribble FM (2016). G protein-coupled receptors as new therapeutic targets for type 2 diabetes. Diabetologia 59**:** 229-233.

Ren JM, Marshall BA, Mueckler MM, McCaleb M, Amatruda JM, & Shulman GI (1995). Overexpression of Glut4 protein in muscle increases basal and insulin-stimulated whole body glucose disposal in conscious mice. J Clin Invest 95**:** 429-432.

Reynolds THt, Brozinick JT, Jr., Larkin LM, & Cushman SW (2000). Transient enhancement of GLUT-4 levels in rat epitrochlearis muscle after exercise training. J Appl Physiol (1985) 88**:** 2240-2245.

Ribas C, Penela P, Murga C, Salcedo A, Garcia-Hoz C, Jurado-Pueyo M*, et al.* (2007). The G protein-coupled receptor kinase (GRK) interactome: role of GRKs in GPCR regulation and signaling. Biochim Biophys Acta 1768**:** 913-922.

Ribon V, & Saltiel AR (1997). Insulin stimulates tyrosine phosphorylation of the proto-oncogene product of c-Cbl in 3T3-L1 adipocytes. Biochem J 324 (Pt 3)**:** 839-845.

Richter EA, & Hargreaves M (2013). Exercise, GLUT4, and skeletal muscle glucose uptake. Physiol Rev 93**:** 993-1017.

Riddy DM, Cook AE, Diepenhorst NA, Bosnyak S, Brady R, Mannoury la Cour C*, et al.* (2017). Isoform-Specific Biased Agonism of Histamine H3 Receptor Agonists. Mol Pharmacol 91**:** 87-99.

Riddy DM, Delerive P, Summers RJ, Sexton PM, & Langmead CJ (2018). G Protein-Coupled Receptors Targeting Insulin Resistance, Obesity, and Type 2 Diabetes Mellitus. Pharmacol Rev 70**:** 39-67.

Risson V, Mazelin L, Roceri M, Sanchez H, Moncollin V, Corneloup C*, et al.* (2009). Muscle inactivation of mTOR causes metabolic and dystrophin defects leading to severe myopathy. J Cell Biol 187**:** 859-874.

Roberts SJ, & Summers RJ (1998). Cyclic AMP accumulation in rat soleus muscle: stimulation by β_2- but not β_3-adrenoceptors. Eur J Pharmacol 348**:** 53-60.

Robitaille AM, Christen S, Shimobayashi M, Cornu M, Fava LL, Moes S*, et al.* (2013). Quantitative phosphoproteomics reveal mTORC1 activates de novo pyrimidine synthesis. Science 339**:** 1320-1323.

Roder PV, Wu B, Liu Y, & Han W (2016). Pancreatic regulation of glucose homeostasis. Exp Mol Med 48**:** e219.

Rogers S, Macheda ML, Docherty SE, Carty MD, Henderson MA, Soeller WC*, et al.* (2002). Identification of a novel glucose transporter-like protein-GLUT-12. Am J Physiol Endocrinol Metab 282**:** E733-738.

Roh E, Song DK, & Kim MS (2016). Emerging role of the brain in the homeostatic regulation of energy and glucose metabolism. Exp Mol Med 48**:** e216.

Rokosh DG, Bailey BA, Stewart AF, Karns LR, Long CS, & Simpson PC (1994). Distribution of α_{1C}-adrenergic receptor mRNA in adult rat tissues by RNase protection assay and comparison with α_{1B} and α_{1D}. Biochem Biophys Res Commun 200**:** 1177-1184.

Rokosh DG, & Simpson PC (2002α). Knockout of the $\alpha_{1A/C}$-adrenergic receptor subtype: the $\alpha_{1A/C}$ is expressed in resistance arteries and is required to maintain arterial blood pressure. Proc Natl Acad Sci U S A 99**:** 9474-9479.

Romero G, von Zastrow M, & Friedman PA (2011). Role of PDZ proteins in regulating trafficking, signaling, and function of GPCRs: means, motif, and opportunity. Adv Pharmacol 62**:** 279-314.

Rominger DH, Cowan CL, Gowen-MacDonald W, & Violin JD (2014). Biased ligands: pathway validation for novel GPCR therapeutics. Curr Opin Pharmacol 16**:** 108-115.

Rorabaugh BR, Ross SA, Gaivin RJ, Papay RS, McCune DF, Simpson PC*, et al.* (2005). α_{1A}- but not α_{1B}-adrenergic receptors precondition the ischemic heart by a staurosporine-sensitive, chelerythrine-insensitive mechanism. Cardiovasc Res 65**:** 436-445.

Ros-Baro A, Lopez-Iglesias C, Peiro S, Bellido D, Palacin M, Zorzano A*, et al.* (2001). Lipid rafts are required for GLUT4 internalization in adipose cells. Proc Natl Acad Sci U S A 98**:** 12050-12055.

Rosenbaum DM, Rasmussen SG, & Kobilka BK (2009). The structure and function of G-protein-coupled receptors. Nature 459**:** 356-363.

Sajan MP, Bandyopadhyay G, Kanoh Y, Standaert ML, Quon MJ, Reed BC*, et al.* (2002). Sorbitol activates atypical protein kinase C and GLUT4 glucose transporter translocation/glucose transport through proline-rich tyrosine kinase-2, the extracellular signal-regulated kinase pathway and phospholipase D. Biochem J 362**:** 665-674.

Salt I, Celler JW, Hawley SA, Prescott A, Woods A, Carling D*, et al.* (1998). AMP-activated protein kinase: greater AMP dependence, and preferential nuclear localization, of complexes containing the α 2 isoform. Biochem J 334 (Pt 1)**:** 177-187.

Saltiel AR, & Kahn CR (2001). Insulin signalling and the regulation of glucose and lipid metabolism. Nature 414**:** 799-806.

Santti E, Huupponen R, Rouru J, Hanninen V, Pesonen U, Jhanwar-Uniyal M*, et al.* (1994). Potentiation of the anti-obesity effect of the selective β_3-adrenoceptor agonist BRL 35135 in obese Zucker rats by exercise. Br J Pharmacol 113**:** 1231-1236.

Santulli G, Lombardi A, Sorriento D, Anastasio A, Del Giudice C, Formisano P*, et al.* (2012). Age-related impairment in insulin release: the essential role of β_2-adrenergic receptor. Diabetes 61**:** 692-701.

Sarbassov DD, Ali SM, Sengupta S, Sheen JH, Hsu PP, Bagley AF*, et al.* (2006). Prolonged rapamycin treatment inhibits mTORC2 assembly and Akt/PKB. Mol Cell 22**:** 159-168.

Sargeant RJ, & Paquet MR (1993). Effect of insulin on the rates of synthesis and degradation of GLUT1 and GLUT4 glucose transporters in 3T3-L1 adipocytes. Biochem J 290 (Pt 3)**:** 913-919.

Sasaoka T, Wada T, & Tsuneki H (2006). Lipid phosphatases as a possible therapeutic target in cases of type 2 diabetes and obesity. Pharmacol Ther 112**:** 799-809.

Satake S, Moore MC, Igawa K, Converse M, Farmer B, Neal DW*, et al.* (2002). Direct and indirect effects of insulin on glucose uptake and storage by the liver. Diabetes 51**:** 1663-1671.

Sato M, Dehvari N, Oberg AI, Dallner OS, Sandstrom AL, Olsen JM*, et al.* (2014a). Improving type 2 diabetes through a distinct adrenergic signaling pathway involving mTORC2 that mediates glucose uptake in skeletal muscle. Diabetes 63**:** 4115-4129.

Sato M, Dehvari N, Oberg AI, Summers RJ, Hutchinson DS, & Bengtsson T (2014b). Response to Comment on Sato et al. Improving type 2 diabetes through a distinct adrenergic signaling pathway

involving mTORC2 that mediates glucose uptake in skeletal muscle. Diabetes 2014;63:4115-4129. Diabetes 63**:** e22-23.

Sato M, Evans BA, Sandstrom AL, Chia LY, Mukaida S, Thai BS*, et al.* (2018). α_{1A}-Adrenoceptors activate mTOR signalling and glucose uptake in cardiomyocytes. Biochem Pharmacol 148**:** 27-40.

Sato M, Horinouchi T, Hutchinson DS, Evans BA, & Summers RJ (2007). Ligand-directed signaling at the β_3-adrenoceptor produced by 3-(2-Ethylphenoxy)-1-[(1,S)-1,2,3,4-tetrahydronapth-1-ylamino]-2S-2-propanol oxalate (SR59230A) relative to receptor agonists. Mol Pharmacol 72**:** 1359-1368.

Satoh S, Nishimura H, Clark AE, Kozka IJ, Vannucci SJ, Simpson IA*, et al.* (1993). Use of bismannose photolabel to elucidate insulin-regulated GLUT4 subcellular trafficking kinetics in rat adipose cells. Evidence that exocytosis is a critical site of hormone action. J Biol Chem 268**:** 17820-17829.

Satoh T (2014). Molecular mechanisms for the regulation of insulin-stimulated glucose uptake by small guanosine triphosphatases in skeletal muscle and adipocytes. Int J Mol Sci 15**:** 18677-18692.

Saunders C, & Limbird LE (1999). Localization and trafficking of α_2-adrenergic receptor subtypes in cells and tissues. Pharmacol Ther 84**:** 193-205.

Schindelin J, Arganda-Carreras I, Frise E, Kaynig V, Longair M, Pietzsch T*, et al.* (2012). Fiji: an open-source platform for biological-image analysis. Nat Methods 9**:** 676-682.

Schutzer WE, Reed JF, & Mader SL (2005). Decline in caveolin-1 expression and scaffolding of G protein receptor kinase-2 with age in Fischer 344 aortic vascular smooth muscle. Am J Physiol Heart Circ Physiol 288**:** H2457-2464.

Sciarretta S, Volpe M, & Sadoshima J (2014). Mammalian target of rapamycin signaling in cardiac physiology and disease. Circ Res 114**:** 549-564.

Scott MG, Le Rouzic E, Perianin A, Pierotti V, Enslen H, Benichou S*, et al.* (2002). Differential nucleocytoplasmic shuttling of β-arrestins. Characterization of a leucine-rich nuclear export signal in β-arrestin2. J Biol Chem 277**:** 37693-37701.

Seibold A, January BG, Friedman J, Hipkin RW, & Clark RB (1998). Desensitization of β_2-adrenergic receptors with mutations of the proposed G protein-coupled receptor kinase phosphorylation sites. J Biol Chem 273**:** 7637-7642.

Seibold A, Williams B, Huang ZF, Friedman J, Moore RH, Knoll BJ*, et al.* (2000). Localization of the sites mediating desensitization of the β_2-adrenergic receptor by the GRK pathway. Mol Pharmacol 58**:** 1162-1173.

Selvetella G, Hirsch E, Notte A, Tarone G, & Lembo G (2004). Adaptive and maladaptive hypertrophic pathways: points of convergence and divergence. Cardiovasc Res 63**:** 373-380.

Selvetella G, & Lembo G (2005). Mechanisms of cardiac hypertrophy. Heart Fail Clin 1**:** 263-273.

Semiz S, Park JG, Nicoloro SM, Furcinitti P, Zhang C, Chawla A*, et al.* (2003). Conventional kinesin KIF5B mediates insulin-stimulated GLUT4 movements on microtubules. EMBO J 22**:** 2387-2399.

Sesti G (2006). Pathophysiology of insulin resistance. Best Pract Res Clin Endocrinol Metab 20**:** 665-679.

Shende P, Plaisance I, Morandi C, Pellieux C, Berthonneche C, Zorzato F*, et al.* (2011). Cardiac raptor ablation impairs adaptive hypertrophy, alters metabolic gene expression, and causes heart failure in mice. Circulation 123**:** 1073-1082.

Shenoy SK, Drake MT, Nelson CD, Houtz DA, Xiao K, Madabushi S*, et al.* (2006). β-arrestin-dependent, G protein-independent ERK1/2 activation by the β$_2$ adrenergic receptor. J Biol Chem 281**:** 1261-1273.

Shigematsu S, Watson RT, Khan AH, & Pessin JE (2003). The adipocyte plasma membrane caveolin functional/structural organization is necessary for the efficient endocytosis of GLUT4. J Biol Chem 278**:** 10683-10690.

Shiina T, Arai K, Tanabe S, Yoshida N, Haga T, Nagao T*, et al.* (2001). Clathrin box in G protein-coupled receptor kinase 2. J Biol Chem 276**:** 33019-33026.

Shioi T, McMullen JR, Tarnavski O, Converso K, Sherwood MC, Manning WJ*, et al.* (2003). Rapamycin attenuates load-induced cardiac hypertrophy in mice. Circulation 107**:** 1664-1670.

Siehler S (2009). Regulation of RhoGEF proteins by G12/13-coupled receptors. Br J Pharmacol 158**:** 41-49.

Simpson IA, Dwyer D, Malide D, Moley KH, Travis A, & Vannucci SJ (2008). The facilitative glucose transporter GLUT3: 20 years of distinction. Am J Physiol Endocrinol Metab 295**:** E242-253.

Smith JS, Lefkowitz RJ, & Rajagopal S (2018). Biased signalling: from simple switches to allosteric microprocessors. Nat Rev Drug Discov 17**:** 243-260.

Smith RM, Charron MJ, Shah N, Lodish HF, & Jarett L (1991). Immunoelectron microscopic demonstration of insulin-stimulated translocation of glucose transporters to the plasma membrane of isolated rat adipocytes and masking of the carboxyl-terminal epitope of intracellular GLUT4. Proc Natl Acad Sci U S A 88**:** 6893-6897.

Somwar R, Niu W, Kim DY, Sweeney G, Randhawa VK, Huang C*, et al.* (2001). Differential effects of phosphatidylinositol 3-kinase inhibition on intracellular signals regulating GLUT4 translocation and glucose transport. J Biol Chem 276**:** 46079-46087.

Sprague JE, & Arbelaez AM (2011). Glucose counterregulatory responses to hypoglycemia. Pediatr Endocrinol Rev 9**:** 463-473; quiz 474-465.

Stenbit AE, Burcelin R, Katz EB, Tsao TS, Gautier N, Charron MJ*, et al.* (1996). Diverse effects of Glut 4 ablation on glucose uptake and glycogen synthesis in red and white skeletal muscle. J Clin Invest 98**:** 629-634.

Stenbit AE, Tsao TS, Li J, Burcelin R, Geenen DL, Factor SM*, et al.* (1997). GLUT4 heterozygous knockout mice develop muscle insulin resistance and diabetes. Nat Med 3**:** 1096-1101.

Stockli J, Fazakerley DJ, & James DE (2011). GLUT4 exocytosis. J Cell Sci 124**:** 4147-4159.

Stuart CA, Yin D, Howell ME, Dykes RJ, Laffan JJ, & Ferrando AA (2006). Hexose transporter mRNAs for GLUT4, GLUT5, and GLUT12 predominate in human muscle. Am J Physiol Endocrinol Metab 291**:** E1067-1073.

Summers RJ, Kompa A, & Roberts SJ (1997). β-adrenoceptor subtypes and their desensitization mechanisms. J Auton Pharmacol 17**:** 331-343.

Suryawan A, & Davis TA (2010). The abundance and activation of mTORC1 regulators in skeletal muscle of neonatal pigs are modulated by insulin, amino acids, and age. J Appl Physiol (1985) 109: 1448-1454.

Susulic VS, Frederich RC, Lawitts J, Tozzo E, Kahn BB, Harper ME, *et al.* (1995). Targeted disruption of the β_3-adrenergic receptor gene. J Biol Chem 270: 29483-29492.

Sutherland EW, & Robison GA (1969). The role of cyclic AMP in the control of carbohydrate metabolism. Diabetes 18: 797-819.

Svalo J, Nordling J, Bouchelouche K, Andersson KE, Korstanje C, & Bouchelouche P (2013). The novel β_3-adrenoceptor agonist mirabegron reduces carbachol-induced contractile activity in detrusor tissue from patients with bladder outflow obstruction with or without detrusor overactivity. Eur J Pharmacol 699: 101-105.

Sylow L, Jensen TE, Kleinert M, Mouatt JR, Maarbjerg SJ, Jeppesen J, *et al.* (2013). Rac1 is a novel regulator of contraction-stimulated glucose uptake in skeletal muscle. Diabetes 62: 1139-1151.

Sylow L, Kleinert M, Richter EA, & Jensen TE (2017a). Exercise-stimulated glucose uptake - regulation and implications for glycaemic control. Nat Rev Endocrinol 13: 133-148.

Sylow L, Moller LLV, Kleinert M, D'Hulst G, De Groote E, Schjerling P, *et al.* (2017b). Rac1 and AMPK Account for the Majority of Muscle Glucose Uptake Stimulated by Ex Vivo Contraction but Not In Vivo Exercise. Diabetes 66: 1548-1559.

Szablewski L (2017). Glucose transporters in healthy heart and in cardiac disease. Int J Cardiol 230: 70-75.

Talwar KK, Bhargava B, Upasani PT, Verma S, Kamlakar T, & Chopra P (1996). Hemodynamic predictors of early intolerance and long-term effects of propranolol in dilated cardiomyopathy. J Card Fail 2: 273-277.

Tang H, Inoki K, Lee M, Wright E, Khuong A, Khuong A, *et al.* (2014). mTORC1 promotes denervation-induced muscle atrophy through a mechanism involving the activation of FoxO and E3 ubiquitin ligases. Sci Signal 7: ra18.

Teerlink JR, Pfeffer JM, & Pfeffer MA (1994). Progressive ventricular remodeling in response to diffuse isoproterenol-induced myocardial necrosis in rats. Circ Res 75: 105-113.

Tepper D (1999). Frontiers in congestive heart failure: Effect of Metoprolol CR/XL in chronic heart failure: Metoprolol CR/XL Randomised Intervention Trial in Congestive Heart Failure (MERIT-HF). Congest Heart Fail 5: 184-185.

Thorens B (1992). Molecular and cellular physiology of GLUT-2, a high-Km facilitated diffusion glucose transporter. Int Rev Cytol 137: 209-238.

Thorens B, & Mueckler M (2010). Glucose transporters in the 21st Century. Am J Physiol Endocrinol Metab 298: E141-145.

Thorpe LM, Yuzugullu H, & Zhao JJ (2015). PI3K in cancer: divergent roles of isoforms, modes of activation and therapeutic targeting. Nat Rev Cancer 15: 7-24.

Torgan CE, Brozinick JT, Jr., Banks EA, Cortez MY, Wilcox RE, & Ivy JL (1993). Exercise training and clenbuterol reduce insulin resistance of obese Zucker rats. Am J Physiol 264: E373-379.

Tortorella LL, & Pilch PF (2002). C2C12 myocytes lack an insulin-responsive vesicular compartment despite dexamethasone-induced GLUT4 expression. Am J Physiol Endocrinol Metab 283**:** E514-524.

Tsuchiya A, Kanno T, & Nishizaki T (2014). PI3 kinase directly phosphorylates Akt1/2 at Ser473/474 in the insulin signal transduction pathway. J Endocrinol 220**:** 49-59.

Tsuga H, Kameyama K, Haga T, Kurose H, & Nagao T (1994). Sequestration of muscarinic acetylcholine receptor m2 subtypes. Facilitation by G protein-coupled receptor kinase (GRK2) and attenuation by a dominant-negative mutant of GRK2. J Biol Chem 269**:** 32522-32527.

Turner RC, Millns H, Neil HA, Stratton IM, Manley SE, Matthews DR*, et al.* (1998). Risk factors for coronary artery disease in non-insulin dependent diabetes mellitus: United Kingdom Prospective Diabetes Study (UKPDS: 23). BMJ 316**:** 823-828.

Uldry M, Ibberson M, Horisberger JD, Chatton JY, Riederer BM, & Thorens B (2001). Identification of a mammalian H(+)-myo-inositol symporter expressed predominantly in the brain. EMBO J 20**:** 4467-4477.

Um SH, Frigerio F, Watanabe M, Picard F, Joaquin M, Sticker M*, et al.* (2004). Absence of S6K1 protects against age- and diet-induced obesity while enhancing insulin sensitivity. Nature 431**:** 200-205.

Usui I, Imamura T, Babendure JL, Satoh H, Lu JC, Hupfeld CJ*, et al.* (2005). G protein-coupled receptor kinase 2 mediates endothelin-1-induced insulin resistance via the inhibition of both Gαq/11 and insulin receptor substrate-1 pathways in 3T3-L1 adipocytes. Mol Endocrinol 19**:** 2760-2768.

Usui I, Imamura T, Satoh H, Huang J, Babendure JL, Hupfeld CJ*, et al.* (2004). GRK2 is an endogenous protein inhibitor of the insulin signaling pathway for glucose transport stimulation. EMBO J 23**:** 2821-2829.

Utermark T, Rao T, Cheng H, Wang Q, Lee SH, Wang ZC*, et al.* (2012). The p110 α and p110 β isoforms of PI3K play divergent roles in mammary gland development and tumorigenesis. Genes Dev 26**:** 1573-1586.

Vakhrusheva O, Smolka C, Gajawada P, Kostin S, Boettger T, Kubin T*, et al.* (2008). Sirt7 increases stress resistance of cardiomyocytes and prevents apoptosis and inflammatory cardiomyopathy in mice. Circ Res 102**:** 703-710.

Valentine RJ, Coughlan KA, Ruderman NB, & Saha AK (2014). Insulin inhibits AMPK activity and phosphorylates AMPK Ser(4)(8)(5)/(4)(9)(1) through Akt in hepatocytes, myotubes and incubated rat skeletal muscle. Arch Biochem Biophys 562**:** 62-69.

van der Westhuizen ET, Breton B, Christopoulos A, & Bouvier M (2014). Quantification of ligand bias for clinically relevant β2-adrenergic receptor ligands: implications for drug taxonomy. Mol Pharmacol 85**:** 492-509.

Vardanega-Peicher M, Lopes G, Lima FB, Curi R, Nakano LC, & Bazotte RB (2000). Time sequence of changes in the responsiveness of glycogen breakdown to adrenergic agonists in perfused liver of rats with insulin-induced hypoglycemia. Braz J Med Biol Res 33**:** 805-813.

Vichaiwong K, Purohit S, An D, Toyoda T, Jessen N, Hirshman MF*, et al.* (2010). Contraction regulates site-specific phosphorylation of TBC1D1 in skeletal muscle. Biochem J 431**:** 311-320.

Vinge LE, Oie E, Andersson Y, Grogaard HK, Andersen G, & Attramadal H (2001). Myocardial distribution and regulation of GRK and β-arrestin isoforms in congestive heart failure in rats. Am J Physiol Heart Circ Physiol 281**:** H2490-2499.

Violin JD, Crombie AL, Soergel DG, & Lark MW (2014). Biased ligands at G-protein-coupled receptors: promise and progress. Trends Pharmacol Sci 35**:** 308-316.

Violin JD, DiPilato LM, Yildirim N, Elston TC, Zhang J, & Lefkowitz RJ (2008). β$_2$-adrenergic receptor signaling and desensitization elucidated by quantitative modeling of real time cAMP dynamics. J Biol Chem 283**:** 2949-2961.

Wachten S, Masada N, Ayling LJ, Ciruela A, Nikolaev VO, Lohse MJ*, et al.* (2010). Distinct pools of cAMP centre on different isoforms of adenylyl cyclase in pituitary-derived GH3B6 cells. J Cell Sci 123**:** 95-106.

Walker PS, Ramlal T, Donovan JA, Doering TP, Sandra A, Klip A*, et al.* (1989). Insulin and glucose-dependent regulation of the glucose transport system in the rat L6 skeletal muscle cell line. J Biol Chem 264**:** 6587-6595.

Wallberg-Henriksson H, & Zierath JR (2001). GLUT4: a key player regulating glucose homeostasis? Insights from transgenic and knockout mice (review). Mol Membr Biol 18**:** 205-211.

Wang BT, Ducker GS, Barczak AJ, Barbeau R, Erle DJ, & Shokat KM (2011). The mammalian target of rapamycin regulates cholesterol biosynthetic gene expression and exhibits a rapamycin-resistant transcriptional profile. Proc Natl Acad Sci U S A 108**:** 15201-15206.

Wang L, & Proud CG (2002). Ras/Erk signaling is essential for activation of protein synthesis by Gq protein-coupled receptor agonists in adult cardiomyocytes. Circ Res 91**:** 821-829.

Wang L, Shen M, Wang F, & Ma L (2012). GRK5 ablation contributes to insulin resistance. Biochem Biophys Res Commun 429**:** 99-104.

Wang Q, Bilan PJ, Tsakiridis T, Hinek A, & Klip A (1998). Actin filaments participate in the relocalization of phosphatidylinositol3-kinase to glucose transporter-containing compartments and in the stimulation of glucose uptake in 3T3-L1 adipocytes. Biochem J 331 (Pt 3)**:** 917-928.

Wasserman DH, Kang L, Ayala JE, Fueger PT, & Lee-Young RS (2011). The physiological regulation of glucose flux into muscle in vivo. J Exp Biol 214**:** 254-262.

Watari K, Nakaya M, & Kurose H (2014). Multiple functions of G protein-coupled receptor kinases. J Mol Signal 9**:** 1.

Watson-Wright WM, & Wilkinson M (1986). The muscle slice--a new preparation for the characterization of β-adrenergic binding in fast- and slow-twitch skeletal muscle. Muscle Nerve 9**:** 416-422.

Watson SJ, Brown AJ, & Holliday ND (2012). Differential signaling by splice variants of the human free fatty acid receptor GPR120. Mol Pharmacol 81**:** 631-642.

Weichhart T, Hengstschlager M, & Linke M (2015). Regulation of innate immune cell function by mTOR. Nat Rev Immunol 15**:** 599-614.

Weiler M, Blaes J, Pusch S, Sahm F, Czabanka M, Luger S*, et al.* (2014). mTOR target NDRG1 confers MGMT-dependent resistance to alkylating chemotherapy. Proc Natl Acad Sci U S A 111**:** 409-414.

Weiss ER, Raman D, Shirakawa S, Ducceschi MH, Bertram PT, Wong F, *et al.* (1998). The cloning of GRK7, a candidate cone opsin kinase, from cone- and rod-dominant mammalian retinas. Mol Vis 4**:** 27.

Widen E, Ekstrand A, Saloranta C, Franssila-Kallunki A, Eriksson J, Schalin-Jantti C, *et al.* (1992). Insulin resistance in type 2 (non-insulin-dependent) diabetic patients with hypertriglyceridaemia. Diabetologia 35**:** 1140-1145.

Wilden PA, Siddle K, Haring E, Backer JM, White MF, & Kahn CR (1992). The role of insulin receptor kinase domain autophosphorylation in receptor-mediated activities. Analysis with insulin and anti-receptor antibodies. J Biol Chem 267**:** 13719-13727.

Wilson C, Wilson S, Piercy V, Sennitt MV, & Arch JR (1984). The rat lipolytic β-adrenoceptor: studies using novel β-adrenoceptor agonists. Eur J Pharmacol 100**:** 309-319.

Woodall BP, Woodall MC, Luongo TS, Grisanti LA, Tilley DG, Elrod JW, *et al.* (2016). Skeletal Muscle-specific G Protein-coupled Receptor Kinase 2 Ablation Alters Isolated Skeletal Muscle Mechanics and Enhances Clenbuterol-stimulated Hypertrophy. J Biol Chem 291**:** 21913-21924.

Worzfeld T, Wettschureck N, & Offermanns S (2008). G(12)/G(13)-mediated signalling in mammalian physiology and disease. Trends Pharmacol Sci 29**:** 582-589.

Wright DC, Geiger PC, Holloszy JO, & Han DH (2005). Contraction- and hypoxia-stimulated glucose transport is mediated by a Ca2+-dependent mechanism in slow-twitch rat soleus muscle. Am J Physiol Endocrinol Metab 288**:** E1062-1066.

Wu Y, Ding Y, Tanaka Y, & Zhang W (2014). Risk factors contributing to type 2 diabetes and recent advances in the treatment and prevention. Int J Med Sci 11**:** 1185-1200.

Xavier S, Sadanandan J, George N, & Paulose CS (2012). β_2-adrenoceptor and insulin receptor expression in the skeletal muscle of streptozotocin induced diabetic rats: antagonism by vitamin D(3) and curcumin. Eur J Pharmacol 687**:** 14-20.

Xiang Y, & Kobilka B (2003). The PDZ-binding motif of the β_2-adrenoceptor is essential for physiologic signaling and trafficking in cardiac myocytes. Proc Natl Acad Sci U S A 100**:** 10776-10781.

Xiao B, Heath R, Saiu P, Leiper FC, Leone P, Jing C, *et al.* (2007). Structural basis for AMP binding to mammalian AMP-activated protein kinase. Nature 449**:** 496-500.

Yang F, Yu X, Liu C, Qu CX, Gong Z, Liu HD, *et al.* (2015). Phospho-selective mechanisms of arrestin conformations and functions revealed by unnatural amino acid incorporation and (19)F-NMR. Nat Commun 6**:** 8202.

Yang J, & Holman GD (1993). Comparison of GLUT4 and GLUT1 subcellular trafficking in basal and insulin-stimulated 3T3-L1 cells. J Biol Chem 268**:** 4600-4603.

Yang X, Pratley RE, Tokraks S, Bogardus C, & Permana PA (2002). Microarray profiling of skeletal muscle tissues from equally obese, non-diabetic insulin-sensitive and insulin-resistant Pima Indians. Diabetologia 45**:** 1584-1593.

Yang Z, Yang F, Zhang D, Liu Z, Lin A, Liu C, *et al.* (2017). Phosphorylation of G Protein-Coupled Receptors: From the Barcode Hypothesis to the Flute Model. Mol Pharmacol 92**:** 201-210.

Yeh JI, Gulve EA, Rameh L, & Birnbaum MJ (1995). The effects of wortmannin on rat skeletal muscle. Dissociation of signaling pathways for insulin- and contraction-activated hexose transport. J Biol Chem 270**:** 2107-2111.

Yoon MS (2017a). mTOR as a Key Regulator in Maintaining Skeletal Muscle Mass. Front Physiol 8**:** 788.

Yoon MS (2017b). The Role of Mammalian Target of Rapamycin (mTOR) in Insulin Signaling. Nutrients 9.

Yuan N, Friedman J, Whaley BS, & Clark RB (1994). cAMP-dependent protein kinase and protein kinase C consensus site mutations of the β-adrenergic receptor. Effect on desensitization and stimulation of adenylylcyclase. J Biol Chem 269**:** 23032-23038.

Yuan T, Lupse B, Maedler K, & Ardestani A (2018). mTORC2 Signaling: A Path for Pancreatic β Cell's Growth and Function. J Mol Biol 430**:** 904-918.

Zerial M, & McBride H (2001). Rab proteins as membrane organizers. Nat Rev Mol Cell Biol 2**:** 107-117.

Zhang D, Contu R, Latronico MV, Zhang J, Rizzi R, Catalucci D*, et al.* (2010). MTORC1 regulates cardiac function and myocyte survival through 4E-BP1 inhibition in mice. J Clin Invest 120**:** 2805-2816.

Zhang D, Zhao Q, & Wu B (2015). Structural Studies of G Protein-Coupled Receptors. Mol Cells 38**:** 836-842.

Zhang J, Barak LS, Anborgh PH, Laporte SA, Caron MG, & Ferguson SS (1999). Cellular trafficking of G protein-coupled receptor/ β-arrestin endocytic complexes. J Biol Chem 274**:** 10999-11006.

Zhao X, Balaji P, Pachon R, Beniamen DM, Vatner DE, Graham RM*, et al.* (2015). Overexpression of Cardiomyocyte α_{1A}-Adrenergic Receptors Attenuates Postinfarct Remodeling by Inducing Angiogenesis Through Heterocellular Signaling. Arterioscler Thromb Vasc Biol 35**:** 2451-2459.

Zhu H, McElwee-Witmer S, Perrone M, Clark KL, & Zilberstein A (2000). Phenylephrine protects neonatal rat cardiomyocytes from hypoxia and serum deprivation-induced apoptosis. Cell Death Differ 7**:** 773-784.

Zhu WZ, Wang SQ, Chakir K, Yang D, Zhang T, Brown JH*, et al.* (2003). Linkage of β_1-adrenergic stimulation to apoptotic heart cell death through protein kinase A-independent activation of Ca2+/calmodulin kinase II. J Clin Invest 111**:** 617-625.

Zhu Y, Pires KM, Whitehead KJ, Olsen CD, Wayment B, Zhang YC*, et al.* (2013). Mechanistic target of rapamycin (Mtor) is essential for murine embryonic heart development and growth. PLoS One 8**:** e54221.

Zierath JR (1995). In vitro studies of human skeletal muscle: hormonal and metabolic regulation of glucose transport. Acta Physiol Scand Suppl 626**:** 1-96.

Zierath JR, & Wallberg-Henriksson H (2002). From receptor to effector: insulin signal transduction in skeletal muscle from type II diabetic patients. Ann N Y Acad Sci 967**:** 120-134.

Zimmermann G, & Taussig R (1996). Protein kinase C alters the responsiveness of adenylyl cyclases to G protein α and βγ subunits. J Biol Chem 271**:** 27161-271

Zinzalla V, Stracka D, Oppliger W, & Hall MN (2011). Activation of mTORC2 by association with the ribosome. Cell 144**:** 757-768.

APPENDIX 1

Adrenoceptors promote glucose uptake into adipocytes and muscle by an insulin-independent signalling pathway involving mechanistic target of rapamycin complex 2

Adrenoceptors promote glucose uptake into adipocytes and muscle by an insulin-independent signaling pathway involving mechanistic target of rapamycin complex 2

Saori Mukaida [a], Bronwyn A. Evans [a], Tore Bengtsson [b], Dana S. Hutchinson [a], Masaaki Sato [a],*

[a] Drug Discovery Biology, Monash Institute of Pharmaceutical Sciences, Monash University, 381 Royal Parade, Parkville, Victoria 3052, Australia
[b] Department of Molecular Biosciences, The Wenner-Gren Institute, Stockholm University, SE-10691 Stockholm, Sweden

ARTICLE INFO

ABSTRACT

Uptake of glucose into skeletal muscle and adipose tissue plays a vital role in metabolism and energy balance. Insulin released from β-islet cells of the pancreas promotes glucose uptake in these target tissues by stimulating translocation of GLUT4 transporters to the cell surface. This process is complex, involving signaling proteins including the mechanistic (or mammalian) target of rapamycin (mTOR) and Akt that intersect with multiple pathways controlling cell survival, growth and proliferation. mTOR exists in two forms, mTOR complex 1 (mTORC1), and mTOR complex 2 (mTORC2). mTORC1 has been intensively studied, acting as a key regulator of protein and lipid synthesis that integrates cellular nutrient availability and energy balance. Studies on mTORC2 have focused largely on its capacity to activate Akt by phosphorylation at Ser473, however recent findings demonstrate a novel role for mTORC2 in cellular glucose uptake. For example, agonists acting at β_2-adrenoceptors (ARs) in skeletal muscle or β_3-ARs in brown adipose tissue increase glucose uptake *in vitro and in vivo via* mechanisms dependent on mTORC2 but not Akt. In this review, we will focus on the signaling pathways downstream of β-ARs that promote glucose uptake in skeletal muscle and brown adipocytes, and will highlight how the insulin and adrenergic pathways converge and interact in these cells. The identification of insulin-independent mechanisms that promote glucose uptake should facilitate novel treatment strategies for metabolic disease.

© 2016 Elsevier Ltd. All rights reserved.

1. Introduction

The mechanistic (or mammalian) target of rapamycin (mTOR) integrates cellular sensing of nutrient, oxygen and energy levels with protein and lipid synthesis, cell survival, growth and proliferation. mTOR exists in two forms, the rapamycin-sensitive mTOR complex-1 (mTORC1) and the rapamycin-insensitive mTOR complex-2 (mTORC2) [1,2]. These complexes are unambiguously defined by binding of raptor (mTORC1) or rictor (mTORC2). mTORC1 regulates cell growth and protein synthesis through p70S6 kinase (S6K1), 4E-binding protein (4EBP) and protein phosphatase-2A (PP2A) [3], while mTORC2 is known to regulate Akt activation [4] and cytoskeletal reorganization [5,6]. Although mTORC2 is resistant to acute inhibition by rapamycin, prolonged treatment interferes with mTORC2 assembly and prevents the full activation of Akt [7].

Activation of mTORC1 is positively regulated by growth factors and mitogen-activated protein kinase (MAPK) pathways, due to phosphorylation and consequent inactivation of the upstream suppressor protein tuberous sclerosis complex 2 (TSC2) [8]. In contrast,

TSC2 activity is increased upon phosphorylation at distinct sites by adenosine monophosphate-activated kinase (AMPK), resulting in suppression of mTORC1 activity (reviewed by [9]). This mechanism governs the coordination of cell growth with energy status, as AMPK is activated due to AMP/ADP elevation or other forms of cellular stress. AMPK also phosphorylates raptor, further inhibiting mTORC1 activity [10]. mTORC2 is known to play a role in regulating glucose homeostasis. For example, skeletal muscle-specific ablation of rictor (and hence of mTORC2) depresses insulin-stimulated glucose uptake while at the same time increasing basal glycogen synthase activity [11]. This indicates that under conditions of low nutrient status, mTORC2 has the capacity to increase glucose uptake and suppress glycogen storage. We will discuss the manner in which this finding may relate to recent studies demonstrating that activation of β_2-adrenoceptors (ARs) in skeletal muscle or β_3-ARs in brown adipocytes increases activation of mTOR, and also mTORC2-mediated glucose uptake in vivo and in vitro [12,13].

2. The role of mTORC2 in skeletal muscle glucose uptake

Skeletal muscle is responsible for 75% of insulin-mediated glucose uptake and utilization in the fed state, making it an important target for diabetic therapies [14]. In muscle, stimulation by insulin or β_2-AR agonists increases glucose uptake via a common downstream mechanism involving the translocation of glucose transporter 4 (GLUT4) from the cytosol to the plasma membrane [15]. The upstream pathways utilized by β_2-ARs, on the other hand, are independent of proteins involved in insulin-stimulated glucose uptake.

2.1. Insulin-mediated glucose uptake

Insulin regulates whole-body glucose homeostasis by acting on the insulin receptor, a heterotetrameric membrane glycoprotein consisting of dimeric ligand-binding α-subunits and two tyrosine kinase β-subunits [16,17]. Insulin binding to the extracellular α-subunit of the receptor causes rapid autophosphorylation of tyrosine residues through a conformational change that brings the α-subunits closer. Also, tyrosine phosphorylation of insulin receptor substrates (IRS) promotes binding to phosphoinositide 3-kinase (PI3K) through SRC homology 2 (SH2) domains [18]. PI3K converts phosphatidylinositol 4,5-bisphosphate (PI(4,5)P_2) to the lipid second messenger phosphatidylinositol (3,4,5)-trisphosphate (PI(3,4,5)P_3), inducing the recruitment of 3-phosphoinositide-dependent protein kinase-1 (PDK1) to the plasma membrane, which in turn phosphorylates the serine kinase Akt at Thr308 (Fig. 1) [19]. A recent study demonstrates that Akt-pThr308 phosphorylates Thr86 of SIN1 (stress-activated protein kinase interacting protein 1), another key component of mTORC2 that increases mTOR kinase activity [20]. This results in a positive feedback loop in which mTORC2 phosphorylates Akt at Ser473, thereby fully activating Akt [21]. Like Erk1/2 (extracellular signal regulated kinase 1/2), phosphorylation by Akt inactivates the inhibitor TSC2, allowing mTORC1 phosphorylation at Ser2448 and activation of downstream effectors. Akt also phosphorylates AS160 (Akt substrate of 160 kDa) at Thr642, facilitating release of GLUT4 from intracellular storage vesicles (Fig. 1). Translocation, docking and fusion with the plasma membrane are promoted by re-organization of the actin cytoskeleton governed by Rac-1 (Ras-related C3 botulinum toxin substrate 1), and by interaction of AS160 with the molecular switches Rab8A and Rab13. The final stages of GLUT4 translocation are driven by α-actinin-4, the motor proteins MyoVa (myosin Va) and Myo1c (myosin 1c), and the adapter protein Mical-L2 (molecule interacting with CasL-like 2) (reviewed by [22]).

2.2. β_2-AR mediated glucose uptake in skeletal muscle

Skeletal muscle expresses abundant β-ARs that are predominantly β_2-ARs, with 7–10% of β_1-ARs present [23]. Recent findings have shown that stimulation with the β-AR agonist isoprenaline promotes glucose uptake in L6 myoblasts and myotubes, and intact skeletal muscle in vitro and in vivo [13,24]. Notably, isoprenaline increases glucose uptake to a greater extent than insulin in vivo in wild type mice, but not in β_1/β_2-AR knockout mice [13]. Furthermore, β_2-AR stimulation greatly improves glucose tolerance in two different models of type 2 diabetes, Goto-Kakizaki rats and high-fat diet–fed C57BL/6J mice [13]. Skeletal muscle from streptozotocin-induced diabetic rats has increased β_2-adrenoceptor mRNA levels compared to non-diabetic control rats, associated with an increase in the number of β_2-adrenoceptors as measured by [^{3}H] propranolol binding [25]. However in another study, there was no change in β_2-adrenoceptor expression in skeletal muscle from streptozotocin-induced Wistar diabetic rats [26]. In humans, there are similar β_2-adrenoceptor mRNA levels in the lateralis muscle from insulin-sensitive and insulin-resistant equally obese, non-diabetic Pima Indians [27] and in myotubes established from obese patients with type 2 diabetes and matched obese healthy participants [28].

β_2-ARs in skeletal muscle are primarily Gαs-coupled receptors [24], and increase glucose uptake via stimulation of adenylyl cyclase and production of the second messenger, cyclic AMP (cAMP), which activates protein kinase A (PKA) [13,24]. Although the mechanism is not fully understood, PKA promotes phosphorylation of mTORC2 at S2481, which is required for GLUT4 translocation and glucose uptake [13] (Fig. 1).

2.3. Comparison between β_2-AR and insulin-mediated glucose uptake

Unlike insulin, agonist stimulation of β_2-ARs does not increase PI(3,4,5)P_3 levels nor phosphorylate Akt at either Thr308 or Ser473. β_2-AR mediated glucose uptake is not blocked by selective Akt inhibitors in L6 cells, indicating that stimulation of β_2-ARs increases glucose uptake without activating Akt [13]. In addition, glucose uptake is increased by the cell permeable cAMP analogs (8-bromoadenosine 3′,5′-cAMP and N6,2′-O-dibutyryladenosine 3′,5′-cAMP) in L6 cells, indicating that increases in cAMP levels are tightly linked to increased glucose uptake [13]. Treatment with a specific inhibitor of mTOR, KU0063794, confirmed that mTOR is involved not only in insulin signaling but also β_2-AR stimulated glucose uptake [13]. mTOR has two primary phosphorylation sites at Ser2448 and at Ser2481. In complex 1, mTOR is predominantly phosphorylated at S2448 while in complex 2, mTOR is phosphorylated at S2481 [11,29]. It has been reported that alterations to the mTORC1 signaling pathway in skeletal muscle directly affect whole-body energy homeostasis [30], yet siRNA knockdown of mTORC2 (rictor), but not mTORC1 (raptor), markedly inhibits both insulin-mediated and β_2-AR mediated glucose uptake [13]. This confirms mTORC2 as a key regulator of glucose uptake in skeletal muscle. Indeed, in muscle lacking rictor, insulin-stimulated Akt phosphorylation at Ser473 and AS160 at Thr642 are dramatically decreased. The muscle-specific rictor knockout mice display glucose intolerance and decreased insulin-stimulated glucose uptake [11].

Although mTORC2 is activated in cells stimulated with β_2-AR agonists, it is unable to phosphorylate Akt-Ser473 because this reaction requires prior phosphorylation of Thr308 [21]. Hence, the upstream β_2-AR pathway differs from the insulin pathway at the level of cAMP versus Akt and PIP3, but both pathways involve mTORC2 as a key component. The β_2-AR pathway produces cAMP to activate mTORC2 while the insulin pathway activates PI3K,
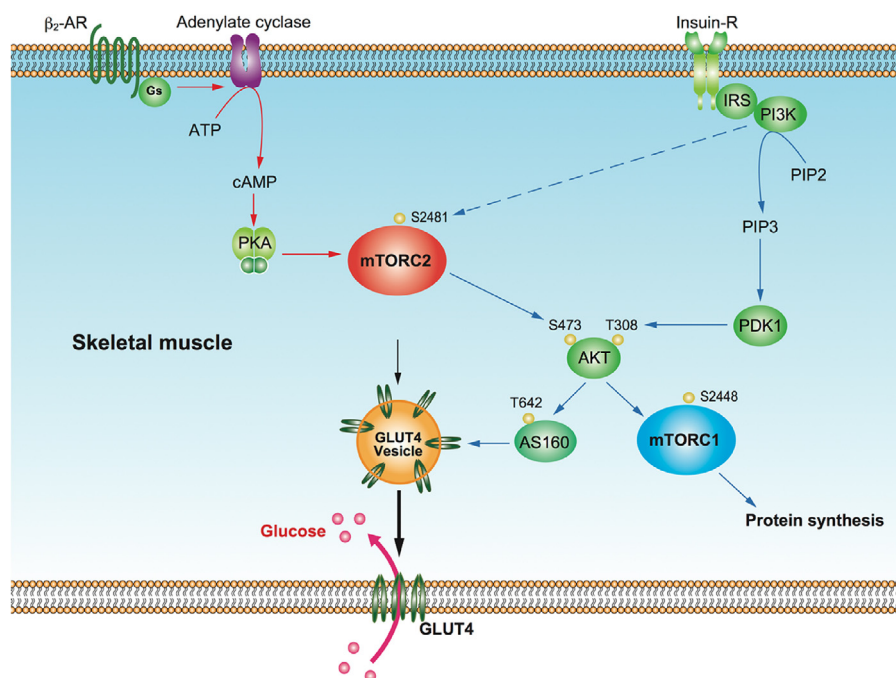
Fig. 1. Currently proposed mechanisms for insulin- and β_2-AR-stimulated glucose uptake. In skeletal muscle, activation of the β_2-AR coupled to Gαs stimulates adenylate cyclase, leading to the production of cAMP. cAMP activates PKA which then phosphorylates mTORC2 at Ser2481. The phosphorylated mTORC2 stimulates translocation of GLUT4 from cytosol to the plasma membrane, and increased localization of GLUT4 at the plasma membrane enhances glucose uptake. Insulin binds to the insulin receptor (Insulin-R), resulting in phosphorylation of insulin receptor substrate (IRS) and activation of PI3K. PI3K then increases levels of PIP3, which activates PDK1 to phosphorylate Akt at Thr308. PI3K also activates mTORC2 (Ser2481) which acts as a kinase of Akt at Ser473. Fully activated Akt phosphorylates AS160 to promote GLUT4 translocation to the plasma membrane leading to increased glucose uptake. Akt also phosphorylates mTORC1 at Ser2448 and thereby promotes protein synthesis.

leading to activation of Akt and mTORC2 (Fig. 1). Like insulin, glucose uptake in response to β_2-AR stimulation is blocked by GLUT inhibitors and by pretreatment with GLUT4 siRNA [13]. It has been known that type 2 diabetes is closely associated with defects in insulin signaling mechanisms such as defects in IRS, PI3K activity and Akt phosphorylation [31,32], but β_2-ARs expressed in skeletal muscle could bypass these defects through mTORC2-mediated regulation of GLUT4 trafficking, providing a compensatory pathway following loss of insulin sensitivity [13,33]. This is of particular interest considering that β_2-AR expression is unaltered in skeletal muscle from diabetic patients [27,28]. An insulin-independent pathway for glucose uptake is physiologically relevant and is highlighted by the mechanism whereby the type 2 diabetic drug metformin exerts its effects. Metformin increases glucose uptake in skeletal muscle through activation of AMPK [34,35]. In skeletal muscle, stimulation of α_1-ARs but not β_2-ARs increase glucose uptake via AMPK [36].

3. The role of mTORC2 in brown adipocyte glucose uptake

Brown adipose tissue (BAT) plays an important role in body temperature regulation owing to its ability to generate heat by uncoupling mitochondrial respiration, a process mediated by uncoupling protein 1 (UCP1) [37]. BAT depots are highly innervated and are activated by centres in the brain responsive to cold exposure, leading to the release of norepinephrine from sympathetic nerves. The energy-utilizing capacity of BAT gives it the potential to influence whole-body energy homeostasis. For example, BAT has been shown to play an important role in the regulation of glucose homeostasis and insulin secretion [38]. Glucose uptake is significantly increased in BAT in vivo by exposure of animals to cold [39,40] and by activation of the sympathetic nervous system, independently of insulin [41]. Chronic norepinephrine infusion mimics the effect of cold exposure on stimulation of glucose uptake into

BAT and white adipose tissue (WAT) [41–43]. This activation by the sympathetic nervous system can be mimicked by adrenergic agonists in brown adipocytes in vitro [44–50]. In animal models these effects are primarily due to actions at the β_3-AR, the predominant β-AR expressed, although actions involving β_1- or α_1-ARs are evident in some studies, particularly in cells or animals devoid of β_3-ARs [49–51]. β_3-AR agonists were originally developed for the treatment of obesity and diabetes, and are effective in animal models [52]. Humans were thought to lose BAT after infancy, but positron emission tomography scans of ^{18}F-fluorodeoxyglucose (FDG) uptake have revealed that adult humans possess BAT in the supraclavicular and neck regions. Human BAT is activated upon cold exposure [53–56] and contains UCP1 protein [57,58]. Cells cultured from biopsies of these regions are found to be phenotypically brown or beige/brite adipocytes [59–61]. Mirabegron (YM-178) was developed as a selective human β_3-AR agonist, approved in 2012 for the treatment of overactive bladder. In lean male subjects [62], a single dose of 200 mg mirabegron increases BAT [18]FDG uptake and resting metabolic rate by 203 ± 40 kcal/d (+13%), comparable to cold exposure (2 h at 14 °C). Thus activation of human β_3-ARs has a whole-body impact on energy expenditure. Supraclavicular brown adipocytes express substantially more β_3-AR mRNA than neighbouring white adipocytes [63]. No studies have addressed the question of relative β_3-AR levels in BAT from lean, obese or diabetic subjects, however obesity correlates with decreases in cold-induced BAT activation [55,56], possibly reflecting a lower abundance of brown adipocytes positive for β_3-ARs.

The β_3-AR is a Gαs-coupled G protein-coupled receptor (GPCR) and there is strong evidence that glucose uptake mediated by the β_3-AR occurs via a Gαs-cAMP-PKA mediated mechanism, based on pharmacological inhibitors of this pathway [12,49]. In addition, cholera toxin and 8-bromo-cAMP increase glucose uptake in primary brown adipocytes [12,49]. Other mechanisms shown to be involved in β_3-AR mediated glucose uptake include localisation of
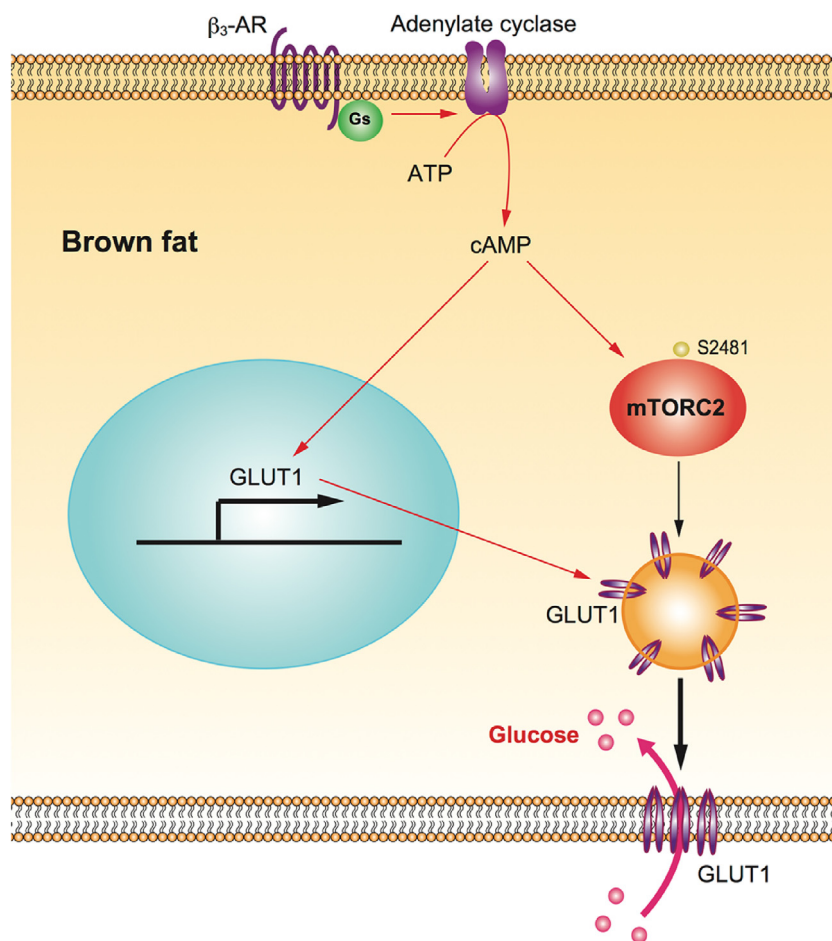
Fig. 2. Signaling pathways of β_3-AR-mediated glucose uptake in BAT. Stimulation of β_3-ARs increases the production of cAMP *via* Gαs-adenylyl cyclase in brown adipocytes. cAMP promotes the transcription and translation of GLUT1 mRNA, resulting in increased expression of GLUT1 protein. cAMP also phosphorylates mTORC2 at Ser2481 through unknown mechanisms, and activated mTORC2 causes translocation of GLUT1 to the plasma membrane leading to increased glucose uptake.

the β_3-AR in lipid-rich microenvironments in the plasma membrane [64], conventional and novel protein kinase C (PKC) isoforms [49,50], and AMPK [65,66]. As demonstrated in skeletal muscle, mTORC2 plays a pivotal role in adipocyte glucose uptake stimulated by β-AR agonists as well as insulin.

Cai et al. recently reviewed the literature on the role of both mTORC1 and mTORC2 in adipose tissue function, including adipogenesis, lipogenesis, lipolysis, thermogenesis, and regulation of endocrine function [67]. Here we will focus on the role of mTOR in glucose metabolism in adipose tissue. The contributions of mTORC1 and mTORC2 have been dissected by generating mice with adipocyte-specific ablation of raptor or rictor [68,69]. Ablation of raptor in adipose tissue increases mitochondrial uncoupling, but has no effect on insulin-mediated Akt phosphorylation or glucose tolerance profiles of chow-fed mice [68]. In contrast, adipocytes isolated from mice with fat-specific ablation of rictor (and hence disruption of mTORC2) display reduced insulin-stimulated Akt-Ser473 phosphorylation, GLUT4 translocation to the cell surface and glucose uptake, and these mice have impaired glucose tolerance profiles *in vivo* [69]. These studies indicate that mTORC2 is the complex involved in adipocyte glucose homeostasis.

A recent study from our laboratory also demonstrated that mTORC2 is involved in β_3-AR mediated glucose uptake in brown adipocytes [12] (Fig. 2). Interestingly, β_3-AR glucose uptake can be inhibited by a range of PI3K inhibitors [49], yet there is no phosphorylation of Akt at either Ser473 or Thr308 [12]. A series of experiments showed that these PI3K inhibitors are effective against

a range of related kinases, including mTOR [70,71]. Using more specific PI3K and Akt inhibitors, we confirmed that PI3K-Akt is not involved in β_3-AR mediated glucose uptake, whereas inhibition of mTOR by either Torin-1 or KU0063794 reduces glucose uptake. Several lines of evidence demonstrate the involvement of mTORC2 rather than mTORC1: (i) Stimulation of β_3-ARs increases mTOR phosphorylation at Ser2481 (which is associated with mTORC2 activity), but not at Ser2448 (which is associated with mTORC1 activity) [29], (ii) Long-term but not short-term rapamycin treatment attenuates β_3-AR mediated glucose uptake (as outlined above, rapamycin acutely inhibits mTORC1, whereas long-term treatment prevents mTORC2 assembly), (iii) siRNA against rictor, but not raptor, attenuates glucose uptake by β_3-ARs. In brown adipocytes, β_3-AR mediated glucose uptake depends on the *de novo* synthesis and translocation of GLUT1 [72]. mTORC2 is involved only in the translocation of the newly synthesized GLUT1 to the plasma membrane, but is not required for the *de novo* synthesis of GLUT1 [12] (Fig. 2).

A recent study by Michael Hall's group also demonstrated a pivotal role for mTORC2 in brown adipocyte glucose uptake, both *in vitro* and *in vivo* [73]. Mice lacking rictor in adipose tissue (AdRiKO) are hypothermic, and display increased sensitivity to cold and have impaired cold-induced glucose uptake and glycolysis. Surprisingly cold exposure of control or AdRiKO mice did not cause any alterations in GLUT1/4 content in the plasma membrane. Immortalized brown adipocytes were used to study the signaling pathways involved in mTORC2-mediated glucose uptake. As

observed in our study [12], norepinephrine was found to stimulate phosphorylation of mTOR at Ser2481. In contrast, Albert and coworkers also observed norepinephrine-induced phosphorylation of Akt at Ser473 both in immortalized brown adipocytes and in BAT following *in vivo* treatment of control mice [73]. Reasons for these conflicting findings on the role of Akt in β-AR mediated mTORC2 signaling and glucose uptake need to be clarified further.

4. Conclusions

This review has provided evidence for the metabolic role of β-AR signaling in skeletal muscle and brown adipocytes. In muscle, the action of β-agonists facilitates protein synthesis and glucose uptake, which are impaired in severe disease states such as type 2 diabetes and muscle wasting disorders [74,75]. Type 2 diabetes is associated with defects in insulin signaling including insulin receptor substrate, PI3K, Akt phosphorylation, causing impaired GLUT4 translocation and protein synthesis. These defects can be bypassed by the skeletal muscle β$_2$-AR-mTORC2 pathway which is independent of insulin signaling pathways. Likewise, BAT β-ARs play a significant role in thermogenesis and can contribute significantly to whole body energy expenditure, and consequently have recently received substantial attention as a therapeutic strategy in the treatment of obesity and Type 2 diabetes. The capacity of key GPCRs to promote glucose uptake by modulating mTORC2 activation represents a novel paradigm that holds great potential in the identification of drug targets for treating a range of metabolic disorders.

Acknowledgements

References

[1] D.D. Sarbassov, S.M. Ali, D.M. Sabatini, Growing roles for the mTOR pathway, Curr. Opin. Cell Biol. 17 (6) (2005) 596–603.

[2] S. Wullschleger, R. Loewith, M.N. Hall, TOR signaling in growth and metabolism, Cell 124 (3) (2006) 471–484.

[3] I.H. Park, E. Erbay, P. Nuzzi, J. Chen, Skeletal myocyte hypertrophy requires mTOR kinase activity and S6K1, Exp. Cell Res. 309 (1) (2005) 211–219.

[4] D.A. Guertin, D.M. Stevens, C.C. Thoreen, A.A. Burds, N.Y. Kalaany, J. Moffat, M. Brown, K.J. Fitzgerald, D.M. Sabatini, Ablation in mice of the mTORC components raptor, rictor, or mLST8 reveals that mTORC2 is required for signaling to Akt-FOXO and PKCα, but not S6K1, Dev. Cell 11 (6) (2006) 859–871.

[5] E. Jacinto, R. Loewith, A. Schmidt, S. Lin, M.A. Ruegg, A. Hall, M.N. Hall, Mammalian TOR complex 2 controls the actin cytoskeleton and is rapamycin insensitive, Nat. Cell Biol. 6 (11) (2004) 1122–1128.

[6] D.D. Sarbassov, S.M. Ali, D.H. Kim, D.A. Guertin, R.R. Latek, H. Erdjument-Bromage, P. Tempst, D.M. Sabatini, Rictor, a novel binding partner of mTOR, defines a rapamycin-insensitive and raptor-independent pathway that regulates the cytoskeleton, Curr. Biol. 14 (14) (2004) 1296–1302.

[7] D.D. Sarbassov, S.M. Ali, S. Sengupta, J.H. Sheen, P.P. Hsu, A.F. Bagley, A.L. Markhard, D.M. Sabatini, Prolonged rapamycin treatment inhibits mTORC2 assembly and Akt/PKB, Mol. Cell 22 (2) (2006) 159–168.

[8] J.N. Winter, L.S. Jefferson, S.R. Kimball, ERK and Akt signaling pathways function through parallel mechanisms to promote mTORC1 signaling, American journal of physiology, Cell Physiol. 300 (5) (2011) C1172–C1180.

[9] R.J. Shaw, LKB1 and AMP-activated protein kinase control of mTOR signalling and growth, Acta Physiol. 196 (1) (2009) 65–80.

[10] D.M. Gwinn, D.B. Shackelford, D.F. Egan, M.M. Mihaylova, A. Mery, D.S. Vasquez, B.E. Turk, R.J. Shaw, AMPK phosphorylation of raptor mediates a metabolic checkpoint, Mol. Cell 30 (2) (2008) 214–226.

[11] A. Kumar, T.E. Harris, S.R. Keller, K.M. Choi, M.A. Magnuson, J.C. Lawrence Jr., Muscle-specific deletion of rictor impairs insulin-stimulated glucose

[12] J.M. Olsen, M. Sato, O.S. Dallner, A.L. Sandstrom, D.F. Pisani, J.C. Chambard, E.Z. Amri, D.S. Hutchinson, T. Bengtsson, Glucose uptake in brown fat cells is dependent on mTOR complex 2-promoted GLUT1 translocation, J. Cell Biol. 207 (3) (2014) 365–374.

[13] M. Sato, N. Dehvari, A.I. Oberg, O.S. Dallner, A.L. Sandstrom, J.M. Olsen, R.I. Csikasz, R.J. Summers, D.S. Hutchinson, T. Bengtsson, Improving type 2 diabetes through a distinct adrenergic signaling pathway involving mTORC2 that mediates glucose uptake in skeletal muscle, Diabetes 63 (12) (2014) 4115–4129.

[14] E.A. Richter, M. Hargreaves, Exercise, GLUT4, and skeletal muscle glucose uptake, Physiol. Rev. 93 (3) (2013) 993–1017.

[15] A.F. Rowland, D.J. Fazakerley, D.E. James, Mapping insulin/GLUT4 circuitry, Traffic 12 (6) (2011) 672–681.

[16] J. Lee, M. Miyazaki, G.R. Romeo, S.E. Shoelson, Insulin receptor activation with transmembrane domain ligands, J. Biol. Chem. 289 (28) (2014) 19769–19777.

[17] J.W. Ryder, A.V. Chibalin, J.R. Zierath, Intracellular mechanisms underlying increases in glucose uptake in response to insulin or exercise in skeletal muscle, Acta Physiol. Scand. 171 (3) (2001) 249–257.

[18] M. Bjornholm, J.R. Zierath, Insulin signal transduction in human skeletal muscle: identifying the defects in Type II diabetes, Biochem. Soc. Trans. 33 (Pt. 2) (2005) 354–357.

[19] K.S. Walker, M. Deak, A. Paterson, K. Hudson, P. Cohen, D.R. Alessi, Activation of protein kinase B beta and gamma isoforms by insulin in vivo and by 3-phosphoinositide-dependent protein kinase-1 in vitro: comparison with protein kinase B alpha, Biochem. J. 331 (Pt. 1) (1998) 299–308.

[20] G. Yang, D.S. Murashige, S.J. Humphrey, D.E. James, A positive feedback loop between akt and mTORC2 via SIN1 phosphorylation, Cell Rep. 12 (6) (2015) 937–943.

[21] V. Facchinetti, W. Ouyang, H. Wei, N. Soto, A. Lazorchak, C. Gould, C. Lowry, A.C. Newton, Y. Mao, R.Q. Miao, W.C. Sessa, J. Qin, P. Zhang, B. Su, E. Jacinto, The mammalian target of rapamycin complex 2 controls folding and stability of Akt and protein kinase C, EMBO J. 27 (14) (2008) 1932–1943.

[22] A. Klip, Y. Sun, T.T. Chiu, K.P. Foley, Signal transduction meets vesicle traffic: the software and hardware of GLUT4 translocation: american journal of physiology, Cell Physiol. 306 (10) (2014) C879–86.

[23] D.M. Rosenbaum, S.G. Rasmussen, B.K. Kobilka, The structure and function of G-protein-coupled receptors, Nature 459 (7245) (2009) 356–363.

[24] J. Nevzorova, B.A. Evans, T. Bengtsson, R.J. Summers, Multiple signalling pathways involved in β$_2$-adrenoceptor-mediated glucose uptake in rat skeletal muscle cells, Br. J. Pharmacol. 147 (4) (2006) 446–454.

[25] S. Xavier, J. Sadanandan, N. George, C.S. Paulose, β$_2$-adrenoceptor and insulin receptor expression in the skeletal muscle of streptozotocin induced diabetic rats: antagonism by vitamin D(3) and curcumin, Eur. J. Pharmacol. 687 (1–3) (2012) 14–20.

[26] G.R. Willsky, L.H. Chi, Y. Liang, D.P. Gaile, Z. Hu, D.C. Crans, Diabetes-altered gene expression in rat skeletal muscle corrected by oral administration of vanadyl sulfate, Physiol. Genomics 26 (3) (2006) 192–201.

[27] X. Yang, R.E. Pratley, S. Tokraks, C. Bogardus, P.A. Permana, Microarray profiling of skeletal muscle tissues from equally obese, non-diabetic insulin-sensitive and insulin-resistant Pima Indians, Diabetologia 45 (11) (2002) 1584–1593.

[28] C.M. Frederiksen, K. Hojlund, L. Hansen, E.J. Oakeley, B. Hemmings, B.M. Abdallah, K. Brusgaard, H. Beck-Nielsen, M. Gaster, Transcriptional profiling of myotubes from patients with type 2 diabetes: no evidence for a primary defect in oxidative phosphorylation genes, Diabetologia 51 (11) (2008) 2068–2077.

[29] J. Copp, G. Manning, T. Hunter, TORC-specific phosphorylation of mammalian target of rapamycin (mTOR): phospho-Ser2481 is a marker for intact mTOR signaling complex 2, Cancer Res. 69 (5) (2009) 1821–1827.

[30] S. Frojdo, H. Vidal, L. Pirola, Alterations of insulin signaling in type 2 diabetes: a review of the current evidence from humans, Biochim. Biophys. Acta 1792 (2) (2009) 83–92.

[31] K. Cusi, K. Maezono, A. Osman, M. Pendergrass, M.E. Patti, T. Pratipanawatr, R.A. DeFronzo, C.R. Kahn, L.J. Mandarino, Insulin resistance differentially affects the PI 3-kinase- and MAP kinase-mediated signaling in human muscle, J. Clin. Invest. 105 (3) (2000) 311–320.

[32] M. Bjornholm, Y. Kawano, M. Lehtihet, J.R. Zierath, Insulin receptor substrate-1 phosphorylation and phosphatidylinositol 3-kinase activity in skeletal muscle from NIDDM subjects after in vivo insulin stimulation, Diabetes 46 (3) (1997) 524–527.

[33] M. Sato, N. Dehvari, A.I. Oberg, R.J. Summers, D.S. Hutchinson, T. Bengtsson, Response to Comment on Sato et al. Improving type 2 diabetes through a distinct adrenergic signaling pathway involving mTORC2 that mediates glucose uptake in skeletal muscle. Diabetes 2014;63:4115-4129, Diabetes 63 (12) (2014) e22–3.

[34] N. Kumar, C.S. Dey, Metformin enhances insulin signalling in insulin-dependent and-independent pathways in insulin resistant muscle cells, Br. J. Pharmacol. 137 (3) (2002) 329–336.

[35] K.A. Coughlan, R.J. Valentine, N.B. Ruderman, A.K. Saha, AMPK activation: a therapeutic target for type 2 diabetes? Diabetes Metab. Syndr. Obes. 7 (2014) 241–253.

[36] D.S. Hutchinson, T. Bengtsson, AMP-activated protein kinase activation by adrenoceptors in L6 skeletal muscle cells: mediation by α$_1$-adrenoceptors causing glucose uptake, Diabetes 55 (3) (2006) 682–690.

[37] B. Cannon, J. Nedergaard, Brown adipose tissue: function and physiological significance, Physiol. Rev. 84 (1) (2004) 277–359.

[38] C. Guerra, P. Navarro, A.M. Valverde, M. Arribas, J. Bruning, L.P. Kozak, C.R. Kahn, M. Benito, Brown adipose tissue-specific insulin receptor knockout shows diabetic phenotype without insulin resistance, J. Clin. Invest. 108 (8) (2001) 1205–1213.

[39] S. Cunningham, P. Leslie, D. Hopwood, P. Illingworth, R.T. Jung, D.G. Nicholls, N. Peden, J. Rafael, E. Rial, The characterization and energetic potential of brown adipose tissue in man, Clin. Sci. 69 (3) (1985) 343–348.

[40] R. Greco-Perotto, D. Zaninetti, F. Assimacopoulos-Jeannet, E. Bobbioni, B. Jeanrenaud, Stimulatory effect of cold adaptation on glucose utilization by brown adipose tissue. Relationship with changes in the glucose transporter system, J. Biol. Chem. 262 (16) (1987) 7732–7736.

[41] X. Liu, F. Perusse, L.J. Bukowiecki, Chronic norepinephrine infusion stimulates glucose uptake in white and brown adipose tissues, Am. J. Physiol. 266 (3 Pt. 2) (1994) R914–20.

[42] G.J. Cooney, I.D. Caterson, E.A. Newsholme, The effect of insulin and noradrenaline on the uptake of 2-[1-14C]deoxyglucose in vivo by brown adipose tissue and other glucose-utilising tissues of the mouse, FEBS Lett. 188 (2) (1985) 257–261.

[43] K. Tsukazaki, H. Nikami, Y. Shimizu, T. Kawada, T. Yoshida, M. Saito, Chronic administration of β-adrenergic agonists can mimic the stimulative effect of cold exposure on protein synthesis in rat brown adipose tissue, J. Biochem. 117 (1) (1995) 96–100.

[44] H. Nikami, Y. Shimizu, M. Sumida, Y. Minokoshi, T. Yoshida, M. Saito, T. Shimazu, Expression of β_3-adrenoceptor and stimulation of glucose transport by β_3-agonists in brown adipocyte primary culture, J. Biochem. 119 (1) (1996) 120–125.

[45] Y. Shimizu, T. Shimazu, Effects of wortmannin on increased glucose transport by insulin and norepinephrine in primary culture of brown adipocytes, Biochem. Biophys. Res. Commun. 202 (2) (1994) 660–665.

[46] Y. Shimizu, D. Kielar, Y. Minokoshi, T. Shimazu, Noradrenaline increases glucose transport into brown adipocytes in culture by a mechanism different from that of insulin, Biochem. J. 314 (Pt. 2) (1996) 485–490.

[47] X. Liu, F. Perusse, L.J. Bukowiecki, Mechanisms of the antidiabetic effects of the β_3-adrenergic agonist CL-316243 in obese Zucker-ZDF rats, Am. J. Physiol. 274 (5 Pt. 2) (1998) R1212–9.

[48] M. Omatsu-Kanbe, H. Kitasato, Insulin and noradrenaline independently stimulate the translocation of glucose transporters from intracellular stores to the plasma membrane in mouse brown adipocytes, FEBS Lett. 314 (3) (1992) 246–250.

[49] E. Chernogubova, B. Cannon, T. Bengtsson, Norepinephrine increases glucose transport in brown adipocytes via β_3-adrenoceptors through a cAMP, PKA, and PI3-kinase-dependent pathway stimulating conventional and novel PKCs, Endocrinology 145 (1) (2004) 269–280.

[50] E. Chernogubova, D.S. Hutchinson, J. Nedergaard, T. Bengtsson, α_1- and β_1-adrenoceptor signaling fully compensates for β_3-adrenoceptor deficiency in brown adipocyte norepinephrine-stimulated glucose uptake, Endocrinology 146 (5) (2005) 2271–2284.

[51] C.L. Mattsson, R.I. Csikasz, E. Chernogubova, D.L. Yamamoto, H.T. Hogberg, E.Z. Amri, D.S. Hutchinson, T. Bengtsson, β_1-adrenergic receptors increase UCP1 in human MADS brown adipocytes and rescue cold-acclimated β_3-adrenergic receptor-knockout mice via nonshivering thermogenesis, Am. J. Physiol. Endocrinol. Metab. 301 (6) (2011) E1108–E11018.

[52] J.R. Arch, S. Wilson, Prospects for β_3-adrenoceptor agonists in the treatment of obesity and diabetes, Int. J. Obes. Relat. Metab. Disord. 20 (3) (1996) 191–199.

[53] J. Nedergaard, T. Bengtsson, B. Cannon, Unexpected evidence for active brown adipose tissue in adult humans, Am. J. Physiol. Endocrinol. Metab. 293 (2) (2007) E444–52.

[54] A.M. Cypess, S. Lehman, G. Williams, I. Tal, D. Rodman, A.B. Goldfine, F.C. Kuo, E.L. Palmer, Y.H. Tseng, A. Doria, G.M. Kolodny, C.R. Kahn, Identification and importance of brown adipose tissue in adult humans, N. Engl. J. Med. 360 (15) (2009) 1509–1517.

[55] M. Saito, Y. Okamatsu-Ogura, M. Matsushita, K. Watanabe, T. Yoneshiro, J. Nio-Kobayashi, T. Iwanaga, M. Miyagawa, T. Kameya, K. Nakada, Y. Kawai, M. Tsujisaki, High incidence of metabolically active brown adipose tissue in healthy adult humans, Diabetes 58 (7) (2009) 1526–1531.

[56] W.D. van Marken Lichtenbelt, J.W. Vanhommerig, N.M. Smulders, J.M. Drossaerts, G.J. Kemerink, N.D. Bouvy, P. Schrauwen, G.J. Teule, Cold-activated brown adipose tissue in healthy men, N. Engl. J. Med. 360 (15) (2009) 1500–1508.

[57] S. Cinti, Transdifferentiation properties of adipocytes in the adipose organ, Am. J. Physiol. Endocrinol. Metab. 297 (5) (2009) E977–86.

[58] M.C. Zingaretti, F. Crosta, A. Vitali, M. Guerrieri, A. Frontini, B. Cannon, J. Nedergaard, S. Cinti, The presence of UCP1 demonstrates that metabolically active adipose tissue in the neck of adult humans truly represents brown adipose tissue, FASEB J. 23 (9) (2009) 3113–3120.

[59] J. Wu, P. Bostrom, L.M. Sparks, L. Ye, J.H. Choi, A.H. Giang, M. Khandekar, K.A. Virtanen, P. Nuutila, G. Schaart, K. Huang, H. Tu, W.D. van Marken Lichtenbelt, J. Hoeks, S. Enerback, P. Schrauwen, B.M. Spiegelman, Beige adipocytes are a distinct type of thermogenic fat cell in mouse and human, Cell 150 (2) (2012) 366–376.

[60] A.M. Cypess, A.P. White, C. Vernochet, T.J. Schulz, R. Xue, C.A. Sass, T.L. Huang, C. Roberts-Toler, L.S. Weiner, C. Sze, A.T. Chacko, L.N. Deschamps, L.M. Herder, N. Truchan, A.L. Glasgow, A.R. Holman, A. Gavrila, P.O. Hasselgren, M.A. Mori, M. Molla, Y.H. Tseng, Anatomical localization, gene expression profiling and functional characterization of adult human neck brown fat, Nat. Med. 19 (5) (2013) 635–639.

[61] M.E. Lidell, M.J. Betz, O. Dahlqvist Leinhard, M. Heglind, L. Elander, M. Slawik, T. Mussack, D. Nilsson, T. Romu, P. Nuutila, K.A. Virtanen, F. Beuschlein, A. Persson, M. Borga, S. Enerback, Evidence for two types of brown adipose tissue in humans, Nat. Med. 19 (5) (2013) 631–634.

[62] A.M. Cypess, L.S. Weiner, C. Roberts-Toler, E.F. Elia, S.H. Kessler, P.A. Kahn, J. English, K. Chatman, S.A. Trauger, A. Doria, G.M. Kolodny, Activation of human brown adipose tissue by a β_3-adrenergic receptor agonist, Cell Metab. 21 (1) (2015) 33–38.

[63] K.A. Virtanen, M.E. Lidell, J. Orava, M. Heglind, R. Westergren, T. Niemi, M. Taittonen, J. Laine, N.J. Savisto, S. Enerback, P. Nuutila, Functional brown adipose tissue in healthy adults, N. Engl. J. Med. 360 (15) (2009) 1518–1525.

[64] M. Sato, D.S. Hutchinson, M.L. Halls, S.G. Furness, B.A. Evans, R.J. Summers, Interaction with caveolin-1 modulates G protein coupling of mouse β_3-adrenoceptor, J. Biol. Chem. 287 (24) (2012) 20674–20688.

[65] D.S. Hutchinson, E. Chernogubova, O.S. Dallner, B. Cannon, T. Bengtsson, β-adrenoceptors, but not α-adrenoceptors, stimulate AMP-activated protein kinase in brown adipocytes independently of uncoupling protein-1, Diabetologia 48 (11) (2005) 2386–2395.

[66] K. Inokuma, Y. Ogura-Okamatsu, C. Toda, K. Kimura, H. Yamashita, M. Saito, Uncoupling protein 1 is necessary for norepinephrine-induced glucose utilization in brown adipose tissue, Diabetes 54 (5) (2005) 1385–1391.

[67] H. Cai, L.Q. Dong, F. Liu, Recent advances in adipose mTOR signaling and function: therapeutic prospects, Trends Pharmacol. Sci. 37 (4) (2016) 303–317.

[68] P. Polak, N. Cybulski, J.N. Feige, J. Auwerx, M.A. Ruegg, M.N. Hall, Adipose-specific knockout of raptor results in lean mice with enhanced mitochondrial respiration, Cell Metab. 8 (5) (2008) 399–410.

[69] A. Kumar, J.C. Lawrence Jr., D.Y. Jung, H.J. Ko, S.R. Keller, J.K. Kim, M.A. Magnuson, T.E. Harris, Fat cell-specific ablation of rictor in mice impairs insulin-regulated fat cell and whole-body glucose and lipid metabolism, Diabetes 59 (6) (2010) 1397–1406.

[70] S.I. Gharbi, M.J. Zvelebil, S.J. Shuttleworth, T. Hancox, N. Saghir, J.F. Timms, M.D. Waterfield, Exploring the specificity of the PI3K family inhibitor LY294002, Biochem. J. 404 (1) (2007) 15–21.

[71] Z.A. Knight, B. Gonzalez, M.E. Feldman, E.R. Zunder, D.D. Goldenberg, O. Williams, R. Loewith, D. Stokoe, A. Balla, B. Toth, T. Balla, W.A. Weiss, R.L. Williams, K.M. Shokat, A pharmacological map of the PI3-K family defines a role for p110α in insulin signaling, Cell 125 (4) (2006) 733–747.

[72] O.S. Dallner, E. Chernogubova, K.A. Brolinson, T. Bengtsson, β_3-adrenergic receptors stimulate glucose uptake in brown adipocytes by two mechanisms independently of glucose transporter 4 translocation, Endocrinology 147 (12) (2006) 5730–5739.

[73] V. Albert, K. Svensson, M. Shimobayashi, M. Colombi, S. Munoz, V. Jimenez, C. Handschin, F. Bosch, M.N. Hall, mTORC2 sustains thermogenesis via Akt-induced glucose uptake and glycolysis in brown adipose tissue, EMBO Mol. Med. 8 (3) (2016) 232–246.

[74] H. Elayan, M. Milic, P. Sun, M. Gharaibeh, M.G. Ziegler, Chronic β_2 adrenergic agonist, but not exercise, improves glucose handling in older type 2 diabetic mice, Cell. Mol. Neurobiol. 32 (5) (2012) 871–877.

[75] R.T. Hinkle, K.M. Hodge, D.B. Cody, R.J. Sheldon, B.K. Kobilka, R.J. Isfort, Skeletal muscle hypertrophy and anti-atrophy effects of clenbuterol are mediated by the β_2-adrenergic receptor, Muscle Nerve 25 (5) (2002) 729–734.